

**Microalgae for wastewater treatment and biomass production:
A comparative analysis of growth and nutrient removal including
shotgun proteomics**

Anil Kumar Patel

Department of Bioresource Engineering

21111 Lakeshore Road, Ste. Anne de Bellevue, Quebec H9X 3V9

McGill University, Quebec, Canada

December 2015

A dissertation submitted to the Faculty of Graduate Studies and Research,
McGill University, in partial fulfillment of the requirements of the degree of
Doctor of Philosophy

© Anil Kumar Patel, 2015

Dedication

In loving memory of my father, Dr. Popatlal M. Patel (1933-2012).

Abstract

Post-industrial activities have amplified global cycles of nitrogen and phosphorus by 100% and 400%, respectively. Projections for biofuel production from microalgae are based on optimistic assumptions and projections of achievable productivities. Feedstock and biofuel production can be feasible when a second function is added, such as wastewater treatment. Experiment 1 consisted of a candidate screen of three freshwater and three marine unsequenced species that quantified total phosphorus removal and growth as a function of phosphorus loading. Phosphorus uptake was found to be dependent on species, duration of exposure, and treatment, with significant interaction effects. Growth was dependent on species and treatment. Not all species showed increased P removal with increasing P addition, and unexpectedly no species demonstrated higher biomass accumulation. Two dual-purpose candidates – *Monoraphidium minutum* sp. and *Tetraselmis suecica* sp. – were identified as capable of high rates of phosphorus removal and growth. In Experiment 2 the sequenced eukaryotic green microalga *Chlamydomonas reinhardtii* was cultured in batch mode at the bench scale for 12 days in order to investigate nitrogen and phosphorus uptake and the response of biomass accumulation to wastewater processing. *Chlamydomonas* removed total phosphorus and nitrogen in solution efficiently in both culture conditions, however, final biomass concentration did not differ significantly. Label-free shotgun proteomics identified 2358 non-redundant proteins, of which 92 were significantly differentially abundant. Functional analysis found enrichment of photosynthetic antennae proteins, enzymes related to carbon fixation, and biosynthesis of secondary metabolites in wastewater cells. Control cells showed enrichment of enzymes and proteins related to nitrogen metabolism and assimilation, synthesis and utilization of carbohydrates, amino acid recycling, evidence of oxidative stress, and little lipid biosynthesis.

Up-regulated pathways in artificial wastewater, notably photosynthetic carbon fixation and biosynthesis of plant hormones, and the up-regulated pathways in nitrate only control, notably nitrogen, amino acid, and starch metabolism, represent potential targets for genetic improvement. In Experiment 3, the same strain of *Chlamydomonas* was cultured in batch mode for 5 days using a pilot scale photobioreactor system in order to investigate and compare nutrient uptake and growth responses to scale up wastewater processing. *Chlamydomonas* removed nitrogen and phosphorus efficiently in both conditions, and final biomass concentration was significantly higher in wastewater-cultured cells. Nonetheless, *Chlamydomonas* did not accumulate biomass quickly at either the bench or pilot scales compared to top performers identified in Experiment 1. Cells cultured in wastewater medium showed higher final biomass concentration and biomass productivity in the photobioreactor cultures over flask cultures from Experiment 2. Cells cultured in control medium had comparable final biomass yields at both scales, but higher biomass productivity in the photobioreactor cultures, which suggested nutrient starvation.

Abrégé

Les activités des sociétés post-industrielles ont amplifié les cycles globaux d'azote et de phosphore de 100% et de 400% respectivement. Les projections de production de biocarburant à partir de microalgues sont fondées sur des hypothèses et projections optimistes concernant la productivité atteignable. La production de matière première et de biocarburants est envisageable lorsqu'une seconde fonction est ajoutée, telle qu'avec le traitement des eaux usées. L'expérience 1 consistait en un processus de sélection parmi trois espèces d'eau douce et trois espèces marines non séquencées qui a permis de quantifier l'élimination totale de phosphore ainsi que la croissance en fonction de la charge de phosphore. L'assimilation de phosphore s'est avérée dépendante de l'espèce, de la durée d'exposition et du traitement, avec des effets d'interaction significatifs. La croissance a été dépendante de l'espèce et du traitement. Les espèces n'ont pas toutes exhibé une élimination de P croissante avec un ajout graduel de P et, étonnamment, aucune espèce n'a démontré une accumulation en biomasse plus élevée. Deux candidats à double vocation – *Monoraphidium minutum* sp. et *Tetraselmis suecica* sp. – ont été identifiés pour leur capacité d'élimination du phosphore et de croissance à des taux élevés. Lors de l'expérience 2 une microalgue eucaryote verte *Chlamydomonas reinhardtii* fut cultivée en lots sur un banc d'essai durant 12 jours pour étudier l'assimilation d'azote et de phosphore ainsi que la réponse d'accumulation de biomasse lors de traitements d'eaux usées. *Chlamydomonas* éliminait efficacement le phosphore total et l'azote en solution dans les deux conditions de culture, cependant, la concentration finale en biomasse ne différait pas significativement. Un flux de travail sans marquage de protéomique en vrac (« shotgun ») a identifié 2358 protéines non redondantes dont 92 étaient significativement différentiellement abondantes. L'analyse fonctionnelle a permis de constater un enrichissement de protéines antennes photosynthétiques,

des enzymes liées à la fixation de carbone et la biosynthèse de métabolites secondaires parmi les cellules des eaux usées. Les cellules témoins ont présenté un enrichissement des enzymes et des protéines associées au métabolisme et à l'assimilation de l'azote, une synthèse et une utilisation des glucides, un recyclage des acides aminés, une évidence de stress oxydatif et peu de biosynthèse des lipides. Les voies régulées à la hausse des eaux usées artificielles, notamment la fixation photosynthétique du carbone et la biosynthèse d'hormones végétales, et les voies régulées à la hausse des témoins de nitrate seulement, dont l'azote, les acides aminés et le métabolisme de l'amidon, représentent des cibles potentielles d'amélioration génétique. Pour l'expérience 3, la même souche de *Chlamydomonas* a été cultivée en lots pendant 5 jours en utilisant un photobioréacteur pilote afin d'étudier et de comparer les réponses sur l'absorption de nutriments et la croissance dues à ce changement d'échelle de traitement des eaux usées. Le *Chlamydomonas* a éliminé efficacement l'azote et le phosphore dans les deux conditions, et la concentration finale en biomasse était significativement plus élevée dans les cellules cultivées en eaux usées. Néanmoins, le *Chlamydomonas* n'a pas fait d'accumulation de biomasse rapidement tant pour le banc d'essai qu'à l'échelle pilote comparativement aux souches les plus performantes identifiées dans l'expérience 1. Les cellules cultivées en milieu d'eaux usées ont démontré une concentration finale et une productivité plus grandes en biomasse dans les cultures en photobioréacteur contrairement aux cultures en flasques de l'expérience 2. Les cellules cultivées en milieu contrôlé ont atteint des rendements en biomasse finale comparables aux deux échelles, mais une plus grande productivité de biomasse dans les cultures en photobioréacteur, suggérant un appauvrissement en nutriments.

Acknowledgements

I thank my supervisor Dr. Mark G. Lefsrud for the opportunity, guidance and support to pursue this research, and for imparting a spirit of originality in research and academic freedom. I thank members serving on the Ph.D. advisory and defense committees for their effort and interest: Drs. Suzelle Barrington, Gregor Fussmann, W. Hayes McDonald, Ajjamada Kushalappa, Valérie Orsat, Vijaya Ragahavan and Don Smith. I thank Dr. Eric Huang for technical support in adapting and optimizing proteomic methods, training with instrumentation, and a very productive friendship. I thank Dr. Etienne Low-Décarie for his encouragement in pursuing a doctorate, instruction in R, and a collaborative friendship. I thank Dr. Todd Greco for invaluable assistance and guidance with proteome informatics, computational and software resources, and critical review of the manuscript. I thank the instructors, assistants and guest speakers of the 2013 Proteomics Course, Cold Spring Harbor Laboratory, for training and an introduction to the larger proteomics community. I thank Dr. Olivier Collin for help troubleshooting all things LC-MS. I thank the academic and support staff at the Department of Bioresource Engineering, and Drs. Darwin Lyew and Robert Williams for advice and technical support in microbiology and biochemistry, and Blake Bissonnette for assistance with the photobioreactors. I thank my fellow lab mates and graduate students, including, Manual Ivan Villalobos Solis, Louis-Martin Dion, Kumaran Sivagnanam, and Kevin MacDonald. I thank Drs. Gabrielle and Viktor Zacek for their hospitality on Durocher Street in the McGill Ghetto. I thank Ramanand Patel, Hart Lazer, Donna Read and the faculty and students at United Yoga Montreal. Finally, I owe a tremendous debt of gratitude to my parents, Joan and Popat Patel, whose support never waived, and my sisters Ila and Tara and their families for their love and encouragement. Most of all I thank my beautiful, loving, and talented wife, Anita. Without her love and support, I would be lost at sea.

Thesis office statement

Candidates have the option, **subject to the approval of their Department**, of including, as part of their thesis, copies of the text of a paper(s) submitted for publication, or the clearly duplicated text of the published paper(s) provided that these copies are bound as an integral part of the thesis. If this option is chosen, **connecting texts, providing logical bridges between the different papers are mandatory.**

The thesis must still conform to all other requirements of the “Guidelines Concerning Thesis Preparation” and should be in literary form that is more than a mere collection of manuscripts published or to be published. The thesis must include, as separate chapters or sections: (1) a Table of Contents, (2) a general abstract in English and French, (3) an introduction which clearly states the rationale and objectives of the study, (4) a comprehensive general review of the background literature to the subject of the thesis, when this review is appropriate, and (5) a final overall conclusion and/or summary.

Additional material (procedural and design data, as well as description of the equipment used) must be provided where appropriate and in sufficient detail (*e.g.* in appendices) to allow a clear and precise judgment to be made of the importance and originality of the research reported in the thesis.

In the case of manuscripts co-authored by the candidate and others, **the candidate is required to make an explicit statement in the thesis as to who contributed to such work and to what extent**; supervisors must attest to the accuracy of such claims at the Ph.D. Oral defense. Since the task of examiners is made more difficult in these cases, it is in the candidate’s interest to make perfectly clear the responsibilities of all the authors of the co-authored papers.

Statement of contributing authors

In accordance with the McGill “Guidelines for a Manuscript Based Thesis,” the contributions made by the candidate and co-authors of the PhD dissertation chapters are specified below by chapter manuscript. Dr. Mark Lefsrud served as thesis advisor and was involved in experimental design, editing and review of chapter manuscripts for publication, and provided critical input and guidance.

Chapter 3 (Manuscript I):

This manuscript chapter were co-authored by the candidate, Dr. Suzelle Barrington and Dr. Mark Lefsrud. The candidate was responsible for carrying out culturing of microalgae strains, performance of gravimetric, spectrophotometric and colorimetric assays to determine growth and nutrient removal, statistical analysis, and writing of the manuscript. Dr. Darwin Lyew provided advice and technical support in microbiology. The co-authors Dr. Mark Lefsrud and Dr Suzelle Barrington participated in experimental design, presentation of data and editing and critical review of the published manuscript.

Chapter 4 (Manuscript II) and Chapter 5 (Manuscript II, Supplemental findings):

These manuscript chapters were co-authored by the candidate, Dr. Eric Liu Huang, Dr. Etienne Low-Décarie and Dr. Mark Lefsrud. The candidate was responsible for carrying out microalgae culturing at the bench scale and performance of assays as above. Regarding development of an in-house shotgun proteomics platform suitable for green eukaryotic microalgae, the candidate performed all sample preparation and protein digestion, liquid chromatography (LC), mass spectrometry (MS), statistical and mass informatic analysis, including determination of relative

protein abundance. The candidate also performed functional analysis, including enrichment, metabolic mapping and biological interpretation using the literature and bioinformatics databases. The candidate was responsible for the writing and editing of the manuscript for publication. The specific contributions made by the co-authors or critical assistance provided by individuals in the acknowledgements section is listed below.

Sample preparation and digestion: The candidate was responsible for all proteomic sample generation, including harvesting, preparation, protein extraction/digestion, clean up and optimization for microalgae of cited references. The co-author Dr. Eric Liu Huang provided technical support.

Shotgun proteomic analysis: The candidate was responsible for performing all LC–MS runs and optimization for eukaryotic microalgae of methods (Chapter 9, Section 9.1, Appendix A) referenced from Oak Ridge National Laboratory and yeast proteomics. The co-author Dr. Eric Liu Huang provided technical support and assistance in setting up the mass spectrometer and HPLC system.

Mass informatics: The candidate was responsible for performing all protein identification and statistical analysis at the Cold Spring Harbor Proteomics 2013 course. As listed in acknowledgements, Dr. Todd Greco (Department of Molecular Biology, Princeton University) provided technical support and mentoring, including fast computer and proteome analysis software that generated final protein identification lists based on methods learned and developed in the course.

Differential analysis: The candidate performed parsing of protein attributes using R and differential abundance analysis and data normalization using the online tool QSpec. As listed in

acknowledgements, Dr. Damian Fermin (Yale School of Medicine) & Dr. Hyung Choi (School of Public Health, National University of Singapore) provided technical input on parameters.

Statistical analysis and visualization: The co-author Dr. Etienne Low-Décarie was responsible for producing R scripts that calculated growth and nutrient removal rates and curve plots (Figure 4.1), proteome level multivariate analysis (PCA) and biplot (Figure 4.2), GO slim files based on *Arabidopsis* TAIR 10 functional descriptions, and visualization of nitrogen metabolism related protein spectral counts (Table 4.2) (Figure 4.4).

Functional enrichment and pathway analysis: The candidate performed all manual curation and confirmation of identified and differentially abundant proteins (Table 5.1), functional enrichment (Table 4.1), pathway analysis and metabolic mapping (Figure 4.3). This included annotation database and literature searches.

Preparation, editing, and submission of the manuscript was performed by the candidate with critical input from co-authors Drs. Huang, Low-Décarie and Lefsrud.

Dr. Mark Lefsrud served as thesis advisor and was involved in experimental design, editing and review of the manuscript and provided critical input on the use of the mass analyzer.

Chapter 6 (Manuscript III):

This manuscript chapter was co-authored by the candidate, Blake Bissonnette and Dr. Mark Lefsrud. The candidate was responsible for carrying out culturing of microalgae at the bench and pilot scale. This included performance of assays as above, statistical analysis, the modification and optimization of an in-house bioreactor system, and the writing and editing of the manuscript. The specific contributions made by the co-authors or critical assistance provided by individuals in the acknowledgements section is listed below.

Dr. Darwin Lyew designed and built the photobioreactor (PBR) system for previous unrelated research, and advised the candidate on conversion for use with liquid media and compressed air. Co-author Blake Bissonnette provided technical and engineering assistance in this modification of the PBR system that included multiplication of glass columns, gas mixture, uniform airflow metering and lighting, and assistance with culturing and sampling during experimental runs. Dr. Mark Lefsrud participated in experimental design, presentation of data, and editing and critical review of the manuscript for publication submission.

Table of contents

Abstract.....	III
Abrégé	V
Acknowledgements	VII
Thesis office statement	VIII
Statement of contributing authors.....	IX
Table of contents	XIII
List of tables	XX
List of figures.....	XXI
List of abbreviations	XXII
Chapter 1: Introduction.....	1
Connecting statement	1
1. Introduction	2
1.1. Background, problem statement and significance.....	2
1.2. Statement of hypotheses and research objectives	8
1.3. Dissertation organization	11
Chapter 2: Literature review.....	13
Connecting statement	13
2. Literature review.....	14
2.1. Microalgal biology and physiology	14
2.1.1. <i>Chlamydomonas reinhardtii</i>	14
2.1.2. Photosynthesis and carbon fixation	15
2.1.3. Nitrogen metabolism and assimilation	17
2.1.4. Phosphorus removal.....	18

2.1.5. Metabolic adaptations to macronutrient limitation	19
2.1.6. Metabolic tradeoffs between growth and the stress response	21
2.2. Microalgal biotechnology	22
2.2.1. Biomass, commodities and co-products	22
2.2.2. Wastewater treatment	23
2.2.3. Biomass production and photo-technology	25
2.2.4. Constraints on yields.....	26
2.3. Summary of microalgal biology and biotechnology	28
2.4. Shotgun proteomics and data analysis	29
2.4.1. Eukaryotic microalgal proteomics	30
2.4.2. Shotgun proteomics	31
2.4.3. Mass informatics.....	35
2.4.4. Label-free quantitation and relative abundance	36
2.4.5. Significance analysis.....	37
2.5. Bioinformatics tools and functional analysis	38
2.5.1. Functional enrichment	39
2.5.2. Ontology tools.....	40
2.5.3. Pathway analysis and metabolic mapping	41
2.6. Summary of shotgun proteomics and data analysis	42
Chapter 3: Manuscript I.....	44
Connecting statement	44
Abstract	46
3.1. Introduction	47
3.2. Materials and methods	50

3.2.1 Experimental organisms	50
3.2.2 Methods	51
3.2.3 Analytical procedures	53
3.2.4. Statistical analysis.....	54
3.3. Results	54
3.3.1. Phosphorus removal.....	54
3.3.2. Biomass accumulation	58
3.3.3. Dual-purpose candidates.....	60
3.4. Discussion	61
3.4.1. Microalgal photosynthesis, growth and phosphorus removal	61
3.4.2. Response of nutrient removal to P addition.....	62
3.4.3. Growth response to P addition.....	64
3.4.4. Batch culturing constraints	66
3.4.5. Industrial application and scale up.....	67
Acknowledgements	68
Chapter 4: Manuscript II.....	69
Connecting statement	69
Abstract	72
4.1. Introduction	73
4.2. Materials and methods	76
4.2.1. Experimental design, organism and culture conditions	76
4.2.2. Growth and nutrient removal	78
4.2.3. Protein extraction and digestion	78
4.2.4. 2D LC–MS/MS.....	79

4.2.5. Database searching	80
4.2.6. Selection of differentially abundant proteins by QSpec	81
4.2.7. Functional enrichment and pathway analysis	82
4.3. Results and discussion.....	83
4.3.1. Comparison of growth and nutrient removal rates	83
4.3.2. Global proteome overview and visualization	87
4.3.3. Differential analysis and functional enrichment.....	91
4.3.3.1. Wastewater cells showed a higher abundance of antenna proteins	94
4.3.3.2. Functional enrichment found that wastewater cells continued to fix carbon and divide.	96
4.3.3.3. Biosynthesis of amino acids, fatty acids, vitamins and chlorophyll continued in wastewater cells.....	99
4.3.3.4. Depletion of extracellular nitrogen activated amino acid recycling, starch metabolism, and oxidative stress in control cells.	101
4.3.3.5. Alterations to proteins related to nitrogen sensing, metabolism and assimilation	105
4.4. Concluding remarks	111
Associated content	113
Acknowledgements	114
Chapter 5: Manuscript II, Supplemental findings	115
Connecting statement	115
Abstract:	117
5.1. Introduction	118
5.2. Materials and methods	119

5.2.1. Selection of differentially abundant proteins, functional enrichment and pathway analysis.....	120
5.3. Results and discussion.....	121
5.3.1. Differential analysis and functional enrichment.....	124
5.3.1.1. Additional biosynthesis proteins enriched in wastewater by AFAT score.....	124
5.3.1.2. Additional proteins enriched in control by AFAT score	124
5.3.1.3. Additional proteins in control lacking AFAT annotation.....	125
5.3.2. Stress response proteins	126
5.3.2.1. Stress related proteins in wastewater.....	127
5.3.2.2. Control cells showed evidence of nutrient limitation.....	127
5.3.2.3. Oxidative stress proteins were enriched in control.....	128
5.3.3. Poorly annotated and unknown proteins.....	130
5.3.3.1. Poorly annotated and unknown proteins with higher levels in wastewater.....	130
5.3.3.2. Poorly annotated and unknown proteins with higher levels in control	132
5.4. Concluding remarks	133
Chapter 6: Manuscript III	135
Connecting statement	135
Abstract	137
6.1. Introduction	138
6.2. Materials and methods	141
6.2.1. Algal strain and culture conditions	141
6.2.2. Pilot scale PBR system	143
6.2.3 Analytical procedures	144
6.2.4 Data and statistical analysis	145

6.3. Results	146
6.3.1. Nutrient removal by culture condition and scale	146
6.3.2. Biomass growth by culture condition and scale	151
6.4. Discussion	152
6.4.1 Nutrient removal response of <i>C. reinhardtii</i> to wastewater processing	152
6.4.1.1. PBR wastewater and control cultures showed nutrient limitation.....	152
6.4.1.2. Control cells in flask cultures showed nutrient limitation.....	154
6.4.2. Growth response of <i>C. reinhardtii</i> to wastewater processing.....	155
6.4.2.1. Biomass yields were higher in wastewater PBR cultures.....	155
6.4.2.2. Biomass yields were not significantly different in flask cultures.....	160
6.4.2.3. Control PBR and flask cultures had similar biomass yields but different productivities	161
6.4.3. A metabolic conundrum between growth and the stress response	162
6.4.4. Development of dual-purpose candidates and consortia	164
Acknowledgements	166
Chapter 7: Final summary, significance and conclusions	168
Connecting statement	168
7. Final summary, significance and conclusions	169
7.1. Dissertation summary.....	169
7.2. Methodology	173
7.3. Microalgae and wastewater treatment.....	177
7.3.1. Chapter 3: Manuscript I	177
7.3.2. Chapter 4: Manuscript II.....	179
7.3.3. Chapter 5: Manuscript II, Supplemental findings.....	182

7.3.4. Chapter 6: Manuscript III	184
7.4. Statement of originality, significance and contribution to knowledge.....	187
7.5. Future research	190
7.5.1. Discovery and targeted proteomics.....	191
7.5.2. Community proteomics and bioprocess monitoring.....	193
Chapter 8: References.....	195
8.1. References	195
Chapter 9: Appendices.....	219
9.1. Appendix A: Proteomic sample preparation and instrument setup.....	219
9.1.1. Sample preparation for small samples of microalgae.....	219
9.1.2. LTQ XL parameters for data-dependent acquisition of tandem MS/MS spectra	219
9.1.3. 2D LC elution gradient	220
9.2. Appendix B: Publishing agreements	224

List of tables

Chapter 3 (Manuscript I)

Table 3.1. Algal group and culture origin of the six strains tested in screening.....	51
---	----

Chapter 4 (Manuscript II)

Table 4.1. Proteins that are significantly increased in abundance by treatment condition with KEGG functional association.....	92
--	----

Table 4.2. Nitrogen-related proteins identified in the experiment by culture condition with GO and Arabidopsis functional association.....	108
--	-----

Chapter 5 (Manuscript II, Supplemental findings)

Table 5.1. Proteins significantly increased in abundance by culture condition with QSpec statistics and normalized spectral counts.....	123
---	-----

Supporting information table as referenced in Chapter 4 (Manuscript II) and Chapter 5 (Manuscript II, Supplemental findings)

Table S1. Proteins identified that contain four or more spectra with QSpec statistics, normalized spectral counts, JGI <i>Chlre</i> v5.3.1 annotation and functional association.....	
.....Accessible at: http://pubs.acs.org/doi/abs/10.1021/pr501316h	

List of figures

Chapter 2: Literature Review

Figure 2.1. Life cycle of *Chlamydomonas reinhardtii*.....15

Figure 2.2. Workflow of MudPIT LC–MS/MS shotgun proteomics experiment.....31

Chapter 3 (Manuscript I)

Figure 3.1. Total phosphorus and biomass growth for six species over 16 days.....55

Figure 3.2. Phosphorus removal efficiency and total phosphorus removed at day 8.....56

Figure 3.3. Final biomass and biomass productivity at day 16.....59

Chapter 4 (Manuscript II)

Graphical abstract.....73

Figure 4.1. Visualizing flask growth and nutrient removal curves.....85

Figure 4.2. PCA visualization of 20 proteins with greatest variance at proteome level...89

Figure 4.3. Pathway-centric visualization of up-regulated pathways of the *C. reinhardtii* genome according to culture condition.....96

Figure 4.4. Nitrogen metabolism and assimilation related proteins.....107

Chapter 6 (Manuscript III)

Figure 6.1. Visualizing photobioreactor growth and nutrient removal curves.....147

Figure 6.2. Nutrient removal efficiency.....149

Figure 6.3. Final biomass concentration and productivities.....159

List of abbreviations

2-cys PRX: 2-cys peroxiredoxin

2DGE: two-dimensional gel electrophoresis

α -KG: α -ketoglutarate

A1F: ADP-ribosylation factor

AA: arachidonic acid

AAT1: alanine aminotransferase

AdoMet: S-adenosylmethionine

ADP: adenosine diphosphate

ADH/ACDH: alcohol/acetaldehyde dehydrogenase

AFAT: Algal Functional Annotation Tool

AIH: agmatine deiminase

ALT: alanine aminotransferase

ALDH: acetaldehyde dehydrogenase

ANOVA: analysis of variance

AS: asparagine synthetase

ASL: argininosuccinate lyase

ASADH: aspartate-semialdehyde dehydrogenase

AspAT: aspartate aminotransferase

ASS: argininosuccinate synthase

ATP: adenosine triphosphate

AWW: artificial wastewater

BCAT: branched-chain amino acid aminotransferase

CA1: carbonic anhydrase

CAD: carbamoyl phosphate synthetase, small subunit

CCM: carbon concentrating mechanism

CHD: choline dehydrogenase

CHLI1: magnesium chelatase subunit I

CMP: carbamoyl phosphate synthetase B

CID: collision-induced dissociation

CEF: cyclic electron flow pathway

C-PC: C-phycoerythrin

CTRL: control

DAG: diacylglycerol

DCM: dry cell mass

DDA: data-dependent acquisition

DHA: docosahexaenoic acid

DLA2: dihydrolipoamide acetyltransferase

E2: dihydrolipoamide acetyltransferase

EC: Enzyme Commission number

EPA: eicosapentaenoic acid

EBPR: enhanced biological phosphorus removal

ER: endoplasmic reticulum

ESI: electrospray ionization

FA: fatty acid

FBA: fructose-bisphosphate aldolase class I

FBP: fructose-1,6-bisphosphatase plastid precursor

FD: ferrdoxin

Fd-GOGAT: ferredoxin-dependent glutamine oxoglutarate aminotransferase

FDR: false discovery rate

FDRup/FDRdown: directional false discovery rate

Fe-SOD: Superoxide dismutase

G3P: glyceraldehyde 3-phosphate

GAPDH: glyceraldehyde 3-phosphate dehydrogenase

GBSS: granule-bound starch synthase 1

GDH: glutamate dehydrogenase

GE: Genetic engineering

GeLC/MS: gel-based liquid chromatography-mass spectrometry

GLA: γ -linolenic acid

GMC: glucose-methanol-choline oxidoreductase family proteins

Glc-6-P: glucose 6-phosphate

GLN 1;3: glutamine synthetase – plasma membrane

GLN 1;4: glutamine synthetase – cytosol

GO: Gene Ontology

GOSLIM: GO slims; subset of terms in whole GO

GPT: glucose-6-phosphate/phosphate translocator-related

GPx: glutathione peroxidase

GS: glutamine synthetase

G3P: glyceraldehyde 3-phosphate

HMMs: hidden Markov models

HPLC: high-performance liquid chromatography

HRAP: high rate algal ponds

HSD: honestly significant difference, Tukey's post-hoc test

HT MS: high throughput mass spectrometry

iTRAQ: Isobaric Tags for Relative and Absolute Quantitation

JGI: Joint Genome Institute

KEGG: Kyoto Encyclopedia of Genes and Genomes

KO: KEGG group association

ko: KEGG pathway association

KOG: Eukaryotic Orthologous Group

LCA: life cycle analysis

LC: liquid chromatography

LC-MS: liquid chromatography mass spectrometry

LEF: linear electron flow

LHCII: light-harvesting complex II

LHCI: light-harvesting complex I

LP1: large subunit ribosomal protein

LTA2: dihydrolipoamide S-acetyltransferase

L7/L12: large subunit ribosomal protein

L28: plastid ribosomal protein

MANOVA: multivariate analysis of variance

MetE: cobalamin-independent methionine synthase

MDLC: multi-dimensional liquid chromatography

MGPB: microalgae growth promoting bacteria

MRM: multiple reaction monitoring

MS/MS: tandem mass spectrometry

MTHFR: methylenetetrahydrofolate reductase (NADPH)

MudPIT: Multi-dimensional Protein Identification Technology

NII1: ferredoxin-nitrite reductase

NAD⁺: nicotinamide adenine dinucleotide (oxidized)

NADH: nicotinamide adenine dinucleotide (reduced)

NADP⁺: nicotinamide adenine dinucleotide phosphate (oxidized)

NADPH: nicotinamide adenine dinucleotide phosphate (reduced)

NADH-GOGAT: NADH-dependent glutamine oxoglutarate aminotransferase

Nmr: nitrogen metabolic regulation

NR: nitrate reductase

NiR: nitrite reductase

OAR: 3-oxoacyl-[acyl-carrier protein] reductase

OD: optical density

PAP: purple acid phosphatase

PAR: photosynthetically active radiation

PBR: photobioreactor

PCA: principal component analysis

PDI: ADP-ribosylation factor family

PET: photosynthetic electron transport chain

Pfam: protein families database

PFD: photon flux densities

pI: protein isoelectric point

polyP: polyphosphate

PRK: phosphoribulokinase chloroplast precursor

PSMs: peptide spectrum matches

PSU: photosynthetic unit

PSII: Photosystem II

PSI: Photosystem I

pTACs: plastid transcriptionally active chromosome proteins

PUFAs: polyunsaturated fatty acids

QSpec: hierarchical model for differential protein analysis

RNA-seq: RNA sequencing

RP: reversed phase column packing material

RuBisCO: ribulose-1,5-bisphosphate carboxylase/oxygenase

RuBP: ribulose-1,5-bisphosphate

SCX: strong cation exchange

SRM: single reaction monitoring

TAG: triacylglycerol

TAIR: The Arabidopsis Information Resource

TCA cycle: tricarboxylic acid cycle

TFE: transcription factor engineering

TKT: transketolase

THI4: thiamine biosynthetic enzyme

TOR: target-of-rapamycin

TP: total phosphorus

TPR: tetratricoptide repeat

TRK1: transketolase

VAP: vertical alveolar panel

WSP: waste stabilization ponds

Chapter 1: Introduction

Connecting statement

This chapter provides background information and the context for experimental questions and research reported in this doctoral dissertation. The problem statement, rational and significance, global hypotheses and research objectives are stated. At the end of Chapter 1 the organization of the dissertation and individual chapter content is outlined.

1. Introduction

1.1. Background, problem statement and significance

Oxygenic photosynthetic microalgae are a diverse and highly specialized group of eukaryotic microorganisms found in freshwater, brackish and marine habitats with a wide range of pH, nutrient availability and temperatures.^{1,2} Microalgal biotechnology seeks to develop unicellular biofactories for the production of biomass, biofuels, high-value co-products and environmental applications, including bioremediation and wastewater treatment.^{3,4} Theoretically algal oil, triacylglycerols (TAGs), can be mass-produced from sunlight, CO₂, water and nutrients.⁵ Projections of biodiesel derived from microalgae as an alternative to land based crops have rested on a number of claims and assumptions. Firstly, microalgae operate closer than plants to the theoretical maximum efficiency of photosynthesis.^{6,7} Secondly, microalgae can be grown on non-arable land and require less hydrocarbon resources such as fertilizer.^{8,9} Finally, and most importantly, mass culturing of biomass with lipid contents approaching 30-80% is metabolically possible.⁹⁻¹¹ Despite the short sexual cycles present in microalgae, and decades of research, as of yet no strain with demonstrably improved productivities under full sunlight in outdoor scale up conditions has been reported.^{7,8,12}

At the time of writing, the renewed interest by industry, government and academia in commercialization of low-margin commodity biofuels from algae has encountered strong headwinds, including: (1) the continued reporting of low yields of biomass and neutral lipids in peer reviewed literature,^{8,12-14} (2) the high cost of harvesting and dewatering algal biomass at scale;¹⁵ (3) disagreement over life cycle analysis;^{16,17} (4) long time horizons for stable genetic and mutagenic strain development;^{11,18} and (5) the dramatic shock to energy markets from the combined adoption of hydraulic fracturing in North American shale oil/gas production, surplus

of foreign oil, and falling demand. It is then increasingly necessary to use microalgae either as sources of high margin secondary compounds and products^{19–22} or for remediation of wastewaters as a subsidy for commodity feedstock production.^{23,24} Indeed, the Department of Energy’s Aquatic Species Program concluded that the most compelling algal production systems would be one that couples an algae-based wastewater treatment process with a biofuel production system.²⁴ Reviews of the potential of algal biofuel production from wastewater,^{25,26} including bioeconomic scenarios of algae-based production,²⁷ suggest that near and mid-term large-scale production is unfavorable without wastewater treatment as the primary function.

Post-industrial anthropogenic activities have amplified global cycles of the nutrients N and P by 100% and 400% respectively.²⁸ This over-enrichment is implicated in large changes to global biodiversity, species assemblages and ecosystem services.²⁹ Treatment of wastewater by microalgae was proposed early on.³⁰ Substantial literature exists on microalgal cell growth and nutrient removal kinetics in different wastewaters.^{25,26,31–33} Nonetheless, high-density culturing of microalgae in wastewater at scale remains poorly understood at the level of cell culture and cell pathway. Two fundamental assumptions exist for coupling an algae-based wastewater treatment system to a biofuel production process: (1) nutrient removal will fund part of the overall systems’ value; and (2) biomass from wastewater contains sufficient TAG’s to compete with other crop based feed stocks.³⁴

Algal cells in nature oscillate between periods of N and P starvation and re-exposure. Current understanding of nitrogen metabolism in microalgae relies significantly on research using *Arabidopsis* or subjecting *Chlamydomonas* or other unsequenced green microalgae to N-limitation or deprivation. Nutrient depletion in *Chlamydomonas* has been shown to trigger early synthesis of starch followed by significant TAG accumulation,³⁵ the default stress response for

microalgae experiencing N-limitation.³⁶ The breakdown of stored fatty acids (FAs) in turn supports the recovery of cell cultures when conditions improve.^{37–39}

It was hypothesized⁴⁰ using *Chlorella* sp. and then demonstrated using *Neochloris oleoabundans* sp.⁴¹ that consumption of chlorophyll occurred after exhaustion of extracellular N pools, causing decreased light absorption in anticipation of limits to cell division. Turn over of less critical nitrogen rich proteins in favor of those needed for survival, in turn frees up available N to sustain growth and balance lipid biosynthesis until conditions change.^{35,42,43} Highly sophisticated biochemical networks, then, govern the metabolic compartmentalization of C and N in an effort to maintain optimal C/N ratios in fluctuating conditions.⁴³ An active area of research seeks to culture lipid rich microalgae by shunting carbon away from carbohydrate synthesis towards TAG biosynthesis while still maintaining growth.^{44–46}

Nonetheless, overcoming the evolutionary tradeoff between biomass accumulation and lipid biosynthesis, starch and oil,⁴⁷ is a metabolic conundrum that continues to confound mass culturing schemes despite decades of research.^{8,36} In contrast to large industrial projects, algal farm design with verifiable yields are based on agricultural engineering standards and methods, and not on more costly civil or municipal engineering practices.^{14,27,48} Thus, just as in crop improvement⁴⁹ and animal science,⁵⁰ the key to increased yields, decreased costs, and extension of geographic range falls to biological research.²⁷ This includes development of application specific strains through breeding,^{11,51,52} natural selection and experimental evolution,^{53–55} overexpression of phenotypic traits,⁵⁶ insertional mutagenesis,⁵⁷ and pursuit of genetic targets in robust and scalable unsequenced strains.^{58,59}

Determination of culture health and monitoring of productivity relies on measurements of photosynthetic activity, pH, gas exchange and nutrient depletion, and often involves the use of

gravimetric, spectrophotometric and colorimetric analysis, including chlorophyll *a* concentration, optical density (OD) and dry cell mass (DCM). These techniques are limited because eukaryotic microalgae respond rapidly to subtle changes in their environment, be it optimal or sub-optimal.^{1,60,61} At best the physiological state at any given time point can be inferred.

Characterizing the genetic and biochemical mechanisms behind these dynamic metabolic adaptations is required for understanding and manipulating the cellular partitioning and compartmentalization of C and N for increased yields.^{43,47} Recently, experiments using sequenced and unsequenced strains and high-throughput (HT) techniques have attempted to elucidate differential gene expression,^{42,55} protein expression,^{58,59} network level responses to N-starvation and/or recovery,^{39,43,62} and a systems biology^{63,64} understanding of metabolic responses by microalgae to changing environmental conditions.

Regardless of strategy, proteomic analysis is needed to confirm identification and perform relative or absolute quantitation of potential targets because of the importance of post-transcriptional and post-translational modifications in eukaryotic algae and plants.^{65–67} The majority of algal proteomic studies in the literature have used the sequenced freshwater green microalga model organism *Chlamydomonas reinhardtii* with a focus on functional groups and sub-cellular compartments.⁶⁸ The use of mass spectrometry (MS) based proteomics for the identification of critical regulators of genes, proteins, and metabolites as promising targets for genetic and metabolic engineering has intensified in algae, including: time-course comparative transcriptomic/proteomic analyses of the unsequenced *C. vulgaris* sp. under N-deprivation-induced lipid accumulation;^{58,59} profiling of oil bodies in *C. reinhardtii* sp. under N-deprivation to identify proteins involved in lipid metabolism;⁶⁹ proteomic analysis of high CO₂-inducible extracellular proteins in *C. reinhardtii* sp.;⁷⁰ and anaerobic response characterization of *C.*

reinhardtii sp. using quantitative proteomics.⁷¹ Multi-dimensional Protein Identification Technology (MudPIT) is a shotgun proteomics technique that uses a two-dimensional liquid chromatography nano-electrospray ionization tandem mass spectrometry (2D LC–nanoESI–MS/MS) approach to identify thousands of proteins in proteolytically digested complex mixtures.⁷² MudPIT has been used to study the proteomes of yeast⁷³ and *Populus*.⁷⁴

Besides the above mentioned studies concerning network level responses to N-starvation and/or recovery,^{39,43,62} there is an absence in the literature of proteomic studies investigating the response of microalgae to simulated or real wastewater processing. To our knowledge no other study using comparative proteomic analysis of wastewater-cultured microalgae, other than that presented in Chapters 4 and 5,⁷⁵ has been reported in the literature.

Three fundamental problems need to be addressed to use algae for wastewater treatment and biomass production:

- 1) Determine which species of eukaryotic microalgae perform best for nutrient uptake and biomass accumulation.
- 2) Determine how can dynamic cellular adaptations to wastewater processing be characterized to provide biological insight.
- 3) Examine what is the effect on culture performance and yields of scaling up culture size.

This dissertation research examined unsequenced and sequenced species of microalgae in order to characterize growth, and nutrient removal dynamics as a function of macronutrient (N and P) loading. Flask cultures at the bench scale, and photobioreactor (PBR) cultures at the pilot scale, were allowed to proceed to steady state. In the principal experiment, *C. reinhardtii* was

used to develop label-free shotgun proteomic and bioinformatics workflows. Cellular responses to simulated high-density wastewater processing at the 330 mL flask culture volume were examined using differential protein analysis, quantitating relative protein abundance, and performing functional enrichment of metabolic pathways. In contrast to other studies that focused on metabolic responses to either ammonia only^{39,43,62} or nitrate only^{35,41,42,58,59} availability and/or starvation, we used subtle manipulation of nitrate-N ($\text{NO}_3\text{-N}$) and ammonia-N ($\text{NH}_3\text{-N}$) as nitrogen sources. In order to achieve photoautotrophic growth conditions⁶⁷ we did not use acetate in the media.^{35,39,42,43,55,62} In further contrast to other time course proteomic studies,^{39,43} we compared group proteomes cultured in batch mode during stationary phase after allowing for long exposure times to the control and treatment mediums by the transforming organism. Statistically significant differentially expressed proteins were identified by condition, their function and metabolic pathway elucidated, and relative quantitation performed on nitrogen related proteins using normalized spectral counts.

In the first experiment of this doctoral dissertation, a candidate screen of three freshwater and three marine unsequenced microalgae species was performed at bench scale using 165 mL flask cultures in batch mode in order to quantify total phosphorus removal and growth as a function of phosphorus loading. The second principal experiment examined the response of the sequenced *C. reinhardtii* to simulated wastewater containing nitrate and ammonia, and samples were subjected to in-house proteomic and bioinformatics analysis to identify candidate pathways of interest for the development of a robust strain suitable for scalable outdoor wastewater treatment. In the third experiment, a pilot scale PBR system comprised of four 10 L culture volume vertical columns, with metered airflow and gas mixing functions, was used to examine the growth and nutrient removal response of the same strain of *C. reinhardtii*, cultured in

identical control and wastewater treatment mediums, under unsterile conditions with CO₂ supplementation. Results are reported and discussed in the context of metabolic constraints to microalgal mass culturing, and with insights obtained from proteomic results at the flask bench scale.

This dissertation research seeks to integrate shotgun proteomics and functional analysis into fundamental biological research concerning algal physiology and the environmental application of wastewater treatment. The effort and results may inform candidate selection and breeding programs, identification of genetic targets, and provide insights for higher plants. In light of accelerating technical developments in HT LC–MS, it may contribute incremental progress towards the use of algal proteomics as a monitoring and diagnostic tools for bioprocess optimization,⁷⁶ and the study of both monocultures and microbial consortia in industrial and wild settings.⁷⁷ Furthermore, the integration⁷⁸ of RNA sequencing (RNA-seq)^{63,64} and MS-based shotgun proteomics⁷⁹ suggests that in the near term, more cost effective and comprehensive understandings of biological systems, including microalgal bioremediation applications, can be achieved.

1.2. Statement of hypotheses and research objectives

Microalgae differ in uptake of macronutrients and growth within and between species, depending on environmental conditions and perturbation. Identification of top performers is fundamental and onerous. Unlike traditional crop⁴⁹ or animal⁵⁰ breeding through genetic improvement, the development of application specific algal hybrids is limited by current knowledge of the sexual cycle and recombination for many algae,^{11,55} a poor understanding of regulatory control mechanisms for cellular processes,^{36,59} and public concern over outdoor pond cultivation of

genetically engineered strains.⁸⁰ Use of the sequenced model organism *C. reinhardtii* to investigate cellular functions can lead to insights into traits desirable in more robust wild type strains suitable for mass culturing.^{46,59} Leveraging HT techniques such as LC–MS and systems biology to understand culture dynamics and metabolic fluxes in high density microalgal cultures may inform strain selection and improvement, growth and nutrient removal efficiency, and industrial scale up of wastewater treatment or secondary compound production.

The proteome consists of the complete set of proteins of an organism and the field of proteomics includes the census, distribution, dynamics and expression patterns, and interactions of proteins.⁸¹ In order to characterize cellular activity for target identification, candidate screening and bioprocess optimization, determination of which proteins are present, in what location, and in what quantities, is fundamental. It is hypothesized that shotgun proteomics can distinguish between treatment group proteomes, and provide insight into the physiological state of cell cultures responding and adapting to different local environments. As such, proteins associated with different cellular processes, metabolic pathways, and regulatory networks will be significantly differentially abundant, and functional enrichment analysis of these differential proteins may reveal interesting targets for further inquiry. It is hypothesized that microalgae cultured in medium over-enriched in N and/or P, including artificial wastewater containing both nitrate-N and ammonia-N, will show higher rates of nutrient removal and accumulate more biomass at both the flask and PBR scales. It is further hypothesized that scale will affect culture productivity and nutrient removal efficiency.

The global research objectives of each three experiments are:

- 1) Identify dual-purpose candidates that remove nutrients efficiently and grow quickly.

- 2) Elucidate cellular responses and identify potential targets for genetic improvement using shotgun proteomics and a systems biology approach.
- 3) Compare nutrient removal and growth at the bench and pilot scales.

The specific objectives of this doctoral research are as follows:

- 1) Screen unsequenced species of microalgae to identify dual-purpose candidates capable of high rates of P removal and growth.
 - Culture in batch mode three freshwater – *Chlorella* sp., *Monoraphidium minutum* sp., and *Scenedesmus* sp. – and three marine – *Nannochloropsis* sp., *N. limnetica* sp., and *Tetraselmis suecica* sp. – species at the 250 mL flask scale to quantify total phosphorus (TP) removal and growth as a function of P loading.
 - Establish in-house platform and protocols for maintaining stable monocultures and axenic seed cultures of different species of microalgae for current and future research.
- 2) Perform experiments using the sequenced eukaryotic green microalga *C. reinhardtii* to examine the growth and nutrient removal responses to simulated wastewater processing at bench and pilot scales.
 - Culture in batch mode *Chlamydomonas* at the 330 mL flask and 10L PBR culture volumes and quantify growth and nutrient removal responses in two conditions: (1) artificial wastewater containing nitrate and ammonia, and (2) nutrient-sufficient control containing nitrate as the sole form of nitrogen.
 - Modify an existing vertical column PBR system for suitability in culturing suspended microalgae in liquid medium with a bubble column, gas mixing and uniform lighting system for current and future research.

- Generate samples for proteomic analysis.
- 3) Perform shotgun proteomic analysis on 4 biological replicates of *C. reinhardtii* at the flask scale, cultured in conditions described in objective 2.
- Modify and optimize an in-house shotgun proteomics platform to produce high-quality and reproducible HT LC–MS data from eukaryotic green microalgae, including pellet harvesting, protein extraction, in-solution digestion, sample clean up, column packing, and instrument methods for performance of 2D LC–nanoESI–MS/MS using a linear ion trap (LTQ XL) mass spectrometer.
 - Operate a linear ion trap mass analyzer with nano-spray high-performance liquid chromatography (HPLC), including development and troubleshooting of a multi-step MudPIT elution gradient with strong reproducibility for current and future work using green algae and plant samples.
 - Establish in-house mass informatics and bioinformatics workflows for comparative shotgun proteomics to analyze *C. reinhardtii* data sets, including mass informatics and statistical analysis, identification of differentially abundant proteins by condition, functional enrichment, biochemical significance, pathway analysis and metabolic mapping.

1.3. Dissertation organization

This doctorate dissertation in Bioresource Engineering is composed of seven chapters, with tables, figures, references, and appendices. Chapter 1 consists of the introduction with background, problem statement, statement of hypotheses, research objectives and rationale, and dissertation organization. Chapter 2 contains a comprehensive general review of the literature

background pertaining to the subject of this research dissertation. Three distinct manuscripts in chapter form – Chapters 3, 4 and 5, and 6 – contain the experimental research and reported results in fulfillment of research objectives (Section 1.2). Each manuscript chapter contains either the clearly duplicated text of a published paper, the text of a paper published online and currently ‘in press’, or the text of a paper for publication submission, with references, tables and figures. Each manuscript chapter is preceded by a connecting statement with an explanation of rationale, purpose and logical bridge to the overall dissertation. Chapter 3 reports findings from Manuscript I. Chapter 4 reports findings from Manuscript II. Chapter 5 contains the Supplemental findings of Manuscript II, Chapter 4. Chapter 6 reports findings from Manuscript III. Chapter 7 contains a final overall conclusion and summary integration of research findings from the three manuscripts, a statement of originality and significance, and future areas for inquiry. Chapter 8, Section 8.1, References contains all citations of the literature used in this dissertation numbered in order of appearance. Chapter 9, Section 9.1, Appendix A contains the methods for sample preparation, parameters for the mass analyzer and the 2D LC elution gradient used for the shotgun proteomics study reported in Chapters 4 and 5. Chapter 9, Section 9.2, Appendix B contains the publishing agreements with John Wiley & Sons for reproducing Chapter 3 (Manuscript 1), and the publishing agreements with ACS Publications for reproducing Chapters 4 and 5 (Manuscript II) and graphic Figure 2.2 in Chapter 2.

Chapter 2: Literature review

Connecting statement

This chapter provides a comprehensive background review of the literature related to experimental findings reported in this doctoral dissertation. The evolutionary origins of microalgae and the suitability of using the model organism *Chlamydomonas reinhardtii* for studying growth and nutrient removal are summarized. Microalgal biology, metabolism, and the highly conserved functions of photosynthesis, nitrogen metabolism, and their influence on photoautotrophic carbon fixation are reviewed. Microalgal biotechnology applications, constraints to mass culturing, and the necessity of a second application function such as wastewater treatment to subsidize feedstock production are examined. A review of algal proteomics to date and literature related to potential mutagenic targets for enhanced growth and nutrient removal is included. Finally, shotgun proteomics, mass spectrometry, differential protein abundance statistics, functional analysis, and bioinformatics tools for elucidating the eukaryotic microalgal proteome are summarized.

2. Literature review

2.1. Microalgal biology and physiology

The photosynthetic organelle of microalgae and plants (the plastid) traces its origin to a primary endosymbiotic event in which a non-photosynthetic protist engulfed a cyanobacterium, thus enslaving it over time to gene loss and continuing to spread oxygenic photosynthesis to a variety of eukaryotic clades.^{1,2,82} To date approximately 40,000 species have been identified, of which cyanobacteria represent the great majority.² For the purpose of this dissertation and reported findings, microalgae refers to eukaryotic unicellular algae, and not the blue green prokaryotes, or multicellular macroalgae such as kelp.

2.1.1. *Chlamydomonas reinhardtii*

C. reinhardtii is a freshwater green microalga model organism (Figure 2.1) used extensively in academic research and biotechnology.^{67,83} This chlorophyte is well suited for nutrient removal studies due to ease of manipulating growth medium composition,^{60,84} and a highly conserved chloroplast genome⁸⁵ with photosynthetic apparatus and nitrogen assimilation functions that allow biochemical and genetic dissection of metabolic pathways,^{60,86} including comparison to *Arabidopsis thaliana*.⁸⁷ The complete sequenced and assembled nuclear genome⁸⁸ of *C. reinhardtii* has enabled large-scale comparative analysis of its proteome.⁶⁷ All three genomes can be transformed (chloroplast, mitochondrial,⁸⁹ and nuclear), with each one comprising distinct transcriptional, translational, and post-translational properties.^{21,90} Other more robust microalga are often used for research into wastewater treatment and biofuel production, including *Chlorella* sp.,¹⁹ *Neochloris oleoabundans* sp.,⁴⁸ and *Chlorella vulgaris* sp.^{58,59} Sustained open pond production continues to rely primarily on three taxa capable of withstanding the effects of

contamination: *Spirulina platensis*, *Dunaliella salina* and *Chlorella*.^{8,91} A common strategy in academia and industry is to identify and overexpress traits in *C. reinhardtii*,^{53–56} that can be pursued in heartier strains suitable for outdoor scale up production.⁴⁶

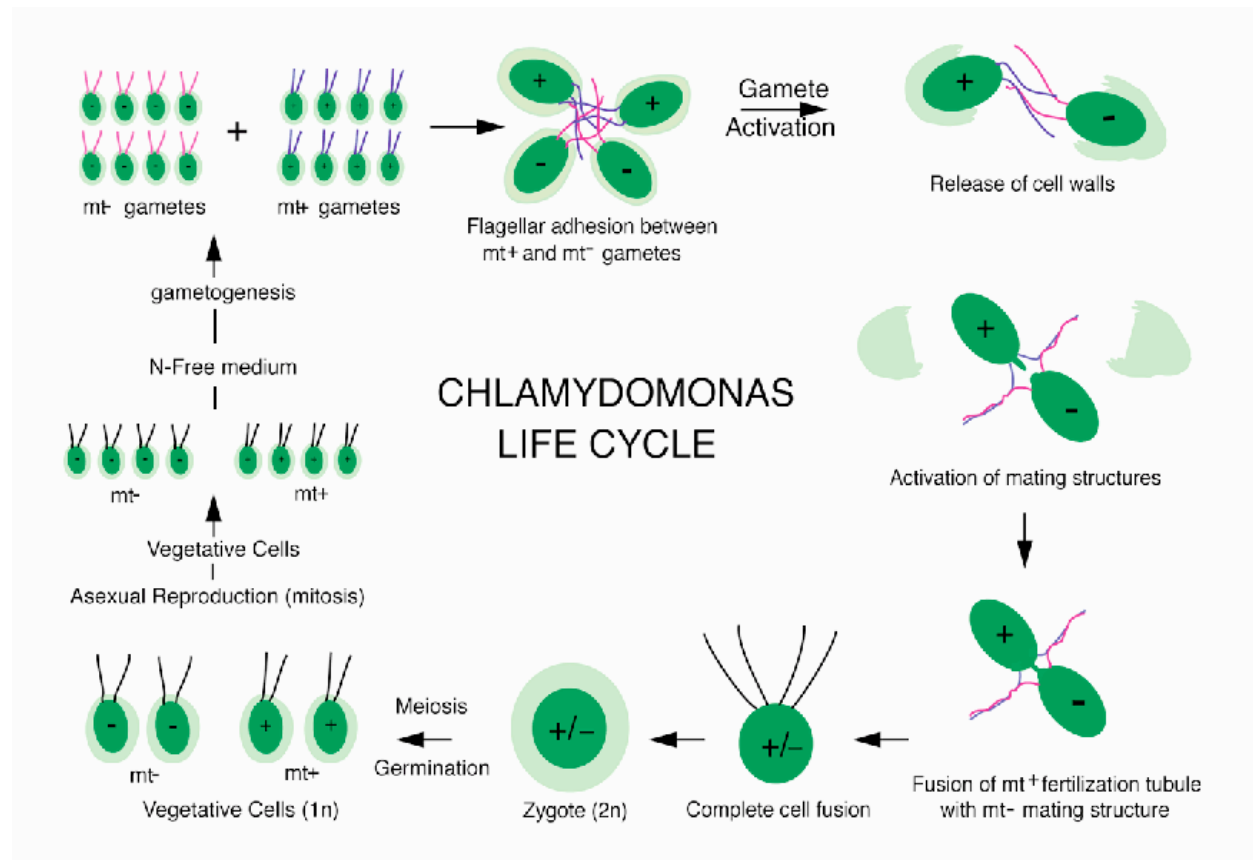


Figure 2.1: Life cycle of *Chlamydomonas reinhardtii*. Credit: Bill Snell, UT Health Science Center at Dallas contributed this figure of the *C. reinhardtii* life cycle to *Chlamydomonas* connection (<http://www.chlamy.org/images/lifecycle.gif>).

2.1.2. Photosynthesis and carbon fixation

Eukaryotic microalgae retain the basic and highly conserved oxygenic photosynthetic apparatus of cyanobacteria located in the chloroplasts.⁸² Photosynthesis refers to the production of photosynthate (ATP and NADPH) by the photosynthetic electron transport (PET) chain, and carbon fixation is the use of photosynthate by the Calvin–Bensen cycle to produce simple organic products.¹ Photosystems II and I (PSII and PSI) operate in series and use light energy to

produce ATP and reducing power (NADPH or NADH) in the light dependent reactions, used in turn by light independent (dark reactions) for carbon fixation (CO_2), primarily in the form of carbohydrates.⁹² The light reaction takes place in the thylakoid, a membrane-bound compartment located in the chloroplast. The proton motive force generated by the light reactions is used by ATP synthase to generate ATP, in a similar way as the mitochondrial respiratory chain. The general equation converting light energy to chemical energy by way of photosynthesis represents a combination of two reactions:



(1) The left hand side represents quantum requirement or energy input, where energy transduction in the two photosystems produces ATP and NADPH via electron transfer due to photon absorption, and (2) the right hand side represents carbohydrate energy content whereby carbon assimilation in the Calvin–Benson cycle using ATP and NADPH produced in the photosystems, fixes CO_2 into chemical energy.⁵ Thus, energy input from 8 mol per mol of CO_2 is reduced to the basic form of chemical energy CH_2O (actual form is triosephosphate ($\text{C}_3\text{H}_5\text{O}_3\text{P}$), representing a consensus median of $482.5 \text{ kJ} \cdot \text{mol}^{-1}$ of carbohydrate energy content, often calculated from glucose ($\text{C}_6\text{H}_{12}\text{O}_6$).⁵

Carbon fixation in oxygenic photosynthesis, then, is primarily driven by linear electron flow (LEF) and reductant generated in photosynthesis. Of importance for wastewater processing, and any biomass production scheme, is that even in non-limited nutrient conditions, LEF coupled ATP/NADPH cannot exceed a stoichiometry of 1.5 required for CO_2 fixation, nor can it generate sufficient ATP/NADPH for the export of glyceraldehyde-3-phosphate (G3P) from the Calvin–Benson cycle.^{61,92} Consequently, photosynthesis is unable to power nitrogen metabolism, gene expression, and biosynthesis of amino acids, lipids, pigments, and proteins simultaneously with

the Calvin–Benson cycle, requiring alternate and competing electron flow pathways in the light reactions to synthesize additional ATP for carbon fixation.^{1,61,93} ATP generation is accomplished without net generation of NADPH to avoid over-reduction of electron carriers,⁶¹ and the cyclic electron flow (CEF) pathway around PSI has been demonstrated in *C. reinhardtii*.⁹⁴

Also of importance to mass culturing is that evolution in low light water columns conferred the ability to produce an overabundance of light pigments in individual microalgal cells competing for photons.^{8,11} Photosynthesis becomes saturated at 30% of total terrestrial solar radiation (solar radiation $\sim 1,700\text{--}2,000\ \mu\text{mol m}^{-2}\ \text{s}^{-1}$) for most strains, and the rate of photosynthesis is directly proportional to light intensity at illumination intensities above the light compensation point up to high intensities that damage photosynthetic receptor systems and cause photoinhibition.⁹⁵ Contrary to claims from carefully controlled low light studies, on balance microalgae are no more efficient at photosynthesis in high light than land plants.^{6,7}

2.1.3. Nitrogen metabolism and assimilation

Nitrogen source, availability and assimilation are critical factors that affect microalgal cellular physiology, growth, and metabolic function.^{40,96–98} Nitrogen assimilation plays a vital role in plant growth and development, where inorganic N is assimilated into N carrying amino acids such as glutamine, glutamate, asparagine, and aspartate in plants and green algae.⁹⁷ Ammonium is the preferred source of fixed N for photosynthetic phytoplankton, requiring less energy than the more abundant nitrate, which first must be reduced to nitrite, and then ammonium in the chloroplasts.⁹⁹ In the absence of biologically available ammonia (NH_3), nitrogen metabolism and assimilation of nitrate (NO_3) necessitates three consecutive reduction steps delimited intracellularly by the plasma and chloroplast membrane barriers: (1) the 2-electron reduction of

nitrate to nitrite (NO_2) catalyzed by nitrate reductase (NR) in the cytosol; (2) the 6-electron reduction of NR produced nitrite to ammonium ions catalyzed by ferredoxin-dependent nitrite reductase (NiR) in the chloroplast stroma using reduced ferredoxin from PSI; and finally (3), the 2-electron reductive transfer of an amido-group from one molecule of glutamine to one molecule of 2-oxoglutarate to form 2 molecules of glutamate.^{98,99} The glutamine synthetase-glutamate synthase pathways then determine the fate of ammonium ions and their incorporation into carbon skeletons essential for amino acids, nucleic acids, and chlorophyll.^{97,100}

The glutamate synthases play a central role in the regulation of N assimilation in photosynthetic eukaryotes.⁹⁷ The glutamate synthases – NADH-dependent and ferredoxin-dependent glutamine oxoglutarate aminotransferase (NADH-GOGAT and Fd-GOGAT) – produce glutamate from glutamine and α -ketoglutarate, using oxidoreductase activity on the CH-NH_2 group of donors with an iron-sulfur protein or NAD^+ as acceptors in the chloroplast stroma. Additional enzymes critical in the biosynthesis of these N carrying amino acids include cytoplasmic and chloroplastic glutamine synthetase (GS), glutamate dehydrogenase (GDH), aspartate aminotransferase (AspAT), and asparagine synthetase (AS).

2.1.4. Phosphorus removal

Phosphorus is an essential ingredient in the conversion of solar energy to biochemical energy by plants and is understood to play a critical role as part of the electron donor mechanism in photosynthesis. Phosphorus is commonly measured as total phosphorus (TP) – the sum of particulate and dissolved fractions of phosphorus – where soluble reactive phosphorus (PO_4^{-3}) is the most available fraction of P for algal uptake, followed by the most labile portion of particulate P which can be rapidly converted to PO_4^{-3} and taken up by cells. Aquatic primary

production is thought to be limited by P, although N-limitation may be higher than previously thought.^{101,102} Meta-analysis found responses of autotrophs to single enrichment of N or P is not as effective in provoking the growth response as N + P enrichment.¹⁰³ Aslan & Kapdan (2006) attributed lower performance of nutrient removal at high P and N concentrations to light limitation, evidenced by high chlorophyll *a* concentrations, and the need to optimize both the N/P ratio and light/dark cycles.³³

2.1.5. Metabolic adaptations to macronutrient limitation

Phytoplankton growth and productivity are determined primarily by light, macro and micronutrients, and temperature. Dramatic shifts in this 'integrated growth environment' caused microalgae to evolve mechanisms that optimize the allocation of photosynthate among cellular processes in order to maximize growth and survival.^{1,61} Reductant generated in photosynthesis has three primary fates – carbon fixation, direct use and ATP generation – and partitioning among the 3 sinks is tied to cellular events in turn determining the relationships between light-harvesting (pigment), photosynthetic electron transport and carbon fixation.¹ This adaptive trait is accomplished in part by the diversity of lipids produced and a capacity to modify lipid metabolism rapidly to suit environmental conditions.^{104,105}

Of the complex lipids found in eukaryotic cells, phospholipids are the most abundant lipid class.¹⁰⁶ Optimal growth conditions in microalgae are associated with the synthesis of fatty acids (FAs) for esterification into glycerol-based membrane lipids which serve a structural role, constitute 5-20% of dry cell mass (DCM) and include medium chain (C10-C14, long chain (C16-C18) and very long chain (C20 species and FA derivatives).³⁶ Under sub-optimal growth conditions microalgae orient the lipid biosynthesis pathways towards production of neutral lipids

(20-50%), primarily triacylglycerols (TAGs), in response to chemical stimuli (salinity, nutrient deprivation and pH) and physical stimuli (temperature and light intensity), where de-novo TAG synthesis acts as an electron sink to prevent damage to membrane lipids and is coordinated with secondary synthesis of carotenoids which sequester in the lipid bodies and act as 'sun-screen' to prevent excess light striking the chloroplasts.^{36,46} TAGs are neutral FAs composed primarily of C14-C18 saturated or monounsaturated fatty acids, and as exceptions very long (>C20) PUFAs.^{36,107}

Reitan *et al.* (1994) examined the effect of nutrient limitation on fatty acid and lipid content in marine microalgae.³⁸ Phosphorus limitation was found to result in a higher relative content of 16:0 and 18:1 fatty acids, and a lower relative content of 18:4n-3, 20:5n-3 and 22:6n-3, suggesting a reduced synthesis of n-3 polyunsaturated fatty acids. Phosphorus deprivation was found to elicit a similar response as N-deprivation in the marine eustigmatophyte *Nannochloropsis* sp., although requiring longer to decrease productivity and halt growth.³⁷ Fatty acid content also increased in this study, and the FAs responsible for the increase were the same as under N-limitation, although synthesis of 18:1n9 was further stimulated. Tellingly, upon resumption of P supply, growth immediately resumed and FA levels resumed initial values and composition within 1 week. Just as in N-sufficient and N-starved cells,³⁶ the main lipid classes in P-sufficient and P-starved cells were polar lipids and sterols, and TAGs, respectively.

Spoehr & Milner (1949) first hypothesized that N-starvation caused *Chlorella pyrenoidosa* sp. to accumulate up to 85% lipids in its biomass and decrease overall levels of chlorophyll.⁴⁰ During N-deficiency, photosynthesis continues, cell division ceases and storage of lipids occurs at the same rate as non N-limited cells, causing dry mass lipid contents to double or triple from normal growth conditions (ie. *Botryococcus braunii* sp. 25–75%, *Nannochloropsis*

sp. 31–68%).¹⁰⁸ Transcript abundance^{35,42} in N-deprived *C. reinhardtii* has been shown to trigger early synthesis of starch, followed by activation of gametogenesis, down-regulation of protein synthesis, and a redirection of metabolism that funnels carbon towards TAG biosynthesis and storage in lipid bodies after prolonged conditions persist.^{36,40} As hypothesized,⁴⁰ the consumption of chlorophyll occurred after exhaustion of extracellular N pools,⁴¹ leading to less light absorption in anticipation of limits to cell division. Turnover of less critical proteins provides carbon/energy for TAG biosynthesis and frees up available N for synthesis of proteins critical in the survival response.^{35,42,43} The breakdown of stored fatty acids (FAs) supports the recovery of cell cultures when conditions improve.^{37–39}

2.1.6. Metabolic tradeoffs between growth and the stress response

Of importance to wastewater processing, and any large-scale biomass/feedstock production scheme, is a fundamental metabolic contradiction between growth through starch synthesis and cell division, and inducement of the stress response for oil accumulation.⁴⁷ Chlorophytes, just like higher plants, utilize starch as their primary carbohydrate store.¹⁰⁹ An active area of research seeks to culture lipid rich microalgae by shunting carbon away from carbohydrate synthesis towards TAG biosynthesis while still maintaining growth.^{44–46} It remains unclear if invoking the default stress response is co-terminal with maintaining optimal growth and cell division in a strain cultured outdoors in high light.^{7,12,47} Cellular metabolism in prokaryotes is governed by sophisticated biochemical networks. In eukaryotic microalgae this complexity is compounded further by the important role of post-transcriptional and post-translational regulation of protein expression and cellular metabolism.^{59,110–112}

Two fundamental assumptions exist for coupling an algae-based wastewater treatment system to a biofuel production process: (1) nutrient removal will fund part of the overall systems' value, and (2) biomass from wastewater contains sufficient TAG's to compete with other crop based feed stocks.³⁴ At present, the metabolic conundrum between growth and lipid biosynthesis means that maximizing biomass growth is deemed a more viable strategy for commodity feedstock production than producing low yields of biomass sufficiently rich in TAGs via N-deprivation.^{8,47} If wastewater processing is to subsidize feedstock production, or remain attractive as a standalone application, then development of fast growing and efficient nutrient removers is fundamental.^{23,24,55}

2.2. Microalgal biotechnology

2.2.1. Biomass, commodities and co-products

Algal biomass is primarily composed of carbohydrates, proteins and lipids. Nutritional composition of the marine eustigmatophyte *Nannochloropsis* sp. cultured in laboratory chemostats found 37.6% (w/w) available carbohydrates, 28.8% crude protein, and 18.4% total lipids, with FA content (% dry mass) at 0.6% of 14:0, 5.0% of 16:0; 4.7% of 16:1 ω 7, 3.8% of 18:1 ω 9, 0.4% of 18:2 ω 6; 0.7% of 20:4 ω 6, and 2.2% of 20:5 ω 3. Minerals in 100 g of dry biomass were as follows: Ca (972 mg), K (533 mg), Na (659 mg), Mg (316 mg), Zn (103 mg), Fe (136 mg), Mn (3.4 mg), Cu (35.0 mg), Ni (0.22 mg), and Co (< 0.1 mg), and negligible toxic heavy metals including Cd and Pb.¹¹³ Commercially valuable co-products include polyunsaturated fatty acids (PUFAs) – including docosahexaenoic acid (DHA), eicosapentaenoic acid (EPA), γ -linolenic acid (GLA) and arachidonic acid (AA) – and carotenoids such as astaxanthin, beta-carotene, lutein and C-phycocyanin (C-PC).¹¹⁴ Other high-value co-products include R-

phycoerythrins for immunofluorescence, industrial enzymes, and the potential development of chloroplast bioreactor platforms for therapeutic protein production.^{4,21,22,115,116} Low margin commodity products from biomass include biofuels, biomass for direct combustion, organic fertilizer, and fish and animal feeds.^{3,18}

Use of algal biomass as a feedstock for renewable liquid biofuels has been proposed for a number of years.^{24,117} Once extracted, algal oil can be chemically reacted via industrial alkali-catalyzed transesterification to yield mono-alkyl esters (biodiesel) and the byproduct glycerin.^{9,36} Weyer *et al.* (2010) based a theoretical calculation of the upper limit of algal oil production using physical laws and assumptions of ideal efficiencies and compared it to a best-case analysis of realistic efficiencies for six global sites using sunlight and outdoor ponds.⁵ This study proposed a theoretical maximum yield of $354,000 \text{ L} \cdot \text{ha}^{-1} \cdot \text{year}^{-1}$ ($38,000 \text{ gal} \cdot \text{ac}^{-1} \cdot \text{year}^{-1}$) and a best-case range of $40,700\text{--}53,200 \text{ L} \cdot \text{ha}^{-1} \cdot \text{year}^{-1}$ ($4,350\text{--}5,700 \text{ gal} \cdot \text{ac}^{-1} \cdot \text{year}^{-1}$) of unrefined oil. Estimates agreed with Department of Energy predictions,²⁴ were less optimistic than Chisti (2007),⁹ and more aggressive than a scale up photobioreactor (PBR) field study in the Mediterranean.³⁷ Reported lipid yields from real world experiments and small-scale research projects in the literature^{13,14,37} continue to fall short by 10 to 20 times projected yields.^{8,91} Industry claims remain difficult to verify due to intellectual property and patents. At the time of this dissertation, no company has yet produced a commercially viable mass scale algae based biofuel production platform.^{7,12,27}

2.2.2. Wastewater treatment

Applications and services using microalgae include CO₂ capture from power plants, bioremediation of metals and hazardous material, and nutrient removal from wastewaters.^{4,26}

Using microalgae for wastewater treatment was first proposed by Oswald *et al.* (1957).³⁰ Cultivation of algal biomass using N and P from animal manure effluent offers an alternative to land application,^{118,119} and could recycle nutrients as part of a larger biofuel production process, resulting in a decrease of anthropogenic effects and lower biomass production costs.^{16,34,120} The Department of Energy's Aquatic Species Program concluded that the most compelling algal production system would be one that couples an algae-based wastewater treatment process with a biofuel production system.²⁴ Reviews of the potential of algal biofuel production from wastewater,^{25,26} including bio-economic scenarios of microalgae-based production,²⁷ suggest near and mid-term large-scale production is unfavorable without wastewater treatment as the primary function.

Substantial literature exists on microalgal cell growth and nutrient removal kinetics in different wastewaters.^{25,26,31-33} Microalgae can efficiently remove N and P from wastewater.^{33,121-125} Phosphorus removal is especially cost effective compared to chemical techniques.¹²⁶ Microalgae have a proven track record in the developing world for wastewater treatment, including low cost high rate algal ponds (HRAP),¹²⁷ and waste stabilization ponds (WSP).¹²⁸ The majority of studies on algal wastewater treatment focus on nutrient removal of N and P at the laboratory scale and pilot-scale, including WSP,³⁰ and only a few recent studies focus on wastewater-grown microalgae as a feedstock for biofuels.¹²⁹⁻¹³¹ Levine *et al.* (2010) batch cultured *N. oleoabundans* sp. in both synthetic media and anaerobic digester effluent and found 90 - 95% of the initial nitrate and ammonium was assimilated after 6 days, with a 10 - 30% fatty acid methyl esters yield on a dry mass basis.⁴⁸ Cellular lipid content was found to be inversely correlated with the N concentration in the growth media, and the proportion of PUFAs (i.e. C16:3, C18:2, and C18:3) decreased with N concentration over time while the proportion of

C18:1 fatty acid increased, suggesting potential for high quality biodiesel from wastewater. A challenge for agricultural wastewater treatment lies in the higher N & P loadings than those found in municipal sewage effluent.³⁴

While treatment of wastewater by continuous cultivation is possible at the small-scale, systems move to saturation over time depending on levels of nutrient concentration and the removal traits of different microalgae strains,¹³² with large implications for biomass yields. The advantage found in semi-continuous culturing is likely due to longer exposure times of wastewater to the transforming microorganisms, versus rapid replacement of effluents before nutrients can be assimilated in continuous cultures, which experience saturation of the system due to the high medium exchange rate.¹³² Lipid profiling as an analytical technique can effectively infer cellular physiology. Nonetheless, the dynamic metabolic adaptations associated with high-density culturing of microalgae in wastewater remains poorly understood at the level of cell culture and metabolic pathways, and the majority of studies focus on N-limitation and manipulating nitrate only or ammonia only for enhanced algal biofuel production.

2.2.3. Biomass production and photo-technology

Huntley and Redalje (2007) provide a thorough history of algae biomass cultivation, from the first photosynthetic microbe (*Chlorella vulgaris* sp.) isolated and grown up in pure culture in 1890 on through to modern day mass culturing techniques.⁹¹ The development of laboratory scale PBRs in the 1940's allowed for precise control of nutrient, light and temperature inputs. Following this came the observation that culture conditions dramatically altered the chemical composition of *Chlorella pyrenoidosa* sp., including protein and lipid content.⁴⁰ The first open ponds were then developed in Germany to investigate food production.

Modern production of commodity feedstock necessitates inexpensive culturing of large quantities of microalgal biomass. Microalgal biomass has been successfully cultured at different volumes ranging from 2.6 to 300 L using tubular and flat panel PBRs.^{13,19,37,133,134} Vertical column PBRs allow optimization of temperature, pH, mixing, media and gas levels, and exposure to light.^{9,134} Additional advantages include high surface to volume ratios, low shear force and wall growth, high CO₂ efficiency and volumetric gas transfer rates, and long stable cultivation periods with minimal interference or competition.^{135,136} Despite advances in engineering, and multiplication of columns, the technology is limited in scale due to dependence of culture volume on column height, where taller columns demonstrate reduced volumetric productivity.¹³⁷ The technology is deemed feasible only for high-value compounds, seed cultures, or laboratory scale experiments, and outdoor ponds continue to offer the lowest cost of production.^{8,19,138} A two-step cultivation process incorporating PBRs and outdoor ponds has been proposed as a strategy for maximizing biomass concentration, followed by N-limitation for enhanced lipid content.³⁷ Despite limitations, laboratory PBRs are very useful to investigate nutrient removal and growth dynamics, screen potential candidates, and produce high quality samples for high-throughput (HT) analysis.

2.2.4. Constraints on yields

In nature microalgae are typically subjected to the following conditions: maximum cell densities of 10^3 cells ml⁻¹, average distance between cells of 1,350 μ m or 250 times cell diameter, spatial displacements of 5×10^{-3} to 3×10^{-5} m s⁻¹, light supply according to daily rhythm with photon flux densities (PFD) within the light limited area, sub optimal nutrient and CO₂ conditions, and stable pH, temperature range and ion concentrations.⁹⁵ In contrast, closed cultivation systems

typically apply cell densities approaching 10^8 cells ml^{-1} , average distance between cells of $60\text{ }\mu\text{m}$ or 10 times cell diameter, spatial displacements in the range of 0.3 to 1.2 m s^{-1} , turbulence-conditioned PFD variations with frequencies of 0.1 – $1,000\text{ s}$ superseding the daytime rhythm, either optimal or enriched nutrient and CO_2 conditions, non-physiological variations in pH and temperature, and near constant mechanical stress on microalgal cells and cell walls.⁹⁵ Furthermore, growth and formation of pigments and products occur at greatly slower rates than reactor dynamics,¹³⁹ where cell density directly affects physiology and metabolic activity due to quorum and product sensing.¹¹

A scale down analysis of tubular systems for microalgae cultivation highlights three critical areas of constraint arising from cell and bioreactor interactions, namely, light attenuation, fluid dynamics and the algal cell metabolism itself.¹³⁹ A major input into PBR systems is the transfer of mechanical energy to the fluid phase in order to enhance gas exchange and prevent sedimentation and/or reactor wall attachment by algal cells.¹⁴⁰ Typically in vertical column reactors fluid flow is accomplished using a bubble column, and ambient or injected CO_2 serves as the carbon source in photoautotrophic culturing. As the carbon is consumed, oxygen is evolved into the culture fluid medium due to photolysis of water.¹⁴¹ In high density cultures, maintaining a high photosynthetic rate requires adjusting the CO_2/O_2 balance such that the carboxylating enzyme RuBisCO supplies CO_2 for the Calvin–Benson cycle, but evolving O_2 does not reach inhibitory concentrations where cells enter photorespiration.⁹⁵ Local turbulences move microalgal cells randomly through good and poorly illuminated elements. As density increases, cells receive heterogeneous intensities of light causing antenna pigments to pick up more light energy than that transferred in the enzymatic step, in turn causing dissipation of energy as fluorescence photons and heat, and resultant declines in biomass and product

yields.^{139,140} Thus, light attenuation due to cell shading is a fundamental constraint for photo-technology and mass culturing of microalgae in pond and PBR alike.

2.3. Summary of microalgal biology and biotechnology

Evolution over millions of years has conferred the ability on microalgae to adapt and proliferate across widely different habitats.¹ Microalgae are characterized by rapid growth with certain species and strains within species capable of doubling times in hours during the exponential growth phase.⁹ Microalgae rapidly respond to growth limiting constraints by dynamically adapting photosynthesis, nitrogen metabolism, carbon fixation and lipid biosynthesis to suit environmental conditions. Under low nutrient conditions that inhibit cell division, microalgae continue photosynthetic carbon fixation, and store the photoassimilates in neutral lipid form as a survival mechanism.^{35,41} Regardless of cultivation system used, metabolic tradeoffs^{8,47} exist between growth through carbon fixation and cellular division under nutrient-sufficient conditions, and the default stress response of hyper-lipid accumulation. Furthermore, dynamic changes in culture conditions occur within a bioreactor environment due to the relatively fast photosynthetic processes of CO₂ uptake and O₂ evolution, and the relatively slow algal metabolic processes of growth and product formation.^{95,139}

Ongoing research into low-cost harvesting, dewatering and extraction of algal biomass and lipids may portend future breakthrough technologies.¹⁵ Advances in photo-technology, including next generation PBR and pond systems will also likely play a role. Nonetheless, despite decades of research the fundamental metabolic conundrum between growth and lipid biosynthesis continues to confound mass culturing yields and prevent lower cost feedstock

production. Mitigating costs of production through high-value compounds is one strategy. Cultivating oleaginous microalgae using wastewaters as a nutrient supply is another.

As in other eukaryotic microorganisms, the basic cell cycle in microalgae evolved signaling networks that involve post-transcriptional and translational modifications as a strategy to respond rapidly to changes in environmental conditions and stressors. Of importance for biomass growth and nutrient removal, and any scale up production of feedstock, is a systems biology understanding of cellular processes. The role of N source and availability has large implications for the distribution of N in the cell, and the shunting of carbon into different metabolic compartments – lipids or starch.⁴³ As such, high throughput (HT) expression data can greatly inform identification and location of cell cycle regulators and potential mutagenic targets.

2.4. Shotgun proteomics and data analysis

The proteome consists of the complete set of proteins of an organism and the field of proteomics includes the census, distribution, dynamics and expression patterns, and interactions of proteins.⁸¹ The terms proteomics and functional proteomics refer to the application of global (proteome-wide or system-wide) experimental approaches to elucidate protein function.¹⁴² At present, two HT analytical techniques are used: DNA microarrays (DNA chips) and mass spectrometry (MS). DNA chips analyze the mRNAs in a cell to discern expression patterns and gene products. Microarrays can compare concentrations of probe oligonucleotides and responses to different experimental treatments. Nonetheless, their precision is low because mRNA levels detected by the array do not quantitatively reflect protein levels because mRNAs are first reverse-transcribed into stable cDNAs for microarray analysis, and yields are not uniform.⁸¹

Mass spectrometry is a physical technique that characterizes protein molecules using the masses of their ions. Tandem MS (MS/MS) fragments peptides to determine their amino acid sequences,^{142,143} and is suitable for complex protein mixtures without isolation.¹⁴⁴ The power of MS-based proteomics resides in the confirmation of protein synthesis in the ribosome using the mRNA copy from the DNA template, the ability to capture post-translational and transcriptional modifications, and suitability for determination of relative abundance or absolute quantitation of protein levels. The following is a summary of algal proteomics studies to date relevant to this dissertation research, a description of shotgun proteomics, mass informatics, differential protein abundance and statistical analysis, functional analysis, and bioinformatics tools useful for extracting biological meaning and insight from HT MS-based proteomic data.

2.4.1. Eukaryotic microalgal proteomics

The majority of microalgal proteomic studies have used *C. reinhardtii* with a focus on functional groups and sub-cellular compartments.⁶⁸ These include the chloroplast 70S ribosome,¹⁴⁵ eyespot,¹⁴⁶ and centrioles.¹⁴⁷ Comparative proteomic studies performed to elucidate metabolic pathways in microalgae are comparatively sparse,¹⁴⁸ and include light induced changes to the proteome,¹⁴⁹ iron deficiency,¹⁵⁰ cadmium exposure,^{151,152} and oxidative stress.¹⁵³

Recently, the effects of decreasing sequencing costs,¹⁵⁴ increased curation and annotation of algae and plant databases,¹⁵⁵ and the adoption of large-scale MS-based proteomic and molecular genetic studies portend new biological insights that may inform higher yields of algal products and services. To that end using MS-based proteomics for the identification of critical regulators of genes, proteins, and metabolites as promising targets for genetic and metabolic engineering has intensified in microalgae: time-course comparative transcriptomic/proteomic analyses of the unsequenced *C. vulgaris* to nitrate-N limitation induced lipid accumulation;^{58,59}

profiling of oil bodies in *C. reinhardtii* under N-deprivation to identify proteins involved in lipid metabolism;⁶⁹ network level responses of *C. reinhardtii* to ammonia-N starvation and/or recovery;^{39,43,62} proteomic analysis of high CO₂-inducible extracellular proteins in *C. reinhardtii*;⁷⁰ and anaerobic response characterization of *C. reinhardtii* using quantitative proteomics.⁷¹

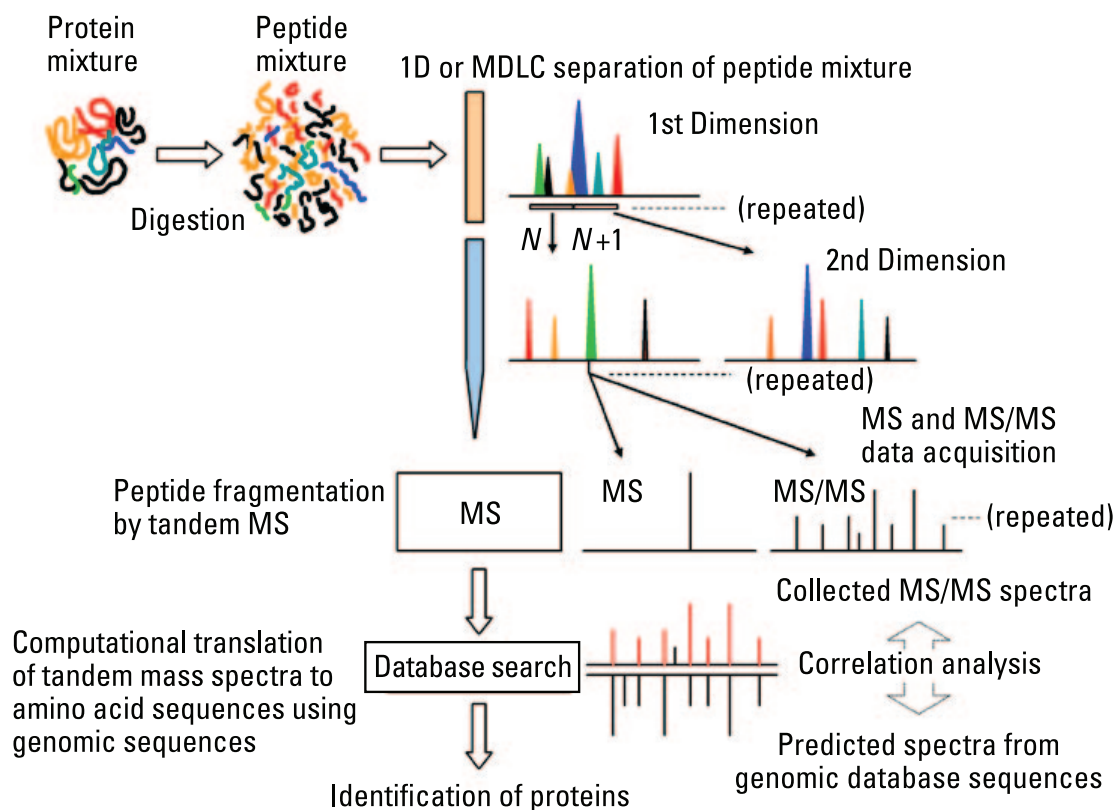


Figure 2.2: Workflow of MudPIT 2D LC-MS/MS shotgun proteomics experiment. Steps include digestion, chromatographic separation, peptide fragmentation and database matching of tandem mass spectra to identify proteins in a complex mixture.¹⁵⁶ (Reprinted with permission from Motoyama, A.; Yates, J. R. Multidimensional LC separations in shotgun proteomics. *Anal. Chem.*, 2008, 80 (19), 7187–7193. Copyright 2008, American Chemical Society.) (Chapter 9, Section 9.2, Appendix B).

2.4.2. Shotgun proteomics

Mass spectrometry is a technique for the generation, separation and detection of charged molecular species in vacuum by magnetic and/or electric fields based on the mass to charge ratio (m/z). It is a powerful analytical tool for absolute molecular specificity. At the ion source,

components of a sample are ionized into charged particles (ions), typically cations by loss of an electron. Scanning by the mass analyzer separates and sorts ions according to m/z values. These separated ions are then measured in the detector and the results plotted. In this way the ion signal is converted into mass spectra. A mass spectrum plots intensity (y-axis) versus m/z (x-axis) and represents the distribution of ions in a given sample by m/z (ie. mass). This provides information on the number of components in a sample, the m/z for each component, abundance information, and by using tandem MS (MS/MS), the sequence information of peptides can be determined.

Shotgun proteomics combines the use of liquid chromatography (LC) for separation of a peptide mixture prior to introduction to the mass spectrometer, and MS detectors for identification (Figure 2.2). It is a large-scale strategy for protein identification in complex mixtures involving pre-digestion of intact proteins, peptide separation, fragmentation using MS/MS, acquisition of mass spectra from resultant peptides, and database searches to identify the proteins found in the original sample.^{73,143,144} The term comes from DNA shotgun sequencing and uses the same analogy of a shotgun's quasi-random firing pattern and dispersion to ensure a target is hit.¹⁵⁷ Separation of peptides by LC is based on the unique physical properties of hydrophobicity and charge, and multi-dimensional LC (MDLC) techniques such as two dimensions (2D) of liquid chromatography (LC/LC), increases the peak capacity and resolving power of separations, improves fractionation of peptides, reduces the complexity of peptide ions entering the MS, and results in decreased ion suppression, and improved ionization efficiency.^{144,158} Multi-dimensional Protein Identification Technology (MudPIT) is a shotgun proteomics technique that uses this 2D LC–MS/MS approach to identify thousands of proteins in proteolytically digested complex mixtures.⁷² It has been used effectively for yeast cells,⁷³ and for protein complexes in yeast and human ribosomes.¹⁵⁹ In plant proteomics the technique was used

in the construction of a detailed proteome atlas for *Populus*, notwithstanding the size and complexity of its genome, dynamic range of protein identification, and abundance of protein variances.⁷⁴

Figure 2.2 summarizes the workflow and informatics for identification of proteins from a complex mixture using 2D LC–MS/MS. In summary, samples (biological or technical replicates) are processed in a single tube proteolytic digest reaction, where cell pellet is lysed, proteins extruded, and then digested. Most large-scale HT MS studies use trypsin to convert the complex mixture of proteins into analyzable peptide populations.¹⁶⁰ Trypsin cleaves the peptide chains at the carboxyl side of the amino acids lysine or arginine, except when either is followed by proline. Peptides are then systematically separated depending on their charge and hydrophobicity in the MDLC phase. Unlike fractionation of proteins using 2D gel electrophoresis (2DGE), where low-throughput separation is performed at the protein level by protein isoelectric point (pI) and molecular weight, the direct analysis of complex protein mixtures using reduction of peptides achieves separation at the peptide level and greatly increases the dynamic range of protein identification.^{156,159} 2D LC–MS/MS uses high-performance liquid chromatography (HPLC) instrumentation to pass the sample in liquid (mobile phase) at high pressure through a column packed with particles (stationary phase). MudPIT separation of peptides using this on-line approach relies on two independent physicochemical properties and uses columns of strong cation exchange (SCX) and reversed phase (RP) material, back-to-back, and contained in fused silica capillaries.¹⁵⁹ During cycles of chromatography, increasing salt concentration serves to "bump" peptides off the SCX, and this is followed by a hydrophobic gradient to progressively elute peptides from the RP into the ion source for identification using MS/MS.^{72,157}

Data-dependent acquisition (DDA) is a mode of data collection that employs tandem MS, and involves multiple steps of MS selection with a fragmentation step between stages (Figure 2.2). Tandem MS involves the selection of ions of a single m/z for transmission to a collision cell for collision-induced dissociation (CID), whereby peptides are fragmented into patterns of specific amino acid sequences.^{159,161} In DDA tandem MS, a fixed number of precursor ions (peptides) whose m/z values were recorded in the initial mass analyzer survey scan (MS1), are selected based on predetermined rules, where the corresponding peak ions are subjected to CID fragmentation in the collision cell, which in turn generates product ions (amino acid sequences) for determination using the second mass analyzer (MS2).^{72,156,162} For example, this dissertation research employs a method using DDA mode where after each MS1 survey scan, the top 5 most intense peak ions are selected for fragmentation, followed by determination of resultant masses of the product ions in the second MS2 scan.⁷⁵

A significant limitation of this electrospray ionization (ESI) approach in biological MS stems from the injection of a dynamic population of peptides into the mass analyzer, of which only a small fraction is then selected for sequencing using MS/MS.¹⁶³ As a result, the sampling and identification of low abundant proteins is limited by a bias towards sequencing of highly abundant proteins.⁷⁴ Data analysis in eukaryotic organisms is further complicated due to the peptide-centric nature of shotgun proteomics, where the same peptide sequence can be present in multiple different proteins or protein isoforms, and shared peptides create ambiguities in sample protein identification.¹⁶⁴

2.4.3. Mass informatics

The masses of peptides are then determined with high accuracy using the tandem MS fragments (Figure 2.2). Interpretation of a CID spectrum of unknown sequence was accomplished by identifying a consecutive series of fragment ions – type-*b* or –*y* ion series or both – whose differences correspond to the residue masses for amino acids.¹⁶¹ The Proteome Discoverer(v1.4)/SEQUEST HT algorithm (v1.3) (Thermo Fisher Scientific, San Jose, CA) converts the character-based amino acid sequences in a protein database to the fragmentation pattern, in turn matching fragment ions in a tandem mass spectrum.^{159,161} When searching peptide fragmentation spectra against the sequence database, potentially matching peptide sequences can be required to conform to tryptic specificity (tryptic peptides), namely, cleavage exclusively C-terminal to arginine or lysine.¹⁶⁰ This process of database matching is dependent on using a sequenced organism and constructing a homemade database using amino acid sequences of known proteins. For example, in this dissertation tandem MS spectra are searched against a polypeptide sequence database of theoretical tryptic peptide sequences comprising the protein complement of *C. reinhardtii* (*Chlre* v 5.3.1 JGI build, released in 2013, containing 19,526 entries, available at: <ftp://ftp.jgi-psf.org/pub/compngen/phytozome/v9.0/Creinhardtii/>), and common laboratory contaminant proteins (human keratin and others).⁷⁵

Once the algorithm correlates the peptide fragmentation spectra with amino acid sequences in the database, DTASelect creates a scoring correlation system for peptide fragment spectra and observed proteins from the genetic database.¹⁴⁴ Identified proteins are then filtered based on Xcorr score or SEQUEST probability scores to filter out false positives, where XCorr measures how close the spectrum fits to the ideal spectrum. Proteome Discoverer filters SEQUEST results for false positives, contaminants, and sorts unique peptides for protein

identification. Protein grouping is enabled, and only rank 1 peptides are counted in the top scored proteins, where each protein identified has at least one unique peptide. This avoids protein redundancy such as isoforms, same sequences, and homologues. Finally, an identical search against the reverse sequence database is performed to allow estimation of global false discovery rate (FDR) using the reverse database method ($\text{false-positive rate} = 2[n_{\text{rev}}/(n_{\text{rev}} + n_{\text{real}})] \times 100$; n_{rev} = the number of peptides identified from the reverse database; n_{real} = the number of peptides identified from the real database).¹⁵⁸

2.4.4. Label-free quantitation and relative abundance

Two general approaches exist for quantitative MS-based proteomics – relative quantitation and absolute quantitation. Relative quantitation relies on stable isotope labeling or label-free methods, whereas absolute measurement of protein abundances involves the use of synthetic peptides as a reference standard or artificial proteins.¹⁶⁵ Technical advances in chromatography (nano-HPLC separation), MS instrumentation (high-resolution, sensitivity and mass-accuracy) and data processing have enabled low cost label-free quantitation.¹⁶⁶ Label-free approaches employ either ion intensity changes from peptide peak areas or heights during LC separation, or make use of spectral counting (counting of peptide spectra) of detected peptides after MS/MS fragmentation.¹⁶⁶ The former is reliant on the reproducibility of sample processing and LC steps that generate peak retention time and m/z values, whereas spectral counting estimates the relative protein abundance using the frequency at which peptides are selected for fragmentation.¹⁶⁶ The number of tandem mass spectra obtained for each protein, the spectral count, was demonstrated to have linear correlation with protein abundance in a mixture for two orders of magnitude.¹⁶⁷ Label-free 2D LC–MS/MS produces semi-quantitative data using spectral counts by summing

the number of MS/MS spectra for a given protein across multiple samples as a surrogate for relative protein abundance. Protein content from two *C. reinhardtii* strains used for biofuel research were compared using iTRAQ labeling and label-free quantitative methods,¹⁶⁶ and results found both methods provided high quality quantitative and qualitative data.

2.4.5. Significance analysis

Shotgun proteomic data is typically highly complex and not normally distributed. A data set often contains thousands of identified proteins with dynamic ranges (ratio of most abundant signal to lowest detectable signal) up to five orders of magnitude in abundance,¹⁶⁸ where variances in high expression proteins tend to be larger than in low abundance proteins. Analysis of which proteins have different relative abundances between two biological states using spectral count data requires normalization and determination of statistical significance. One statistical method for estimating relative protein abundance uses normalized spectral abundance factors (NSAF). In order to account for more peptides/spectra from larger proteins, this method divides the spectral count for each protein by the protein length, and then divides this number by the sum of all length-normalized spectral counts for each run.^{77,169}

Another method, QSpec, is an implementation of a Bayesian approach for the robust differential expression analysis of spectral counts (number of peptides), with direct estimation of directional FDRs for up and down regulation of identified proteins.¹⁷⁰ QSpec is based on hierarchical Bayes estimation of generalized linear mixed effects model (GLMM).¹⁷¹ Spectral counts are considered by QSpec to be random numbers from a large population of proteins, and model parameters are directly shared within replicates and across proteins in a powerful alternative to signal-to-noise ratio types of differential expression test statistics.¹⁷⁰ The QSpec

program normalizes total spectral counts by adjusting data using a Poisson distribution by the total sum sample-by-sample, and normalized length of proteins across all samples, and reports the significance statistic (Z-statistic), computed as the natural log of average fold change (numerator) divided by the variability of the fold changes using standard error (denominator). Fold change is often used to measure change in expression levels of genes from expression data from gene chips.¹⁷² A potential bias of the fold change approach – using fold change ratios to determine changes from initial to final values – lies in failing to detect differentially expressed genes that have large differences in expression, but small ratios.¹⁷³ The log fold change reported by QSpec is not simply the log of the ratios of the treatment versus controls, but is instead derived from the linear model constructed from the spectral counts.¹⁷⁰ Blocking of paired treatment and control samples can also be used to reduce systemic bias and variance from known sources of experimental variation.¹⁷⁴

2.5. Bioinformatics tools and functional analysis

Finding meaningful and legitimate biological insight from genome-scale data necessitates identifying biological functions that are enriched in a set of genes or gene products (proteins) by culture condition. Functional enrichment analysis involves the use of statistics to derive functional annotations – cellular processes, locations, and metabolic pathways – that gene lists are associated with. As such, functional analysis relies heavily on the use of pathway databases (KEGG, MetaCyc, Panther and Reactome), ontology terms (GO, MapMan, KOG), and protein families (Pfam, InterPro).¹⁵⁵ Model organism specific resources such as JGI's Phytozome online databases (*Chlamydomonas* and *Arabidopsis*) compile gene function, annotation and location information for transcript queries. A continuing challenge in plant and algae proteomics is the

complexity of the respective eukaryotic genomes, gaps in annotation databases and tools, and not an insignificant number of proteins with unknown or poorly described functions. Association with a protein family would at the very least indicate functional units present to hypothesize a biological role.⁷⁴ The Pfam database represents a large collection of protein families, where each family is represented by multiple sequence alignments and hidden Markov models (HMMs).¹⁷⁵

2.5.1. Functional enrichment

Enrichment analysis involves assigning biological meaning to a given group of genes. The objective is to identify larger patterns within this group that evidence significant differential expression of characteristics that have biological implications. The web-based annotation integration tool Algal Functional Annotation Tool (AFAT) contains integrated annotation and expression data from pathway, ontology, and protein family databases for *Chlamydomonas reinhardtii* to enable functional interpretation of gene lists and elucidate underlying biological themes *in silico*.¹⁵⁵ Hypergeometric testing by AFTA allows determination of the significance of functional enrichment terms with rank and assignment of a *p*-value, where each enrichment test is considered independent.¹⁵⁵ At present, limiting the enrichment background of identifiers with this *in silico* tool is not possible. Differential proteins must be queried against the entire *Chlamydomonas* genome, with no mechanism for disassociating a gene from a subset of its annotations when performing the enrichment tests. Nonetheless, a given list of proteins with statistically significant differences in relative abundance, using QSpec for example, can be rapidly queried using the AFAT tool to determine enriched functional annotations by condition.

2.5.2. Ontology tools

Ontology tools are useful for generating biological insight from altered levels of protein abundance associated with different metabolic pathways, molecular functions, and cellular localizations.¹⁷⁶ Tatusov *et al.* (1997) developed the functional database Clusters of Orthologous groups of proteins (COG) using the phylogenetic classification of proteins from different sequenced prokaryote genomes.¹⁷⁷ The objective was to leverage the annotation of sequenced genomes into an understanding of genome evolution. The database uses sequence alignments to infer conservation of protein functions, with individual COGs including proteins deemed to be orthologous, although the lineage of genes can be one-to-many or many-to-one. Tatusov *et al.* (2003) developed the functional database Eukaryotic Orthologous Group (KOG) in a similar fashion to COG, and containing the clusters of predicted eukaryotic genome functions for eukaryotes.¹⁷⁸ Eukaryotic KOGs were built using annotated proteins encoded from the *Homo sapiens*, *Drosophila melanogaster*, *Caenorhabditis elegans*, *Arabidopsis thaliana*, *Saccharomyces cerevisiae*, and *Schizosaccharomyces pombe* genomes.

Gene Ontology (GO) provides a controlled vocabulary applicable to eukaryotes based on a knowledge of gene and protein functions from various model organisms.¹⁷⁹ Three categories are contained in GO: biological process, molecular function, and cellular components. Biological process identifies the biological contribution of a gene or gene product. Molecular function defines the biochemical activity of a gene product. Finally, cellular component refers to the intercellular location where a gene product is active. GO terms are linked by nodes connecting parent and child terms and visualization of these multiple paths between terms is possible.¹⁷⁹ At present *Chlamydomonas reinhardtii* has not been added to GO annotations in the GO database. Many gene functions can be inferred using *Arabidopsis thaliana*, especially concerning

photosynthesis and nitrogen metabolism.^{60,86,96} Pattern searches of GO annotation data from *Arabidopsis* (available at: ftp://ftp.arabidopsis.org/home/tair/Ontologies/Gene_Ontology/) can be used to produce GOSLIM files targeting specific processes and functions of interest.

2.5.3. Pathway analysis and metabolic mapping

Biological interpretation and visualization can be achieved by overlaying differential protein abundance data onto metabolic pathways to highlight pathways with altered activities.¹⁷⁶ The Kyoto Encyclopedia of Genes and Genomes (KEGG) is an online resource for functional annotations of genes, including cellular processes and biological functions and pathways. KEGG group (ie., KEGG KO) association is useful for elucidating biological functions, and visualizing KEGG pathway (ie., KEGG ko) terms on metabolic maps. The web-based annotation tool iPath2.0 allows the visualization and analysis of cellular pathways.¹⁸⁰ The primary map provides a summary of the metabolism of a selected organism as annotated to date, where nodes in the map correspond to chemical compounds and map edges represent series of enzymatic reactions.¹⁸⁰ Responsive proteins can be mapped to metabolic map elements by using KEGG KO and/or Enzyme EC numbers in order to elucidate a global pathway-centric overview of specific functional reactions by treatment condition.

In practice, ontology tools and pathway analysis are limited by the degree of database curation. Metabolic maps for many non-model organisms are not experimentally verified and are determined *in silico*. For this reason functional attributes of data sets must be examined manually and verified using resources such as the Joint Genome Institute's (JGI) Phytozome annotation sites (*Chlamydomonas* v9.1 available at: <http://www.phytozome.net/chlamy.php#A>), and the (*Arabidopsis* v9.1 available at:

http://www.phytozome.net/search.php?show=text&method=Org_Athaliana), as well as the *Arabidopsis* TAIR10 site (available at The Arabidopsis Information Resource, <http://www.arabidopsis.org>).

2.6. Summary of shotgun proteomics and data analysis

Microalgae differ in uptake of nutrients and growth between species and within species depending on local environmental conditions. In order to characterize cellular activity for target identification and bioprocess optimization, determination of which proteins are present, in what location, and in what quantities, is fundamental. High throughput MS-based proteomics can provide a snapshot of the proteins present in a biological sample. Extracting biological meaning from HT MS data requires generation of a list of proteins (attributes list) with an abundance ratio relative to a reference condition, and a statistical measurement of the likelihood of an abundance difference. This list of proteins is almost identical to the final results from transcriptome microarrays, but representing protein and not RNA levels, and can be analyzed using many of the same bioinformatics tools.¹⁷⁶

Label-free MudPIT is a shotgun proteomics technique that uses 2D LC–MS/MS. It is a rapid, sensitive technique for comprehensively identifying proteins in complex mixtures that uses MDLC to separate peptides, and then tandem MS to fragment the precursor ions into product ions for sequence determination.¹⁵⁹ Generating legitimate biological insights from LC–MS/MS data requires rigorous data analysis and bioinformatics tools. Firstly, the SEQUEST algorithm relies on translated genomic sequences in a database to infer amino acid sequences from the fragment ions.¹⁵⁹ Secondly, differential analysis¹⁷⁰ determines relative protein abundances, followed by functional enrichment to determine the role of responsive proteins by treatment

condition.¹⁵⁵ Lastly, bioinformatic tools and databases are used to further determine the cellular location, protein function, and biological meaning of differential proteins, and the visualization of enriched cellular pathways using metabolic maps.

Chapter 3: Manuscript I

Microalgae for phosphorus removal and biomass production: A six species screen for dual-purpose organisms.

Anil Patel, Suzelle Barrington and Mark Lefsrud

Received 30 July 2011; revised version received 17 November 2011; accepted for publication 31 December 2011; published 11 February 2012.

Published: *GCB Bioenergy* (2012) 4 (5), pp 485–495, DOI: 10.1111/j.1757-1707.2012.01159.x

(Reprinted with permission from Patel, A.; Barrington, B.; Lefsrud, M. Microalgae for phosphorus removal and biomass production: a six species screen for dual-purpose organisms. *GCB Bioenergy* **2011**, 4 (5), 485-495. Copyright 2012, John Wiley and Sons.) (Chapter 9, Section 9.2, Appendix B).

Connecting statement

Microalgae biofuel production may be feasible when a second function is added, such as wastewater treatment. A fundamental problem for wastewater treatment and biomass production lies in determining which species of eukaryotic microalgae perform best for nutrient removal and biomass accumulation. The global research objective of Experiment 1 was to identify dual-purpose candidates capable of high rates of phosphorus (P) removal and growth. To accomplish this a candidate screen of three freshwater and three marine unsequenced species was performed at the bench scale using 165 mL flask cultures in batch mode in order to quantify total phosphorus removal and growth as a function of phosphorus loading. This required the

establishment of a in-house platform of protocols, techniques and instrumentation for culturing, assaying and maintaining pure monocultures of microalgae for use in this experiment and subsequent research reported in this dissertation.

Microalgae for phosphorus removal and biomass production: A six species screen for dual-purpose organisms

Running title: Dual-purpose microalgae for P removal and biomass

Anil Patel¹, Suzelle Barrington¹ and Mark Lefsrud¹

¹Department of Bioresource Engineering, McGill University, Saints-Anne-de-Bellevue, Quebec H9X 3V9, Canada

Correspondence: Anil Patel, tel. +514 398 8740, fax + 514 398 8387, e-mail: anil.patel@mail.mcgill.ca

Abstract

Microalgae biofuel production can be feasible when a second function is added, such as wastewater treatment. Microalgae differ in uptake of phosphorus (P) and growth, making top performer identification fundamental. The objective of this screen was to identify dual-purpose candidates capable of high rates of P removal and growth. Three freshwater – *Chlorella* sp., *Monoraphidium minutum* sp. and *Scenedesmus* sp. – and three marine – *Nannochloropsis* sp., *N. limnetica* sp., and *Tetraselmis suecica* sp. – species were batch cultured in 250 mL flasks over 16 days to quantify total phosphorus (TP) removal and growth as a function of P loads (control, and 5, 10, and 15 mg L⁻¹ enrichment of control). Experimental design used 100 µmol m⁻² s⁻¹ of light, a light/dark cycle of 14/10 hours, and no CO₂ enrichment. Phosphorus uptake was dependent on species, duration of exposure, and treatment, with significant interaction effects. Growth was dependent on species and treatment. Not all species showed increased P removal with increasing P addition, and no species demonstrated higher growth. *Nannochloropsis* sp. and *N. limnetica* sp. performed poorly across all treatments. Two dual-purpose candidates were identified. At the 10 mg L⁻¹ treatment *Monoraphidium minutum* sp. removed 67.1 % (6.66 mg L⁻¹ ± 0.60 SE) of TP at day 8, 79.3 % (7.86 mg L⁻¹ ± 0.28 SE) at day 16, and biomass accumulation of 0.63 g L⁻¹ ± 0.06

SE at day 16. At the same treatment *Tetraselmis suecica* sp. removed 79.4 % ($6.98 \text{ mg L}^{-1} \pm 0.24$ SE) TP at day 8, 83.0 % ($7.30 \text{ mg L}^{-1} \pm 0.60$ SE) at day 16, and biomass of $0.55 \text{ g L}^{-1} \pm 0.02$ SE at day 16. These species merit further study using high-density wastewater cultures and lipid profiling to assess suitability for a nutrient removal and biomass/biofuel production scheme.

Keywords: *Biodiesel, Biofuel, Biomass production, Microalgae, Phosphorus, Wastewater*

3.1. Introduction

Using algal biomass as a feedstock for renewable liquid biofuels was first proposed by Oswald *et al.* (1957).³⁰ Global change, food and energy security,¹⁸¹ nutrient additions to watersheds,²⁸ and significant investments by government and the private sector are all factors driving renewed interest in biofuels. Small-scale studies and theoretical reviews have concluded that biofuel production from algae is both sustainable and economically viable.^{5,9,91} Disagreement exists over the carbon footprint of algae as a biofuel feedstock according to life cycle analysis (LCA),^{16,182,183} and photosynthetic productivity of algae versus land plants.^{7,184,185} Recent LCA of algae methane also highlights opportunities and drawbacks for nutrient recycling.¹⁸⁶ The main drawback of heterotrophic cultivation of microalgae is that it ultimately relies on photosynthetic crop production for an organic carbon source.⁹ In the case of combustion of microalgae biomass, it is unclear how biogas can compete with the current boom in shale gas drilling, supply, and overall price deflation seen in North American natural gas markets.

Despite decades of research and aggressive production goals cited by industry such as Sapphire Energy Inc. (San Diego, CA) and Solazyme Inc. (South San Francisco, CA), the continued low lipid production yields reported from real world experiments suggest that this

technology is not mature or commercially viable due to high cost of producing and processing algal biomass.⁸ While recent advances in the field of synthetic biology hold out promise,¹⁸⁷ the complexity of the microalgal metabolism and long time horizons for genetic engineering (GE) or transcription factor engineering (TFE) necessitates following other strategies for commercialization of algal oil.¹⁸ One strategy for narrowing the feasibility gap for large-scale commercialization is to use a dual-purpose organism suitable for feedstock production and bio-remediation. The Department of Energy's Aquatic Species Program concluded that the most compelling algal production systems would be one that couples an algae-based wastewater treatment process with a biofuel production system.²⁴ Post-industrial anthropogenic activities have amplified global cycles of N and P by 100% and 400%, respectively.²⁸ This over-enrichment is implicated in large changes to global biodiversity, species assemblages and ecosystem services.²⁹ A strong correlation exists between P loads and algal growth in Quebec lakes.¹⁸⁸ An increasing trend in frequency and number of algal blooms is associated with rising P levels in soils surrounding the St. Lawrence due to proximity to high-density animal production centers, cash cropping, septic systems, municipal wastewater and non-point source P additions.¹⁸⁹ Cultivation of microalgae using nutrients from manure effluent is an alternative to land application, and biomass could be used as a slow release fertilizer and low-grade animal feed.¹¹⁸

Microalgae have a proven track record in small-scale nutrient removal studies and pilot scale high rate algal ponds (HRAP) and waste stabilization ponds (WSP) in the developing world, and are an attractive means of low cost wastewater treatment.^{126,190} Studies showed the efficacy of removing N, P, and toxic metals from wastewater, where phosphorus removal is especially compelling and cost effective when compared to chemical techniques.^{26,122,191}

Common microalgae cultures for nutrient removal include the freshwater species *Chlorella* sp.,¹⁹² and *Scenedesmus* sp.^{123,193} The marine species *Nannochloris* sp. was reported to have relatively high nutrient uptake rates¹⁹⁴ and the marine eustigmatophyte *Nannochloropsis* sp. high lipid productivity.³⁷

The present experiment was designed to identify robust species of microalgae displaying the dual-purpose traits of high biomass growth and high assimilation of P suitable for a commercial strategy of wastewater treatment and biomass production. The laboratory setup tested three freshwater – *Chlorella* sp., *Monoraphidium minutum* sp. and *Scenedesmus* sp. – and three marine species – *Nannochloropsis* sp., *N. limnetica* sp., and *Tetraselmis suecica* sp. The experiment quantified the effects of P addition perturbation, besides monitoring biomass growth and P uptake for four levels of P exposure (control, and 5, 10 and 15 mg L⁻¹ enrichment of control). Total P as phosphate at treatment loadings of 5 – 15 mg L⁻¹ in this experiment are an order of magnitude larger than that found in nature (3-34 µg L⁻¹),¹⁸⁸ significantly higher than those reported in HRAP (1.19 – 1.82 mg L⁻¹),¹²⁷ and within the range of reported values for WSP.¹²⁸

The experimental approach included a more true reproduction of natural or industrial facility conditions in the attempt to avoid fine manipulation of cultures to boost observed or projected nutrient removal and biomass yields, a charge often leveled at academic and startup company groups.⁸ Firstly, with the exception of phosphorus enrichment, uniform temperature, and axenic lines, this screen did not use: (1) continuous high light, (2) CO₂ enrichment, or (3) media buffer and constant pH. Secondly, nitrogen was not added in excess to restore balance in the high phosphorus treatments. Thirdly, maximizing and measuring percent lipid content was deemed a less important strategy than maximizing biomass growth and nutrient uptake, due to

the evolutionary tradeoff between biomass growth and lipid biosynthesis, the default pathway for microalgae under environmental stress.³⁶

3.2. Materials and methods

3.2.1 Experimental organisms

The six microalgal strains used in this study are listed in Table 3.1 along with their origin. The experimental organisms were comprised of freshwater and marine eukaryotic phytoplankton from the chorophyta and heterokontophyta taxa. The freshwater green algae *Chlorella* sp. and *Scenedesmus* sp. (Fussmann Lab, McGill University) were chosen because of their use in numerous nutrient removal studies, and *Monoraphidium minutum* sp. (SAG 243-1) because of its lack of appearance in the bioremediation and biofuel literature. The marine green algae *Tetraselmis suecica* sp. (CCMP 906) was chosen for its large size (8-15 μm), potential ease in harvesting, and reported high biomass and lipid productivity.³⁷ The two eustigmatophytes, *Nannochloropsis* sp. (CCMP 531) and *N. limnetica* sp. (CCMP 505) were selected because of reported high biomass and lipid productivity of *Nannochloropsis* sp.,³⁷ and recent interest by microalgal researchers in using picoplankton (2-4 μm) as model organisms. All three marine species were included because of the relatively high salt content of agricultural wastewaters, and very few studies in the literature have used marine species of microalgae for nutrient removal from wastewater.

Table 3.1. Algal group and culture origin of the six strains tested in screening

Algal group	Strain	Culture collection	Freshwater/marine
Freshwater			
Green Algae	<i>Chlorella</i> sp.	Fussmann Lab, McGill University, Canada	Freshwater
	<i>Monoraphidium</i> sp. SAG 243-1	Sammlung von Algenkulturen (SAG), Germany	Freshwater
	<i>Scenedesmus</i> sp.	Fussmann Lab, McGill University, Canada	Freshwater
Marine			
Eustigmatophytes	<i>Nannochloropsis</i> sp. CCMP 531	Provasoli-Guillard NCMA, USA	Marine
	<i>N. limnetica</i> sp. CCMP 505	Provasoli-Guillard NCMA, USA	Marine
Green Algae	<i>Tetraselmis suecica</i> sp. CCMP 906	Provasoli-Guillard NCMA, USA	Marine

3.2.2 Methods

The experimental design consisted of 6 species (3 freshwater, 3 marine) cultured for approximately 16 days, with 4 treatment levels (control and 5, 10, and 15 mg L⁻¹ enrichment of nutrient-sufficient control), replicated 3 times, where each flask was considered a biological replicate ($n = 6 \times 4 \times 3 = 72$). It was determined through trials that each species should be cultivated in a single batch of 4 treatments with 3 biological replicates ($n = 12$) because the marine picoplankton (*Nannochloropsis* sp. and *N. limnetica* sp.) demonstrated an ability to spread through air and confound axenic techniques. Slots on a shaker platform were randomly assigned and reassigned after each sampling to prevent bias and account for any variance in lighting.

For each species, 15 mL of axenic culture in exponential phase with dry cell mass (DCM) density of $0.045 \text{ mg L}^{-1} \pm 0.006 \text{ SE}$ was inoculated into 150 mL of sterile medium in 250 mL flasks stoppered with autoclavable foam. Growth media included COMBO¹⁹⁵ for freshwater algae containing the following molar concentrations in final medium of major stock chemicals: NaNO₃ ($1.00 \times 10^{-3} \text{ M}$), KH₂PO₄ ($1.00 \times 10^{-4} \text{ M}$), Na₂SiO₃·9H₂O ($1.00 \times 10^{-4} \text{ M}$), CaCl₂·2H₂O ($2.50 \times 10^{-4} \text{ M}$), MgSO₄·7H₂O ($1.50 \times 10^{-4} \text{ M}$), NaHCO₃ ($1.50 \times 10^{-4} \text{ M}$), H₃BO₃ ($2.5 \times 10^{-4} \text{ M}$), and KCl ($1.00 \times 10^{-4} \text{ M}$). For the marine species, f/2 medium¹⁹⁶ was prepared using filtered natural seawater (Provasoli-Guillard National Center for Marine Algae and Microbiota, West Boothbay

Harbor, ME) containing the following final concentrations: NaNO_3 (8.82×10^{-4} M), $\text{NaH}_2\text{PO}_4 \cdot \text{H}_2\text{O}$ (3.62×10^{-5} M), and $\text{Na}_2\text{SiO}_3 \cdot 9\text{H}_2\text{O}$ (1.06×10^{-4} M). Algae were cultivated in nutrient-replete medium with 1.55 mg L^{-1} of P as K_2HPO_4 (freshwater control) or 1.12 mg L^{-1} of P as $\text{NaH}_2\text{PO}_4 \cdot \text{H}_2\text{O}$ (marine control), or enrichment of control using treatments of an additional 5, 10 or 15 mg L^{-1} of P as KH_2HPO_4 .

The culture flasks were incubated in laboratory conditions with an air space of ambient CO_2 at 450 ppm, air temperature of 25 ± 2 °C, and initial pH at 8.0 - 8.2 (marine) and 7.0 – 7.2 (freshwater). Three banks of cool white portable fluorescent lights set on a timer provided an average photosynthetically active radiation of $100.4 \mu\text{mol m}^{-2} \text{ s}^{-1} \pm 2.0$ SE of light³⁷ on a light/dark regimen of 14/10 hours to simulate day and night.¹²⁸ A quantum meter (OMSS-ELEC, Apogee Instruments, Logan, UT) was used to measure irradiance and ensure all flasks received the same average irradiance. A continuous shaker platform (Forma 420, Thermo Fisher Scientific, San Jose, CA) was set at rotation speed 100 rpm in order to keep all 6 species of different cell diameters well mixed.

Optical density (OD) was assayed 16 times, at time initial and approximately every 24 hours, for each biological replicate. For a growth sample assay, 1 mL of culture was removed from each experimental flask on a clean bench and growth was followed using OD at 750 nm (OD_{750})³⁷ with a Novapac II spectrophotometer (Pharmacia Biotech, Piscataway, NJ) and zero calibration before each sampling. Technical replicates were not performed due to the trials showing reliability of OD_{750} as a proxy for following biomass growth, the limited culture volume of 165 mL, and determination of final biomass gravimetrically using DCM. Total phosphorus was assayed 5 times, at time initial and approximately every 4 days, at the same time as the OD_{750} assay was taken. For a TP assay an additional 1 mL was taken from each experimental

flask and combined with the 1 mL from the OD₇₅₀ assay for a total of 2 mL. Samples were centrifuged, the supernatant removed, diluted, and divided into 3 technical replicate samples for analysis of TP. This method was chosen to better account for variance seen in trials using the Hach instrument and method described below.

3.2.3 Analytical procedures

Phosphorus is commonly measured as total phosphorus (TP) – the sum of particulate and dissolved fractions of phosphorus – where soluble reactive phosphorus (orthophosphate PO₄-P) is the most available fraction of P for algal uptake, followed by the most labile portion of particulate P which can be rapidly converted to PO₄⁻³ and taken up by cells. Total phosphorus in solution, and not biomass, was measured in this study using a Hach DR 2800 spectrophotometer (Hach Company, Loveland, CO, USA) and Hach reagent pillows according to Method 8190 (Standard Methods 4500 P-E) and similar to Wetzel & Likens, (2000).¹⁹⁷ The persulfate acid digestion step used to convert organic P bound in microalgae cells to orthophosphate was omitted because biomass pellet was removed from supernatant by centrifugation, and the phosphate in the supernatant was soluble. Orthophosphate in biomass free solution reacts with molybdate under acidic conditions to produce a mixed phosphate/molybdate complex. Ascorbic acid reduces the complex to produce an intense blue color. Test results were measured at 880 nm and compared to a standard curve to determine TP in solution.

Total biomass concentration (g L⁻¹) and biomass productivity (g L⁻¹ day⁻¹) was measured using triplicate 10 mL assays from monoculture inoculum and experimental cultures at the end of the experiment. Samples were centrifuged (IEC MUHIRF, Thermo Fisher Scientific, San Jose, CA) at 10,000 rpm for 15 minutes to separate pellet from supernatant, where the picoplankton

species determined this speed and duration. All pellets were washed, re-suspended with distilled water and centrifuged three times to remove minerals and salts. Dewatering was accomplished by freeze drying (Gamma 1-16 LSC, Martin Christ, MBI, Kirkland, QC) for 24 hours followed by DCM determination from the difference between cell masses at the start and end of the experiment, and divided by the time in days to determine biomass productivity.

3.2.4. Statistical analysis

Statistical analysis was performed using SPSS statistical package (version 19; IBM inc., Chicago, IL). Regression and a 3-way ANOVA using species, treatment and time was used for phosphorus removal, and regression and a 2-way ANOVA using species and treatment was used for determination of final biomass concentration from dry cell mass. Statistical analysis was not performed on OD data, given the differences in cell sizes and masses in Daltons. Post hoc multiple comparison was performed using Tukey's HSD (Honestly Significant Difference) and all variables were reported as significant at 95% confidence ($p\text{-value} \leq 0.05$) using standard error (SE).

3.3. Results

3.3.1. Phosphorus removal

Figure 3.1 shows P removal (mg L^{-1}) over 16 days for the six species screened. Curve fits for all species showed exponential uptake of TP from solution. The phosphorus uptake by microalgae biomass was found to be dependent on species, duration of exposure in days, and treatment, where interaction effects among all three factors were significant ($F = 7.17$; $R^2 = 0.97$). Figure

3.2a and 3.2b show P removal efficiency (%) and total phosphorus (TP) removed (mg L^{-1}) by species and treatment at day 8.

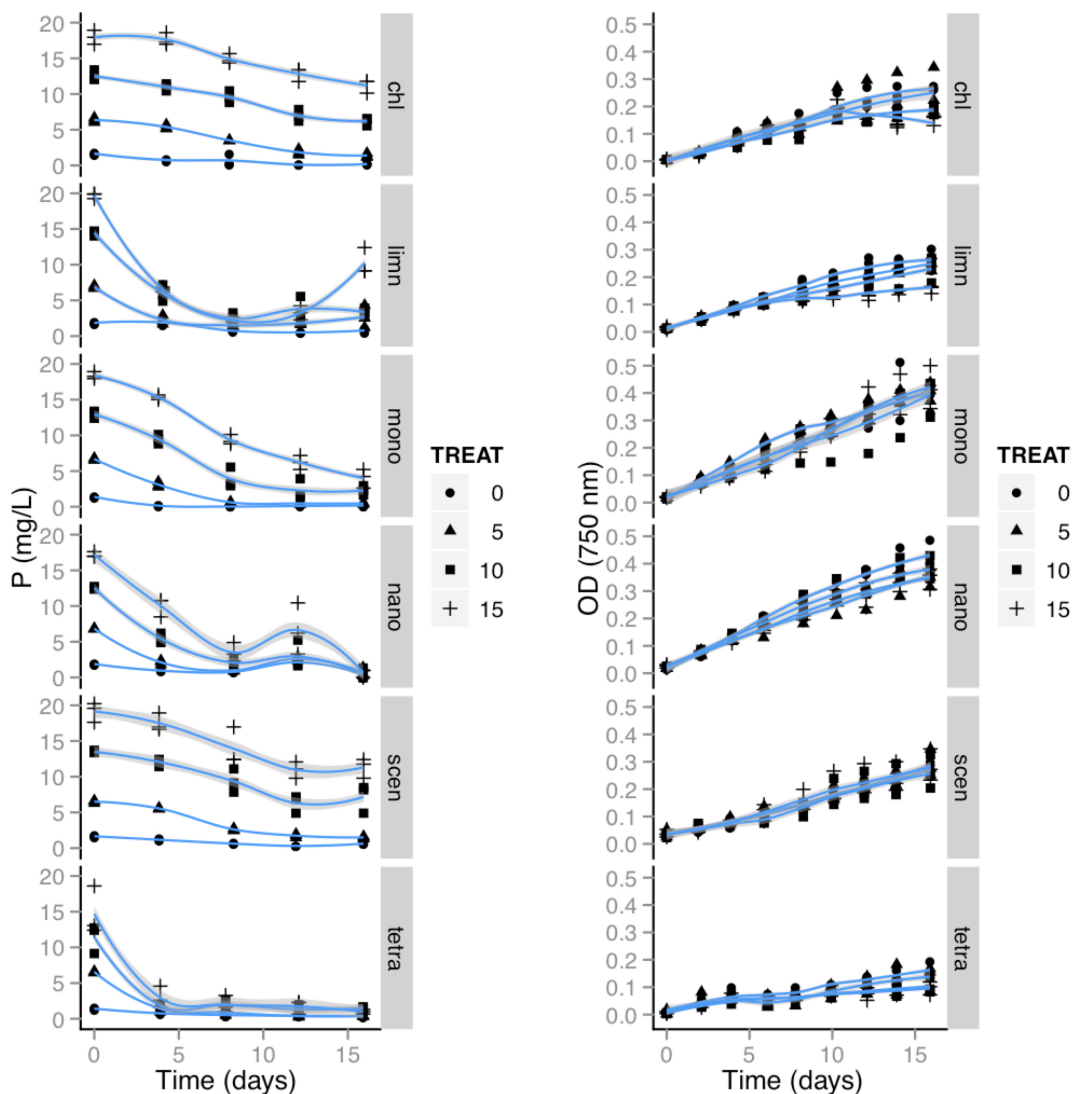
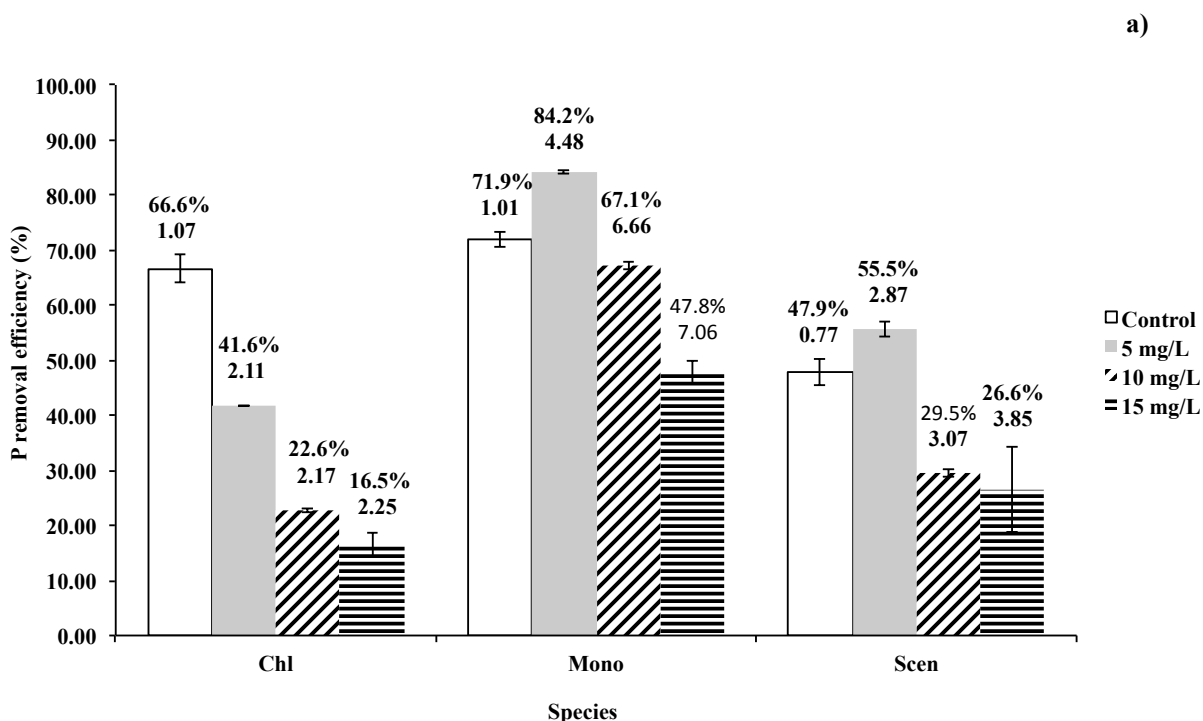


Figure 3.1: Total phosphorus (mg L^{-1}) and biomass growth (OD_{750}) for six species over 16 days. Bands show 95% point wise confidence intervals with standard error for triplicate biological replicates ($n = 3$). Treatments represent nutrient-sufficient control (0), and 5 mg L^{-1} P (5), 10 mg L^{-1} P (10), and 15 mg L^{-1} P (15) enrichment of control. Abbreviation of algal species: Chl., *Chlorella* sp., Limn., *Nannochloropsis limnetica* sp., Mono., *Monoraphidium* sp., Nano., *Nannochloropsis* sp., Scen., *Scenedesmus* sp., Tetra., *Tetraselmis suecica* sp. Due to larger cell diameter, *Tetraselmis suecica* sp. showed a lower OD_{750} and higher final biomass as measured by DCM (g L^{-1}).

The most efficient P removers at day 8 (Figure 3.2a,b) and day 16 (not shown) were the three marine species and the freshwater species *Monoraphidium* sp. All three marine species showed

higher rates of P removal with the increasing additions of P at the 5, 10 and 15 mg L⁻¹ treatments, however the two eustigmatophytes, *Nannochloropsis* sp. and *N. limnetica* sp., released P back into solution after day 12 (Figure 3.1) and were also poor biomass accumulators (discussed below). The freshwater species *Monoraphidium* sp. and *Scenedesmus* sp. showed higher removal rates for the 5 mg L⁻¹ treatment and a decrease in P uptake at the higher loadings of 10 and 15 mg L⁻¹ (Figure 3.2a). *Chlorella* sp. showed a dramatic decrease in P uptake for all treatments compared to control.



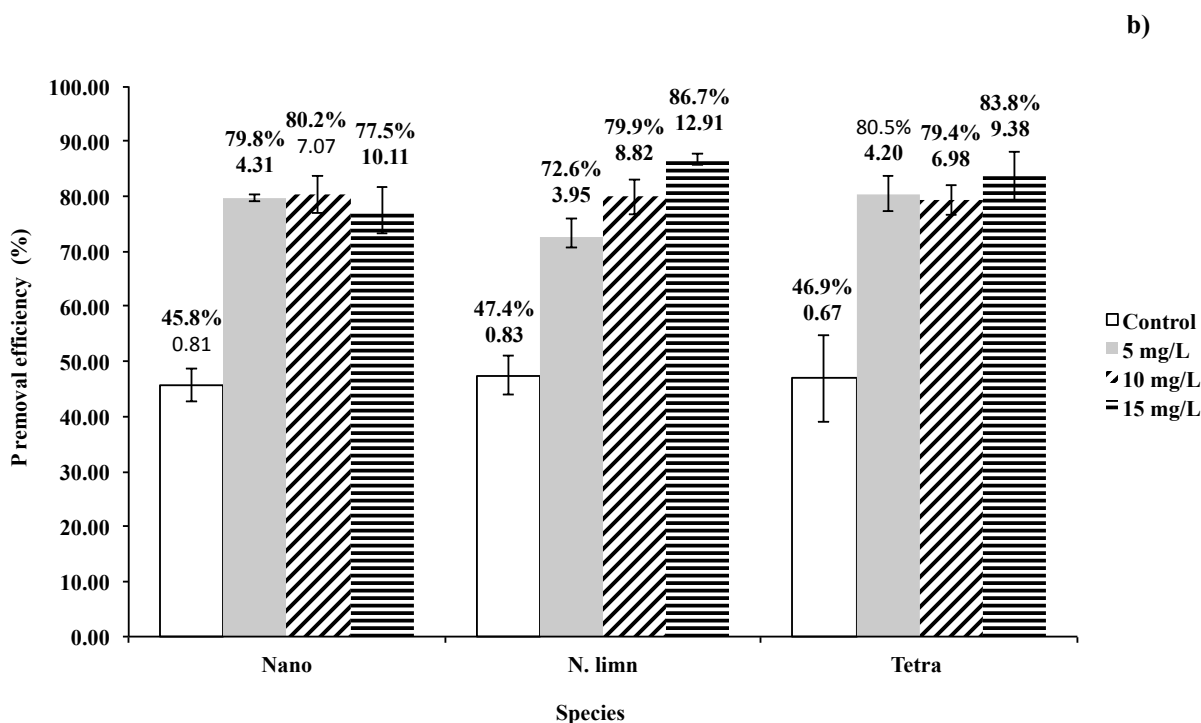


Figure 3.2: Phosphorus removal efficiency (%) and total phosphorus (TP) removed (mg L⁻¹) in superscript by species and treatment at day 8. Phosphorus removal efficiency (%) is calculated using initial and final TP concentration according to: $E_i = (C_o - C_i)/C_o \times 100 = \% \text{ TP}$. Treatments represent nutrient-sufficient control (0), and 5 mg L⁻¹ P (5), 10 mg L⁻¹ P (10), and 15 mg L⁻¹ P (15) enrichment of control. Abbreviation of algal species: Chl., *Chlorella* sp., Mono., *Monoraphidium minutum* sp., Scen., *Scenedesmus* sp., Nano., *Nannochloropsis* sp., N. limn., *Nannochloropsis limnetica* sp., Tetra., *Tetraselmis suecica* sp. Confidence intervals are shown using standard error of the mean with triplicate biological replicates ($n = 3$).

Phosphorus removal results show the two best microalgae candidates to be the freshwater green *Monoraphidium* sp. and the marine green *Tetraselmis suecica* sp. Curve fits for *Monoraphidium* sp. showed exponential uptake of P in all loadings: control, 5, 10, and 15 mg L⁻¹ ($R^2 = 0.45, 0.85, 0.93$, and 0.99 , respectively). The maximum TP removed by *Monoraphidium minutum* sp. for the 10 mg L⁻¹ treatment was 67.1 % ($6.66 \text{ mg L}^{-1} \pm 0.60 \text{ SE}$) at day 8 (Figure 3.2a), and 79.3 % ($7.86 \text{ mg L}^{-1} \pm 0.28 \text{ SE}$) at day 16. Curve fits for *Tetraselmis suecica* sp. showed exponential uptake of P for all loadings: control, 5, 10, and 15 mg L⁻¹ ($R^2 = 0.86, 0.82, 0.60$, and 0.80 , respectively). The maximum TP removal by *Tetraselmis suecica* sp. for the

treatment 10 mg L⁻¹ was 79.4 % (6.98 mg L⁻¹ ± 0.24 SE) at day 8 (Figure 3.2b), and 83.0 % (7.30 mg L⁻¹ ± 0.60 SE) at day 16.

3.3.2. Biomass accumulation

Figure 3.1 shows biomass growth as followed by OD₇₅₀ over 16 days. Curve fits for all species showed linear biomass growth. Species and treatment were found to have a significant effect on final biomass with no significant interaction effects ($F = 1.71$; $p = 0.08$, $R^2 = 0.90$). Figure 3.3a and 3.3b show final biomass (g L⁻¹), and biomass productivity (g L⁻¹ day⁻¹) by species and treatment at day 16.

Post hoc comparison for mean biomass by species showed that the green algae species *Monoraphidium* sp, *Scenedesmus* sp, and *Tetraselmis suecica* sp. produced the highest final biomass, while not significantly different from each other, and accumulated significantly more biomass than *Chlorella* sp. and the two eustigmatophytes, *Nannochloropsis* sp. and *N. limnetica* sp. These two species of picoplankton showed dramatically lower biomass accumulation than the other species. Post hoc comparison of mean biomass by treatment for all species showed no difference between control and 5 mg L⁻¹ enrichment, but a difference between control and the 10 and 15 mg L⁻¹ treatments. Post hoc comparison of mean biomass by treatment within species showed a significant difference between control and 15 mg L⁻¹ treatments only for *Chlorella* sp., and no significant difference between treatments except control for *N. limnetica* sp. (Figure 3.3a,b). Error bars for *Nannochloropsis* sp. suggest high within group variance prevented detection of significant differences between P loadings. No significant decrease in yield was found within any other species by treatment, including 10 and 15 mg L⁻¹ loadings of P.

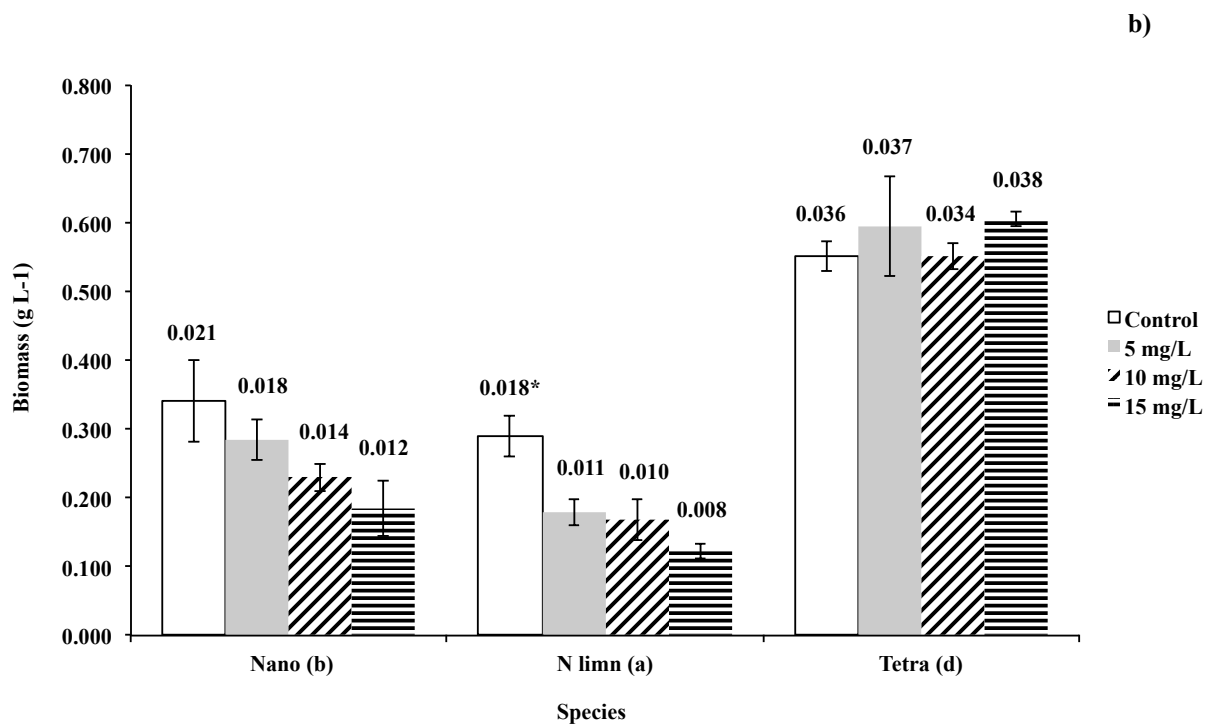
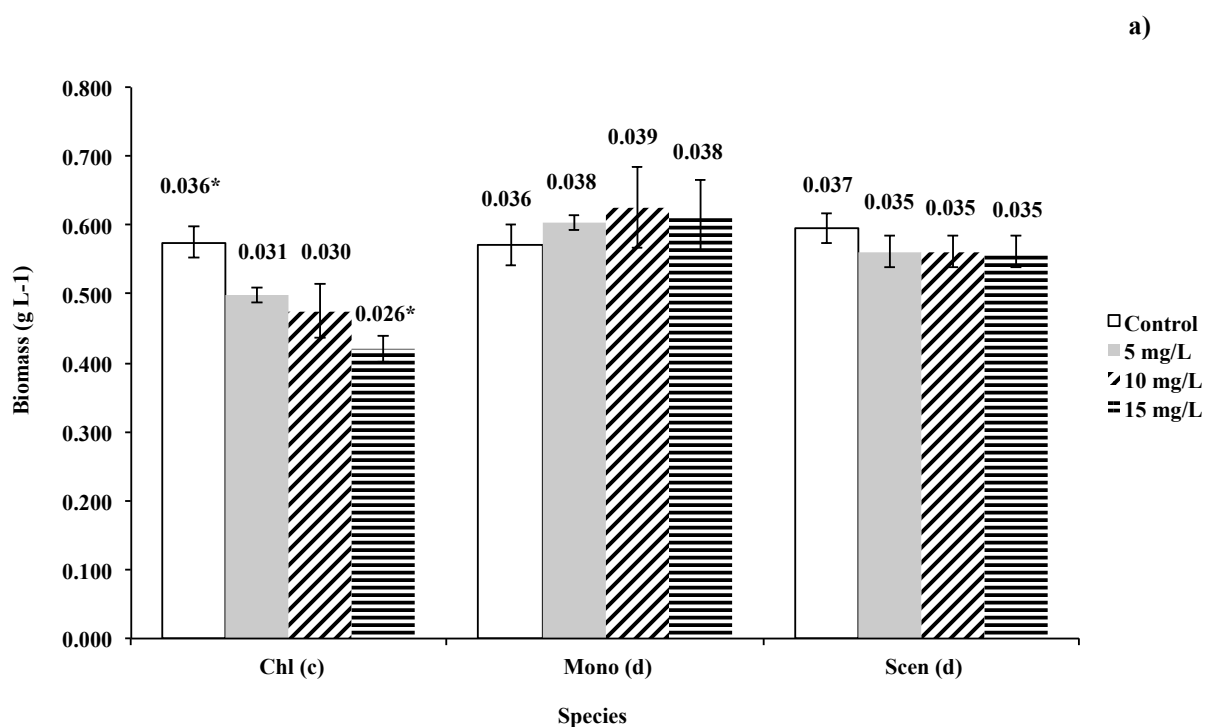


Figure 3.3: Final biomass concentration (g L⁻¹) and biomass productivity (g L⁻¹ day⁻¹) by species and treatment at day 16. Biomass productivity is shown in superscript calculated using initial and final dry cell

mass (DCM) divided by days in culture. Results of post hoc Tukey HSD between species are shown by bracketed letter, and within species by treatment in superscript using *. Treatments represent nutrient-sufficient control (0), and 5 mg L⁻¹ P (5), 10 mg L⁻¹ P (10), and 15 mg L⁻¹ P (15) enrichment of control. Abbreviation of algal species: Chl., *Chlorella* sp., N. limn., *Nannochloropsis limnetica* sp., Mono., *Monoraphidium* sp., Nano., *Nannochloropsis* sp., Scen., *Scenedesmus* sp., Tetra., *Tetraselmis suecica* sp. Confidence intervals are shown using standard error of the mean with triplicate biological replicates (*n* = 3).

Biomass accumulation and productivity results are as follows for the two best P removers, *Monoraphidium* sp. and *Tetraselmis suecica* sp. Curve fits showed linear biomass growth for *Monoraphidium* sp. at all treatments: control, 5, 10 and 15 mg L⁻¹ ($R^2 = 0.99, 0.97, 0.98, \text{ and } 0.99$, respectively). Maximum biomass achieved by *Monoraphidium* sp. for the 10 mg L⁻¹ treatment was 0.63 g L⁻¹ \pm 0.06 SE at day 16 (Figure 3.3a). Curve fits showed linear biomass growth for *Tetraselmis suecica* sp. at all treatments: control, 5, 10 and 15 mg L⁻¹ ($R^2 = 0.93, 0.86, 0.95, \text{ and } 0.83$, respectively). Maximum biomass achieved by *Tetraselmis suecica* sp. for the 10 mg L⁻¹ treatment was 0.55g L⁻¹ \pm 0.02 SE at 16 days (Figure 3.3b).

3.3.3. Dual-purpose candidates

In only two cases were the best phosphorus removers also the best biomass producers. The freshwater chlorophyte *Monoraphidium* sp. achieved biomass productivities of 0.036, 0.038, 0.039 and 0.038 g L⁻¹ day⁻¹ at the control, and 5, 10 and 15 mg L⁻¹ enrichment treatments, respectively, and an initial algal density of 0.052 mg L⁻¹ \pm 0.002 SE (Figure 3.3a). The marine prasinophyte *Tetraselmis suecica* sp. achieved biomass productivities of 0.036, 0.037, 0.034 and 0.038 g L⁻¹ day⁻¹ at the control, 5, 10 and 15 mg L⁻¹ treatments, respectively, and an initial algal density of 0.049 mg L⁻¹ \pm 0.004 SE (Figure 3.3b). These two dual-purpose candidates emerged from the screen as the top performers as measured by biomass growth and P removal efficiency. The two marine eustigmatophytes, *Nannochloropsis* sp. and *N. limnetica* sp., did not show a

biomass gain with increasing P loadings, and a poor overall yield across all treatments, suggesting their lack of potential as dual-purpose organisms. The two freshwater greens, *Chlorella* sp. and *Scenedesmus* sp., showed lower uptake of P at the higher loadings than all the marine species and the freshwater *Monoraphidium* sp.

3.4. Discussion

3.4.1. Microalgal photosynthesis, growth and phosphorus removal

Phosphorus is an essential ingredient in the conversion of solar energy to biochemical energy by plants and is understood to play a critical role as part of the electron donor mechanism in photosynthesis. Community proteogenomics of microbial communities found enhanced biological phosphorus removal (EBPR) selects for polyphosphate (polyP) accumulating organisms to achieve phosphate removal from wastewaters.¹⁹⁸ Similar protein abundances between anaerobic and aerobic phases in this study suggest that in the EBPR metabolic model polyphosphate AMP phosphotransferase hydrolyses polyP to produce ADP, and this in turn is converted to ATP by adenylate kinase. The cycle can be reversed during the aerobic phase, allowing the replenishment of polyP.

Microalgae retain the basic oxygenic photosynthetic apparatus of cyanobacteria situated in the chloroplasts.² The general equation converting light energy to chemical energy by way of photosynthesis represents a combination of two reactions:



1) The left hand side represents quantum requirement or energy input, where energy transduction in the two photosystems produces ATP and NADPH via electron transfer due to photon absorption, and 2) the right hand side represents carbohydrate energy content whereby

carbon assimilation in the Calvin–Benson cycle using ATP and NADPH produced in the photosystems, fixes CO₂ into chemical energy.⁵ The Eilers-Peeters model for photosynthesis hypothesized 3 states of the Photosynthetic Unit (PSU) where light saturation of reaction centers in PSII, and the interconnection of fast photon-associated reactions with slower dark reactions implicated in biomass synthesis, will in turn impact growth, and by implication nutrient uptake.^{199,200} A recent study estimates that algae convert 1 – 2% of incident light to chemical energy, much as land plants do under optimal conditions.⁸ In general, when N and P become scarce photosynthesis can still proceed where microalgal cells continue to fix CO₂ and store photoassimilates in starch and neutral lipid form, conferring survival functions in low nutrient conditions where cell growth is inhibited.³⁶

3.4.2. Response of nutrient removal to P addition

The expected physiological response of higher loadings of P was an enhanced P removal efficiency. Not all species showed increased P removal with increasing P loading, suggesting that phosphorus was not always a limiting nutrient. The effect of increasing P additions on freshwater species was a decline in P removal efficiency as measured at day 8 and day 16, with the exception of *Monoraphidium* sp., and *Scenedesmus* sp., at the control and 5 mg L⁻¹ treatments. The effect of increasing P additions on marine species was a marked increase in P removal efficiency, with the exception of the picoplankton, which released P into solution at day 12 only to take it back up by day 16.

The results of this study are consistent with findings that phosphate concentration strongly affects P uptake and content of microalgae, where stimulated phosphate and polyphosphate uptake are the specific effects of phosphate starvation. This takes place when

excess phosphate is supplied with the required light and air for provision of energy.²⁰¹ Algal cells in natural settings are typically starved of P for periods of time before re-exposure,¹²⁸ as shown by meta-analysis,¹⁰³ and demonstrated experimentally in mono-culture,³⁷ and using co-immobilized alginate beads of *A. brasilense* sp, a microalgae growth promoting bacteria (MGPB), and *Chlorella* sp.²⁰² As mentioned TP as phosphate at treatment loadings of 5 – 15 mg L⁻¹ in this experiment are within the range of reported values for WSP.¹²⁸ Powell *et al.* (2008) found no direct effect of WSP levels on P uptake, and a direct significance for temperature, light intensity and interactions between these factors.¹²⁸ The superior performance of the marine species and the two eustigmatophytes in this study is likely due to evolution in marine environments with extreme and frequent alternations in nutrient availability.¹⁰³

Results were significantly better than 8 - 20% P removal reported for *C. kessleri* sp. grown in batch culture flasks of 100 mL artificial wastewater using diurnal illumination of 12 h light/12 h dark (L/D), 30 °C, irradiance of 45 $\mu\text{mol m}^{-2} \text{s}^{-1}$, and PO₄-P concentration of 10 mg L⁻¹.¹⁹² Aslan & Kapdan (2006) achieved 78% P removal efficiency using batch cultures of *C. vulgaris* sp. at varying N and P concentrations under continuous illumination, 20 °C, in 1000 mL flasks of artificial wastewater and initial PO₄-P concentration of 7.7 mg L⁻¹, where higher concentrations saw on average 30% removal.³³ *Scenedesmus* sp. cultured in artificial wastewater under continuous lighting, with 30-50% daily replacement of volume showed more than 50% P removal after 24 hours in both cases.²⁰³ *Scenedesmus obliquus* batch cultured in urban wastewater in 1.5 L photobioreactor (PBR) columns with continuous lighting, temperature of 25 °C, air bubbling and magnetic stirring removed 97% of phosphorus at the nutrient concentration of 11.8 mg L⁻¹.¹²³

3.4.3. Growth response to P addition

The expected physiological response of higher loadings of P was enhanced biomass accumulation and productivity. No species demonstrated significantly more growth with higher additions of P, again suggesting that P was not the limiting nutrient, at least up until cultures reach a saturation state not attained in 16 days. Rather, the effect of increasing P additions on freshwater species was a significant decline in biomass between the control and 15 mg L⁻¹ treatments for *Chlorella* sp., and no significant difference for *Monoraphidium* sp., and *Scenedesmus* sp. at all loadings. The effect of increasing P additions on marine species was no significant decline in growth between treatments except compared to the control for *N. limnetica* sp., and no significant difference between treatments for *Nannochloropsis* sp. and *Tetraselmis suecica* sp. Observations of all 6 species suggest that increasing P loading may effect stoichiometric production of biomass only up to a certain level due to the P utilization traits of the given species (Figure 3.3a,b).

The green algae species grew well at the higher P treatments, and in the case of *Monoraphidium* sp., *Scenedesmus* sp., and the marine *Tetraselmis suecica* sp., showed consistent growth at all treatments as measured by biomass productivity (g L⁻¹ day⁻¹) (Figure 3.3a,b) and OD₇₅₀ (Figure 3.1). Species-specific rates of P uptake and growth responses to higher additions of P were expected. However, the high rate of P removal efficiency and corresponding dramatic declines in biomass yields with increasing additions of P, as seen in the two eustigmatophytes, was not expected. Both these species released P back into solution at day 12, and this phenomenon is likely explained due to ruptured cells spilling their P content.²⁰⁴ The overall decrease in P eliminations and/or biomass accumulation can be explained due to aging cultures,¹²³ assuming cultures are reaching steady state.

Results on biomass productivity are not entirely consistent with findings in the field on the correlations between P loads and algal growth in lakes,¹⁸⁸ or non-point source additions of P to watersheds,¹⁸⁹ although these additions are at an order of magnitude less than those made in this study, or studies cited here using WSP or HRAP. Comparing final biomass yields from bioprocessing experiments using flask, PBR and pond experiments is problematic due to differences in light regime, treatment loads, microalgal species, scale and growth media. Furthermore, direct comparisons of artificial wastewater and municipal or agricultural wastewater cultures showed that nutrient removal rates are equivalent but that biomass yields are higher in artificial wastewater.^{205,206} Results in this study are significantly lower than yields from a 30 strain screen by Rodolfi *et al.* (2009) using continuous light, CO₂ enrichment and nutrient-sufficient phosphorus growth media in batch flask cultures over 10 days.³⁷ The authors reported biomass productivities (g L⁻¹ day⁻¹) of 0.20 – 0.23 for *Chlorella* sp., 0.21 – 0.26 for *Scenedesmus* sp., 0.17 – 0.21 for *Nannochloropsis* sp., and 0.28 – 0.32 for *Tetraselmis suecica* sp. This compares with the mean control sample productivities (g L⁻¹ day⁻¹) from this study adjusted for time in days of 0.036 ± 0.001 SE for *Chlorella* sp., 0.037 ± 0.001 SE for *Scenedesmus* sp., 0.021 ± 0.003 SE for *Nannochloropsis* sp., and 0.036 ± 0.001 SE for *Tetraselmis suecica* sp., or a roughly ten fold difference. Biomass productivity (g L⁻¹ day⁻¹) falls in the range of reported studies using municipal, agricultural and artificial wastewater as compiled by Pittman *et al.* (2011),²⁶ with an adjusted biomass productivity of 0.026 g L⁻¹ day⁻¹ for *Scenedesmus obliquus* sp. grown in municipal (primary treated) wastewater,¹²³ 0.126 g L⁻¹ day⁻¹ for *Scenedesmus* sp. cultured with artificial wastewater, no CO₂ enrichment and continuous lighting,²⁰³ and 0.081 g L⁻¹ day⁻¹ for *Chlorella* sp. grown in agricultural dairy wastewater (20% dilution).¹³⁰

3.4.4. Batch culturing constraints

Factors affecting growth besides nutrient availability and CO₂ enrichment, are light and temperature,¹⁹² stable pH²⁰⁷ and density of inoculum at time initial.²⁰⁵ A strong correlation has been shown between final cell concentration and linear growth rates due to the onset of light limitation, as shown in batch cultivation of photosynthetic *Chlorella pyrenoidosa* and *Spirulina platensis* in four different types of small-scale PBRs.²⁰⁸ Aslan & Kapdan (2006) attributed lower performance of nutrient removal at higher nutrient concentrations to light limitation, evidenced by high chlorophyll *a* concentrations, and the need to optimize both the N/P ratio and light/dark cycles.³³ Presumably, TP in excess abundance is no longer inhibiting growth, and other parameters, particularly light, becomes limiting. Studying factors affecting luxury uptake of P in WSP, Powell *et al.* (2008) found that increasing light intensity had no effect on acid-insoluble polyphosphate but had a “negative effect” on the acid-soluble polyphosphate.¹²⁸ One explanation is that a faster growth rate at high light intensity causes this form of polyphosphate to be utilized by the cells for synthesis of cellular constituents at a rate that exceeds replenishment.

The observed linear growth rate data from this study was not expected. Growth curves (Figure 3.1) suggest cell density is not limited and the same cohort (species) can be expected to continue growing at a linear growth rate until population density is sufficiently large to cause a saturation effect. At higher P loads it was expected that cultures would maintain longer than control cultures, show higher biomass and cell densities, and a J curve. Exponential growth of microalgae was reported in a recent screen of 30 strains of microalgae that included *Chlorella* sp., *Scenedesmus* sp., *Nannochloropsis* sp., and *Tetraselmis suecica* sp.,³⁷ and also in *Neochloris oleoabundans* sp. cultured in anaerobically digested dairy manure.⁴⁸

Linear growth rates and lower biomass productivities are most likely caused by excess P addition with insufficient supply of required light and/or air through the foam stoppers for the provision of energy,²⁰¹ and also by shading and statistical light/dark cycles due to variations in radial distance from illuminated surface and scattering.¹⁴⁰ Hessen *et al.* (2002) reported the phosphorus to carbon ratio increased in *Selenastrum capricornutum* with reduced light intensity as an adaptive response to self-shading,²⁰⁹ and Martínez Sancho *et al.* (1999) reported similar results for phosphorus metabolism in *Scenedesmus*.²⁹ Finally, the very low N/P ratio may have affected P uptake and growth, where responses of autotrophs to single enrichment of N or P was not as effective in provoking the growth response as N + P enrichment.¹⁰³

3.4.5. Industrial application and scale up

Cultivation of algal biomass using N and P from animal manure effluent and municipal wastewater could recycle nutrients as part of a larger biofuel production process, resulting in decreased anthropogenic effects and lower biomass production costs for lipid production. This screen of six microalgae species in batch flasks showed that biological removal of phosphorus by microalgae biomass was dependent on species, duration of exposure, treatment, and interaction effects among the factors. Biomass accumulation was dependent on species and treatment, with no significant interaction effects. Two promising candidates emerged from the screen, *Monoraphidium* sp., and *Tetraselmis suecica* sp., which demonstrated the dual-purpose traits of high phosphorus removal efficiency and consistent biomass productivity across all P loadings. Biomass yields are lower than many published reports and literature for biomass and biofuel applications, however the biomass yields and P removal efficiencies are within the range of studies for many recent peer reviewed studies using microalgae cultured in wastewater.

Using the maximum biomass achieved by *Monoraphidium* sp. for the 10 mg L⁻¹ treatment of 0.63 g L⁻¹ ± 0.06 SE at day 16 (0.039 g L⁻¹ day⁻¹), and removing 7.86 mg L⁻¹ ± 0.28 SE of TP also at day 16, it is feasible to envision an outdoor scale up PBR or pond system able to treat 100 L of wastewater, remove 5.90×10^{-4} kg of P and produce 4.70×10^{-2} kg of algal biomass, assuming 75% efficiency. The second stage of investigation is to determine lipid productivities from this scale up system. The two dual-purpose species identified is this screen warrant further study to examine the effect of high density wastewater culturing on growth, nutrient removal, and lipidomic profiles of oil content and yields for industrial potential as part of a nutrient removal and biomass/biodiesel production scheme.

Acknowledgements

We wish to thank Drs. Darwin Lyew and Vijaya Raghavan, Department of Bioresource Engineering for their support on culturing during this project, Dr. Gregor Fussmann, Department of Biology for donating freshwater microalgae, the McGill BGSA statistical workshop, and McGill University, Montreal, QC for the financial support. This study received funding support from the Natural Sciences and Engineering Research Council of Canada (NSERC).

Chapter 4: Manuscript II

Comparative shotgun proteomic analysis of wastewater-cultured microalgae: Nitrogen sensing and carbon fixation for growth and nutrient removal in *Chlamydomonas reinhardtii*

Anil K. Patel, Eric L. Huang, Etienne Low-Décarie and Mark G. Lefsrud

Received 22 December 2014; revised version received 8 May 2015; accepted for publication 22 May 2015; published 8 July 2015.

***Journal of Proteome Research* (2015), 14 (8), pp 3051-3067. DOI: 10.1021/pr501316h**

(Reprinted with permission from Patel, A.K.; Huang, E.L.; Low-Décarie, E.; Lefsrud, M. G.

Comparative shotgun proteomic analysis of wastewater-cultured microalgae: nitrogen sensing and carbon fixation for growth and nutrient removal in *Chlamydomonas reinhardtii*. *J. Proteome Res.* **2015**, 14 (6), 3051-3067. Copyright 2015, American Chemical Society.) (Chapter 9, Section 9.2, Appendix B).

Connecting statement

Chapter 3 examined the growth and nutrient removal responses of six unsequenced species of microalgae cultured at the bench scale to different phosphorus loadings. This was in an attempt to determine which species of eukaryotic microalgae performed best for nutrient uptake and biomass accumulation, and two top-performers were identified. A second fundamental problem that needs to be addressed to use microalgae for wastewater treatment and biomass production is how can dynamic cellular adaptations to wastewater treatment be characterized to provide

biological insight. The global research objective of Experiment 2 was to elucidate cellular responses and identify potential targets for genetic improvement using shotgun proteomics and a systems biology approach.

To accomplish this, Experiment 2 (reported in Chapters 4, 5, and 6) examined the growth and nutrient removal responses of a single sequenced strain of *Chlamydomonas reinhardtii* to simulated wastewater processing where both nitrate-N and ammonia-N are present in the growth medium. The specific objective of Chapter 4, Manuscript II, was to perform comparative shotgun proteomic analysis of samples collected in stationary phase using an in-house platform capable of yielding high-quality and reproducible HT MS data from eukaryotic green microalgae. This included performance of pellet harvesting, protein extraction, in-solution digestion, sample clean up, column packing, and development/optimization of instrument methods for performance of two-dimensional liquid chromatography nano-electrospray ionization tandem mass spectrometry (2D LC–nanoESI–MS/MS) using a linear ion trap (LTQ XL) mass spectrometer. This study further required the establishment of in-house mass informatics and bioinformatics workflows to analyze *C. reinhardtii* MS data sets. The bioinformatics workflow leveraged publicly available online resources and databases for *C. reinhardtii* and *A. thaliana*, including tools for data normalization, differential protein abundance analysis, functional enrichment, pathway analysis and visualization. The workflow enabled elucidation of protein function, location, and regulation in both eukaryotic microalgae and higher plants. Metabolic pathways and potential targets for genetic manipulation are identified and discussed in the context of the dual-purpose traits of high rates of nutrient removal and biomass accumulation. The additional objective was to inform and further advance the development of robust microalgae suitable for scale up production of commodity feedstock and/or high-value secondary compounds and metabolites. Chapter 4

(Manuscript II) and Chapter 5 (Manuscript II, Supplemental findings) reports findings from proteomic analysis at the bench scale, and Chapter 6 (Manuscript III) compares biomass yields and nutrient removal from this bench scale experiment to findings at the pilot scale.

Comparative shotgun proteomic analysis of wastewater-cultured microalgae: Nitrogen sensing and carbon fixation for growth and nutrient removal in *Chlamydomonas reinhardtii*

Anil K. Patel^{*1}, Eric L. Huang¹, Etienne Low-Décarie² and Mark G. Lefsrud¹

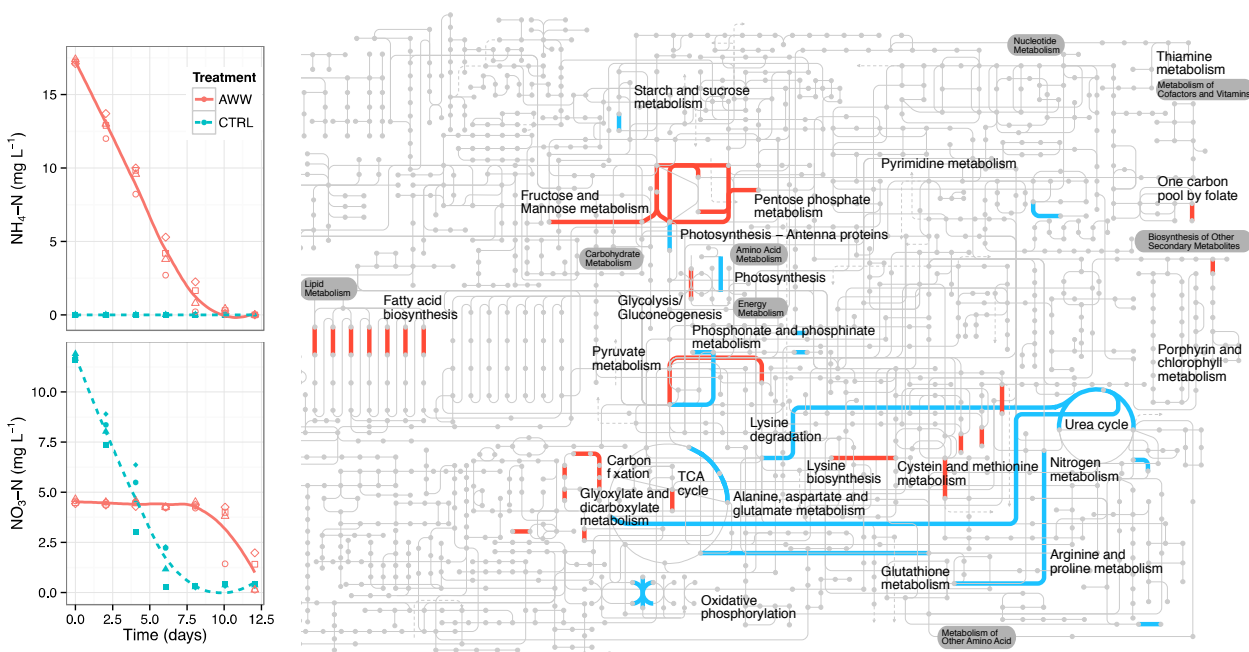
¹Department of Bioresource Engineering, McGill University, Ste. Anne de Bellevue, Quebec H9X 3V9, Canada

²School of Biological Sciences, University of Essex, Colchester CO4 3SQ, United Kingdom

Abstract

Chlamydomonas reinhardtii was batch cultured for 12 days under continuous illumination to investigate nitrogen uptake and metabolic responses to wastewater processing. Our approach compared two conditions: (1) artificial wastewater containing nitrate and ammonia and (2) nutrient-sufficient control containing nitrate as the sole form of nitrogen. Treatments did not differ in final biomass; however, comparison of group proteomes revealed significant differences. Label-free shotgun proteomic analysis identified 2358 proteins, of which 92 were significantly differentially abundant. Wastewater cells showed higher relative abundances of photosynthetic antenna proteins, enzymes related to carbon fixation, and biosynthesis of amino acids and secondary metabolites. Control cells showed higher abundances of enzymes and proteins related to nitrogen metabolism and assimilation, synthesis and utilization of starch, amino acid recycling, evidence of oxidative stress, and little lipid biosynthesis. This study of the eukaryotic microalgal proteome response to nitrogen source, availability, and switching highlights tightly controlled pathways essential to the maintenance of culture health and productivity in concert with light absorption and carbon assimilation. Enriched pathways in artificial wastewater, notably photosynthetic carbon fixation and biosynthesis of plant hormones,

and those in nitrate only control, most notably, nitrogen, amino acid, and starch metabolism, represent potential targets for genetic improvement requiring targeted elucidation.



Graphical abstract: Summary figure included in *JPR* publication.

Keywords: Shotgun proteomics, label-free, MudPIT, *Chlamydomonas reinhardtii*, wastewater treatment, nitrogen sensing, nitrogen metabolism, biomass production

4.1. Introduction

Microalgal biotechnology seeks to develop unicellular biofactories for environmental applications, including bioremediation and the production of biomass and high-value co-products.^{3,4} Microalgae have a proven track record in wastewater treatment,²⁶ and one potential strategy to offset feedstock costs is the development of dual-purpose organisms suitable for wastewater treatment and biomass/biofuel production.^{23,24,48} Unlike traditional crop breeding through strain improvement, the development of application-specific algal hybrids is limited by

current knowledge of the sexual cycle and recombination of many algae,⁵⁵ a poor understanding of regulatory control mechanisms for cellular processes,³⁶ and public concern over outdoor pond cultivation of genetically engineered strains.⁸⁰ Alternative approaches include the selection of desirable traits using experimental evolution^{54–56} and eliciting specific phenotypes through harsh environmental or chemical perturbation.^{66,148,153,210} Nitrogen availability greatly affects microalgal cellular physiology, and any imbalance of the carbon-to-nitrogen ratio elicits rapid metabolic modifications that affect nitrogen assimilation, photosynthetic activity, cellular division, carbon fixation, and biosynthesis.^{39,43,211–213} Use of MS-based proteomics for the identification of critical regulators of genes, proteins, and metabolites in microalgae has intensified.^{58,69–71} Recently, proteomic studies using nitrogen limitation and/or starvation have investigated biochemical adaptation in microalgae related to lipid accumulation, including system-level enzymatic abundance and metabolic responses to total available ammonia,⁴³ starvation,⁶² starvation and recovery,³⁹ and translational proteomic responses to nitrate limitation.⁵⁹

The strategy of shunting carbon toward fatty acid biosynthesis and triacylglycerol (TAG) accumulation, the default stress response of microalgae to nitrogen deprivation, is an active area of algal biofuel research.^{35,45} Nonetheless, overcoming the evolutionary trade-offs between lipid biosynthesis and biomass accumulation has remained a metabolic conundrum despite decades of research.^{8,36,47} Leveraging high-throughput techniques and systems biology to understand culture dynamics and metabolic fluxes in high-density microalgal cultures may inform strain selection and improvement, growth and nutrient removal efficiency, and industrial scale up of wastewater treatment or secondary compound production. We report here research that examined the response of *Chlamydomonas reinhardtii* to a simple two-state system of simulated wastewater

containing ammonia and nitrate and a nutrient-sufficient control containing only nitrate. *C. reinhardtii* is a haploid unicellular freshwater chlorophyte model organism that is well-suited for nutrient removal studies due to ease of growth medium manipulation,^{60,84} a sequenced genome,⁸⁸ proteomic database,⁶⁷ functional annotation,^{155,214} and three transformable genomes (plastid,⁸⁵ nuclear,²¹⁵ and mitochondrial⁸⁹) that enable genetic dissection of metabolic pathways.^{98,215} Green plant lineage and a highly conserved chloroplast genome with photosynthetic apparatus and nitrogen assimilation functions^{60,86} allows comparison of biochemical, enzymatic, and ‘omics data to *Arabidopsis thaliana*.⁸⁷

Current understanding of nitrogen metabolism in microalgae relies significantly on research using *Arabidopsis*⁹⁶ and N-limitation in *Chlamydomonas*^{35,42,213} and other green microalga.^{40,58,212} Because eukaryotic microalgae respond so rapidly to subtle changes in their environment,^{35,60,61} it is important to elucidate genetic and biochemical mechanisms in these dynamic adaptations that successfully ensure continued growth and survival in optimal and suboptimal nutrient conditions. In contrast to other differential gene expression studies on nitrogen stress response in *C. reinhardtii*^{35,42} and proteomic and/or metabolomic time-course studies manipulating only ammonia^{39,43,62} or nitrate,⁵⁹ we sought to characterize protein expression, growth, and nutrient removal dynamics in batch cultured high-density wastewater microalgae cultures allowed to proceed to steady state. In further contrast, we did not use acetate in the media^{39,43,62} and compared group proteomes in stationary phase.^{39,43} Differentially abundant proteins were identified by condition, their function and metabolic pathway were elucidated, and relative quantitation was performed on nitrogen-related proteins using normalized spectral counts. This effort and results may inform selection of mutagenic targets, provide insights into higher plants, and, in light of accelerating technical developments,

contribute incremental progress toward the use of proteomics for environmental applications⁷⁷ and as monitoring and diagnostic tools for bioprocess optimization.⁷⁶ We discuss the effect of culturing a green microalga in simulated wastewater containing nitrate and ammonia and identify candidate pathways of interest for development of a robust strain suitable for scalable outdoor wastewater treatment.

4.2. Materials and methods

4.2.1. Experimental design, organism and culture conditions

Experimental design consisted of 1 microalgal strain of *Chlamydomonas* batch cultured for approximately 12 days, with 2 treatment levels, artificial wastewater (AWW) containing nitrate and ammonia and nutrient-replete control (CTRL) containing nitrate only, replicated 4 times, where each flask was considered a biological replicate for injection in the mass analyzer ($n = 1 \text{ strain} \times 2 \text{ conditions} \times 4 \text{ replicates} = 8$). This label-free study design incorporated randomization, blocking, and biological replication in an effort to avoid systematic bias due to experimental procedure and detect true differences in relative protein abundances between groups.¹⁷⁴

The *C. reinhardtii* strain (CC-2936 wild type mt+, *Chlamydomonas* Resource Center, St. Paul, MN) isolated from soil²¹⁶ and containing a cell wall and nit+ background was used in this study. Culture media, conditions and assay techniques for quantifying biomass growth and nutrient removal have been described previously.²³ The strain was cultivated at $25 \pm 1^\circ\text{C}$, ambient CO₂ at 450 ppm, continuous (24 h) cool white fluorescent illumination ($110.3 \mu\text{mol m}^{-2} \text{s}^{-1} \pm 1.4 \text{ SD}$), and agitation of 110 rpm on a continuous shaker platform. The strain was propagated in sterile nutrient-replete COMBO medium¹⁹⁵ containing major stock chemicals, algal trace elements (ATE), no animal trace elements (ANIMATE), and no vitamins. No acetate

was used in order to achieve photoautotrophic growth conditions.⁶⁷ The medium was set to pH 7.2, buffered against changes in pH using 5mM HEPES buffer,²¹⁷ and stoppered with autoclavable foam.

Axenic cell cultures derived from a single isolated colony were maintained by serial transfer in exponential phase and used to inoculate a starter culture, which was harvested at late-log phase and used to inoculate a new flask culture for use as inoculum.⁴³ Four independent cultures were propagated under two different growth conditions (described below) by transferring 30 mL of inoculum from the same flask at day 7 of exponential growth into eight 500 mL Erlenmeyer flasks containing 300 mL of sterile medium, for a total initial culture volume of 330 mL. Dry cell mass of the inoculum was $0.014 \text{ mg L}^{-1} \pm 0.001 \text{ SD}$. Cell density at inoculation of approximately $8.50 \times 10^5 \text{ cells mL}^{-1}$ was estimated from previously determined standard curves relating cell count measurements to optical density (OD_{680}) using a 0.1 mm depth, Hy Lite hemacytometer (Hausser Scientific, Horsham, PA). Treatment conditions included (1) nutrient-replete COMBO media, control (CTRL), described above and containing 1.55 mg L^{-1} of phosphate-P as K_2HPO_4 , 14.01 mg L^{-1} of nitrate-N as NaNO_3 , and no ammonia-N, and (2) over-enriched COMBO media, artificial wastewater (AWW), modified to contain 5 mg L^{-1} phosphate-P as K_2HPO_4 , 5 mg L^{-1} nitrate-N as NaNO_3 , and 20 mg L^{-1} ammonia-N as NH_4Cl . Treatment levels of N and P were selected based on nutritional requirements²¹⁸ and findings that responses of autotrophs to single enrichment of N or P are not as effective in provoking the growth response as N + P enrichment.^{23,103} Nutrient-sufficient control is based on a previous report.²³ Nutrient-enriched artificial wastewater¹²¹ was modified to mimic the composition of reported secondary effluents of wastewater treatment plants^{123,219,220} and diluted,

anaerobically digested dairy manure.⁴⁸ Lighting, temperature, pH, buffering and agitation were maintained as described for the 12 day duration.

4.2.2. Growth and nutrient removal

Biomass accumulation was followed using OD₆₈₀ and measured gravimetrically using dry cell mass. Total biomass concentration (g L⁻¹) was determined from the difference between average cell masses of triplicate assays at the beginning and end of the experiment using inoculum and final experimental cultures. Samples were centrifuged, washed to remove minerals and salts, and dewatered by freeze drying. Optical density was assayed 12 times for each flask: at the initial time and approximately every 24 h. Total phosphorus (orthophosphate PO₄-P), nitrate-N (NO₃-N) and ammonia-N (NH₃-N) in extracellular solution, not pellet, was assayed 7 times at the initial time and approximately every 2 days at the same time as that for the OD₆₈₀ assay. For a nutrient concentration colorimetric assay, samples were centrifuged, the pellet was discarded, and the supernatant analyzed using Hach TNT kits (TNT 830, 832, 835, 843, 844, 845) (Hach Company, Loveland, CO).

4.2.3. Protein extraction and digestion

At the end of the 12 day culture period, all 8 flask samples were immediately harvested and processed in a random order as a single batch. Cell pellets were processed through a single tube cell lysis and protein digestion method previously described^{76,104,221} and adapted here for eukaryotic microalgae. A 150 mL sample of each flask culture was harvested via centrifugation at 25 °C for 15 min at 3000g (Beckman Avanti J25-I, Brea, CA). Approximately 25 mg of wet cell pellet was immediately quenched in liquid nitrogen, thawed, and solubilized on ice in 100

μ L of lysis buffer to extrude proteins (Tris/10 mM CaCl_2 at pH 7.6 and 6 M guanidine/10 mM dithiothreitol (DTT)) (Sigma-Aldrich Canada, Oakville, ON). Cells were then sonicated (Crystal Electronics, Stamina-XP ultrasonicator, Newmarket, ON) in an ice slurry bath for 5 cycles of 30 s each, with a 30 s cool-down period between cycles. Guanidine solution sample tubes were vortexed every 2 min for the first hour, placed on a tube rotator for a 12 h incubation at 37 °C, and diluted further with 50 mM Tris/10 mM CaCl_2 .

Sequencing grade trypsin (Promega, Madison, WI, USA) was diluted with 50 mM Tris/10 mM CaCl_2 and added to each sample, which was then incubated a further 12 h at 37 °C, followed by addition of a second aliquot of trypsin and incubation for 6 h, followed by addition of 1 M DTT to a final concentration of 20 mM and further incubation for 1 h.²²¹ After digestion, samples were centrifuged for 10 min at 5585g (VWR Costar model V, Radnor, PA), the pellet was discarded, and the supernatant was cleaned and desalted via solid-phase extraction with Sep-Pak Plus C-18 cartridges (WAT020515, Waters Limited, Mississauga, ON), concentrated, solvent exchanged, filtered (Ultrafree-MC UFC30HV00, pore size 0.45 μ m, EMD Millipore, Billerica, MA), and frozen at -80 °C.^{76,198}

4.2.4. 2D LC-MS/MS

We performed label-free shotgun proteomics using Multi-dimensional Protein Identification Technology (MudPIT).⁷³ Peptide analysis was accomplished using online two-dimensional liquid chromatography interfaced with a linear ion trap mass spectrometer (LTQ, Thermo Fisher Scientific, San Jose, CA).^{221,222} Peptides from each biological flask sample (2 conditions \times 4 replicates) were randomly analyzed for a total of 8 MS injections. For each sample injection, peptides were bomb-loaded²²¹ onto a biphasic MudPIT back column packed with ~ 5 cm strong

cation exchange (SCX) resin followed by ~ 5 cm C₁₈ reversed phase (RP) (Luna 5 μ m 100A and Aqua 5 μ m 100A, Phenomenex, Torrance, CA).²²³ Peptide-loaded columns were first washed for 30 min off-line with LC–MS grade H₂O (0.1% F.A) to remove salts and algal cell impurities, then placed in-line with a front column with an integrated nanospray emitter tip (100 μ m i.d., 360 μ m o.d., 15 μ m i.d. tip, New Objective, Woburn, MA) packed with ~15 cm of C₁₈ RP material, and analyzed via 24 h, 12-step MudPIT 2D LC–nanoESI–MS/MS adapted from previously described methods.^{198,223} Parameters for data-dependent acquisition of tandem mass spectra using XCalibur (v2.0.7 SP1) included collision-activated dissociation (35% energy) of the 5 most intense MS/MS following every full scan with a 3 m/z isolation width and dynamic exclusion repeat of 1 with duration of 30 s.¹⁹⁸

4.2.5. Database searching

MS/MS spectra were extracted from Thermo RAW files that corresponded to a single biological replicate and then compared to theoretical tryptic peptide sequences using Proteome Discoverer (v1.4)/SEQUEST HT algorithm (v1.3, Thermo Fisher Scientific, San Jose, CA) using a database comprising the full protein complement of *C. reinhardtii* (*Chlre* v5.3.1 JGI build, released in 2013, containing 19 526 entries, available at: <ftp://ftp.jgi-psf.org/pub/compugen/phytozome/v9.0/Creinhardtii/>) and common laboratory contaminant proteins (human keratin and others).^{74,76} SEQUEST HT database search parameters employed were as follows: full trypsin enzyme specificity with a maximum of 2 missed cleavages, parent ion mass tolerance of 1.6 Da, a fragment mass tolerance of 0.5 Da units, and variable modification of methionine oxidation. An identical search against the reverse sequence database was performed to allow estimation of global false discovery rate (FDR). SEQUEST HT-assigned

peptide spectrum matches (PSMs) across 8 biological samples (2 conditions \times 4 replicates) were loaded into Scaffold (v4.0.7, Proteome Software, Inc., Portland, OR) using the X! Tandem database re-search option. The X! Tandem search^{224,225} was performed against a subset database containing only proteins (and their reverse entries) identified during the primary SEQUEST-HT search and allowing for dynamic modification of N-terminal acetylation and semi-specific cleavages. This refinement search approach provides increased confidence in existing PSMs and increased spectral counts while mitigating decreases in identification sensitivity that often accompanies traditional semi-specific searches. For both SEQUEST HT and X! Tandem PSMs, Scaffold's local FDR Bayesian algorithm was used to assign peptides probabilities. Peptide and protein identifications were controlled at $\leq 1\%$ FDR by (1) empirically selecting Scaffold probability filters according to reverse database hits and (2) requiring ≥ 3 unique peptides in at least one biological sample. Protein accessions, unique peptides, and total spectrum counts were exported to Excel for spectral counting and bioinformatic analysis.

4.2.6. Selection of differentially abundant proteins by QSpec

A minimum of 4 spectra per protein was required for spectral counting and bioinformatics analysis.²²⁶ We first compared *Arabidopsis* TAIR 10 functional descriptions by culture group using multivariate data analysis²²⁷ and performed MANOVA on the raw PCA score to detect if significant differences existed at the level of the global proteome to warrant differential analysis. Statistically significant differentially abundant proteins were then selected using the QSpec software (v1.2.2, available at: <http://www.nesvilab.org/qspect.php/>).¹⁷⁰ The QSpec program normalized total spectral counts by adjusting data using a Poisson distribution by the total sum sample-by-sample and normalized the length of proteins across all samples. All spectral counting

of identified proteins reported in this study used QSpec-normalized spectral counts for a given replicate by treatment condition. The QSpec software reported the significance statistic (Z-statistic), computed as the natural log of the average fold change divided by the variability of the fold changes using standard error. We used blocking of paired control and wastewater samples to reduce bias and variance from known sources of experimental variation.¹⁷⁴ All proteins were evaluated with a Z-statistic $\geq |3.69|$ threshold, corresponding to a directional FDRup or FDRdown of 5% (0.05), unless the less stringent Z-statistic $\geq |3.14|$ threshold, corresponding to a FDRup or FDRdown of 10% (0.10), was specified.

4.2.7. Functional enrichment and pathway analysis

Functional attributes of the data sets were analyzed using Phytozome annotation

(*Chlamydomonas* v9.1 available at:

http://www.phytozome.net/search.php?show=text&method=Org_Creinhardtii), and *Arabidopsis* v9.1, available at: http://www.phytozome.net/search.php?show=text&method=Org_Athaliana).

This incomplete annotation of the *Chlre* v5.3.1 JGI build included the Kyoto Encyclopedia of Genes and Genomes (KEGG), Eukaryotic Orthologous Group (KOG), Panther, Pfam, and best *Arabidopsis* TAIR10 hits (available at: The Arabidopsis Information Resource,

<http://www.arabidopsis.org>). Pattern searches of GO annotation data from *A. thaliana* (available at: ftp://ftp.arabidopsis.org/home/tair/Ontologies/Gene_Ontology/) was used to produce

GOSLIM files targeting specific processes and functions. Functional enrichment was performed using the web-based annotation integration tool Algal Functional Annotation Tool (AFAT)

(available at: <http://pathways.mcdb.ucla.edu/algal/index.html>) and containing integrated

annotation data for biological pathways, ontology terms, and protein families for *C. reinhardtii* and *A. thaliana*.

Hypergeometric testing by AFAT determined the significance of functional enrichment terms with rank and assignment of a p -value, where each enrichment test was considered independent.¹⁵⁵ Phytozome v5 alphanumerical transcript IDs of significantly differentially abundant proteins identified by QSpec were queried against the entire *C. reinhardtii* genome. Trade-offs to this *in silico* approach included: (1) the inability to limit the background universe for hypergeometric testing to proteins identified only in the experiment and (2) the inability to disassociate a gene from a subset of its annotations, leading to multiple pathway hits and significance scores for the same differentially accumulated protein. Manual curation of enrichment results was performed for all proteins discussed, including those that received multiple hits in AFAT-assigned KEGG pathways. Significantly differentially abundant proteins were represented in both tabular and graphical format, where metabolic mapping was performed using the KEGG pathway mapping software iPath2.0 (available at: <http://pathways.embl.de/iPath2.cgi#>) to visualize differences between treatment conditions on a global, metabolic pathway-centric level.^{74,180} The open source R statistical package (R Development Core Team, Vienna, Austria) was used for data analysis and generation of plots not performed with the aforementioned software.

4.3. Results and discussion

4.3.1. Comparison of growth and nutrient removal rates

Our experimental design involved propagating *C. reinhardtii* cells in batch cultures for 12 days under continuous illumination to compare two treatment conditions: (1) artificial wastewater

containing nitrate and ammonia and (2) nutrient-sufficient control containing nitrate as sole form of nitrogen. The expected physiological response of higher nutrient loadings in the wastewater flask cultures was enhanced P and N removal efficiency. We followed ammonia-N, total phosphorus, and nitrate-N in solution over 12 days (Figure 4.1b–d) and found *C. reinhardtii* consumed phosphorus at an exponential rate in both treatments (ANOVA $F_{1,8} = 0.33$ $p = 0.58$), with a half-life in the media of 0.71 ± 0.21 SD days (Figure 4.1c). *C. reinhardtii* consumed ammonia at an exponential rate in the wastewater treatment, halving the concentration every 3.13 ± 0.18 SD days (Figure 4.1b). When ammonia was nearly depleted after 10 days of growth, *C. reinhardtii* started consuming nitrate at a rate of 1.7 ± 0.34 SD days (Figure 4.1d). In the control treatment, which lacked ammonia, nitrate was consumed at an exponential rate, with a halving of the concentration every 2.25 ± 0.26 SD days. Thus, once uptake was initiated, the rate of nitrate consumption was comparable in both treatments. Nutrient removal efficiencies in this study are consistent with other studies of microalgae using control and artificial wastewater.^{23,26,48,121}

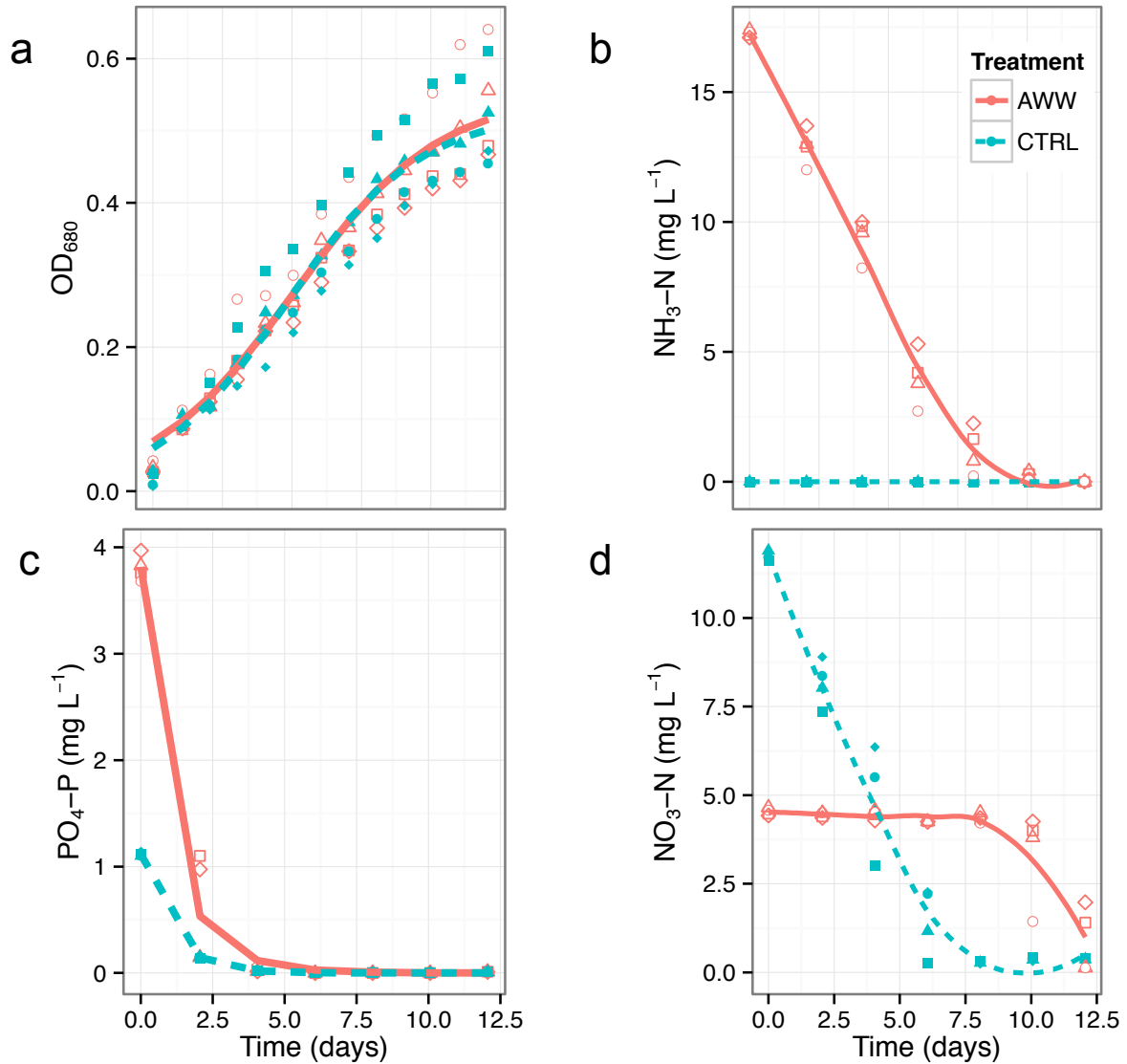


Figure 4.1: Visualizing growth (a) and nutrient removal curves (b–d) for artificial wastewater (AWW; red with open symbols) and control (CTRL; blue with closed symbols) flask cultures over 12 days for $n = 4$ biological replicates. Control contained no ammonia.

The expected response to higher nutrient loadings in the wastewater group was enhanced biomass accumulation. We followed vegetative growth using OD₆₈₀ and found that *C. reinhardtii* cells grew at indistinguishable rates ($F_{1,8} = 2.62$, $p = 0.16$, mean 0.39 ± 0.03 SD day⁻¹) and reached equal abundance ($F_{1,8} = 0.205$, $p = 0.67$, mean 0.54 ± 0.08 SD OD₆₈₀ units) under

wastewater treatment and control conditions (Figure 4.1a). Cultures grew to a final density of approximately 1.78×10^7 cells mL⁻¹ in wastewater and 2.58×10^7 cells mL⁻¹ in control. Final biomass measured gravimetrically using triplicate dry mass samples for each flask was $0.19 \text{ g L}^{-1} \pm 0.02 \text{ SD}$ and $0.23 \text{ g L}^{-1} \pm 0.06 \text{ SD}$ for wastewater and control groups, respectively, where treatment had no significant effect on final biomass (ANOVA $F_{1,8} = 3.807$; $p = 0.063$). These flask scale yields are significantly lower than those of other green alga cultured in similar control and artificial wastewater studies^{23,26,37,48} and are not unexpected. *C. reinhardtii* is a very useful organism for studying desirable phenotypic traits^{47,54–56} for replication in heartier production strains suitable for large-scale and outdoor culturing.^{37,59} The insignificant difference in final biomass between treatment groups, however, was not expected.

Despite the increased availability of nitrogen in the form of ammonia, a preferred source of nitrogen for green algae and higher plants,^{60,99} wastewater cells did not grow faster, accumulate higher biomass, or uptake nutrients faster. The use of gravimetric, spectrophotometric, and colorimetric analysis to infer the physiological responses of *Chlamydomonas* to simulated wastewater processing suggested two explanations: (1) another resource, such as carbon or light, was limiting or (2) treatment levels were not sufficiently different despite over-enrichment using ammonia-N in the artificial wastewater. As mentioned, *Chlamydomonas* has a remarkable ability to adapt to unfavorable nutrient conditions,^{35,42,213} including dynamic metabolic adjustments to maintain a favorable C/N balance.^{43,47,88} We hypothesized, then, that proteomic and functional analysis of samples collected in stationary phase at the end of the experiment would show significant metabolic adaptations to local environments in the growth medium, including nitrogen availability and nitrogen source, that explain the surprising result in final biomass.

4.3.2. Global proteome overview and visualization

Since our proteome analysis was performed using a low mass accuracy ion trap for MS and MS/MS, we employed Scaffold software to apply empirical and statistical approaches to the entire replicate data set. We selected individual peptide and protein probability thresholds to limit false positive identifications, as determined by reverse database hits. Therefore, despite using a low mass accuracy detector, this target-decoy approach allowed specificity to be maintained (see additional details in the Materials and Methods). In other words, our data set achieved similar false positive protein identification rates as could be obtained with high mass accuracy data, albeit at reduced sensitivity.

We analyzed and compared the proteomes of *C. reinhardtii* after 12 days of culturing. 2D LC–MS/MS identified a total of 2358 proteins across all injections ($n = 8$). The peptide-centric nature of shotgun proteomics complicates analysis of eukaryotic proteomes,¹⁶⁴ and 19 ambiguous proteins were identified, of which 18 had 1 other possibility and 1 protein had 2 possibilities. In each case, the longest sequence was selected, and only one of these ambiguous proteins had less than 10 normalized spectral counts across all injections (7 counts total). A minimum requirement of 4 spectra per protein²²⁶ for spectral counting and bioinformatics analysis resulted in 2346 proteins (Supporting information Table S1 can be accessed at: <http://pubs.acs.org/doi/abs/10.1021/pr501316h>). Comparison of treatment groups revealed a highly resembled proteome: 2295 proteins were observed under both conditions, with 38 identified only in the wastewater group and 13 proteins identified only in the control group. Proteins unique to only one group showed low spectral counts (4–13 counts) and did not support uniqueness in identification or further inquiry.

The absence of aggressive perturbation by way of N-starvation is evidenced by the lack of a dramatic shift at the proteome level between treatment groups. This contrasts with recent proteomic studies investigating N-deprivation,^{59,62} ammonia-N availability,⁴³ and ammonia-N starvation and recovery³⁹ for potential biofuel applications. It has to be mentioned that the high degree of overlap between group proteomes in our study can be attributed primarily to three factors: (1) subtle manipulation of macronutrients including nitrogen source in the wastewater treatment, (2) proteomic analysis of samples from stationary phase, and (3) the omission of acetate in the media. First, treatment levels were selected to examine growth and nutrient removal responses of *Chlamydomonas* to simulated wastewater processing and not the induction of lipid biosynthesis via N-starvation. Addition of ammonia-N in the wastewater group ensured over-enrichment of N, not different levels of under-enrichment using only bioavailable ammonia-N, for comparative proteomic analysis to a nutrient-replete nitrate-N only control. Second, in this study, cell cultures were batch cultured^{37,48,132} and allowed to proceed to steady state to ensure long exposure times to simulated wastewater by the transforming microorganism.^{121,132} Proteomic studies of cells adapting to harsh N perturbation sampled at early time points in exposure have demonstrated dramatic and immediate changes in primary metabolism,^{39,43,62} with changes in C/N balance occurring only under sustained chronic conditions,⁴³ as was first hypothesized.⁴⁰ Third, the presence of acetate⁴⁷ in the growth medium^{35,39,42,43,55,62} can alter cellular sensitivities to the maintenance of favorable C/N ratios²²⁸ and cause heightened responsiveness to oxidative stress due to the down-regulation of carbon fixation and photosynthesis.^{39,43,229}

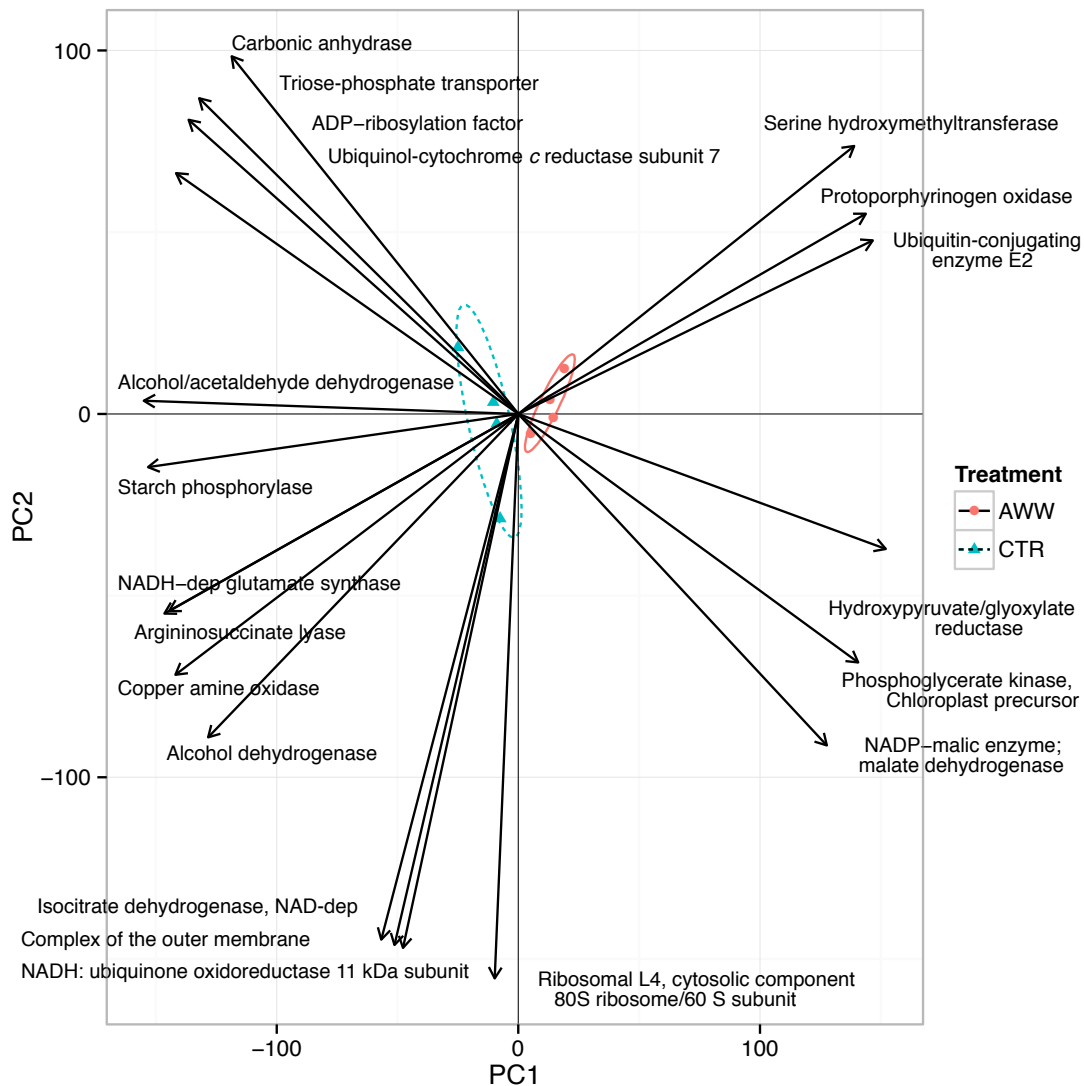


Figure 4.2: First (PC1 24% of variance) and second (PC2 21% of variance) principal components of global PCA analysis showing 20 proteins with greatest variance at the proteome level using *Arabidopsis* TAIR 10 functional descriptions. Labels show corresponding *Chlamydomonas* Phytozome protein descriptions. MANOVA on the raw PCA score ($p = 0.008$) showed a significant difference in protein expression between artificial wastewater (AWW; red circles) and control (CTRL; blue triangles).

We next sought to determine if differences existed at the level of the global proteome by comparing *Arabidopsis* TAIR 10 functional descriptions by culture group using multivariate PCA. The limitation to this approach is the incomplete annotation of *A. thaliana* TAIR 10 functional descriptions for *C. reinhardtii*. Moreover, unsupervised analysis does not distinguish between noisy and highly variable proteins lacking biological significance from those variable

proteins containing a meaningful signal.²³⁰ MANOVA on the raw PCA score showed a significant difference ($p = 0.008$) between the two groups, and biplot visualization shows the 20 proteins with the most variance (longest arrows) for PC1 and PC2 (Figure 4.2).

A fundamental question presented itself, namely, whether the biological variability detected at the proteome level by multivariate PCA was caused by differences in nitrogen source and loading associated with wastewater processing and not by simply indirect compensatory effects, i.e., the control group cells employing physiological mechanisms to reverse the onset of nutrient perturbation in stationary phase. A pattern search of *A. thaliana* GO annotation terms related to nitrogen starvation found no proteins identified in this experiment. Furthermore, only one protein related to fatty acid biosynthesis or TAG accumulation with significantly higher abundance was identified in the control group (Section 4.3.3.4). Comparable growth curves (Figure 4.1a), final biomass, and rates of nutrient removal (Figure 4.1b–d) suggested that neither culture group was in a complete stress response. Overall, no clear pattern is discernable for differentially abundant proteins related to a stress response (Chapter 5, Supplemental findings, Table 5.1), although evidence of oxidative stress was detected in control cells, and iron deficiency, in wastewater cells (Chapter 5, Supplemental findings, Section 5.3.1–5.3.2). At the proteome level, it remained unclear whether the two conditions also exhibited highly resembled functional attributes. Multivariate PCA is useful in the ordering of data with respect to covariance of variables (proteins) and parameters (scope of nutrient availability), but it falls short in providing a biochemical overview.⁴³ The significant result from preliminary PCA, however, warranted further investment in differential abundance statistics and functional enrichment analysis.

4.3.3. Differential analysis and functional enrichment

In addition to controlling for false positive protein identifications, it was equally important to control the false discovery rate when screening for differential abundance on a proteome scale. Towards this goal, we first applied a minimum spectral count filter of four spectral counts.²²⁶ Then, significant differential relative abundance was assessed using the QSpec algorithm, which computes Z-statistics and allows global FDR to be controlled (see Materials and Methods).

QSpec software identified 92 statistically significant differentially abundant proteins with a directional FDRup of 5% (0.05), of which 42 and 50 showed higher levels of relative abundance in wastewater and control, respectively (Chapter 5, Supplemental findings, Table 5.1). Of these 92 differential proteins, 58 (32 in wastewater and 26 in control) were assigned KEGG group association (ie., KEGG KO) by the AFAT tool. Of the 34 differential proteins lacking KEGG association, 8 in wastewater and 20 in control had some functional annotation or description in the Phytozome databases, AFAT tool, and literature. The remaining 6 differential proteins, 2 and 4 in wastewater and control, respectively, were unknown proteins lacking any annotation including description or Pfam¹⁷⁵ family membership. Despite this limitation in functional annotation, the AFAT tool matched the 58 responsive differential proteins to 61 KEGG pathway terms (ie., KEGG ko) under both conditions. This overlap raised a second fundamental question concerning proteins from the same culture group that received multiple hits in AFAT assigned KEGG pathways, including proteins from different culture groups enriched in the same KEGG pathway. Manual curation of AFAT functional enrichment results (described in detail in Materials and Methods) was performed by evaluating the significance *p*-value score for each protein in each treatment group and within the context of wastewater processing and algal/plant biochemistry and metabolism. Shared KEGG pathways were found to

be significant only under one condition or the other, except for Photosynthesis and Photosynthesis–antenna proteins (Section 4.3.3.1), and Nitrogen metabolism (Section 4.3.3.4 and 4.3.3.5), which showed proteins enriched from both treatment groups.

Table 4.1. Proteins that are significantly increased in abundance by treatment condition with KEGG functional association^{a,b}

Wastewater group (AWW)									
KEGG Pathway ^c	Score ^c	Protein description/function ^d	Abbre. ^d	Gene accession ^d	Alias ^d	FDR up ^e	Log2 FC ^e	KO ^e	
Photosynthesis-antenna proteins (ko 00196)	2.19E-07	Chlorophyll <i>a/b</i> binding protein of LHCII		Cre03.g156900.11.2	LHCBM5	3.44E-04	0.724	KO 8912	
		Chlorophyll <i>a/b</i> binding protein of LHCII		g6631.11	LHCBM6	4.00E-05	0.78	KO 8912	
		Chlorophyll <i>a/b</i> binding protein of LHCII		Cre12.g548950.11.2	LHCBM7	4.24E-03	0.54	KO 8913	
		Chlorophyll <i>a/b</i> binding protein of LHCII		Cre17.g720250.11.2	LHCB4	3.31E-03	0.434	KO 8915	
		Chlorophyll <i>a/b</i> binding protein of LHCII		g15011.1	LHCA3	1.00E-05	0.786	KO 8909	
		Chlorophyll <i>a/b</i> binding protein of LHCI		Cre16.g687900.11.2	LHCA7	0.033	0.881	KO 8911	
Carbon fixation in photosynthetic organisms (ko 00710)	3.18E-05	Light-harvesting protein of LCHI		Cre02.g080200.11.2	TRK1	1.66E-04	0.593	KO 0615	
		Transketolase [EC: 2.2.1.1]	TKT	Cre10.g451950.11.2	AAT1	1.35E-03	2.08	KO 0814	
		Alanine aminotransferase [EC: 2.6.1.2]	ALT	Cre05.g234550.12.1	FBA3	4.73E-03	0.466	KO 1623	
		Fructose-bisphosphate aldolase class I [EC: 4.1.2.13]	FBA	Cre12.g510650.11.2	FBP1	0.036	0.884	KO 3841	
		Fructose-1,6-bisphosphatase plastid precursor [EC: 3.1.3.11]	FBP	Cre12.g510650.11.2	PRK1	1.65E-03	0.691	KO 0855	
		Phosphoribulokinase chloroplast precursor [EC: 2.7.1.19]	PRK	g15094.11	FDX1	0	1.935	KO 2639	
Photosynthesis (ko 00195)	2.02E-03	Ferredoxin	FD	Cre02.g082500.11.3	PSAN	0.02	0.843	KO 2701	
		Chloroplastic PS1 reaction center subunit N		Cre16.g651050.11.2	CYC6	4.73E-03	0.466	KO 8906	
		Cytochrome <i>c6</i>		g9648.11	ASD1	0	1.935	KO 0133	
Biosynthesis of plant hormones (ko 01070)	4.36E-03	Aspartate-semialdehyde dehydrogenase [EC: 1.2.1.11]	ASADH	Cre03.g180750.11.2	MES1	0	3.543	KO 0549	
		Cobalamin-independent methionine synthase [EC: 2.1.1.14]	MetE	Cre03.g158900.11.2	DLA2	0.035	0.744	KO 0627	
		Dihydrodipicolinate acetyltransferase [EC: 2.3.1.12]	E2	Cre05.g245900.11.2	BCA2	0.02	1.812	KO 0826	
Biosynthesis of alkaloids from shikimate pathway (ko 01063)	4.90E-03	Branched-chain amino acid aminotransferase [EC: 2.6.1.42]	BCAT	Cre05.g245900.11.2	BCA2	0.02	1.812	KO 0826	
		Choline dehydrogenase [EC: 1.1.99.1]	CHD	Cre12.g514200.11.2		1.36E-03	2.401	KO 0108	
		Choline dehydrogenase [EC: 1.1.99.1]	CHD	Cre12.g514200.11.2		1.36E-03	2.401	KO 0119	
		Acidic ribosomal protein P1		g17858.11	RPP1	1.00E-04	1.562	KO 2942	
		Plastid ribosomal protein L7/L12		Cre13.g581650.11.2	PRPL7	1.46E-03	0.7	KO 2935	
		Plastid ribosomal protein L28		Cre06.g265800.11.2	PRPL28	0.044	1.41	KO 2902	
One carbon pool by folate (ko 00670)	0.137	Methylenetetrahydrofolate reductase (NADPH) [EC: 1.5.1.20]	MTMFR	Cre10.g433600.11.2		2.58E-03	1.597	KO 0297	
		3-oxoacyl-[acyl-carrier protein] reductase [EC: 1.1.1.100]	OAR	Cre03.g172000.11.2	OAR1	4.32E-04	1.525	KO 0059	
		3-oxoacyl-[acyl-carrier protein] reductase [EC: 1.1.1.100]	OAR	Cre03.g172000.11.2	OAR1	4.32E-04	1.525	KO 0059	
		Cobalamin synthesis protein		g15619.11		9.20E-05	2.562	K1 2605	
		Cobalamin synthesis protein		g15199.11		0	3.679	K1 2605	
		Hydroxypyruvate reductase		Cre06.g295450.11.2	HPR1	4.50E-04	0.769	KO 0015	
Nitrogen metabolism (ko 00910)	0.218	Ferredoxin-nitrite reductase [EC: 1.7.7.1]		Cre09.g410750.11.2	NI1	3.64E-03	1.717	KO 0366	
		Porin/voltage-dependent anion-selective channel protein		Cre05.g241950.11.2	ASC2	3.41E-03	0.475	KO 5862	
		Superoxide dismutase [Fe] [EC: 1.15.1.1]		Cre10.g436050.11.2	FSD1	0.042	0.606	KO 4564	
Porphyrin and chlorophyll metabolism (ko 00860)	0.353	Magnesium chelatase subunit I [EC: 6.6.1.1]		Cre06.g306300.11.2	CHL1	0.043	0.86	KO 3405	
		Thiazole biosynthetic enzyme		Cre04.g214150.11.3	TH4	0.024	1.417	KO 3146	
Thiamine metabolism (ko 00730)	N/A								
Control group (CTRL)									
KEGG Pathway ^c	Score ^c	Protein description/function ^d	Abbre. ^d	Gene accession ^d	Alias ^d	FDR up ^e	Log2 FC ^e	KO ^e	
Nitrogen metabolism (ko 00910)	1.02E-03	NADH-dependent glutamate synthase [EC: 1.4.1.14]	NADH-GOGAT	Cre13.g592200.11.2	GSN1	1.40E-05	0.967	KO 0264	
		Ferredoxin-dependent glutamate synthase [EC: 1.4.7.1]	Fd-GOGAT	Cre12.g514050.11.2	GSF1	0.013	0.462	KO 0284	
		Carbonic anhydrase (Carbonate dehydratase 1) [EC 4.2.1.1]	CA1	Cre04.g223100.11.2	CAH1	0	0.912	KO 1674	
Photosynthesis (ko 00195)	1.20E-03	Photosystem I reaction center subunit III		Cre09.g412100.11.2	PSAF	3.30E-05	0.527	KO 2694	
		Photosystem I reaction center subunit VI		Cre07.g330250.11.2	PSAH	0.024	0.297	KO 2695	
		Pre-apoplastocyanin		g3784.11	PCY1	0	0.623	KO 2638	
Alanine, aspartate and glutamate metabolism (ko 00250)	1.30E-03	Argininosuccinate synthase [EC: 6.3.4.5]	ASS	Cre09.g416050.11.2	AGS1	0.025	0.483	KO 1940	
		Argininosuccinate lyase [EC: 4.3.2.1]	ASL	Cre01.g021250.11.3	ARG7	0.017	0.743	KO 1755	
		NADH-dependent glutamate synthase [EC: 1.4.1.14]	NADH-GOGAT	Cre13.g592200.11.2	GSN1	1.40E-05	0.967	KO 0264	
Pyrimidine metabolism (ko 00240)	N/A	Carbamoyl-phosphate synthase small subunit [EC: 6.3.5.5]	CAD	Cre06.g308500.11.2	CMP2	0.094 ^f	0.695	KO 1956	
		Carbamoyl-phosphate synthase small subunit [EC: 6.3.5.5]	CAD	Cre06.g308500.11.2	CMP2	0.094 ^f	0.695	KO 1956	
		Alcohol/acetaldehyde dehydrogenase [EC: 1.1.1.1 2.1.10]	ADH/ACDH	g18056.11	ADH1	0	0.808	KO 4072	
Glycolysis/Gluconeogenesis (ko 00010)	0.013	Alcohol dehydrogenase [EC: 1.1.1.2]	ADH	g15030.11	ADH7	6.80E-05	1.997	KO 0002	
		Glyceraldehyde 3-phosphate dehydrogenase [EC: 1.2.1.12]	GAPDH	Cre12.g485150.11.2	GAP1	0	1.337	KO 0134	
		Agmatine iminohydrolase [EC: 3.5.3.12]	AIH	Cre01.g009350.11.2	AIH2	5.00E-06	2.415	K1 0536	
Arginine and proline metabolism (ko 00330)	0.014	Sodium/potassium-transporting ATPase [EC: 3.6.3.9]		Cre06.g263950.11.3		0.009	2.428	K1 1539	
		Histone H2A		Cre13.g567700.11.2	HAV	0.038	1.062	K1 1251	
		Histone H2B		Cre13.g590750.11.2	HTB37	3.60E-05	0.946	K1 1252	
Systemic lupus erythematosus (ko 05322)	0.043	Histone 3		Cre06.g265000.11.2	HTR13	0.026	1.291	K1 1253	
		Starch phosphorylase [EC: 2.4.1.1]		Cre07.g336950.11.1	PHO2	0.032	0.612	KO 0688	
		Granule-bound starch synthase 1 [EC: 2.4.1.242]	GBSS	Cre17.g721500.11.2	GBS1	6.22E-04	0.515	KO 0703	
Starch and sucrose metabolism (ko 00500)	0.091	Aconitate hydratase [EC: 4.2.1.3]		Cre01.g042750.11.2	ACH1	0.016	0.446	KO 1681	
		Chlorophyll <i>a/b</i> binding protein of LHCII		g5059.11	LHCBM3	0	1.15	KO 8912	
		Glutathione peroxidase [EC: 1.11.1.9]	GPx	g8342.11		0.046	2.173	KO 0432	
Biosynthesis alkaloids from terpenoid/polyketide (ko 01066)	0.115	ADP/ATP carrier protein, mitochondrial		Cre09.g386650.11.2	ANT1	0.002	0.44	KO 5863	
		2-cysteine peroxidoreductin [EC: 1.11.1.15]	2-cys Prx	Cre02.g114600.11.2	PRX2	3.70E-05	0.671	KO 3386	
		Ubiquinol-cytochrome <i>c</i> reductase subunit 7 [EC: 1.10.2.2]	complex III	g5901.11	QC77	2.03E-04	0.981	KO 0417	
Photosynthesis-antenna proteins (ko 00196)	0.342	Protein disulfide isomerase 1 [EC: 5.3.4.1]	PDI	Cre02.g088200.11.2	RB60	0.034	0.465	KO 9580	
		Arf/Sar family, other (ko 04031)		g2791.11		0.034	1.411	KO 7977	
		ADP-ribosylation factor family							

^aThis list was generated by the AFAT tool using differentially abundant proteins identified by QSpec at Z-statistic $\geq |3.69|$, corresponding to directional false discovery rate (FDRup) $\leq 5\%$ (0.05). Only proteins with KEGG association are shown. ^bSupplemental information Table 5.1 lists all 92 differentially abundant proteins identified by QSpec, and Table S3 (<http://pubs.acs.org/doi/abs/10.1021/pr501316h>) lists all 2346 proteins identified that contain 4 or more spectra, with associated QSpec statistics and JGI *ChIre* v5.3.1 annotation. ^cAlgal Functional Annotation Tool significance score and assigned KEGG association. ^dJGI Phytozome v9.1 protein functional descriptions, protein abbreviation, gene transcript name, alias/gene symbol. ^eQSpec directional false discovery rate (FDRup) and Log 2 fold change. ^fSignificant at the Z-statistic $\geq |3.14|$ threshold, corresponding to a FDRup $\leq 10\%$ (0.10).

Manual curation produced 32 proteins enriched in 17 KEGG pathways in the wastewater group and 26 proteins enriched in 16 pathways in control (Table 4.1). In wastewater, Photosynthesis–antenna proteins, Carbon fixation in photosynthetic organisms, Pentose phosphate pathway, Biosynthesis of plant hormones, and Biosynthesis of alkaloids derived from

shikimate pathway make up the top-5 enriched pathways by AFAT significance score and manual curation. In the control group Nitrogen metabolism, Alanine, aspartate and glutamate metabolism, Pyrimidine metabolism, Glycolysis/Gluconeogenesis, and Arginine and proline metabolism made up the top-5 enriched pathways. In order to visualize functional differences between treatment groups, differentially abundant proteins from Table 4.1 were mapped to KEGG-derived metabolic pathways using iPath2.0.^{74,180} Only those differential proteins with an assigned function from AFAT (KEGG KO and/or Enzyme EC number) could be inputted, omitting several differentially abundant proteins (Chapter 5, Supplemental findings, Table 5.1), and not all protein functions were matched by the current iPath2.0 metabolic map. Despite the current limitations in functional annotation, responsive proteins mapped to 97 metabolic map elements (60 in wastewater and 37 in control) to elucidate a pathway-centric overview of specific functional reactions of potential interest for wastewater processing (Figure 5.3).^{74,180}

Significant proteins with KEGG association (Table 4.1 and Figure 4.3) and select differential proteins lacking KEGG association (Chapter 5, Supplemental findings, Table 5.1) are discussed in Sections 4.3.3.1 – 4.3.3.4. Section 4.3.3.5 discusses nitrogen-related proteins in both groups found to be significant, those identified but not significant, and also those expected but not identified. Chapter 5 (Manuscript II, Supplemental findings) reports all remaining differentially abundant proteins not discussed in the article, including those lacking KEGG association, biosynthesis related proteins, stress related proteins, and poorly annotated and unknown proteins (Chapter 5, Supplemental findings, Table 5.1). At first mention, the putative functional name/description of a significant differential protein is given, followed by the Phytozome gene accession name in brackets and gene alias, if any, in italics. Subsequent mention uses putative enzyme abbreviations, or gene aliases, if any. Upper case is used for

nuclear-encoded genes and proteins, and lower case, for organelle-encoded proteins, where all genes in Phytozome are nuclear encoded.²¹⁴

4.3.3.1. Wastewater cells showed a higher abundance of antenna proteins

The wastewater group showed functional enrichment of 5 differential proteins in the KEGG pathway Photosynthesis–antenna proteins (Table 4.1 and Figure 4.3). All 5 proteins belonged to the Pfam family group of Chlorophyll *a/b* binding proteins (PF00504) located in the light-harvesting chlorophyll protein complexes. Antenna proteins enable efficient absorption of diffused light energy in the water column. Of these, 4 were from light-harvesting complex II (LHCII), and 1 was from light-harvesting complex I (LHCI). An additional light-harvesting protein of LHCI (Cre16.g687900.t1.2; *LHCA7*) was also significant, but it lacked an AFAT score. In the control group, only one LHCII Chlorophyll *a/b* binding protein (g5059.t1; *LHCBM3*) of the same Pfam family group was enriched. The wastewater group saw 3 electron transfer agents enriched in the Photosynthesis pathway, the reductant ferredoxin (g15094.t1; *FDXI*), chloroplastic photosystem I (PSI) reaction center subunit N (Cre02.g082500.t1.3; *PSAN*), and cytochrome *c6* (Cre16.g651050.t1.2; *CYC6*). The control group also saw 3 proteins enriched in the Photosynthesis pathway, 2 of which were PS1 reaction center subunits III (Cre09.g412100.t1.2; *PSAF*) and IV (Cre07.g330250.t1.2; *PSAH*), both with GO biological process of carbohydrate synthesis, and preapoplastocyanin (g3784.t1; *PCYI*). This shared pathway between groups suggested a bias in the control group toward higher levels of PSI proteins. Cyclic electron flow (CEF) proteins have been found to peak under nitrogen stress, aiding in the production of ATP by pumping H⁺ to the thylakoid lumen, only to reduce in abundance after repletion of nitrogen in the media.³⁹ Additional ATP synthesis by CEF without generation of reducing power (NADPH or NADH) by way of linear electron flow (LEF) is a

response to nutrient limitation and constraints on carbon fixation and respiration.⁹⁴ This metabolic response agreed with green alga adaptations to available ammonia or nitrate, where intracellular mechanisms detected nitrogen levels and budgeted usage under nonlimited conditions toward protein or nucleotide biosynthesis, and under limiting conditions, decreased light absorption in anticipation of limits to cell division.^{35,41,43} The enrichment of photosynthesis in both groups, particularly the higher levels of antenna proteins in wastewater, contrasts with the immediate metabolic modifications associated with N-starvation. Here the survival response is characterized by a marked reduction in photosynthesis and antennas that limit oxidative damage, conserve and recycle nitrogen pools, and shunt both carbon and energy toward neutral lipids for use in future recovery, membrane stabilization, and shading from high light.^{36,39,62}

Light limitation due to cell shading poses a fundamental constraint on yields in scale up mass cultures. As cell density increases, fluctuating light causes antenna pigments to pick up more light energy than what is transferred to the enzymatic step.¹³⁹ One solution advanced for light saturation is to genetically reduce the overabundance of antenna chlorophylls.²³¹ To date, no stable mutant has been reported, and adaptation, performance, and public acceptance of such a mutant in outdoor ponds is highly dubious. The insertion and expression of the algal cytochrome *c6* gene in *Arabidopsis* has been shown to enhance photosynthesis and growth.²³² Contrary to claims from carefully controlled low light studies, microalgae are no more efficient at photosynthesis under high light than land plants.^{6,7} On balance, the ancient and highly conserved chloroplast photosynthetic machinery offers few targets for mutagenic or metabolic engineering. Nonetheless, even under nonlimited nutrient conditions, alternative competing electron flow pathways to ATP/NADPH coupled LEF exist that power functional reactions

specific to nitrogen metabolism and product biosynthesis⁶¹ and merit further targeted proteomic analysis.

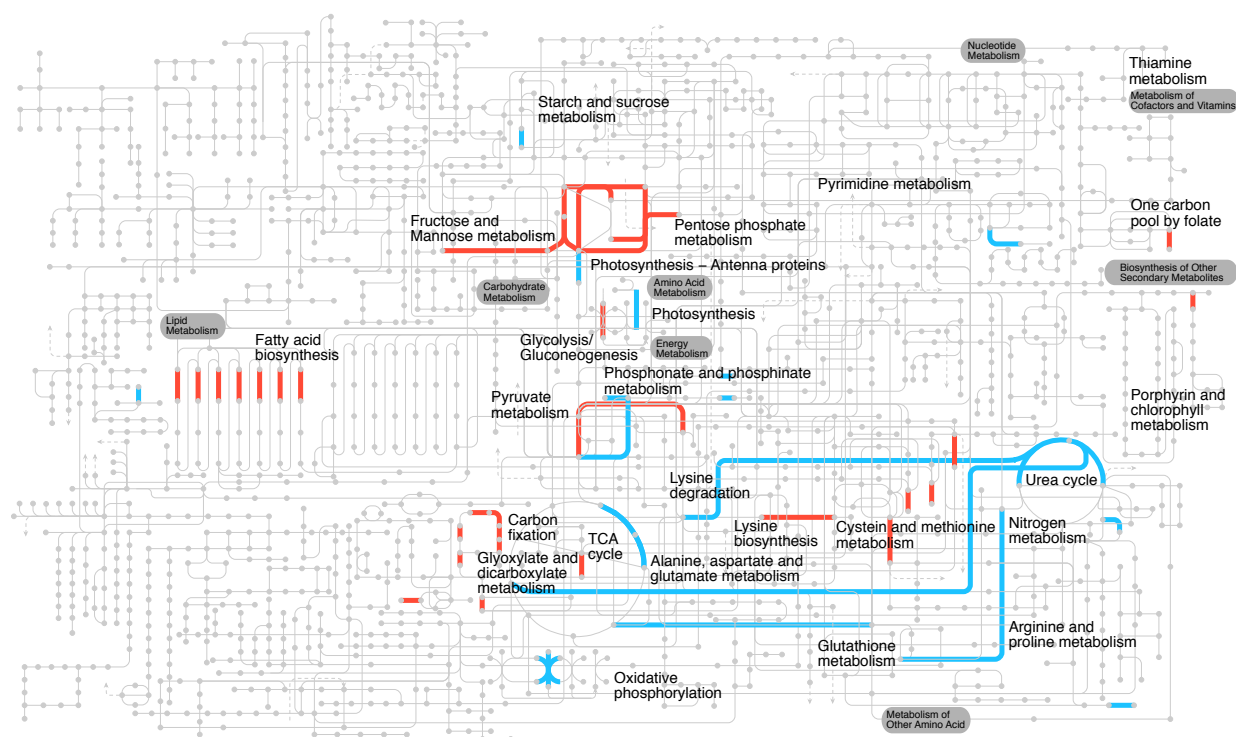


Figure 4.3: Pathway-centric visualization of proteins with differential abundance patterns according to culture condition mapped to KEGG pathways using iPath2.0. The enzymes and proteins colored in red showed significantly higher relative abundance under the artificial wastewater (AWW) conditions, and those colored in blue showed higher levels in the control (CTRL) conditions. Highlighted KEGG pathways include photosynthetic antenna proteins, carbon fixation, and biosynthesis of amino acids and lipids in wastewater cells. Control cells showed enrichment related to nitrogen metabolism and assimilation, synthesis and utilization of starch, and amino acid recycling. Not all proteins in Table 4.1 were successfully mapped.

4.3.3.2. Functional enrichment found that wastewater cells continued to fix carbon and divide.

Synthesis of proteins is required for cellular growth, and ribosomes are required for the synthesis of proteins.²³³ In the wastewater group, 3 ribosomal proteins were enriched in the Ribosome KEGG pathway (Table 4.1 and Figure 4.3). The acidic ribosomal protein P1 (g17858.t1; *RPPI*) had GO biological process of translation elongation during protein

biosynthesis. The plastid ribosomal proteins L7/L12 (Cre13.g581650.t1.2; *PRPL7*) and L28 (Cre06.g265800.t1.2) (*PRPL28*) both showed GO molecular function of contributing to the structural integrity of the ribosome. The lack of enrichment of ribosomal polypeptides in the control group is consistent with the progressive loss of plastidial functions such as amino acid biosynthesis and cytosolic protein translation due to the onset of nitrogen limitation.³⁵ Interestingly, the control group saw higher levels of the previously unknown protein (Cre17.g708750.t1.2; *NSGI*) (Chapter 5, Supplemental findings, Table 5.1) associated with N-limitation induced gametogenesis.²³⁴ Proteomic analysis⁶² found lower levels of *NSGI* were linked to the destruction and resynthesis of ribosomes experiencing N-starvation and was consistent with *Chlamydomonas* cells recycling nitrogen²³⁵ and undergoing autophagy by way of the target-of-rapamycin (TOR) pathway.^{62,236} *NSGI* is an interesting candidate for further targeted proteomic analysis to confirm and quantitate its functional role in ribosomal destruction and resynthesis under nitrogen-induced stress.

Also enriched in wastewater were 5 enzymes in Carbon fixation in photosynthetic organisms, and the utilization of photosynthate (ATP and NADPH) in other enriched pathways such as Fructose and mannose metabolism and Pentose phosphate pathway. Under nonstress conditions, synthesis and degradation of starch is a normal part of the light/dark process in microalgae fixing atmospheric carbon (CO₂).⁴⁷ The Calvin–Benson cycle phosphoribulokinase chloroplast precursor (PRK) (Cre12.g554800.t1.2; *PRK1*) is implicated in the transfer of phosphorus-containing groups in the reductive pentose phosphate pathway (C3) for photoautotrophic assimilation of CO₂ in higher plants.²³⁷ We saw a higher abundance of a putative ALT, an alanine aminotransferase (Cre10.g451950.t1.2; *AAT1*), also enriched in Biosynthesis of alkaloids derived from ornithine, lysine and nicotinic acid. ALT plays a critical

role in transamination reactions for nonessential amino acid synthesis, and the incorporation of nitrogen in the photorespiratory C2 cycle.²³⁸ Three other putative carbon fixation enzymes were enriched in the KEGG Pentose phosphate pathway: transketolase (TKT) (Cre02.g080200.t1.2; *TRK1*) which catalyzes the formation of intermediates, in turn generating NADPH for reductive biosynthesis including fatty acids, starches, nucleic acids and amino acids; fructose-bisphosphate aldolase class I (FBA) (Cre05.g234550.t2.1; *FBA3*), which has GO molecular function of catalyzing the formation of glyceraldehyde 3-phosphate (G3P) for immediate use, conversion to glucose, or storage as starch; and fructose-1,6-bisphosphatase plastid precursor (FBP) (Cre12.g510650.t1.2; *FBP1*), with GO biological process involvement in carbohydrate metabolism. Hydroxypyruvate reductase (Cre06.g295450.t1.2; *HPRI*) is used in the biosynthesis of macromolecules such as carbohydrates from dicarboxylate compounds or 2 carbon precursors that enter as acetyl-CoA. It is listed in AFAT and KEGG as glyoxylate reductase [EC: 1.1.1.26] and enriched in the Glyoxylate and dicarboxylate metabolism pathway. Glyoxylate reductase regulates photosynthesis in the cytoplasm by reducing peroxisome synthesized glyoxylate under low-CO₂ conditions.

The lack of enrichment in control cells suggested the turn over of nitrogen-rich compounds to provide carbon and energy for growth and respiration in increasingly nitrogen-limited conditions.³⁵ This adaptation has been clearly demonstrated in ammonia-N-starved cultures.^{39,43,62} Moreover, an immediate response to N-limitation not only includes lower abundances of enzymes associated with carbon fixation but also the down-regulation of *PRK1* and *TRK1*, resulting in lower abundances of enzymes needed to complete the Calvin–Benson cycle in preparation for slower growth.⁴³ Of the differentially abundant putative enzymes identified in this study, the CO₂-responsive ALT presents *AAT1* as an interesting target.

Elucidating and quantifying enzymatic abundances in photorespiratory pathways, and the response of these mechanisms to different nitrogen and carbon loadings, could further regulatory understanding of how plant/algae cells counter the wasteful effects of oxygenation of RuBP by RuBisCO, the main determinant of photosynthetic inefficiency in C3 plants. A known potential target also identified is *HPRI*. In *A. thaliana* the *HPRI* and *HPR2* genes are implicated in photorespiratory metabolism located in chloroplasts, peroxisomes, mitochondria, and extending into the cytosol,²³⁹ and higher expression is correlated with higher cellular growth rates, ribosomal protein content, and protein translation.^{55,233} Similarly, glyoxylate biosynthesis is a target due to its ability to deactivate RuBisCO and/or inhibit activation.

4.3.3.3. Biosynthesis of amino acids, fatty acids, vitamins and chlorophyll continued in wastewater cells

A significant challenge in wastewater processing is decreasing culture productivity with increasing cell density, light attenuation, and culture age. Remarkably, after 12 days of culture time and cell densities $\sim 10^7$ cell mL⁻¹, the wastewater group continued to show significantly higher relative abundances of proteins related to secondary metabolites, amino acids, fatty acids, and vitamins (Table 4.1 and Figure 4.3). Three putative enzymes were enriched in the Biosynthesis of plant hormones pathway: aspartate-semialdehyde dehydrogenase ASADH (g9648.t1; *ASDI*) showed GO annotation of cytoplasm location and cellular amino acid biosynthetic and metabolic processes; cobalamin-independent methionine synthase (MetE) (Cre03.g180750.t1.2; *MESI*) had GO annotation of zinc ion binding and methionine and cellular amino acid biosynthetic processes; and dihydrolipoamide acetyltransferase (E2) (Cre03.g158900.t1.2; *DLA2*) is the E2 component of the pyruvate dehydrogenase complex linking glycolysis to the TCA cycle and predicted to be plastidic based on similarity to *LTA2* in

A. thaliana. Also enriched was the branched-chain amino acid aminotransferase (BCAT) (Cre05.g245900.t1.2; *BCA2*) in the Biosynthesis of alkaloids derived from shikimate pathway. BCAT synthesizes or degrades leucine, isoleucine, and valine using the Calvin–Benson cycle intermediate α -ketoglutarate (α -KG) to produce α -ketoglutaric acid and glutamate. Choline dehydrogenase (CHD) (Cre12.g514200.t1.2) is part of the GMC oxidoreductase family of proteins acting on CH–OH donors and participates in glycine, serine, and threonine metabolism. It scored equally significant hits in the Benzoate degradation via hydroxylation and Phosphonate and phosphinate metabolism pathways. Other enriched proteins involved in biosynthesis included 3-oxoacyl-[acyl-carrier protein] reductase (OAR) (Cre03.g172000.t1.2; *OAR1*), described in *A. thaliana* as NAD(P)-binding Rossmann-fold superfamily protein and enriched in the Fatty acid biosynthesis and Biosynthesis of unsaturated fatty acids pathways. It was the only differential protein in the wastewater group associated with lipid biosynthesis (Figure 4.3), and it had GO cellular chloroplast location, biological process of regulation of nitrogen utilization, and molecular function repressor activity. The magnesium chelatase subunit I (Cre06.g306300.t1.2; *CHL11*) was enriched in the Porphyrin and chlorophyll metabolism pathway, with GO biological function of chlorophyll biosynthetic process. Additional proteins related to the B complex vitamins cobalamin (B₁₂), thiamine (B₁), and folate (B₉) showed higher relative abundance (Table 4.1) (Chapter 5, Supplemental findings, Section 5.3.1.1).

Two putative enzymes identified with higher relative abundance merit further study. MetE is a precursor of S-adenosylmethionine (AdoMet) and plays a central role in cellular metabolism for the interlocked processes of protein synthesis, methyl-group transfer through AdoMet and biosynthesis of polyamines and ethylene.²⁴⁰ BCAT and all 7 enzymes that catalyze the sequential steps of the shikimate pathway are also interesting targets, given that it is the

biosynthetic route leading to aromatic amino acids phenylalanine, tyrosine, and tryptophan, which, in turn, are protein building blocks and precursors for high-value secondary metabolites.²⁴¹

4.3.3.4. Depletion of extracellular nitrogen activated amino acid recycling, starch metabolism, and oxidative stress in control cells.

We next sought to examine whether depleted extracellular nitrate pools in the control group elicited not only less light energy absorption and growth but also synthesis of starch and utilization of intracellular carbon and nitrogen stores. Results of differential proteomic analysis suggested just that, namely, the enrichment of pathways related to amino acid recycling and the synthesis and oxidation of starch, both used to power cellular respiration and continued growth in depleted nitrate medium (Table 4.1 and Figure 4.3). Starch is the preferred reserve molecule in photosynthetic microalgae for future generation of ATP, reducing power, and carbon skeletons.⁴⁷ Nitrogen deprivation in *Chlamydomonas* has been shown to trigger early synthesis of starch, followed by significant TAG accumulation.^{35,39,62} Two putative enzymes were enriched in the Starch and sucrose metabolism pathway: starch phosphorylase (Cre07.g336950.t1.1; *PHO2*), shown as alpha-glucan phosphorylase 2 in *A. thaliana*, catalyzes the break down of starch; and the glycosyltransferase family starch synthase, shown as granule-bound starch synthase 1 (GBSS) (Cre17.g721500.t1.2; *GBS1*) in Phytozome. Similarly, higher levels of the electron transport chain protein ubiquinol-cytochrome *c* reductase subunit 7 (complex 3) (g5901.t1; *QCR7*) in the Oxidative phosphorylation pathway showed that control cells were regenerating ATP from the oxidation of sugars to power cellular respiration. Finally, the triose-phosphate transporter (Cre01.g045550.t1.2; *TPT3*), described as glucose-6-phosphate/phosphate translocator-related in *A. thaliana*, showed higher relative abundance in control. The protein

mediates transport of carbon for glycolysis and oxidation in the pentose phosphate pathway, but did not generate a hit using the AFAT tool (Chapter 5, Supplemental findings, Table 5.1).

Four putative enzymes were enriched in the Alanine, aspartate and glutamate metabolism and Arginine and proline metabolism amino acid metabolism pathways: argininosuccinate synthase (ASS) (Cre09.g416050.t1.2; *AGS1*); argininosuccinate lyase (ASL) (Cre01.g021250.t1.3; *ARG7*); NADH-dependent glutamate synthase (NADH-GOGAT) (Cre13.g592200.t1.2; *GSN1*), also enriched in Nitrogen metabolism (Section 4.3.3.5); and agmatine iminohydrolase (AIH) (Cre01.g009350.t1.2; *AIH2*), found in the soluble mitochondrial proteome and involved in the agmatine pathway of polyamine (putrescine) biosynthesis. Higher relative abundance of these 4 enzymes suggested gluconeogenesis, whereby glucose is derived from the glucogenic amino acids arginine, ornithine, and proline under low-oxygen conditions. In higher plants, arginine exists in both soluble and protein forms, has a high N/C ratio (4:6), and serves as a main nitrogen storage compound.²⁴² Generation of the precursors needed for the TCA requires that arginine be first metabolized to glutamate and converted to α -ketoglutarate, which, in turn, makes available the ornithine component of arginine to be metabolized to form polyamines and proline. The glutamate semialdehyde generated by catabolism of ornithine and proline is then oxidized to glutamate for conversion to α -ketoglutarate. Three putative enzymes were enriched in the Glycolysis/Gluconeogenesis pathway: the dual function alcohol/acetaldehyde dehydrogenase (ADH/ACDH) (g18056.t1; *ADH1*), which catalyzes the conversion of acetyl-CoA to ethanol under oxygen deprivation and enables NAD⁺ recycling and the progression of glycolysis; alcohol dehydrogenase (ADH) (g15030.t1; *ADH7*), called elicitor-activated gene 3-1 in *A. thaliana*, is synthesized preferentially in fermentative metabolism of plants subjected to low-oxygen stress; and glyceraldehyde 3-phosphate dehydrogenase

(GAPDH) (Cre12.g485150.t1.2; *GAP1*), which catalyzes the conversion of G3P in glycolysis to break down glucose for energy and carbon. GAPDH is associated with the stress response to nutrient limitation,²⁴³ and recently, nonmetabolic processes such as apoptosis, transcription activation, ER to Golgi vesicle shuttling, and fast axonal transport.²⁴⁴ Purple acid phosphatase (PAP) indicated the onset of phosphate deprivation (Chapter 5, Supplemental findings, Section 5.3.2.2). Additional proteins in the control group associated with the oxidative stress response were enriched in multiple KEGG pathways (Table 4.1), including glutathione peroxidase (GPx) (g8342.t1) and 2-cys peroxiredoxin (2-cys PRX) (Cre02.g114600.t1.2; *PRX2*), are discussed in Chapter 5, Supplemental findings. Also discussed are the histone DNA binding superfamily proteins enriched in the Systemic lupus erthematosus pathway.

The typical cellular response to N-deprivation by carbon and nitrogen responsive pathways is down-regulation of carbon assimilation and chlorophyll biosynthesis, up-regulation of lipid biosynthesis, and higher levels of oxidative stress response enzymes.^{43,245} The triacylglycerol lipase and flagellar associated protein (g9673.t1; *FAP12*), referred to as mono/diacylglycerol lipase in *A. thaliana*, showed significantly higher levels, but it lacked KEGG pathway annotation (Chapter 5, Supplemental findings, Table 5.1). The enzyme had GO lipid metabolic and catabolic process and GO molecular function of triglyceride lipase activity in catalyzing the hydrolysis reaction: triacylglycerol + H₂O = diacylglycerol + a carboxylate. The N-deprivation-induced lipase encoding *CrLIP1* has been shown in *C. reinhardtii* to facilitate TAG turnover by degrading diacylglycerol (DAG) and polar lipids.²⁴⁶ As mentioned, a pattern search of *A. thaliana* GO annotation terms related to nitrogen starvation found no proteins identified in this experiment. This absence suggested the control group was not in complete stress response due to residual media and intracellular pools of nitrogen (Figure 4.1b,d).

Interestingly, it should be noted that even after N-starvation, the abundances of fatty acid biosynthesis enzymes have been found to remain mostly unchanged.³⁹

On balance, in the absence of full nitrogen deprivation, cells in exponential and stationary growth stages counter a reduction in carbon assimilation by higher abundances of enzymes involved in amino acid metabolism (Table 4.1 and Figure 4.3), including those with carbon backbones, with the net result of no significant difference in biomass growth and cell division.^{43,88} Indeed, whether coping with nitrate availability (control group in this study) or ammonia availability,^{39,43,62} the metabolism of *C. reinhardtii* adapts to decreasing N conditions in a remarkably flexible way and carries on with photosynthesis, carbon fixation, and eventually the shunting of photoassimilates in neutral lipid form as a survival mechanism to N-depletion.^{35,36,45,88} Thus, the insignificant difference in growth rates and final biomass between the treatment groups, taken together with differential proteomic results, supported our initial hypothesis of dynamic adaptations in physiology that traditional gravimetric and colorimetric analyses fail to detect.

Of the differentially abundant enzymes, interesting targets for inquiry include *FAP12* and *CrLIP1* due to association with neutral lipid accumulation and TAG turnover;²⁴⁶ *ARG7* due to the importance of the last enzyme in the arginine biosynthetic pathway, ASL; and *GSN1* due to its role in reassimilation of ammonia during nitrogen remobilization and transport. Because the primary product of CO₂ fixation, 3-phosphoglycerate, can be fed into starch biosynthesis or used as a precursor of acetyl-CoA for lipid biosynthesis and the glycerol backbone of TAGs, metabolic engineering of a mutant capable of shunting carbon away from starch to TAG in unperturbed growth requires targeted proteomic validation of disruptions or modifications of the cell cycle.^{35,45,47}

4.3.3.5. Alterations to proteins related to nitrogen sensing, metabolism and assimilation

We next sought to compare nitrogen-related proteins identified and enriched in control cells lacking ammonia with the wastewater group, which was switching from uptake of ammonia to nitrate at the time of proteomic sampling (Figure 4.1b,d). We examined functional enrichment of significant proteins using the AFAT and iPath2.0 tools (Table 4.1 and Figure 4.3) and then performed a pattern search of GO annotation data against all proteins identified in the experiment using *Arabidopsis* TAIR 10 descriptions of nitrogen-related proteins. Phytozome v9.1 *Chlamydomonas* protein names corresponding to *A. thaliana* TAIR 10 descriptions and log₁₀ transformed counts are shown by culture group in Figure 4.4 and listed in Table 4.2.

The bulk of ammonia generated through deamination is targeted to the chloroplast, which contains the necessary enzymes for the incorporation of ammonia into carbon skeletons by way of the Glu–Gln (GS/GOGAT) cycle to generate glutamate.^{39,62} The control group received 3 hits in the Nitrogen metabolism KEGG pathway (Table 4.1 and Figure 4.3). The glutamate synthases, NADH-GOGAT (Cre13.g592200.t1.2; *GSNI*), and ferredoxin-dependent glutamate synthase (Fd-GOGAT) (Cre12.g514050.t1.2; *GSFI*), produce glutamate from glutamine and α -ketoglutarate, with GO oxidoreductase activity on the CH–NH₂ group of donors with an iron–sulfur protein or NAD⁺ as acceptors in the chloroplast stroma. Both proteins were enriched: NADH-GOGAT is implicated in primary assimilation of ammonia via N₂ fixation, nitrate reduction or direct uptake, and reassimilation of ammonia during nitrogen remobilization and transport; Fd-GOGAT is implicated in reassimilating ammonia released from glycine decarboxylation during photorespiration.²⁴⁷ NADH-GOGAT was also enriched with a higher AFAT score in the amino acid metabolism pathways discussed previously (Section 4.3.3.4).

Ammonia-N starvation studies showed a significant increase in both glutamate synthases⁶² and different abundances of GSN isoforms.³⁹ Also enriched was the low-CO₂ inducible gene regulated carbonic anhydrase (CA1) (Cre04.g223100.t1.2; *CAH1*), described as carbonate dehydratase 1 in *C. reinhardtii*, most likely explained by the lack of ammonia in the medium, which makes CO₂ more available, and aconitate hydratase (Cre01.g042750.t1.2; *ACH1*), involved in transport of nitrate and also enriched in the Biosynthesis of alkaloids derived from terpenoid and polyketide pathway. Carbamoyl phosphate synthetase, small subunit (CAD) (Cre06.g308500.t1.2; *CMP2*) showed higher abundance at the FDRup (0.094) level with KEGG pathway hits in both Pyrimidine metabolism and Alanine, aspartate, and glutamate metabolism. The small subunit of this heterodimeric enzyme contains a glutamine binding site that catalyzes the hydrolysis of glutamine to glutamate and then ammonia. Carbamoyl phosphate synthetase, large subunit (g8395.t1; *CMP1*), which synthesizes carbamoyl phosphate from the ammonia, was identified in both groups, but not significantly (Figure 4.4). Higher levels of carbamoyl phosphate synthetase subunits as well as arginine and ornithine dynamics are associated with ammonia recycling from protein catabolism via the urea cycle (Figure 4.3).³⁹

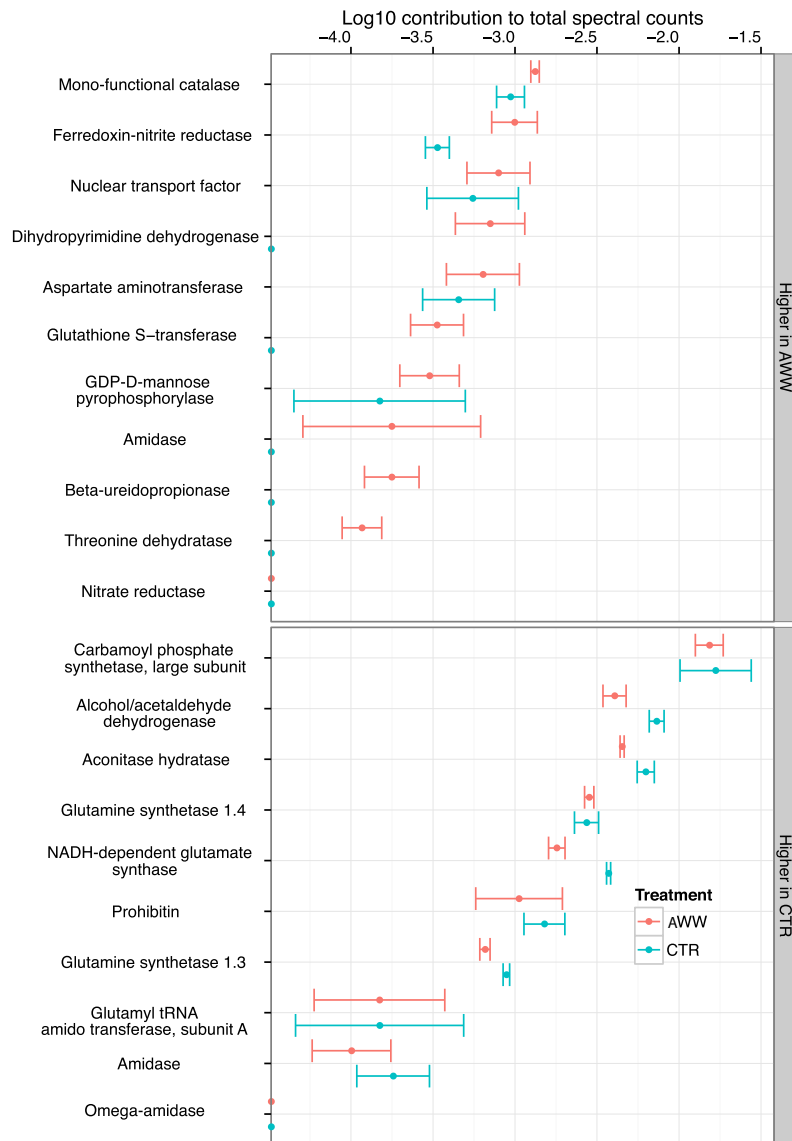


Figure 4.4: Nitrogen metabolism and assimilation related proteins identified in this experiment based on *Arabidopsis* TAIR 10 functional descriptions by culture condition. Labels use corresponding *Chlamydomonas* Phytozome protein descriptions. Standardized spectral counts are shown as a percent contribution, where counts represent normalized spectral counts by length and protein concentration for a given protein in a single sample divided by total normalized spectral counts in a sample across all proteins in experiment. Error bars represent the 95% confidence interval.

Table 4.2. Nitrogen-related proteins identified in the experiment by culture condition with GO and *Arabidopsis* functional association^{a,b}

Wastewater group (AWW)				
Protein description/function ^c	Gene accession ^c	Alias ^c	GO characteristics ^d	TAIR 10 Description ^e
Mono-functional catalase [EC:1.11.1.6]	Cre09.g417150.t1.2	CAT1	involved in cellular response to nitrogen starvation	Catalase 2
Ferredoxin-nitrite reductase [EC: 1.7.7.1]	Cre09.g410750.t1.2	NIII1	has nitrite reductase (NO-forming) activity	Nitrite reductase 1
			involved in nitrate transport	
			has ferredoxin-nitrate reductase activity	
Nuclear transport factor	Cre07.g316000.t1.2		involved in response to nitrate	Nuclear transport factor 2B
Dihydropyrimidine dehydrogenase (NADP+) [EC:1.3.1.2]	Cre13.g578750.t1.2	TBA1	involved in ammonium transport	Pyrimidine 1
Aspartate aminotransferase	g9594.t1	AST1	involved in cellular response to nitrogen levels	Aspartate aminotransferase 3
Glutathione S-transferase [EC:2.5.1.18]	Cre17.g742300.t1.3		related to nitrogen compound metabolic process	Glutathione S-transferase PHI 10
			involved in nitrate transport	
GDP-D-mannose pyrophosphorylase [EC:2.7.7.22]	Cre16.g672800.t1.2	GMP1	involved in response to nitrate	Glucose-1-phosphate adenylyltransferase family protein
Amidase	Cre02.g103350.t1.3		involved in response to ammonium ion	Fatty acid amide hydrolase
Beta-ureidopropionase [EC:3.5.1.6]	Cre01.g022650.t1.2		has carbon-nitrogen ligase activity, with glutamine as amido-N-donor	Beta-ureidopropionase
			involved in nitrogen compound metabolic process	
			involved in cellular response to nitrogen levels	
Threonine dehydratase [EC:4.3.1.19]	Cre02.g073200.t1.2	THD1	has hydrolase activity, acting on carbon-nitrogen (but not peptide) bonds	L-O-methylthreonine resistant 1
Nitrate reductase	Cre09.g410950.t1.2	NIT1	has L-threonine ammonia-lyase activity	Nitrate reductase 2
			has nitrate reductase activity	
			has oxidoreductase activity, acting on other nitrogenous compounds as donors, with NAD or NADP as acceptor	
			involved in nitrate assimilation	
			has nitrate reductase (NADH) activity	
			involved in nitric oxide biosynthetic process	
Control group (CTRL)				
Protein description/function ^c	Gene accession ^c	Alias ^c	GO characteristics ^d	TAIR 10 Description ^e
Carbamoyl phosphate synthase, large subunit [EC:6.3.5.5]	g8395.t1	CMP1	involved in nitrogen compound metabolic process	Carbamoyl phosphate synthetase B
Alcohol / acetaldehyde dehydrogenase [EC: 1.2.1.10]	g18056.t1	ADH1	involved in nitrate transport	Aldehyde dehydrogenase 2C4
			involved in response to nitrate	
Aconitate hydratase [EC: 4.2.1.3]	Cre01.g042750.t1.2	ACH1	involved in response to nitrate	Aconitase 2
			involved in nitrate transport	
Glutamine synthetase [EC:6.3.1.2]	g13061.t1	GLN2	has glutamate-ammonia ligase activity	Glutamine synthetase 1;4
			involved in nitrate assimilation	
			involved in nitrogen compound metabolic process	
NADH-dependent glutamate synthase [EC:1.4.1.14]	Cre13.g592200.t1.2	GSN1	involved in nitrate assimilation	NADH-dependent glutamate synthase 1
			involved in nitrogen compound metabolic process	
Prohibitin	Cre12.g519350.t1.2		involved in ammonia assimilation cycle	Prohibitin 3
			involved in response to nitric oxide	
Glutamine synthetase [EC:6.3.1.2]	Cre02.g113200.t1.3	GLN1	involved in nitrate assimilation	Glutamine synthetase 1.3
			has glutamate-ammonia ligase activity	
			involved in nitrogen compound metabolic process	
Glutamyl tRNA amidotransferase, subunit A	Cre10.g439400.t1.1	GAT1	has carbon-nitrogen ligase activity, with glutamine as amido-N-donor	Amidase family protein
Amidase	g11560.t3	AMI2	has hydrolase activity, acting on carbon-nitrogen (but not peptide) bonds	Amidase 1
			has carbon-nitrogen ligase activity, with glutamine as amido-N-donor	
Omega-amidase [EC:3.5.1.3]	g11647.t1		involved in nitrogen compound metabolic process	Nitrilase/cyanide hydratase and apolipoprotein
			has hydrolase activity, acting on carbon-nitrogen (but not peptide) bonds	

^a This list of N-related proteins identified in the experiment was generated by a pattern search of GO annotation data using *Arabidopsis* TAIR 10 descriptions.

^b Figure 4.4 shows log10 contribution of these N-related proteins listed in Table 4.2 by treatment group using standardized spectral counts.

^c JGI *Chlamydomonas* Phytozome v9.1 corresponding protein functional descriptions, gene accession name (transcript), alias/gene symbol.

^d GO *Arabidopsis* TAIR 10 characteristics.

^e *Arabidopsis* TAIR 10 protein descriptions included in *Chlre* v5.3.1 JGI build and Phytozome v9.1 annotations.

Annotation notes:

JGI *Chlre* v5.3.1 build and Phytozome v9.1 annotations are available at <ftp://ftp.jgi-psf.org/pub/comp/gen/phytozome/v9.0/Creinhardtii/>

JGI Phytozome v9.1 gene accession names (transcripts) are searchable at http://phytozome.jgi.doe.gov/pz/portal.html?search?show=KEYWORD&method=Org_Creinhardtii

TAIR GO slim characteristics are available at http://ftp.arabidopsis.org/home/tair/Ontologies/Gene_Ontology/

Arabidopsis TAIR10 annotation also available at The Arabidopsis Information Resource: <http://www.arabidopsis.org>

In wastewater cells, the oxidoreductase enzyme ferredoxin-nitrite reductase (NII1) (Cre09.g410750.t1.2; *NIII*) was enriched in the Nitrogen metabolism pathway. *NIII* was identified in *C. reinhardtii* due to linkage to loci required for growth using nitrate as sole N source and where nitrate presence was an inducer of higher nitrate reductase levels.²⁴⁸ Normalized spectral counts for NII1 were higher in wastewater replicates than control and lower in the AWW2 replicate compared to other wastewater replicates (Chapter 5, Supplemental findings, Table 5.1). This supported the conclusion that wastewater cells were switching from ammonia to nitrate uptake, that AWW2 had switched earlier, and that cells in control were entering nitrate-N limitation. It also supported rejection of a common assumption that because the rate of ammonium uptake is not dependent on total available ammonium the *C. reinhardtii* metabolism is unchanged and not dynamic in the presence of sufficient ammonium.⁴³

Nitrogen-related proteins we expected to identify included glutamine synthetase (cytoplasmic and chloroplastic), aspartate aminotransferase, glutamate dehydrogenase, and asparagine synthetase. The glutamine synthetases (GS) [EC: 6.3.1.2], GLN 1.3 (Cre02.g113200.t1.3; *GLN1*) and GLN 1.4 (g13061.t1; *GLN2*), were identified in the experiment but did not show significantly higher levels in either treatment. This is in contrast to ammonia-N starvation results showing higher abundances of both GS enzymes.^{39,62} These nitrate assimilation enzymes catalyze the condensation of glutamate and ammonia to form glutamine, with GO cellular location of GLN 1.4 in the cytosol and GLN 1.3 in the plasma membrane, cytosol, and chloroplasts. We expected a higher relative abundance of both enzymes in the control group; however, residual levels of nitrate pools²⁴⁹ and up-regulation of amino acid metabolism may account for the low biosynthetic glutamine synthetase activity. The putative assimilatory glutamate dehydrogenases (GDH) [EC: 1.4.1.3] (Cre09.g388800.t1.2; *GDH1*) and

(Cre05.g232150.t1.2; *GDH2*) were both identified, but not significantly. GDH2 converts glutamate to α -ketoglutarate, and its activity is adaptive under stress, including glutamine synthetase and glutamate synthase inhibition,²⁵⁰ and is highest in high ammonium concentrations and lowest in nitrate-grown cells.²⁴⁹ GDH2 has been found to respond to ammonia-N starvation with a 10-fold decrease, only to respond more slowly than GS and GSN enzymes to ammonia-N repletion after 24 h.³⁹ This further supported switching of nitrogen source in the wastewater group and depletion of nitrate in the control group. Aspartate aminotransferases [EC: 2.6.1.1] play an important part in amino acid metabolism by catalyzing a reversible transfer of an α -amino group between aspartate and glutamate. All four putative enzymes were identified in this experiment, (g9594.t1; *AST1*), (Cre02.g097900.t1.2; *AST3*), (Cre06.g257950.t1.2; *AST4*) and (Cre02.g147200.t1.2; lacking alias), but none significantly under either condition. Finally, asparagine synthetase [EC: 6.3.5.4], which generates asparagine from aspartate in an amidation reaction similar to that of glutamine synthetase, was not identified in either condition in this study.

Proteomic analysis supported the conclusion that wastewater-cultured cells detected available nitrogen pools and budgeted uptake and assimilation to maintain respiration, biosynthesis, and continued growth. Control cells had depleted extracellular nitrate and, by proteomic inference, were up-regulating amino acid metabolism to recycle intracellular nitrogen and continue with photosynthesis and respiration. Of the enriched enzymes involved in nitrogen metabolism, NII1 is a candidate for further study using targeted proteomics, given its linkage to loci required for growth. GLN 1.3, GLN 1.4, and GDH2 are interesting because of their critical role in nitrate assimilation and adaptive response to ammonia and nitrate pools. Although not differentially abundant in this study, the response of GDH2 to switching of nitrogen source also

requires further quantitative proteomic analysis over a prescribed time course using real and/or simulated wastewater. Additional targets for elucidating nitrogen metabolism are *GSN1* and *GSF1* due to participation in the primary assimilation and reassimilation of ammonia, and well as both the small CAD subunit for its role in catalyzing the hydrolysis of glutamine to glutamate and then ammonia, and the large CAD subunit, for synthesis of carbamoyl phosphate from the ammonia.

4.4. Concluding remarks

Differing from studies on harsh nutrient deprivation and/or single N source manipulation, our label-free shotgun proteomic analysis of artificial wastewater-cultured *C. reinhardtii* contributed novel insights into nitrogen metabolism and carbon fixation by using wastewater containing both nitrate and ammonia. This study identified 2346 proteins with 4 or more spectra, of which 92 showed significant changes in protein abundance. Surprisingly, after 12 days, the wastewater group was still engaged in photosynthetic carbon fixation, cell division, and biosynthesis of amino acids, fatty acids, secondary metabolites, and chlorophyll. Control cells showed continued photosynthesis, synthesis and use of starch, recycling of amino acids, evidence of oxidative stress, and little enrichment of lipid biosynthesis. The insignificant difference in final biomass and OD₆₈₀ further demonstrated that even in increasingly N-limited media *C. reinhardtii* continued to grow and attempt to balance its C/N ratio. Overall, our results were in agreement with previous findings on nitrogen sensing, recycling of nitrogen to sustain growth, and decreased overall protein turnover in favor of those critical for survival in cells entering N-limitation.^{35,39,41,43,62,245} This study provided insight into the importance of nitrogen source: ammonia and/or nitrate. The adaptive response of enzymes to nitrogen switching from ammonia

to nitrate uptake in wastewater cells was indicative of tightly controlled and dynamic cellular responses to N availability that dictate cell culture health and productivity in concert with light absorption and carbon assimilation. Proteomic analysis of stationary phase samples reinforced a continued challenge for biofuel applications, namely, how to reconcile the dramatic short-term response and rearrangement of microalgal metabolism subjected to N-starvation with highly conserved molecular survival mechanisms that shunt and compartmentalize C and N to the detriment of culture yields over longer durations and on production scales. In the case of wastewater processing, we found evidence that over-enrichment of N did not adversely affect growth or cellular physiology. This finding is intriguing and supports optimism for improvements in breeding programs, bioprospecting, and bioprocess optimization. Also interesting are the up-regulated pathways identified such as shikimate and biosynthesis of plant hormones that lead to valuable secondary compounds.

Differential abundance analysis and functional enrichment identified a number of enzymes and potential gene targets for multistate and time-course experiments using discovery and targeted proteomic techniques. Future mutagenic selection and/or metabolic dissection of these targets could further enhance understanding of growth and nutrient removal in microalgae and higher plants. Findings also demonstrated the power of LC–MS proteomic analysis to detect metabolic responses to subtle changes in environmental conditions, not just drastic perturbation, that gravimetric and spectrophotometric measures alone fail to detect. Continued technical advances in mass spectrometry and informatics may afford more routine proteomic study and monitoring of candidate strains, cultured outdoors, in secondary municipal effluent and/or agricultural wastewater as part of a larger feedstock production scheme. We will continue

elucidating candidate pathways for development of a robust strain suitable for scalable outdoor wastewater treatment.

Associated content

Supporting information

Report of additional differentially abundant proteins of interest not discussed in the article, including biosynthesis related, stress related, poorly annotated, and unknown proteins. Proteins lacking KEGG pathway association are evaluated by use of functional annotation tools such as Pfam and Panther biological pathway databases, GO and KOG ontology databases, JGI Phytozome, and literature related to *Chlamydomonas* and *Arabidopsis*. Chapter 5, Supplemental findings, Table 5.1: All statistically significant differentially abundant proteins identified by QSpec with normalized spectral counts, statistics, JGI *Chlre* v5.3.1 annotations, and Phytozome functional descriptions. Chapter 4, Table 4.2: Nitrogen-related proteins identified in the experiment based on a pattern search of GO annotation data using *Arabidopsis* TAIR 10 descriptions. Supporting Information Table S1 (accessible at: <http://pubs.acs.org/doi/abs/10.1021/pr501316h>): Complete list of the 2346 proteins identified with 4 or more spectra, including QSpec normalized spectral counts, statistics, and JGI *Chlre* v5.3.1 annotations. The Supporting Information is available free of charge on the ACS Publications website at DOI: 10.1021/pr501316h. The mass spectrometry proteomics data have been deposited to the ProteomeXchange Consortium²⁵¹ via the PRIDE partner repository with the data set identifier PXD002146.

Author information

Corresponding author

*E-mail: anil.patel@mail.mcgill.ca. Phone: 514-531-1700. Fax: 514-398-7990.

Notes

The authors declare no competing financial interest

Acknowledgements

We wish to thank Dr. Todd Greco (Department of Molecular Biology, Princeton University) for assistance and guidance with proteome informatics; Dr. Damian Fermin (Yale School of Medicine) & Dr. Hyungwon Choi (School of Public Health, National University of Singapore) for assistance using QSpec; the instructors, assistants and guest speakers from the 2013 Proteomics Course, Cold Spring Harbor Laboratory; Dr. Taylor Weiss (Department of Biochemistry and Molecular Biology, Michigan State University) for critical review of manuscript; Dr. Huan Qiu (Department of Ecology, Evolution and Natural Resources, Rutgers University) for guidance with annotation tools; Dr. Graham Bell (Department of Biology, McGill University) for providing the *C. reinhardtii* (CC-2936 wild type mt+) strain; and Drs. Vijaya Raghavan, Valérie Orsat, Darwin Lyew, and Robert Williams (Department of Bioresource Engineering, McGill University) for support with engineering and culturing. This research was funded by a Natural Sciences and Engineering Research Council of Canada (NSERC) Discovery grant (RGPIN 355743-13), a Canada Foundation for Innovation (CFI) equipment grant (CFI/Exp/Lefsrud/#23635), and McGill University, QC, Canada.

Chapter 5: Manuscript II, Supplemental findings

Comparative shotgun proteomic analysis of wastewater-cultured microalgae: Nitrogen sensing and carbon fixation for growth and nutrient removal in *Chlamydomonas reinhardtii*

Anil K. Patel, Eric L. Huang, Etienne Low-Décarie and Mark G. Lefsrud

Received 22 December 2014; revised version received 8 May 2015; accepted for publication 22 May 2015; published 8 July 2015.

***Journal of Proteome Research* (2015), 14 (8), pp 3051-3067. DOI: 10.1021/pr501316h**

(Reprinted with permission from Patel, A.K.; Huang, E.L.; Low-Décarie, E.; Lefsrud, M. G.

Comparative shotgun proteomic analysis of wastewater-cultured microalgae: nitrogen sensing and carbon fixation for growth and nutrient removal in *Chlamydomonas reinhardtii*. *J. Proteome Res.* **2015**, 14 (6), 3051-3067. Copyright 2015, American Chemical Society.) (Chapter 9, Section 9.2, Appendix B).

Connecting statement

In Chapter 4, Manuscript II, we performed a label-free comparative shotgun proteomic analysis of wastewater-cultured *C. reinhardtii* at the bench scale. Experiment 2 attempted to address a fundamental problem in wastewater treatment and biomass production of how dynamic cellular adaptations can be characterized to provide biological insight. Experiment 2 accomplished the research objective of elucidating cellular responses and identifying potential targets for genetic improvement by using shotgun proteomics and a systems biology approach. *Chlamydomonas*

demonstrated a remarkable ability to adapt to the availability and source of nitrogen in each respective culture condition, as evidenced by the insignificant difference in final biomass and comparable nutrient removal rates. Here in Chapter 5, additional differentially abundant proteins of interest identified in Experiment 2 are reported. These were not discussed in detail in Chapter 4, and have been published as Supplemental findings of Manuscript II. The specific objective of Chapter 5 is to examine differential proteins that are biosynthesis related, stress related, poorly annotated, and those whose function is unknown, in order to further characterize the cellular responses of *Chlamydomonas* to wastewater processing.

Comparative shotgun proteomic analysis of wastewater-cultured microalgae: Nitrogen sensing and carbon fixation for growth and nutrient removal in *Chlamydomonas reinhardtii*

Anil K. Patel^{*,1}, Eric L. Huang¹, Etienne Low-Décarie² and Mark G. Lefsrud¹

¹Department of Bioresource Engineering, McGill University, Ste. Anne de Bellevue, Quebec H9X 3V9, Canada

²School of Biological Sciences, University of Essex, Colchester CO4 3SQ, United Kingdom

Available at ACS Publication website: <http://pubs.acs.org/doi/suppl/10.1021/pr501316h>

SUPPLEMENTAL FINDINGS

Abstract:

Chlamydomonas reinhardtii was batch cultured for 12 days under continuous illumination to study nitrogen uptake and metabolic responses to wastewater processing. Our approach compared two conditions: (1) artificial wastewater containing nitrate and ammonia and (2) nutrient-sufficient control containing nitrate as sole form of nitrogen. Treatments did not differ in final biomass; however, comparison of group proteomes revealed significant differences. Label-free shotgun proteomic analysis identified 2358 proteins, of which 92 were significantly differentially abundant. We report additional differentially abundant proteins of interest not discussed previously, including biosynthesis related, stress related, poorly annotated, and unknown proteins. Wastewater cells showed higher relative levels of biosynthesis proteins related to B complex vitamins and cobalamin, and stress response proteins related to iron deficiency. Control cells showed higher levels of histone superfamily proteins, sugar metabolism

and nitrogen regulation proteins, and nutrient limitation and oxidative stress response proteins. Control had a higher abundance of poorly annotated and unknown proteins, but not proteins associated with neutral lipid biosynthesis. Enriched pathways in wastewater, included RNA degradation, thiamine metabolism and one carbon pool by folate, and those in nitrate only control, notably, calcium signaling, systemic lupus erythematosus, protein processing in endoplasmic reticulum and Arf/Sar family. Proteome analysis found that N-limitation did not adversely affect growth or biomass yields in control cells at the flask bench scale, due in part to the role of stress response proteins. Over-enrichment of ammonia-N did not adversely affect cellular physiology or yields in wastewater cells. Enriched pathways related to the stress response in control, most notably, glycolysis/gluconeogenesis, glutathione metabolism, oxidative phosphorylation, peroxisome and proximal tubule bicarbonate reclamation represent potential targets for genetic improvement requiring targeted elucidation.

5.1. Introduction

As reported in Chapter 4, Manuscript II,⁷⁵ our experimental design involved propagating *C. reinhardtii* cells in batch cultures for 12 days under continuous illumination to compare two treatment conditions: (1) artificial wastewater containing nitrate and ammonia, and (2) nutrient-sufficient control containing nitrate as sole form of nitrogen. Despite the increased availability of nitrogen in the form of ammonia, a preferred source of nitrogen for green algae and higher plants,^{60,99} the wastewater cells did not grow faster, accumulate higher biomass, or uptake nutrients faster. Nonetheless, *Chlamydomonas* showed a remarkable ability to adapt to local conditions in each treatment. Surprisingly, even after 12 days the wastewater group was still engaged in photosynthetic carbon fixation, cell division, and biosynthesis of amino acids, fatty

acids, secondary metabolites and chlorophyll. Control cells showed continued photosynthesis, synthesis and use of starch, and recycling of amino acids, which suggested adaptations to the onset of N-limitation. The typical cellular response to N-deprivation by C and N responsive pathways is down-regulation of carbon assimilation and chlorophyll biosynthesis, up-regulation of lipid biosynthesis, and higher abundances of oxidative stress response enzymes.^{43,245} Different from other differential gene expression studies on nitrogen stress response in *C. reinhardtii*,^{35,42} and proteomic and/or metabolomic time-course studies manipulating only ammonia^{39,43,62} or nitrate,⁵⁹ higher levels of enzymes and proteins related to lipid biosynthesis was not found in the control condition. Furthermore, a pattern search of *A. thaliana* GO annotation terms related to nitrogen starvation found no proteins identified in this experiment. Here we report additional differentially abundant proteins of interest not discussed in Chapter 4, Manuscript II, including biosynthesis related, stress related, poorly annotated, and unknown proteins. Proteins lacking KEGG pathway association are evaluated by use of functional annotation tools such as Pfam, Panther, GO and KOG ontology databases, JGI Phytozome, and literature related to *Chlamydomonas* and *Arabidopsis*.

5.2. Materials and methods

Details can be found in the Materials and methods section of Chapter 4, Manuscript II, for experimental design, organism, and culture conditions (Section 4.2.1), growth and nutrient removal (Section 4.2.2), protein extraction and digestion (Section 4.2.3), 2D LC–MS/MS (Section 4.2.4), and database searching (Section 4.2.5).

5.2.1. Selection of differentially abundant proteins, functional enrichment and pathway analysis

A minimum of 4 spectra per protein was required for spectral counting and bioinformatics analysis.²²⁶ As described in Chapter 4 (see additional details in Materials and methods, Sections 4.2.6 and 4.2.7, and Results and discussion, Section 4.3),⁷⁵ we used the QSpec software to identify statistically significant differentially abundant proteins by culture group using spectral count normalization and estimates of false discovery rates (FDR).¹⁷⁰ A threshold of Z-statistic $\geq |3.69|$ and corresponding to a directional FDRup of 5% (0.05) was used, unless the less stringent Z-statistic $\geq |3.14|$ threshold, corresponding to a directional FDRup of 10% (0.10) was specified. Functional attributes of the data set were analyzed using Phytozome annotation (*Chlamydomonas* v9.1 and *Arabidopsis* v9.1). Pattern searches of GO annotation data from *A. thaliana* was used to produce GOSLIM files targeting specific processes and functions. Functional enrichment of biological pathways was performed using the web-based annotation integration tool Algal Functional Annotation Tool (AFAT).¹⁵⁵ Phytozome v5 alphanumerical transcript IDs of significantly differentially abundant proteins identified by QSpec were queried against the entire *C. reinhardtii* genome. Manual curation of enrichment results was performed for all proteins discussed, including those that received multiple hits in AFAT-assigned KEGG pathways. Significantly differentially abundant proteins were represented in both tabular and graphical format (Table 4.1 and Figure 4.3), where metabolic mapping was performed using the KEGG pathway mapping software iPath2.0. The open source R statistical package was used for data analysis and generation of plots not performed with the aforementioned software.

5.3. Results and discussion

QSpec software identified 92 statistically significant differentially abundant proteins with a directional FDRup of 5% (0.05), of which 42 and 50 showed higher levels of relative abundance in wastewater and control, respectively (Table 5.1). Of these 92 differential proteins, 58 (32 in wastewater and 26 in control) were assigned KEGG group association (*ie.*, KEGG KO) by the AFAT tool (Chapter 4, Manuscript II, Table 4.1). Of the 34 differential proteins lacking KEGG association, 8 in wastewater and 20 in control had some functional annotation or description in the Phytozome databases, AFAT tool, and the literature. The remaining 6 differential proteins, 2 and 4 in wastewater and control, respectively, were unknown proteins lacking any annotation including description or Pfam¹⁷⁵ family membership. Despite this limitation in functional annotation, the AFAT tool matched the 58 responsive differential proteins to 61 KEGG pathway terms (*ie.*, KEGG ko) in both conditions, and manual curation of functionally enriched KEGG pathway terms (*ie.*, KEGG ko) was performed (described in detail in Chapter 4, Materials and methods). Manual curation produced 32 proteins enriched in 17 KEGG pathways in the wastewater group, and 26 proteins enriched in 16 pathways in control (Table 4.1). In order to visualize functional differences between treatment groups, differentially abundant proteins from Table 4.1 were mapped to KEGG-derived metabolic pathways using iPath2.0.^{74,180} Only those differential proteins with an assigned function from AFAT (KEGG KO and/or Enzyme EC number) could be inputted, omitting several differentially abundant proteins (Table 5.1), and not all protein functions were matched by the current iPath2.0 metabolic map. Despite the limitations in functional annotation, responsive proteins mapped to 97 metabolic map elements (60 in wastewater and 37 in control) to elucidate a pathway-centric overview of specific functional

reactions of potential interest for wastewater processing (Chapter 4, Manuscript II, Figure 4.3).^{74,180}

In wastewater, RNA degradation, Thiamine metabolism pathway, and One carbon pool by folate make up the enriched pathways by AFAT significance score and manual curation not discussed in Chapter 4 (Table 4.1). In the control group Calcium signaling pathway, Systemic lupus erythematosus, Arf/Sar family, and Protein processing in endoplasmic reticulum make up the enriched pathways not discussed in Chapter 4 (Table 4.1). Also, Huntington's disease pathway was enriched in wastewater cells, and suggested iron limitation. In the control group the Glycolysis/Gluconeogenesis pathway was enriched due to the onset of N-limitation, and Glutathione metabolism, Oxidative phosphorylation, Proximal tubule bicarbonate reclamation and Peroxisome pathway due to oxidative stress. Interestingly, KEGG pathways not enriched in control, included Fatty acid biosynthesis and Biosynthesis of unsaturated fatty acids.

Significant supplemental information proteins with KEGG association (Table 4.1 and Figure 4.3) and differential proteins lacking KEGG association (Table 5.1), including biosynthesis related proteins, are discussed in Sections 5.3.1.1 – 5.3.1.3. Sections 5.3.2.1 – 5.3.2.3 discuss stress related proteins found to be significant in both conditions. Poorly annotated and unknown proteins are discussed in Sections 5.3.3.1 – 5.3.3.2. At first mention the putative functional name/description of a significant differential protein is given, followed by the Phytozome gene accession name in brackets and gene alias, if any, in italics. Subsequent mention uses putative enzyme abbreviations, or gene aliases, if any. Upper case is used for nuclear encoded genes and proteins, lower case for organelle encoded proteins, where all genes in Phytozome are nuclear encoded.²¹⁴

Table 5.1. Proteins significantly increased in abundance by culture condition with QSpec statistics and normalized spectral counts^a

Wastewater group (AWW)														
Protein description/function ^b	Alias ^b	Gene accession ^b	Length ^c	CTRL_1 ^d	AWW_1 ^d	CTRL_2 ^d	AWW_2 ^d	CTRL_3 ^d	AWW_3 ^d	CTRL_4 ^d	AWW_4 ^d	Log2 FC ^d	Zstat ^d	FDRup ^d
Chlorophyll a/b binding protein of LHClI	LHCBM5	Cre03.g156900.t1	268	59	73	29	73	50	91	28	128	0.724	5.4361	0.00034
Chlorophyll a/b binding protein of LHClI	LHCBM6	g6631.t1	253	60	77	33	76	45	88	33	146	0.78	6.0387	4.00E-05
Chlorophyll a/b binding protein of LHClI	LHCBM7	Cre12.g548950.t1	249	77	83	42	99	62	97	50	161	0.54	4.6228	0.00424
Chlorophyll a/b binding protein of LHClI	LHCB4	Cre17.g720250.t1	280	75	167	74	155	97	171	120	161	0.434	4.7068	0.00331
Chlorophyll a/b binding protein of LHClI	LHCA3	g11502.t1	267	79	168	17	136	89	80	15	67	0.786	6.3857	1.00E-05
Light-harvesting protein of LHClI	LHCA7	Cre16.g687900.t1	241	14	28	10	30	18	37	11	35	0.881	3.8252	0.03344
Transketolase [EC: 2.2.1.1]	TRK1	Cre02.g080200.t1	718	37	113	69	107	105	183	72	169	0.593	5.6489	0.00017
Alanine aminotransferase [EC: 2.6.1.2]	AAT1	Cre10.g451950.t1	521	2	19	2	9	3	35	5	13	2.08	5.0072	0.00135
Fructose-bisphosphate aldolase class I [EC: 4.1.2.13]	FBA3	Cre05.g234550.t2	377	57	148	68	114	83	185	101	121	0.466	4.5849	0.00473
Fructose-1,6-bisphosphatase plastid precursor [EC: 3.1.3.11]	FBP1	Cre12.g510650.t1	415	13	19	13	29	12	46	17	42	0.884	3.7857	0.03642
Phosphoribulokinase chloroplast precursor [EC: 2.7.1.19]	PRK1	Cre12.g554800.t1	375	30	78	42	82	37	96	51	86	0.691	4.9392	0.00165
Ferredoxin	FDX1	g15094.t1	126	6	39	0	38	24	116	19	75	1.935	9.206	0
Chloroplastic PSI reaction center subunit N	PSAN	Cre02.g082500.t1	139	9	28	16	29	15	55	28	54	0.843	4.0503	0.01991
Cytochrome c6	CYC6	Cre16.g651050.t1	148	0	22	3	21	4	3	2	25	2.337	5.1339	0.00091
Aspartate-semialdehyde dehydrogenase [EC: 1.2.1.11]	ASD1	g9648.t1	370	45	100	15	52	52	87	34	51	0.587	3.8456	0.03202
Cobalamin-independent methionine synthase [EC: 2.1.1.14]	MES1	Cre03.g180750.t1	815	2	63	4	38	4	65	5	68	3.543	9.21	0
Dihydrolipoamide acetyltransferase [EC: 2.3.1.12]	DIA2	Cre03.g158900.t1	494	21	38	18	34	20	63	17	37	0.744	3.8093	0.03453
Branched-chain amino acid aminotransferase [EC: 2.6.1.42]	BCA2	Cre05.g245900.t1	396	4	12	1	6	2	27	4	12	1.812	4.0536	0.01979
Choline dehydrogenase [EC: 1.1.99.1]		Cre12.g514200.t1	611	2	14	3	12	1	23	2	17	2.401	5.0032	0.00136
Acidic ribosomal protein P1	RPP1	g17858.t1	107	12	17	3	26	5	56	11	28	1.562	5.7934	1.00E-04
Plastid ribosomal protein L7/L12	PRPL7	Cre13.g581650.t1	162	30	89	43	61	31	88	54	101	0.7	4.98	0.00146
Plastid ribosomal protein L28	PRPL28	Cre06.g265800.t1	195	4	13	2	12	5	19	5	15	1.41	3.6993	0.04367
Methylenetetrahydrofolate reductase (NADPH) [EC: 1.5.1.20]		Cre10.g433600.t1	600	6	19	3	20	7	25	6	29	1.597	4.7909	0.00258
3-oxoacyl-[acyl-carrier protein] reductase [EC: 1.1.1.100]	OAR1	Cre03.g172000.t1	322	10	41	5	14	10	34	7	35	1.525	5.3657	0.00043
Cobalamin synthesis protein		g15619.t1	518	3	25	1	18	3	15	4	36	2.562	5.8176	9.20E-05
Cobalamin synthesis protein		g15199.t1	316	2	52	3	56	3	57	4	62	3.679	9.8329	0
Hydroxypyruvate reductase	HPRI	Cre06.g295450.t1	418	48	74	15	54	37	91	39	94	0.769	5.3525	0.00045
Ferredoxin-nitrite reductase [EC: 1.7.7.1]	NI11	Cre09.g410750.t1	589	8	22	4	5	3	33	4	26	1.717	4.6738	0.00364
Porin/voltage-dependent anion-selective channel protein	ASC2	Cre05.g241950.t1	276	60	131	85	151	78	136	77	126	0.475	4.6968	0.00341
Superoxide dismutase [Fe] [EC: 1.15.1.1]	FSO1	Cre10.g436050.t1	234	11	64	39	58	32	62	37	55	0.606	3.7158	0.04214
Magnesium chelatase subunit I [EC: 6.6.1.1]	CHLI1	Cre06.g306300.t1	417	12	39	10	24	17	38	16	32	0.86	3.7116	0.04257
Thiazole biosynthetic enzyme	THI4	Cre04.g214150.t1	357	11	18	1	6	7	31	0	20	1.417	3.9704	0.02404
NAD(P)-binding Rossmann-fold superfamily protein		g2755.t1	372	14	35	9	24	5	27	16	26	0.961	3.861	0.03099
Cobalamin synthesis protein		Cre02.g118400.t1	624	0	45	1	32	1	44	2	46	4.146	8.3818	0
Tetrapeptide repeat (TPR)-like superfamily protein		Cre09.g404000.t1	215	10	28	11	22	9	35	16	46	1.076	4.3586	0.00896
X-Pro dipeptidyl-peptidase (S15 family)		Cre12.g524600.t1	485	4	14	0	13	3	16	4	20	1.881	4.399	0.00803
5'-AMP-activated protein kinase, gamma subunit		Cre12.g528000.t1	409	24	39	26	59	35	75	37	78	0.628	3.9622	0.02461
function unknown		Cre07.g340450.t1	4952	26	52	21	49	18	27	21	56	0.723	3.9343	0.02621
Low-CO ₂ inducible protein	LCIB	Cre10.g452800.t1	448	15	58	48	46	27	116	43	53	0.602	3.95	0.02532
Low-CO ₂ inducible protein	LCIC	Cre06.g307500.t1	443	31	69	52	60	36	118	50	78	0.547	3.9629	0.02461
function unknown		Cre07.g352000.t1	453	39	86	25	105	39	175	24	112	1.186	7.7372	0
function unknown		Cre11.g467400.t1	602	5	13	5	10	0	7	3	17	1.535	3.7453	0.03961

Control group (CTRL)

Protein description/function ^b	Alias ^b	Gene accession ^b	Length ^c	CTRL_1 ^d	AWW_1 ^d	CTRL_2 ^d	AWW_2 ^d	CTRL_3 ^d	AWW_3 ^d	CTRL_4 ^d	AWW_4 ^d	Log2 FC ^d	Zstat ^d	FDRup ^d
NADH-dependent glutamate synthase [EC:1.4.1.14]	GSN1	Cre13.g592200.t1	2251	53	24	46	47	50	30	47	30	-0.967	-6.0062	1.40E-05
Ferredoxin-dependent glutamate synthase [EC:1.4.7.1]	GSF1	Cre12.g514050.t1	1629	82	58	67	75	83	92	91	85	-0.462	-4.0489	0.01329
Carbonic anhydrase (Carbonate dehydratase 1) [EC 4.2.1.1]	CAH1	Cre04.g223100.t1	377	55	78	200	52	93	118	105	67	-0.912	-8.649	0
Photosystem I reaction center subunit III	PSAF	Cre09.g412100.t1	227	198	97	179	93	72	80	67	189	-0.527	-5.7988	3.30E-05
Photosystem I reaction center subunit VI	PSAH	Cre07.g330250.t1	130	267	159	146	208	155	286	123	85	-0.297	-3.8079	0.02378
Pre-apoptocytanin	PCY1	g3784.t1	145	46	87	387	102	60	170	113	151	-0.623	-7.4129	0
Argininosuccinate synthase [EC: 6.3.4.5]	AGS1	Cre09.g416050.t1	441	44	48	78	60	62	74	81	68	-0.483	-3.7827	0.02518
Argininosuccinate lyase [EC 4.3.2.1]	ARG7	Cre01.g021250.t1	508	39	31	36	27	32	22	31	27	-0.743	-3.95	0.01689
Carbamoyl phosphate synthase, small subunit ^e	CMP2	Cre06.g308500.t1	461	20	14	17	19	23	23	31	18	-0.695	-3.1595	0.09366 ^g
Alcohol/acetaldehyde dehydrogenase [EC 1.1.1.1 1.2.1.10]	ADH1	g18056.t1	954	87	74	104	70	85	59	111	85	-0.808	-7.0279	0
Alcohol dehydrogenase [EC 1.1.1.2]	ADH7	g15030.t1	395	24	5	13	10	15	3	16	3	-1.997	-5.6199	6.80E-05
Glyceraldehyde 3-phosphate dehydrogenase [EC 1.2.1.12]	GAP1	Cre12.g485150.t1	371	154	67	110	91	181	73	134	73	-1.337	-13.065	0
Agmatine iminohydrolase [EC 3.5.3.12]	AIH2	Cre01.g009350.t1	430	18	0	14	11	19	1	11	0	-2.415	-6.2432	5.00E-06
Sodium/potassium-transporting ATPase [EC 3.6.3.9]		Cre06.g263950.t1	1214	12	0	3	1	8	0	6	3	-2.428	-4.2051	0.00884
Histone H2A	HAV	Cre13.g567700.t1	144	10	11	48	15	17	13	14	15	-1.062	-4.2973	0.00682
Histone H2B	HTB37	Cre13.g590750.t1	155	55	40	91	42	53	44	48	42	-0.946	-6.4297	2.00E-06
Histone 3	HTR13	Cre06.g265000.t1	192	22	4	6	3	6	7	14	11	-1.291	-3.7615	0.02636
Starch phosphorylase [EC: 2.4.1.1]	PHO2	Cre07.g336950.t1	872	40	23	40	37	33	33	35	32	-0.612	-3.6797	0.03172
Granule-bound starch synthase 1 [EC: 2.4.1.242]	GBS1	Cre17.g721500.t1	726	87	83	98	99	99	74	105	99	-0.515	-5.0389	0.00062
Aconitate hydratase [EC 4.2.1.3]	ACH1	Cre01.g042750.t1	828	84	71	94	70	76	91	77	88	-0.446	-3.9758	0.0159
Chlorophyll a/b binding protein of LHClI	LHCBM3	g5059.t1	257	102	97	302	117	217	102	196	169	-1.15	-14.142	0
Glutathione peroxidase [EC: 1.1.1.9]		g8342.t1	259	0	7	0	6	0	5	2	2	-2.173	-3.5142	0.04561
ADP/ATP carrier protein, mitochondrial	ANT1	Cre09.g386650.t1	308	138	125	101	151	133	99	156	133	-0.44	-4.7659	0.00161
2-cys peroxidoredoxin	PRX2	Cre02.g114600.t1	198	60	68	139	71	93	76	66	80	-0.671	-5.7741	3.70E-05
Ubiquinol-cytochrome c reductase subunit 7 [EC:1.10.2.2]	QCR7	g5901.t1	123	24	26	57	23	30	21	38	28	-0.981	-5.3406	0.0002
Protein disulfide isomerase 1 [EC:5.3.4.1]	RB60	Cre02.g088200.t1	532	50	57	96	57	46	59	61	66	-0.465	-3.6548	0.03352
ADP-ribosylation factor family		g2791.t1	181	4	4	17	4	8	5	10	5	-1.411	-3.6563	0.03352
Triacylglycerol lipase and Flagellar Associated Protein	FAP12	g9673.t1	483	3	4	4	3	11	2	21	4	-1.893	-4.3617	0.00571
Triose-phosphate transporter	TPT3	Cre01.g045550.t1	406	2	3	100	3	32	4	41	2	-4.003	-10.383	0
Carbohydrate-binding-like fold protein (<i>A. thaliana</i>)		Cre12.g492750.t1	3466	11	0	1	0	8	0	5	3	-2.181	-3.6707	0.03243
Plastid transcriptionally active 16 (<i>A. thaliana</i>)		Cre02.g081250.t1	763	45	24	85	27	24	49	24	31	-0.812	-4.8128	0.00137
Purple acid phosphatase	MPA9	Cre11.g476700.t1	629	44	4	18	5	33	19	17	5	-2.15	-7.639	0
Ca ²⁺ -dependent phospholipid-binding protein		Cre02.g110350.t1	278	6	13	24	8	12	3	11	5	-1.208	-3.6911	0.03102
Flagella membrane glycoprotein, major form	FMG1-B	g9144.t1	4389	37	36	25	33	39	42	65	26	-0.687	-4.3322	0.00618
Predicted protein with ankrin repeats	ANK22	Cre03.g173350.t1	368	4	3	14	1	3	3	13	4	-1.88	-3.8482	0.02155
Actin regulatory proteins (gelsolin/villin family)		Cre12.g524400.t1	391	6	4	23	4	6	6	8	4	-1.542	-3.9149	0.01848
YbaB/EbfC DNA-binding family protein		Cre10.g458550.t1	157	9	5	2	4	20	7	22	9	-1.48	-4.2715	0.00736
Mitochondrial ATP synthase associated 31.2 kDa protein	ASA4	Cre13.g581600.t1	325	50	55	133	75	58	69	63	60	-0.612	-5.1646	0.00039
Low-CO ₂ inducible protein	LCID	Cre04.g222800.t1	478	34	17	89	13	70	64	47	21	-1.477	-9.1179	0
Chloroplast thylakoid membrane cellular component protein	CGL129	Cre05.g233950.t1	144	4	10	22	4	11	3	10	4	-1.474	-4.0845	0.01209
Chloroplast thylakoid membrane cellular component protein		Cre10.g433950.t1	151	45	7	345	9	8	1	12	5	-4.37	-14.78	0
Flagellar Associated Protein	FAP211	Cre02.g077750.t1	773	112	36	26	40	27	29	28	32	-0.844	-5.2158	0.00032
Cell wall protein perophorin-C8	PHC8	Cre17.g71850.t1	603	10	1	4	2	12	0	5	1	-2.692	-4.5618	0.00312
Cell wall protein perophorin-C3	PHC3	g53838.t1	443	29	7	12	13	22	12	12	13	-1.036	-3.9566	0.01689
Perophorin protein family		g17202.t1	763	27	12	7	11	13	9	19	7	-1.135	-3.9582	0.01659
Perophorin protein family		Cre04.g221450.t1	756	51	9	9	29	19	24	18	8	-0.844	-3.8303	0.02257
Putative ribosome protein	NSG1	Cre17.g708750.t1	314	85	43	90	48	63	32	65	34	-1.311	-9.5242	0
Function unknown		Cre17.g707900.t1	355	5	3	11	2	8	6	10	3	-1.591	-3.6203	0.03619
Function unknown		Cre12.g544450.t1	784	55	46	59	66	68	61	73	58	-0.535	-4.0769	0.01232
function unknown		Cre09.g405500.t1	255	38	1	24	8	38	1	27	0	-3.728	-8.7337	0
function unknown		g2947.t1	2804	33	5	27	7	25	1	15	10	-2.106	-7.216	0

5.3.1. Differential analysis and functional enrichment

5.3.1.1. Additional biosynthesis proteins enriched in wastewater by AFAT score.

Proteins related to the B complex vitamins cobalamin (B₁₂), thiamine (B₁), and folate (B₉) were found to be significantly more abundant in wastewater cells. Two cobalamin synthesis proteins (g15619.t1 and g15199.t1) (Table 4.1 and Figure 4.3), described as plastid transcriptionally active 17 in *A. thaliana*, were enriched in the RNA degradation KEGG pathway. In *Chlamydomonas* cobalamin is a cofactor for enzymes catalyzing rearrangement-reduction reactions or methyl transfer reactions in the cytosol.²⁵² The thiazole biosynthetic enzyme (Cre04.g214150.t1.3; *THI4*), with KOG function of thiamine biosynthesis and DNA damage tolerance was enriched in the Thiamine metabolism pathway, but lacked a score in the AFAT tool. It is involved in the synthesis of the thiazole moiety of thiamine pyrophosphate (B₁), which plays a fundamental role in energy metabolism by acting as an essential cofactor for enzymes such as transketolase and α -ketoglutarate dehydrogenase. Methylenetetrahydrofolate reductase (NADPH) (MTHFR) (Cre10.g433600.t1.2) had higher abundance in the One carbon pool by folate KEGG pathway.

5.3.1.2. Additional proteins enriched in control by AFAT score

In the control group additional proteins enriched in KEGG pathways included the mitochondrial ADP/ATP carrier protein (Cre09.g386650.t1.2; *ANT1*) with higher abundance in the Calcium signaling pathway (Table 4.1 and Figure 4.3); and the histone super family proteins Histone H2B (Cre13.g590750.t1.2; *HTB37*) and Histone 3 (Cre06.g265000.t1.2; *HTR13*), both members of the Pfam Core histone H2A/H2B/H3/H4 protein family (PF00125). The H3 and H4 histone DNA binding superfamily proteins are involved in transcriptional activation through hyperacetylation, and chromatin compaction and gene repression through hypoacetylation, as

shown in gene expression in *Arabidopsis*.²⁵³ Histone H2A (Cre13.g567700.t1.2; *HAV*) a core histone for nucleosome formation. All three histone proteins were enriched in the Systemic lupus erythematosus KEGG pathway. Higher relative abundances of these proteins were not expected. Histone proteins play a critical role in preserving chromatin organization, but are not known to be greatly effected by nutrient deprivation.³⁵ Proteomic analysis of ammonia-N deprived cells showed levels of histones and other core proteins remained mostly unchanged over time.³⁹

The ADP-ribosylation factor family protein (g2791.t1, K0 7977) was enriched in the Arf/Sar family, other KEGG pathway, lacked a score in AFAT, and showed GO biological process of small GTPase mediated signal transduction and molecular function of GTP binding. Protein disulfide-isomerase (Cre02.g088200.t1.2; *RB60*) also lacked an AFAT score and was enriched in the Protein processing in endoplasmic reticulum pathway. This enzyme has Pfam Thioredoxin family membership (PF00085) and GO biological process of cell redox homeostasis. In the chloroplasts of *C. reinhardtii*, PDI RB60 is a redox sensor component of an mRNA-binding protein complex associated with photo-regulation of translation in the dark, and is also implicated in formation of regulatory disulfide bonds in chloroplasts.²⁵⁴

5.3.1.3. Additional proteins in control lacking AFAT annotation

In the control group 3 additional proteins showed higher relative abundances, but lacked KEGG association (Table 5.1). First, triose-phosphate transporter (Cre01.g045550.t1.2; *TPT3*) is described as glucose-6-phosphate/phosphate translocator-related in *A. thaliana*, belongs to the Pfam Triose-phosphate transporter family (PF03151) and is associated with sugar metabolism. Located between the inner and outer membrane of the chloroplast, GPTs mediate the transport of carbon between plastids and the cytosol in the form of glucose 6-phosphate (Glc-6-P) for glycolysis, and the oxidation of glucose in the pentose phosphate pathway.²⁵⁵ This transporter

had KOG function of phosphoenolpyruvate/phosphate antiporter, in the export of triose phosphate in exchange for inorganic phosphate used for ATP regeneration in the light reactions. Second, the *A. thaliana* described carbohydrate-binding-like fold protein (Cre12.g492750.t1.3) has Pfam Starch binding domain family membership (PF00686), GO biological process of carbohydrate metabolic process, and GO molecular function of starch binding. Third, the *A. thaliana* described plastid transcriptionally active 16 (Cre02.g081250.t1.2) showed KOG predicted dehydrogenase function, nitrogen metabolic regulation (Nmr) in Panther (14194), and Nmr-A-like family membership in Pfam (PF05368). It is one of eighteen components, called plastid transcriptionally active chromosome proteins (pTACs). pTACs are associated with plastid gene expression, and may play roles in post-transcriptional processes, including RNA processing and/or mRNA stability.²⁵⁶ Interestingly, pTAC 17 is associated with cobalamin synthesis and showed higher abundance in wastewater cells (Section 5.3.1.1).

5.3.2. Stress response proteins

Similar growth curves suggested cells in neither culture group were in a complete stress response (Figure 4.1a). The absence of aggressive perturbation by nutrient deprivation is also confirmed by the lack of a dramatic shift at the proteome level between treatment groups, and was not unexpected given the subtle manipulation of macronutrients. Our experimental design did not use a control group held in exponential phase with continuous harvesting of cells and nutrient replenishment. Instead, addition of ammonia-N in the wastewater condition ensured over-enrichment of nitrogen, and cells in both groups were allowed to proceed to steady state, similar to high-density wastewater batch cultures. As discussed in Chapter 4, a fundamental question presented itself, namely, whether the biological variability detected and reported here, was

caused by differences in nitrogen source and loading associated with wastewater processing, and not simply indirect compensatory effects i.e., the control group cells employing physiological mechanisms to reverse the onset of nutrient perturbation. A pattern search of *A. thaliana* GO annotation terms related to nitrogen starvation found no proteins identified in this experiment. Furthermore, only 1 differentially expressed protein related to fatty acid biosynthesis or TAG accumulation was identified in the control group (Section 5.3.2.2 below), and none with KEGG pathway enrichment. Overall, no clear pattern is discernable for proteins related to a stress response, although evidence of oxidative stress was detected in control cells, and iron deficiency in wastewater cells.

5.3.2.1. Stress related proteins in wastewater

In the wastewater cultures, the superoxide dismutase [Fe] (Cre10.g436050.t1.2; *FSDI*) was enriched in the Huntington's disease KEGG pathway (Table 4.1 and Figure 4.3). It belongs to the Iron/manganese superoxide dismutase families in Pfam (PF00081, PF02777), has GO biological process of reactions and pathways involving the superoxide anion O_2^- (superoxide free radical) and molecular function of catalyzing $2 \text{ superoxide} + 2 \text{ H}^+ = O_2 + \text{hydrogen peroxide}$. Higher levels of this enzyme increases the capacity of *Chlamydomonas* to detoxify superoxide during Fe limitation stress.²⁵⁷ Also enriched in this KEGG pathway was the Porin/voltage-dependent anion-selective channel protein (Cre05.g241950.t1.2; *ASC2*) with GO cellular component of mitochondrial outer membrane and biological process of regulation of anion transport.

5.3.2.2. Control cells showed evidence of nutrient limitation

In control cells glyceraldehyde 3-phosphate dehydrogenase (GAPDH) [EC 1.2.1.12] (Cre12.g485150.t1.2; *GAP1*), discussed in Chapter 4 (Section 4.3.3.4), was enriched in the

Glycolysis/Gluconeogenesis pathway. This enzyme is associated with a stress response to low nutrient conditions.²⁴³ Purple acid phosphatase 15 (PAP) (Cre11.g476700.t1.2; *MPA9*) showed higher abundance (Table 5.1) and has GO molecular function of protein serine/threonine phosphatase activity. PAPs are metalloenzymes that hydrolyse phosphate esters and anhydrides under acidic conditions, and are implicated in acclimation to nutritional phosphate deprivation.²⁵⁸ In phosphate-starved *Arabidopsis* plants, PAPs have been shown to scavenge phosphate from extracellular phosphate esters by root cells, and function in intracellular vacuolar phosphate recycling.²⁵⁹ Triacylglycerol lipase and Flagellar Associated Protein (g9673.t1; *FAP12*) showed higher abundance, has Lipase (class 3) family membership in Pfam (PF01764) and is discussed in Chapter 4 (Section 4.3.3.4). As mentioned, pathways not enriched in control included Fatty acid biosynthesis and Biosynthesis of unsaturated fatty acids, which demonstrated that the N-deprivation survival response had not been induced in control cells.

5.3.2.3. Oxidative stress proteins were enriched in control

The typical cellular response to N-deprivation by carbon and nitrogen responsive pathways is down-regulation of carbon assimilation and chlorophyll biosynthesis, and up-regulation of lipid biosynthesis and oxidative stress response.^{43,245} A number of proteins associated with oxidative stress were enriched in the control cells. Glutathione peroxidase (GPx) (g8342.t1) was enriched in the Glutathione metabolism KEGG pathway and is associated with the oxidative stress response in GO biological process. The enzyme has GO molecular function of glutathione peroxidase activity and catalyzes the reaction $2 \text{ glutathione} + \text{hydrogen peroxide} = \text{oxidized glutathione} + 2 \text{ H}_2\text{O}$. The ubiquinol-cytochrome *c* reductase subunit 7 protein (complex 3) (g5901.t1; *QCR7*) was enriched in the Oxidative phosphorylation pathway. In *A. thaliana*, GO biological process and GO molecular function identify this multi-subunit enzyme as complex III,

containing ten polypeptide subunits that include four redox centers: cytochrome *b/b6*, cytochrome *c1* and an 2Fe–2S cluster. It is located in the mitochondrial inner membrane and forms part of the mitochondrial respiratory chain that catalyzes oxidation of ubiquinol by oxidized cytochrome *c1*. The sodium/potassium-transporting ATPase (Cre06.g263950.t1.3) was enriched in Proximal tubule bicarbonate reclamation pathway. Described in *A. thaliana* as an endoplasmic reticulum-type calcium-transporting ATPase 3, it has KOG function Na⁺/K⁺ ATPase, alpha subunit (membrane protein, Ca²⁺-transporting ATPase). Alcohol dehydrogenase (ADH) (g15030.t1; *ADH7*) was more abundant. It is a KOG alcohol dehydrogenase (class V) enzyme belonging to the aldehyde dehydrogenase (ALDH) gene superfamily of enzymes performing NAD⁺- or NADP⁺- dependent conversion of aldehydes to carboxylic acids. In *Arabidopsis* and *Chlamydomonas* they function as ‘aldehyde scavengers’ that remove reactive aldehydes during the oxidative degradation of lipid membranes (lipid peroxidation).²⁶⁰ ADH was enriched in the Glycolysis/Gluconeogenesis pathway, and discussed in Chapter 4 (Section 4.3.3.4).

Aconitate hydratase (Cre01.g042750.t1.2; *ACH1*) was enriched in the Biosynthesis of alkaloids derived from terpenoid and polyketide pathway. It is part of the KOG functional group RNA-binding translational regulator IRP (aconitase superfamily). In *A. thaliana* it has multiple GO annotations including biological processes of mitochondrial, isocitrate metabolic process, response to oxidative stress, and GO molecular function of aconitate hydratase activity for the interconversion of citrate and isocitrate. 2-cys peroxiredoxin (2-cys Prx) (Cre02.g114600.t1.2; *PRX2*) was listed as K0 3386 in Phytozome and enriched in the Peroxisome KEGG pathway. The enzyme has KOG (0852) Alkyl hydroperoxide reductase, thiol specific antioxidant and related enzymes membership and GO molecular function of antioxidant activity. It is part of the

antioxidant defense system of chloroplasts in *Arabidopsis* and mitigates oxidative damage in photosynthetic membranes by reducing toxic peroxides to their corresponding alcohols.²⁶¹

Carbonic anhydrase (CA1) (Cre04.g223100.t1.2; *CAH1*), described as carbonate dehydratase 1 in *C. reinhardtii*, was enriched in the Nitrogen metabolism pathway. This enzyme is localized in the periplasmic space, is low-CO₂ inducible gene regulated and has carbonate dehydratase activity.²⁶² Finally, 4 perophroin protein family members showed significantly higher relative abundances but lacked further annotation (Section 5.3.3.2).

5.3.3. Poorly annotated and unknown proteins

A continuing challenge in plant and algae proteomics is the complexity of the respective eukaryotic genomes, gaps in annotation databases and tools, and not an insignificant number of proteins with unknown or poorly described functions.²¹⁴ Association with a protein family would at the very least indicate functional units present to hypothesize a biological role.⁷⁴ Of those proteins lacking KEGG association, 8 wastewater and 20 control proteins had some functional annotation or description, and 2 and 4 proteins, respectively, were unknown proteins lacking any annotation including Pfam family membership or Phytozome description.

5.3.3.1. Poorly annotated and unknown proteins with higher levels in wastewater

The *A. thaliana* described NAD(P)-binding Rossmann-fold superfamily protein (g2755.t1) lacked KEGG pathway association in AFAT, and showed nitrogen metabolic regulation (Nmr) in Panther, and NmrA-like Pfam membership (PF05368). It had GO chloroplast cellular component and biological process of regulation of nitrogen utilization, and molecular function of repressor activity. The cobalamin synthesis protein (Cre02.g118400.t1.3), described in *A. thaliana* as plastid transcriptionally active 17, showed cobalamin synthesis protein function

in KOG, and GO cellular component of plastid chromosome and chloroplast stroma (Section 5.3.1.1). It is one of eighteen components called plastid transcriptionally active chromosome proteins (pTACs) that are associated with plastid gene expression and may play roles in post-transcriptional processes, including RNA processing and/or mRNA stability.²⁵⁶ Interestingly, pTAC 16 is associated with nitrogen metabolism regulation and showed significantly higher abundance in control cells, as mentioned (Section 5.3.1.3).

The tetratricopeptide repeat (TPR)-like superfamily protein (Cre09.g404000.t1.3) in *A. thaliana* belonged to the Pfam Pentapeptide repeats (8 copies) family (PF00805). The protein (Cre12.g524600.t1.2) had GO biological process of proteolysis and molecular function of aminopeptidase activity, and Pfam X-Pro dipeptidyl-peptidase (S15 family) membership (PF02129). The KOG 5'-AMP-activated protein kinase, gamma subunit (Cre12.g528000.t1.2) had Pfam CBS domain (PF00571). The protein (Cre07.g340450.t1.3) had Pfam memberships of IPT/TIG domain (PF01833), G8 domain (PF10162), and PA14 domain (PF07691) and GO molecular function of protein binding. Two proteins (Cre10.g452800.t1.2 and Cre06.g307500.t1.1) had the Phytozome description of Low-CO₂ inducible protein. *C. reinhardtii* has been shown to modulate photosynthesis to acclimate to CO₂-limiting stress by the induction of the carbon concentrating mechanism (CCM) including carbonic anhydrases and inorganic carbon transporters.²⁶³

The remaining two unknown differential proteins (Cre07.g352000.t1.2 and Cre11.g467400.t1.2) lacked any functional annotation whatsoever from Pfam, the KEGG, MetaCyc, Panther, and Reactome biological pathway databases, or GO, Mapman and KOG ontology databases. Using the protein sequence we attempted to elucidate a biological function

by using BLAST to associate sequence homology with higher plants and organisms. Searches did not return any insight into identity or function.

5.3.3.2. Poorly annotated and unknown proteins with higher levels in control

Additional proteins enriched in the control contained a description and minimal annotation, or no annotation whatsoever. The KOG predicted Ca^{2+} -dependent phospholipid-binding protein (Cre02.g110350.t1.2) and showed C2 domain protein family membership (PF00168). The flagella membrane glycoprotein (major form) (g9144.t1; *FMG1-B*) had KOG function of proteins containing Ca^{2+} -binding EGF-like domains. The predicted protein with ankrin repeats (Cre03.g173350.t1.2; *ANK22*) had Ankyrin repeat Pfam membership (PF00023), KOG function of myotrophin and similar proteins and GO molecular function of protein binding. The KOG actin regulatory proteins (gelsolin/villin family) (Cre12.g524400.t1.2) had family membership in Villin headpiece domain (PF02209) and Gelsolin repeat (PF00626). Finally the Pfam YbaB/EbfC DNA-binding family protein (Cre10.g458550.t1.2) (PF02575) also showed higher levels.

The proteins containing only descriptions, included, a mitochondrial F1F0 ATP synthase associated 31.2 kDa protein (Cre13.g581600.t1.2; *ASA4*); the low- CO_2 inducible protein (Cre04.g222800.t1.2; *LCID*); the *A. thaliana* described chloroplast thylakoid membrane cellular component proteins (Cre05.g233950.t1.2; *CGL129*) and (Cre10.g433950.t1.3); and the Flagellar Associated Protein (Cre02.g077750.t1.2; *FAP211*) with Pfam NYN domain membership (PF01936), described in *A. thaliana* as a putative endonuclease or glycosyl hydrolase.

A number of Pfam Pherophorin protein family members (PF12499) showed significantly higher abundance in control. These included, the cell wall protein pherophorin-C8 (Cre17.g717850.t1.3; *PHC8*); the cell wall protein pherophorin-C3 (g6305.t1; *PHC3*); and two

proteins lacking further description (g17202.t1 and Cre04.g221450.t1.2). In the multicellular green alga *Volvox carteri*, and closely related unicellular *C. reinhardtii*, the presence of reactive oxygen species and peroxophorin family proteins suggested an evolutionary connection between sex and stress at the gene level.²⁶⁴ As mentioned, N-starvation is known to induce gametogenesis and sexual reproduction in *C. reinhardtii*.^{84,234}

The control group contained 4 unknown proteins with significantly higher levels that lacked any functional annotation whatsoever from Pfam, the KEGG, MetaCyc, Panther, and Reactome biological pathway databases, or GO, Mapman and KOG ontology databases. The gene accession names were Cre17.g707900.t1.2, Cre12.g544450.t1.2, Cre09.g405500.t1.3 and g2947.t1. Using the protein sequence we attempted to elucidate a biological function by using BLAST to associate sequence homology with higher plants and organisms. Searches did not return any insight into identity or function.

5.4. Concluding remarks

Differing from studies on harsh nutrient deprivation and/or single nitrogen source manipulation, our label-free shotgun proteomic analysis of wastewater-cultured *C. reinhardtii* contributed novel insights into nitrogen metabolism and carbon fixation by using wastewater containing both nitrate and ammonia. Surprisingly, after 12 days, we found no significant difference in final biomass and OD₆₈₀. This finding demonstrated that even in increasingly N-limited media *C. reinhardtii* continued to grow and attempt to balance its C/N ratio. Wastewater cells showed higher relative abundances of biosynthesis proteins related to B complex vitamins and cobalamin, and the stress response proteins related to iron deficiency. Control cells showed higher levels of histone superfamily proteins, proteins associated with carbohydrate metabolism

and nitrogen regulation, and stress proteins in response to nutrient limitation and oxidative stress. Control cells demonstrated a higher relative abundance of poorly annotated and unknown proteins, but not lipid biosynthesis. Up-regulated pathways in wastewater, included, RNA degradation, Thiamine metabolism and one Carbon pool by folate, and those in nitrate only control, notably, Calcium signaling, Systemic lupus erythematosus, Protein processing in endoplasmic reticulum and Arf/Sar family. Up-regulated pathways related to the stress response in the control condition, included, Glycolysis/Gluconeogenesis, Glutathione metabolism, Oxidative phosphorylation, Peroxisome and Proximal tubule bicarbonate reclamation.

Proteome analysis found that N-limitation did not adversely affect growth or biomass yields in control cells at the flask bench scale cultured in nitrate-N only medium after 12 days. This finding is due in part to the role of stress response proteins, and further demonstrated the resilience of *C. reinhardtii* to abiotic stressors.¹ Over-enrichment of ammonia-N did not adversely affect cellular physiology or yields in wastewater cells. Both these findings are intriguing and support optimism for improvements in bioprocess optimization and future yields in outdoor ponds using different sources of wastewater of varying quality and macronutrient concentration. Up-regulated pathways related to the stress response in the control condition merit further study. Also interesting are the up-regulated biosynthesis pathways identified in wastewater cells such as One carbon pool by folate that lead to secondary compounds. Differential abundance analysis and functional enrichment identified a number of enzymes and potential gene targets for genetic improvement requiring further elucidation using discovery and targeted proteomic techniques. We will continue the identification of candidate pathways at the bench and pilot scale for development of robust strains suitable for scalable outdoor treatment of real wastewaters.

Chapter 6: Manuscript III

Microalgae for wastewater treatment and biomass production: A comparative analysis of pilot scale photobioreactor-cultured *Chlamydomonas reinhardtii*

Anil Patel, Blake Bissonnette, and Mark Lefsrud

Original research article for submission to the journal *GCB Bioenergy*

Connecting statement

The previous Chapters 4 and 5 (Manuscript II and Supplemental findings) examined the growth and nutrient removal responses of *Chlamydomonas reinhardtii* cultured in batch mode over 12 days at the 330 mL bench scale to simulated wastewater processing.⁷⁵ *C. reinhardtii* removed nutrients efficiently, and surprisingly, final biomass concentration was not significantly different between culture conditions. Shotgun proteomic analysis was performed on samples harvested in stationary phase at the end of the experiment and revealed dynamic adaptations by *C. reinhardtii* cells to adjust to their respective culture conditions. In comparison to the two promising candidates identified in Chapter 3 (Manuscript I),²³ *Monoraphidium minutum* sp. and *Tetraselmis suecica* sp., *C. reinhardtii* did not demonstrate the dual-purpose traits of nutrient removal efficiency and high rates of biomass accumulation at the bench scale.

A fundamental problem that needs to be addressed to use microalgae for wastewater treatment and biomass production is the effect on culture performance and yields of scaling up culture size. The global research objective of Experiment 3 was to compare nutrient removal and growth at the bench and pilot scales. In order to accomplish this, we scaled up the culture volume

of *C. reinhardtii* from the 330 mL bench scale to the 10 L photobioreactor (PBR) pilot scale. The same strain of *C. reinhardtii* was propagated over 5 days in batch mode using a pilot scale PBR system comprised of four 10 L culture volume vertical columns in order to examine the growth and nutrient removal response. *C. reinhardtii* was cultured in control and artificial wastewater treatment media of identical compositions as that reported in Chapters 4 and 5. Furthermore, extensive modifications of a vertical column PBR system was performed to accommodate microalgae suspended in liquid medium, including metered airflow, gas mixing functions, and a uniform lighting system. *C. reinhardtii* required CO₂ supplementation and different to the flask cultures, the PBR columns were not maintained in sterile conditions. As in Chapters 3 and 4, the dual-purpose traits of high nutrient removal efficiency and biomass growth were sought, and were determined using similar gravimetric, spectrophotometric and colorimetric analyses. Results are reported and discussed in the context of metabolic constraints to the mass culturing of microalgae, and with insights obtained from proteomic results obtained at the flask scale, as reported in Chapters 4 and 5, which elucidated cellular responses to wastewater processing. A comparison of yields is also made to the two dual-purpose candidates identified in Chapter 3.

Microalgae for wastewater treatment and biomass production: A comparative analysis of pilot scale photobioreactor-cultured *C. reinhardtii*

Running title: Sequenced microalgae for wastewater treatment and biomass

Anil Patel¹, Blake Bissonnette¹, and Mark Lefsrud¹

¹Department of Bioresource Engineering, McGill University, Saints-Anne-de-Bellevue, Quebec H9X 3V9, Canada

Correspondence: Anil Patel, tel. +514 398 8740, fax + 514 398 8387, e-mail: anil.patel@mail.mcgill.ca

Abstract

A fundamental problem in the use of microalgae for wastewater treatment and biomass production is the effect of scaling up culture size on culture performance and yields.

Chlamydomonas reinhardtii was cultured in batch mode for 5 days using a pilot scale photobioreactor (PBR) system under continuous illumination in order to investigate phosphorus and nitrogen removal and growth responses to wastewater processing. Our approach compared two conditions: (1) artificial wastewater containing nitrate and ammonia and (2) nutrient-sufficient control containing nitrate as the sole form of nitrogen. The PBR system was comprised of four 10 L culture volume vertical columns, air was supplemented with CO₂ in a ratio of (97/3, v/v), and cultures were propagated under non-sterile conditions. *Chlamydomonas* removed phosphorus and nitrogen from solution efficiently in both culture conditions. Treatment was found to have a significant effect on final biomass. Final dry cell mass and biomass productivity were significantly higher in artificial wastewater cultures. Control cultures showed evidence of the onset of nutrient starvation. Results were compared to biomass yields from the same strain propagated at the bench scale using 330 mL flask culture volumes, identical wastewater and

control media, continuous light, and sterile conditions with no CO₂ supplementation. Cells cultured in control medium showed similar final biomass yields, but higher biomass productivity in the PBR cultures. Cells cultured in wastewater medium showed both higher final biomass and biomass productivity in the PBR cultures. Biomass yields were lower than that of other reported eukaryotic green microalgae cultured in real and artificial wastewater. *Chlamydomonas* did not demonstrate the desired dual-purpose traits of high nutrient removal efficiency and biomass productivity at either scale. The microalga did demonstrate a remarkable ability to adapt to environmental conditions associated with mass culturing, including light attenuation, fluid dynamics, and nutrient limitation. This study highlights the importance of characterizing microalgae cultured in wastewater containing both ammonia and nitrate, and examining the effect of scale. Results are reported and discussed in the context of metabolic constraints to the mass culturing of microalgae, and with insights obtained from proteomic analysis of cultures at the flask scale.

Keywords: *Nutrient removal, Chlamydomonas reinhardtii, Nitrogen, Phosphorus, Feedstock, Biofuel, Scale up*

6.1. Introduction

Microalgal biotechnology seeks to develop unicellular biofactories for the production of commodities, high-value co-products, and environmental services.^{3,4} A renewed interest in the development and commercialization of biofuels and low-margin algal commodities has recently encountered setbacks, including: (1) the continued reporting of low yields of biomass and neutral lipids in peer reviewed literature;^{8,12–14} (2) the high cost of harvesting and dewatering algal

biomass at scale;¹⁵ (3) life cycle analysis;^{16,17} (4) long time horizons for stable genetic and mutagenic strain development;^{11,18} and (5) recent and dramatic shocks to energy markets from the adoption of hydraulic fracturing in North American shale oil/gas production. It is then increasingly necessary to use microalgae either as sources of high margin secondary products^{4,19,20} or for remediation of wastewaters as a subsidy for commodity feedstock production.^{23,24} Treatment of wastewater by microalgae was proposed early on.³⁰ Microalgae can efficiently remove nitrogen (N) and phosphorus (P) from wastewater.^{33,121–125} Phosphorus removal is especially cost effective compared to chemical techniques.¹²⁶ Microalgae have a proven track record in the developing world for wastewater treatment, including low cost high rate algal ponds (HRAP),¹²⁷ and waste stabilization ponds (WSP).¹²⁸ Substantial literature exists on microalgal cell growth and nutrient removal kinetics in different wastewaters.^{25,26,31–33} Nonetheless, high-density culturing of microalgae in wastewater remains poorly understood at the level of cell culture and metabolic pathways.

A fundamental problem in the proposed use of microalgae for wastewater treatment and biomass production is the effect of scaling up culture size on culture performance and yields. Overcoming the evolutionary tradeoff between biomass accumulation and the stress response, biosynthesis of starch versus oil,⁴⁷ is a metabolic conundrum that continues to confound mass culturing schemes despite decades of research.^{8,36} In contrast to large industrial projects, algal farm design with verifiable yields are based on agricultural engineering standards and methods, and not more costly civil or municipal engineering practices.^{14,27,48} Thus, just as in crop improvement⁴⁹ and animal science,⁵⁰ the key to increased yields, decreased costs, and extension of geographic range falls to biological research.²⁷ This includes development of application specific strains through breeding,^{11,51,52} natural selection and experimental evolution,^{53–55}

overexpression of phenotypic traits,⁵⁶ insertional mutagenesis,⁵⁷ and pursuit of genetic targets in robust and scalable unsequenced strains.^{58,59}

The objective of this study was to examine nutrient removal and growth at the pilot scale. We report here the results of research that examined the response of *Chlamydomonas reinhardtii* propagated in 10 L photobioreactor (PBR) cultures to a simple two-state system of simulated wastewater containing ammonia and nitrate, and a nutrient-sufficient control containing only nitrate. Our approach assumed that if wastewater processing is to subsidize commodity feedstock production, or remain attractive as a standalone and scalable environmental application, then development of fast growing and efficient nutrient removers is fundamental.^{23,24,55} In contrast to other studies that used unsequenced microalgae, and focused on bioprospecting,³⁷ and use of municipal¹²¹ and agricultural⁴⁸ wastewater, we used the sequenced green microalga *C. reinhardtii* to further the goal of developing dual-purpose candidates. *C. reinhardtii* is a haploid unicellular freshwater chlorophyte⁸⁴ well suited for nutrient removal studies due to the ease of manipulating growth medium composition.^{60,84} Furthermore, a sequenced nuclear genome⁸⁸ and highly conserved chloroplast genome⁸⁵ with well-characterized photosynthetic apparatus and nitrogen assimilation functions allows for biochemical and genetic dissection,^{60,86} and comparison to *Arabidopsis thaliana*.^{87,96}

In further contrast to other studies on metabolic responses to either ammonia only^{39,43,62} or nitrate only^{35,41,42,58,59} availability and/or starvation, we used subtle manipulation of nitrate-N ($\text{NO}_3\text{-N}$) and ammonia-N ($\text{NH}_3\text{-N}$) as nitrogen sources. We also did not use acetate in the media,^{35,39,42,43,55,62} which can alter cellular sensitivities to the maintenance of favorable C/N ratios,²²⁸ and cause heightened responsiveness to oxidative stress due to the down-regulation of carbon fixation and photosynthesis.^{39,43,229} Microalgal biomass has been successfully cultured at

different volumes ranging from 2.6 to 300 L using tubular and flat panel PBRs.^{13,19,37,133,134} In this study four 10 L biological replicate cultures were propagated in batch mode using a pilot scale PBR system until a steady state was achieved. Our approach included a finer manipulation of culture conditions than would otherwise be expected in an outdoor algal farm or PBR facility.^{8,27} This included use of buffered defined growth medium, uniform temperature, continuous high light, and CO₂ enrichment. Nutrient removal and biomass accumulation results are examined between culture conditions at the pilot scale, and are discussed in relation to the recently reported shotgun proteomic analysis of wastewater-cultured microalgae (Chapter 4),⁷⁵ performed using the same *C. reinhardtii* strain cultured at the bench scale using 330 mL flask volume cultures in identical control and wastewater media. This comparative PBR study may inform culture monitoring, bioprocess optimization, and selection of target pathways towards the long-term goal of developing robust dual-purpose strains suitable for large-scale outdoor wastewater treatment and feedstock production. Final samples from the PBR runs were taken for future proteomic and functional analysis.

6.2. Materials and methods

6.2.1. Algal strain and culture conditions

Experimental design consisted of 1 strain of *Chlamydomonas* cultured in batch mode for approximately 5 days, with 2 treatment levels, artificial wastewater (AWW) containing nitrate and ammonia and nutrient-replete control (CTRL) containing nitrate only, replicated 4 times, where each PBR column was assigned randomly and considered a biological replicate ($n = 1 \text{ strain} \times 2 \text{ conditions} \times 4 \text{ replicates} = 8$). The 4-column system (described below) was run twice under identical conditions.

The *C. reinhardtii* strain (CC-2936 wild type mt+, *Chlamydomonas* Resource Center, St. Paul, MN) was isolated from soil²¹⁶ and contains a cell wall and nit+ background. Culture media, conditions and assay techniques for quantifying nutrient removal and biomass accumulation have been described previously.^{23,75} The strain was cultivated at 25 ± 1 °C, continuous (24 h) cool white fluorescent illumination ($110.3 \mu\text{mol m}^{-2} \text{s}^{-1} \pm 0.58 \text{ SE}$), ambient CO₂ at 450 ppm, and agitation of 110 rpm on a continuous shaker platform. The strain was propagated in sterile nutrient-replete COMBO medium¹⁹⁵ containing major stock chemicals, algal trace elements (ATE), no animal trace elements (ANIMATE), and no vitamins. No acetate was used in order to achieve photoautotrophic growth conditions.⁶⁷ The pH of the medium was set to 7.2 and buffered using 5mM HEPES buffer.²¹⁷

Axenic cell cultures originating from a single isolated colony were maintained by serial transfer in exponential phase, then used to inoculate a starter culture, which was harvested at late-log phase and used to inoculate a single new flask culture for use as inoculum.⁴³ Columns of the PBR system were rinsed with 70% ethanol, flushed with autoclaved distilled water at room temperature, followed immediately by addition of sterile medium, and then inoculum. Independent cultures were propagated by transferring 500 mL of inoculum from the same flask in day 7 of exponential growth with biomass concentration of $0.048 \text{ mg L}^{-1} \pm 0.003 \text{ SE}$ into 10.5L vertical tubular glass columns containing 9.5 L of sterile growth medium, for a total initial culture volume of 10.0 L. The cell density at the time of inoculation was approximately $8.62 \times 10^5 \text{ cells mL}^{-1}$, which was estimated using previously determined standard curves relating cell count measurements under each condition to optical density at a wavelength of 680 nm (OD₆₈₀) using a 0.1 mm depth, Hy Lite hemacytometer (Hausser Scientific, Horsham, PA). Treatments included (1) nutrient-replete COMBO media – control (CTRL) – described above and containing

1.55 mg L⁻¹ of phosphate-P as K₂HPO₄, 14.01 mg L⁻¹ of nitrate-N as NaNO₃ and no ammonia-N, and (2) over-enriched COMBO media – artificial wastewater (AWW) – modified to contain 5 mg L⁻¹ phosphate-P as K₂HPO₄, 5 mg L⁻¹ nitrate-N as NaNO₃ and 20 mg L⁻¹ ammonia-N as NH₄Cl. Concentrations of N and P for nutrient-replete control are based on a previous report.²³ Nutrient-enriched artificial wastewater¹²¹ was modified to match the compositions of secondary effluents of wastewater treatment plants,^{123,219,220} and diluted, anaerobically digested dairy manure.⁴⁸

6.2.2. Pilot scale PBR system

The PBR system consisted of four modular glass vertical tubular columns placed side by side in a row 17.5 cm apart, each with an inner diameter of 10.16 cm, height of 1.37 m, and working culture volume of 10.02 L. Filtered compressed air (RK-02917-00, Cole Parmer, Montréal, QC) was introduced at the base of each column using air spargers to ensure uniform bubble size, decrease entrance velocity, and promote gas exchange and the uniform movement of cells through light and dark regions.^{139,265} Airflow meters (RK-32047-61, Cole Parmer, Montréal, QC) were used to ensure uniform flow. The airflow rate was maintained at 0.3 L min⁻¹ with the airstream continuously supplemented with CO₂ in a ratio of (97/3, v/v) and measured using an electronic mixer (E-7220, Bronkhorst HIGH-TECH B.V, Ruurlo, NL). Cultures were maintained at approximately 25 ± 1 °C. The stability of the temperature and pH were verified at each sampling. Continuous illumination (24 h) using banks of cool white fluorescent bulbs provided an average PAR of 120.3 μmol m⁻² s⁻¹ ± 1.0 SE (front of column) and 101.1 μmol m⁻² s⁻¹ ± 0.5 SE (back of column), as measured by a quantum meter (OMSS-ELEC, Apogee Instruments, Logan, UT). Carbon supplementation was found to be necessary after trials culturing the *C.*

reinhardtii strain in 10 L PBR columns without CO₂ enrichment failed (results not shown). This was in contrast to 3 freshwater and 3 marine strains previously cultured in flasks,²³ all of which grew in the PBR apparatus without CO₂ enrichment, but have not been genetically sequenced prior to this report. After inoculation, PBR cultures were maintained and sampled under non-sterile conditions for the duration of the experiment. This was done to better simulate real conditions, and to mimic the commercial strategy of rapidly growing and harvesting cultures before collapse due to bacterial contamination and/or grazer predation.^{8,37}

6.2.3 Analytical procedures

Biomass accumulation was followed spectrophotometrically by measuring the OD₆₈₀ and determined gravimetrically using dry cell mass (DCM) concentration. The change in total biomass concentration (g L⁻¹) was determined by taking the difference between average cell masses of triplicate 40 mL samples from the axenic inoculum at the beginning of the experiments, and of triplicate 40 mL samples taken at the end of the PBR runs. The samples were centrifuged (Sorvall Legend T, Thermo Fisher Scientific, San Jose, CA) at 10 000 rpm for 15 min, and the resulting cell pellets were washed three times to remove minerals and salts by resuspending in distilled water and centrifugation. Dewatering was accomplished by freeze drying (Martin Christ, Gamma 1–16 LSC; MBI, Kirkland, QC). Optical density was measured at time initial and every 24 hours thereafter. For a growth assay, 10 mL of culture was removed by sterile pipette at the center point of the glass column, 24 cm down the reactor wall from the top. Cells were re-suspended using a vortex mixer and 1 mL of culture was removed for measuring OD₆₈₀ using a Novapac II spectrophotometer (Pharmacia Biotech, Piscataway, NJ).

Nutrient concentrations were determined colorimetrically. Total phosphorus

(orthophosphate $\text{PO}_4\text{-P}$), nitrate-N ($\text{NO}_3\text{-N}$) and ammonia-N ($\text{NH}_3\text{-N}$) content in the supernatant, not pellet, were assayed 3 times, at time initial, day 2, and day 5, at the same time as the OD_{680} assay was performed. For a colorimetric assay, sample tubes from the OD_{680} assay were vortexed, 5 mL of culture was removed and centrifuged at 10,000 rpm for 10 min (VWR Costar model V, Radnor, PA), the pellet discarded and the supernatant analyzed using Hach TNT kits (TNT 830, 832, 835, 843, 844, 845) (Hach Company, Loveland, CO). At the end of each PBR run, samples were immediately harvested via centrifugation at 25 °C for 15 min at 4,117 rpm (Beckman Avanti J25-I, Brea, CA) and approximately 25 mg of wet cell pellet was immediately quenched in liquid nitrogen and stored at -80 °C for future proteomic analysis.

6.2.4 Data and statistical analysis

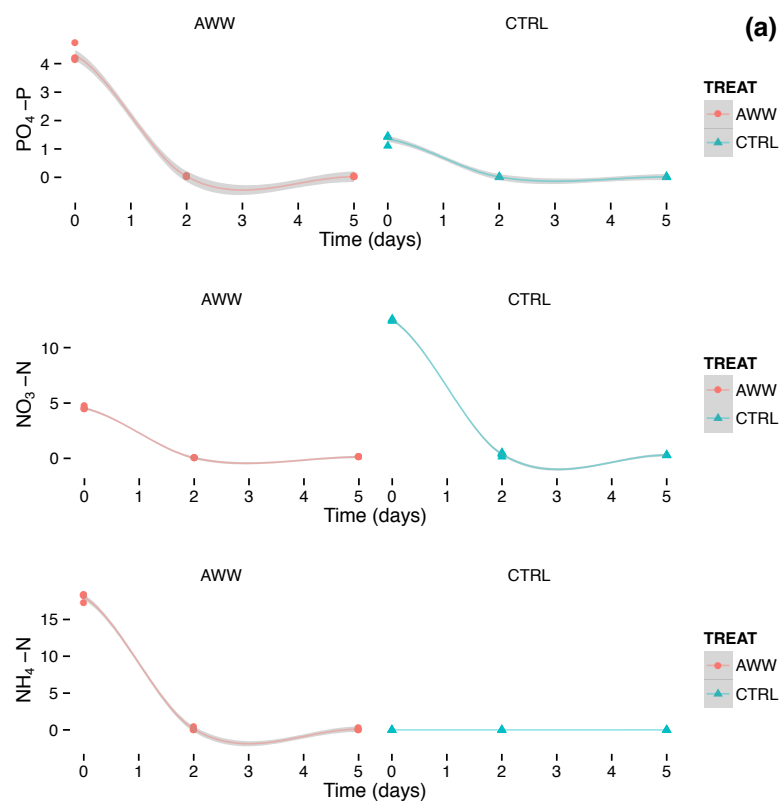
Statistical analysis and plotting was performed using open source R statistical package (R Development Core Team, Vienna, Austria) and ggplot2 (<http://www.ggplot2.org>) packages and tools. We analyzed the effect of treatment on final biomass concentration using a single-factor fixed-effects ANOVA. Nutrient removal efficiency (%) was calculated using initial (C_i) and final (C_o) nutrient concentration according to: $E_i = (C_o - C_i)/C_o \times 100 = \% \text{ removed from solution}$. Due to the use of carbon supplementation and non-sterile culture conditions, pilot scale PBR biomass yields and nutrient removal efficiencies were not statistically comparable to results from flask cultures at the bench scale. Biomass productivity ($\text{g L}^{-1} \text{ day}^{-1}$) in PBR and flask cultures was calculated by dividing the concentration of DCM by the number of days before the onset of stationary phase. Mathematical curve fitting was performed using Microsoft Excel (Microsoft Corp., Redmond, WA). Trend lines for linear and exponential growth functions were fitted to OD_{680} data from the PBR cultures. In each case the trend line with the highest R^2 value

was selected. Due to the fast consumption of N and P, which generated a insufficient number of nutrient depletion data points, trend lines were not applied. Variables are reported as significant at 95% confidence (p -value ≤ 0.05), and all values are reported with the standard error of the mean (SE).

6.3. Results

6.3.1. Nutrient removal by culture condition and scale

Figure 6.1a shows the concentration of total phosphorus (TP), nitrate-N, and ammonia-N in solution over 5 days. Nutrient depletion data showed that N and P were removed from solution completely by day 2, and below the level of detection for the Hach instrument. Figure 6.2a shows nutrient removal efficiency (%) and the final concentration of total nutrients removed (mg L⁻¹) in the PBR cultures. By day 5, *C. reinhardtii* removed 3.79 ± 0.06 mg L⁻¹ (99.4 %) of TP, 4.41 ± 0.04 mg L⁻¹ (97.2 %) of nitrate-N, and 17.15 ± 0.06 mg L⁻¹ (99.4 %) of ammonia-N in the AWW condition, and 1.10 ± 0.02 mg L⁻¹ (98.7 %) of TP and 11.30 ± 0.18 mg L⁻¹ (97.5 %) of nitrate-N in the CTRL condition.



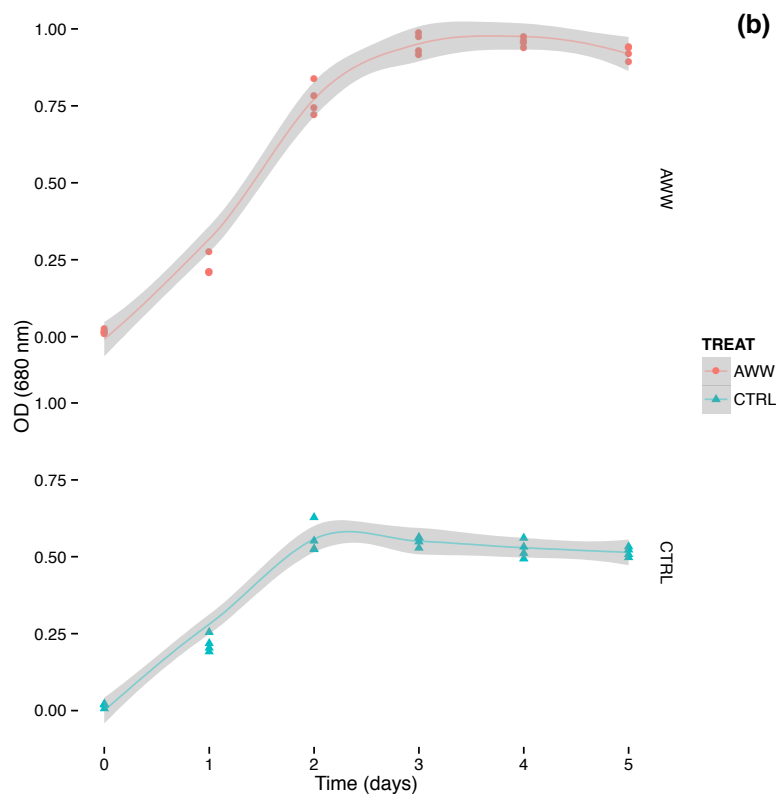
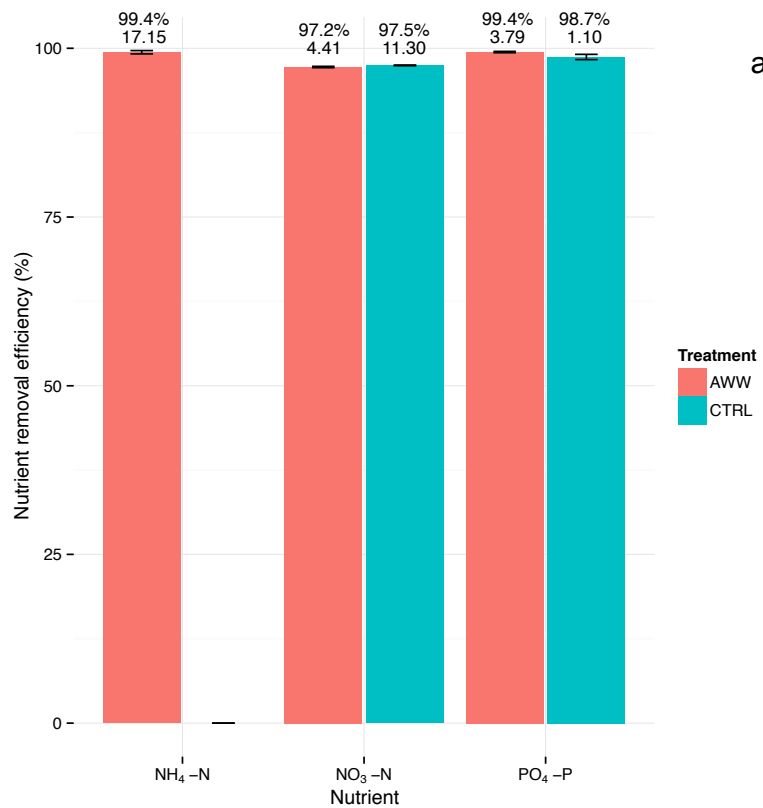


Figure 6.1: Visualizing nutrient removal (a) and growth curves (b) for 10 L PBR cultures. Artificial wastewater (AWW) is shown in red with closed circles and control (CTRL) in blue with closed triangles (one symbol per PBR culture) over 5 days. Bands show 95% point wise confidence intervals with SE for $n = 4$ biological replicates. Control contained no ammonia. The dip below end level in Figure 6.2a is an artifact of the mathematical curve fitting.

As previously reported in Chapter 4 (Results and discussion, Section 4.3.1),⁷⁵ the same strain of *C. reinhardtii* was propagated at bench scale 330 mL volume cultures of identical wastewater and control treatments, under sterile conditions with no CO₂ supplementation. Figure 4.1b–d shows the concentration total phosphorus (TP), nitrate-N, and ammonia-N in solution over 12 days. Nutrient removal efficiency (%) and concentration of total nutrients removed (mg L⁻¹) in the flask experiment are shown at day 8 (Figure 6.2b) and day 12 (Figure 6.2c). *C. reinhardtii* showed preferential uptake of N-ammonia over N-nitrate. By day 8, 3.81 ± 0.06 mg L⁻¹ (99.8 %) of TP, 0.28 ± 0.05 mg L⁻¹ (4.0 %) of nitrate, and 16.02 ± 0.50 mg L⁻¹ (93.1 %) of ammonia was removed from AWW cultures (Figure 6.2b). The maximum concentration of

nutrients removed for CTRL occurred at day 8, with $1.15 \pm 0.01 \text{ mg L}^{-1}$ (99.9 %) removal of TP and $11.28 \pm 0.19 \text{ mg L}^{-1}$ (97.6 %) of nitrate-N in solution (Figure 6.2b). By day 12 in the AWW condition, $3.80 \pm 0.06 \text{ mg L}^{-1}$ (99.7 %) of TP, $3.62 \pm 0.51 \text{ mg L}^{-1}$ (81.1 %) of nitrate-N, and $17.24 \pm 0.07 \text{ mg L}^{-1}$ (99.9 %) of ammonia-N had been removed, while in CTRL $1.10 \pm 0.01 \text{ mg L}^{-1}$ (98.8 %) of TP and $11.22 \pm 0.19 \text{ mg L}^{-1}$ (96.9 %) of nitrate-N were removed (Figure 6.2c).



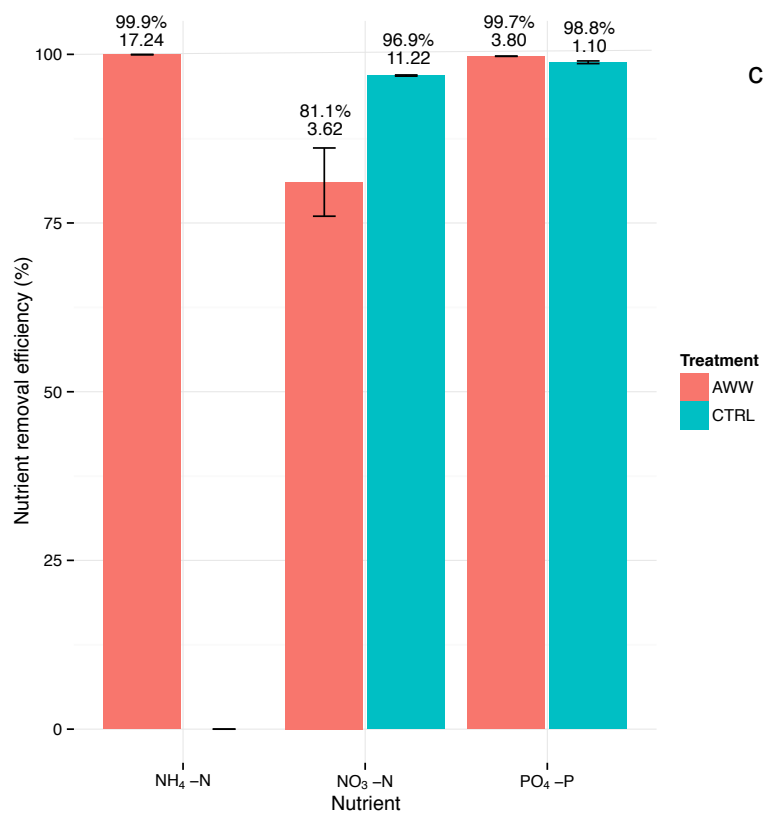
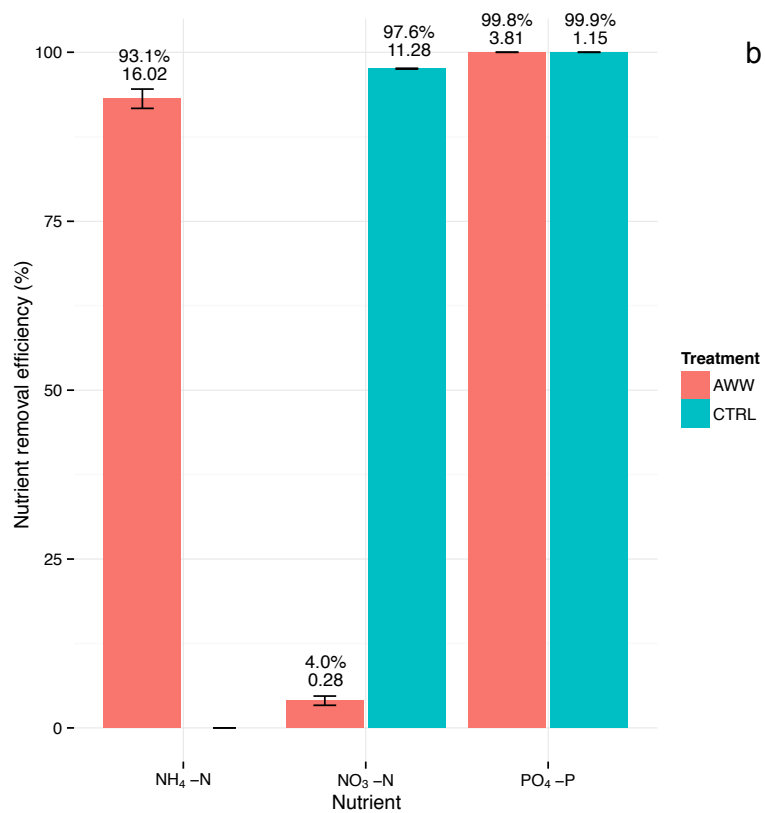


Figure 6.2: Nutrient removal efficiency and total nutrient concentration removed. PBR cultures at day 5 (a), and flask cultures at day 8 (b) and day 12 (c). *Chlamydomonas* efficiently removed total phosphorus (orthophosphate PO₄-P), nitrate-N (NO₃-N) and ammonia-N (NH₃-N) from solution in both treatments at both scales. Artificial wastewater (AWW) is shown in red and control (CTRL) in blue. Mean macronutrient concentration removed (mg L⁻¹) is shown in superscript. Confidence intervals are shown using SE for n = 4 biological replicates.

6.3.2. Biomass growth by culture condition and scale

Figure 6.1b shows growth of PBR cultures as followed by OD₆₈₀ measurements. Mathematical analysis showed exponential growth in the wastewater and control groups occurred over 3 time points between time initial and day 2 for both AWW and CTRL conditions ($R^2 = 0.96, 0.93$, respectively). Figure 6.3a compares final biomass concentration (g L⁻¹) and biomass productivity (g L⁻¹ day⁻¹) between the two PBR culture conditions at day 5. Final biomass concentration was 0.48 ± 0.04 g L⁻¹ for wastewater, and 0.24 ± 0.02 g L⁻¹ in the control group. Culture condition was found to have a highly significant effect on final biomass accumulation (ANOVA F_{1,8} = 37.99; $p = 3.33 \times 10^{-6}$). *C. reinhardtii* achieved biomass productivity of 0.24 g L⁻¹ day⁻¹ in wastewater, and 0.12 g L⁻¹ day⁻¹ in control during exponential growth until day 2.

As previously reported in Chapter 4 (Results and discussion, Section 4.3.1),⁷⁵ culture condition had no significant effect on final biomass concentration at the flask scale (Chapter 4; Figure 4.1a). Figure 6.3b shows final biomass concentration (g L⁻¹) and biomass productivity (g L⁻¹ day⁻¹) between the two flask conditions at day 12. Final biomass measured gravimetrically using DCM was 0.19 ± 0.01 g L⁻¹ for AWW and 0.23 ± 0.02 g L⁻¹ in CTRL, where culture condition had no significant effect (ANOVA F_{1,8} = 3.807; $p = 0.063$). Both conditions achieved the same relatively low biomass productivity rate of 0.02 g L⁻¹ day⁻¹ during linear growth until day 10.

6.4. Discussion

6.4.1 Nutrient removal response of *C. reinhardtii* to wastewater processing

Algal cells in nature oscillate between periods of N and P starvation and re-exposure. Aquatic primary production is thought to be limited by P, although N-limitation may be higher than previously thought.^{101,102} The concentrations of TP being used in the control (1.5 mg L^{-1}) and wastewater (5.0 mg L^{-1}) media in this study are an order of magnitude higher than that found in nature ($3 - 34 \text{ } \mu\text{g L}^{-1}$),²⁶⁶ in HRAP ($1.19 - 1.82 \text{ mg L}^{-1}$),¹²⁷ but is within the range of reported values for WSP.¹²⁸ The concentrations of total nitrate-N for control (14.0 mg L^{-1}) and wastewater (5.0 mg L^{-1}), and that of ammonia-N in the wastewater (20.0 mg L^{-1}) are an order of magnitude higher than that found in nature,^{101,102} but are within the range of those reported in HRAP ($9.8 - 14.5 \text{ mg L}^{-1}$ nitrate-N),¹²⁷ secondarily treated municipal¹²¹ and agricultural⁴⁸ wastewaters.

6.4.1.1. PBR wastewater and control cultures showed nutrient limitation.

The expected physiological response of higher nutrient loadings in the wastewater PBR cultures was enhanced P and N removal. Nutrient depletion curves suggest that *C. reinhardtii* consumed TP at exponential rates in both media conditions, and ammonia-N in wastewater (Figure 6.1a). Nitrate-N appeared to be consumed at an exponential rate in control and a linear rate in wastewater. This result was not unexpected due to ammonia-N as a preferred source of nitrogen for green algae and higher plants,^{60,99} and a similar result reported in Chapter 4 (see below, Section 6.4.1.2). Nutrient removal efficiency (%) for TP and nitrate at day 5 was comparable for both media (Figure 6.2a), and uptake of ammonia from solution was nearly complete. Nutrient removal data for both culture groups showed that by day 2, macronutrients in solution were depleted. This result suggested that intracellular pools of P, N, or both P and N, had become limiting, particularly in the control group. The increase in nutrient concentration

between day 3 and day 5 was also indicative of cell rupturing due to mechanical stress, and age, and possibly the onset of bacterial contamination.

Comparing N and P removal efficiencies to the literature is complicated by different growth media composition, light intensity, light/dark cycle, N/P ratio, culture vessel, scale, aeration, time course, microalgae species, and analytical techniques. Nonetheless, nutrient removal efficiencies at the 10L PBR culture volume for *Chlamydomonas* are consistent with reported efficiencies for other microalgae cultured in artificial, municipal or agricultural wastewaters. Shi *et al.* (2007) found *Chlorella vulgaris* sp. and *Scenedesmus rubescens* sp. immobilized on twin layers removed phosphate, ammonium and nitrate to less than 10% of their initial concentration within 9 days using secondary, synthetic wastewater similar to this study.¹²¹ *Scenedesmus obliquus* sp. batch cultured in urban wastewater for 8 days in 1.5 L PBR columns with continuous lighting and temperature of 25 °C, removed 97% of P and 100% of ammonia at the nutrient concentration of 11.8 mg L⁻¹ and 27.4 mg L⁻¹, respectively.¹²³ Olguín *et al.* (2003) reported 96% ammonia-N and 87% P removal by the cyanobacterium *Spirulina* in an outdoor raceway treating 2% diluted anaerobic effluents from pig wastewater,¹²⁴ which contained similar loadings of N and P as reported by Martinez *et al.* (2000).¹²³ González *et al.* (1997) reported ammonium removal efficiencies of 90%, and TP removal of 55%, using both *Scenedesmus dimorphus* sp. and *C. vulgaris* sp., after 9 days of culturing agro-industrial wastewater in batch mode using 2 L working volumes in a 4 L cylindrical glass bioreactor.¹²⁵ Aslan & Kapdan (2006) achieved 78% P removal efficiency from a initial PO₄-P concentration of 7.7 mg L⁻¹, and complete removal of ammonia-N at concentrations of 13.2 and 21.2 mg L⁻¹, using *C. vulgaris* sp. batch cultured under continuous illumination and 20 °C using 1000 mL flasks of artificial wastewater.³³

6.4.1.2. Control cells in flask cultures showed nutrient limitation

As discussed in Chapter 3,²³ and Chapter 4,⁷⁵ the expected physiological response of higher nutrient loadings was enhanced P and N removal efficiency. In the bench scale study using 330 mL flask cultures of identical control and wastewater media, *C. reinhardtii* consumed TP at exponential rates under both conditions (Chapter 4, Results and discussion, Section 4.3.1; Figure 4.1). Ammonia which was lacking in the control medium was preferentially consumed^{98,100} at an exponential rate in the wastewater cultures, and the uptake of nitrate only started at day 10. Once uptake was initiated, the nitrate removal rate for both groups was comparable (Chapter 4; Figure 4.1d). Nutrient removal efficiency (%) of TP was also comparable between the two growth medium conditions at day 8 (Figure 6.2b) and day 12 (Figure 6.2c). Nitrate-N was nearly completely removed in the control group by day 8. Wastewater cells had removed 93.1 % of ammonia by day 8, and completely removed ammonia in solution by day 12. Colorimetric analysis alone showed that control cultures had nearly depleted macronutrients in the solution, were entering lag phase and the early stages of nutrient limitation. Wastewater cultures were still removing ammonia-N from solution, before switching to a new nitrogen source, and showed little evidence of stress response at the end of the flask experiment (Chapter 4; Figure 4.1b,d). The slightly higher concentrations of nitrate and TP in solution at day 12 compared to day 8 are likely due to an aging culture and lysed cells. Nutrient removal efficiencies for both conditions at the bench scale are consistent with other studies of microalgae using similar wastewater and control media.^{23,26,48,121} For example, *Chlorella* removed ammonia, total nitrogen, and TP by 100%, 75.7–82.5%, and 62.5–74.7%, respectively, in different dilutions of dairy manure cultured in 110 mL cultures with continuous high light.²⁶⁷ In the bench scale study using 330 mL flask cultures, Chapter 3 (Discussion, Section 3.4.3), not

all species showed increased P removal with increasing P loading. The effect of increasing P additions on freshwater microalgae was a decline in P removal efficiency as measured at day 8 and day 16, with the exception of *Monoraphidium* sp. and *Scenedesmus* sp. at the control and 5 mg L⁻¹ PO₄-P treatments, respectively. The effect of increasing P additions on marine species was a marked increase in P removal efficiency. The top performing freshwater green *Monoraphidium* sp. removed most of the phosphorus at day 8 (71.9 %, 64.75%) and day 16 (84.3 %, 86.6%) at the control and 5 mg L⁻¹ PO₄-P treatments, respectively, as compared to *C. reinhardtii* at the bench scale that consumed 98.8 – 99.7% of TP at both treatments levels, control and wastewater. Proteomic analysis determined that control cells of *C. reinhardtii* were entering the early stages of N-limitation at the end of the experiment,⁷⁵ whereas, the low N/P ratio and non-continuous light very likely affected TP uptake and growth of all six strains at higher single enrichment loadings of phosphorus, as reported in Chapter 3.

6.4.2. Growth response of *C. reinhardtii* to wastewater processing

6.4.2.1. Biomass yields were higher in wastewater PBR cultures

The complete removal of macronutrients from solution by day 2 in both the PBR culture groups suggested that differences in biomass accumulation are mainly attributed to N and P loadings. As expected, measurement of growth using OD₆₈₀ (Figure 6.1b) and final DCM concentration (Figure 6.3a) showed significantly more biomass accumulation in wastewater cells than control. At the 10 L pilot scale culture volume, final biomass densities of 0.48 ± 0.04 g L⁻¹ and 0.24 ± 0.02 g L⁻¹ for wastewater and control, respectively, corresponded to biomass productivities of 0.24 g L⁻¹ day⁻¹ and 0.12 g L⁻¹ day⁻¹, respectively, when adjusted for time (2 days exponential growth). Direct comparisons of artificial wastewater and municipal or

agricultural wastewater have shown equivalent nutrient removal rates, but slightly higher growth rates and biomass yields in synthetic wastewater, likely due to optimal N/P balance and less toxicity.^{26,205,268} The productivity rate for control cultures compares to that of 0.12 – 0.13 g L⁻¹ day⁻¹ reported for three *Chlorella* species cultured in 2.6 L vertical alveolar panel (VAP) with continuous illumination, no CO₂ supplementation, and nitrate-N media.¹⁹ Control biomass productivity also matches the 0.13 g L⁻¹ day⁻¹ reported using industrial scale up 300 L Brite-Box tubular PBRs, continuous light, and secondary municipal effluent,¹³ and the productivity of wastewater cultures exceeded it. Both culture conditions, however, are significantly less than the 0.36 (nutrient-sufficient) and 0.30 g L⁻¹ day⁻¹ (nutrient-deprived) productivities reported for the marine eustigmatophyte *Nannochloropsis* sp. using outdoor 110-L Green Wall Panel PBRs, CO₂ enrichment, and nitrate-N media with continuous harvesting.³⁷ As mentioned in Materials and methods, direct statistical comparison of biomass yields between wastewater groups at the 10L PBR column and 330 mL flask culture scales is not possible due to the addition of CO₂ and unsterile culture conditions in the pilot scale experiment. Nonetheless, it was not surprising that both final biomass concentration and biomass productivities were higher in the PBR versus flask cultures: final biomass of ~ 0.48 g L⁻¹ in PBRs versus ~ 0.19 g L⁻¹ in flasks, and biomass productivities of ~ 0.24 g L⁻¹ day⁻¹ in PBRs versus ~ 0.02 g L⁻¹ day⁻¹ in flasks, when adjusted for time (10 days growth before stationary phase), using identical wastewater medium (Figure 6.3a,b).

The use of gravimetric, spectrophotometric, and colorimetric analysis to infer the physiological responses of *Chlamydomonas* growth to wastewater and control conditions suggested a number of explanations, including carbon source, light attenuation, bacterial contamination, and stress from N-deprivation. Firstly, OD₆₈₀ was comparable between day 0 and

day 2 for both PBR culture conditions. Final OD₆₈₀ readings of ~ 0.9 in wastewater and ~ 0.5 in control strongly supported the conclusion that cells were experiencing light attenuation due to cell shading,^{139,140} but not carbon limitation given the CO₂ supplementation. This was not the case in 330 mL flask cultures where the same analytical procedures had suggested light and/or carbon as limiting factors, before proteomic analysis determined that control cells in lag phase were entering the early stages of N-limitation.⁷⁵

Secondly, the non-sterile culture conditions of the PBR system complicated interpretation of the growth response. It has to be mentioned that the majority of pilot and large-scale studies, including this one, do not account for what percentage of actual and projected biomass yields are in fact bacterial mass,^{8,48} and not that of the monocultured microalgae. As mentioned, we followed a commercial strategy of quickly growing photosynthetic cultures before culture collapse from bacterial contamination and/or grazer predation. However, exposure to air during sampling invited bacterial contamination, and presumably more so in wastewater due to higher macronutrient loadings, higher biomass, and more ruptured cells in stationary phase acting as a carbon source. Mixed culturing of algal and bacterial cells has beneficial effects in sterile and non-sterile cultures,²⁰⁵ where microbes still take up N & P from solution. Efficient nutrient removal has been demonstrated by the co-immobilization of *A. brasilense* sp, a microalgae growth promoting bacteria (MGPB), in alginate beads with *Chlorella* sp.²⁰² and *C. vulgaris* sp.¹³² The analytical techniques used were unable to provide further insight into the metabolic response of a monocultured green microalga to contamination, let alone community dynamics or resource partitioning,^{198,269} and future study of microalgae consortia is needed for industrial and environmental applications.

Thirdly, and most likely the primary contributor, the removal of macronutrients from solution by day 2 in both the PBR culture groups strongly suggested that differences in biomass accumulation are mainly attributed to N and P loadings. It was hypothesized⁴⁰ and demonstrated⁴¹ that consumption of chlorophyll continues to support growth after exhaustion of extracellular N pools. In the PBR control cultures cells appeared yellow-green,^{40,62} and larger and globular in shape, compared to a darker green color in wastewater-cultured cells. This observation is supported by proteomic studies of cells adapting to harsh N perturbation, that when sampled at early time points demonstrated dramatic and immediate changes in primary metabolism,^{39,43,62} with changes in C/N balance and lipid accumulation occurring only under sustained chronic conditions.^{43,62} Lower biomass productivities were also found using nutrient-deprived growth medium,³⁷ including comparable neutral lipid accumulation and composition due to P-limitation as that associated with N-limitation, as demonstrated in marine species.^{37,38} The following physiological states (Figure 6.1a,b) can be inferred from PBR samples: (1) intracellular pools of nitrogen were still available for assimilation and use in carbon fixation and cell division in the wastewater group due to over-enrichment of biologically available N-ammonia, P, and CO₂ supplementation; and (2) control cells had likely depleted intracellular pools of nitrogen, including chlorophyll, entered full N-deprivation, and were shunting carbon away from starch synthesis and towards TAG accumulation in a fundamental shift of cellular metabolism towards the survival response.^{35,36,45} Phosphorus deprivation was found to elicit a similar response as N-deprivation in the marine eustigmatophyte *Nannochloropsis* sp., although requiring longer to decrease productivity and halt growth.³⁷

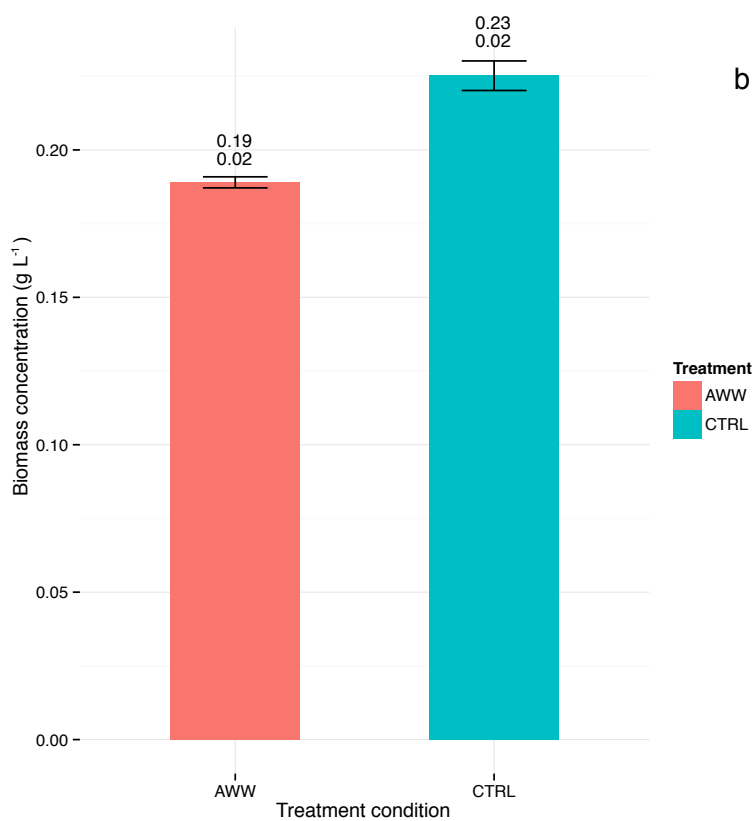
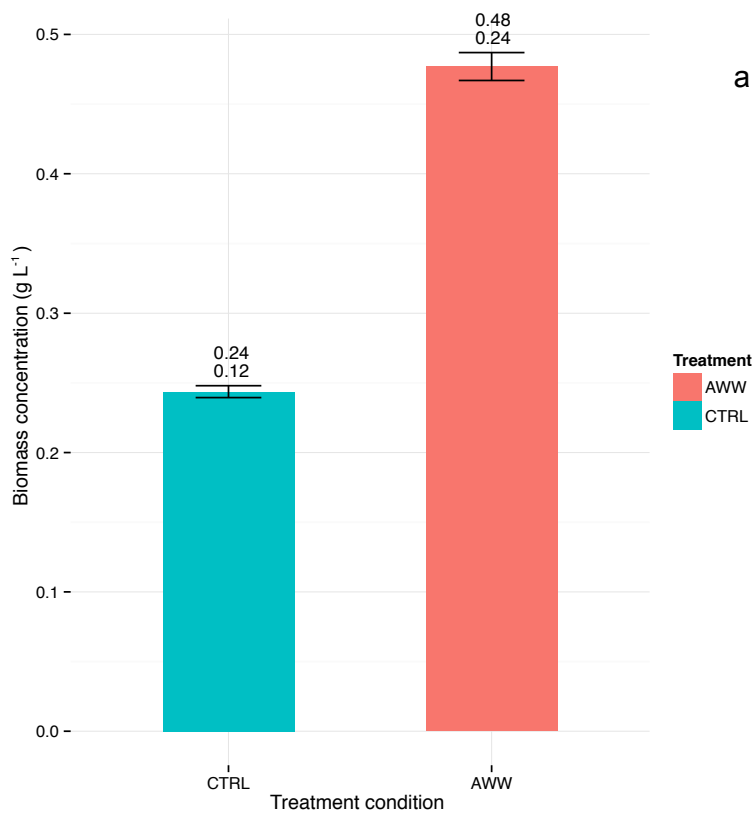


Figure 6.3: Final biomass accumulation between treatment groups at the PBR (a) and flask (b) scale. Final biomass concentration (g L^{-1}) and biomass productivity rates ($\text{g L}^{-1} \text{ day}^{-1}$) are shown in superscript. Confidence intervals show standard error (SE) of the mean for $n = 4$ biological replicates. Biomass productivity is calculated using initial and final dry cell mass (DCM) concentration divided by days in exponential phase or linear growth phase. Artificial wastewater (AWW) is shown in red and control (CTRL) in blue. Treatment had a highly significant effect on biomass accumulation at the PBR scale (a), and no significant effect at the flask scale (b). Final biomass concentration in the control (CTRL) cultures was similar at both scales, despite CO_2 supplementation in PBR columns.

6.4.2.2. Biomass yields were not significantly different in flask cultures

As discussed in Chapter 4 (Section 4.3.1),⁷⁵ despite the presence of the preferred source of inorganic nitrogen in the form of ammonia-N, wastewater cells did not grow faster or reach higher densities (Chapter 4; Figure 4.1a). The final biomass density in flask cultures of $0.19 \pm 0.01 \text{ g L}^{-1}$ for wastewater grown cells and $0.23 \pm 0.02 \text{ g L}^{-1}$ for control media grown cells was not significantly different and translated into biomass productivities of $\sim 0.02 \text{ g L}^{-1} \text{ day}^{-1}$ (Figure 6.3b), when adjusted for time (10 days linear growth). Final biomass concentrations and productivities of *Chlamydomonas* at the bench scale are approximately one third that of the best performing dual-purpose candidates – *Monoraphidium minutum* sp. and *Tetraselmis suecica* sp. – cultured using identical control medium, under non-continuous light at the bench scale for 16 days (Chapter 3).²³ They are an order of magnitude lower than the biomass productivity range of $0.17 - 0.37 \text{ g L}^{-1} \text{ day}^{-1}$ found across 30 strains of freshwater and marine microalgae cultured for 10 days under continuous light with air/ CO_2 (95/5, v/v).³⁷ Finally, they are also significantly lower than yields reported in studies for different species of microalgae cultured in municipal, agricultural and artificial wastewater.^{25,26} This result highlighted the limitations of using *Chlamydomonas*^{39,43,55,75} to identify potential targets suitable for robust, but as yet unsequenced candidates.^{58,59}

As reported in Chapter 4, Sections 4.3.3.2 – 4.3.3.5, the insignificant difference in final biomass and OD_{680} demonstrated that even in increasingly N-limited media, as was the case in

the control flask cultures, *C. reinhardtii* continued to grow and attempt to balance its C/N ratio.⁷⁵ Surprisingly, even after 12 days the wastewater group was still engaged in photosynthetic carbon fixation, cell division, and biosynthesis of amino acids, fatty acids, secondary metabolites and chlorophyll. Control cells showed continued photosynthesis, synthesis and use of carbohydrates, recycling of amino acids, evidence of oxidative stress, and little enrichment of lipid biosynthesis.

6.4.2.3. Control PBR and flask cultures had similar biomass yields but different productivities

A comparison of final biomass yields between pilot and bench scales revealed a remarkable similarity for both control groups: $\sim 0.24 \text{ g L}^{-1}$ in PBRs versus $\sim 0.23 \text{ g L}^{-1}$ in flasks (Figure 6.3a,b). This observation, taken together with a statistically significant difference in final biomass concentration between PBR wastewater and control cultures, supported our initial hypothesis of N-deprivation in nutrient-sufficient control PBR cultures, such that CO_2 supplementation, and approximately two orders of magnitude larger culture volume had no demonstrable effect on final biomass in pilot scale over bench scale. Not surprisingly, a higher rate of biomass productivity is seen between control groups at different scales: $\sim 0.12 \text{ g L}^{-1} \text{ day}^{-1}$ in PBRs versus $\sim 0.02 \text{ g L}^{-1} \text{ day}^{-1}$ in flasks. Just as in nature,^{1,61,103} control cells in the PBR columns rapidly took up nitrate-N and TP, and used CO_2 supplementation to accumulate biomass quickly by cell division and carbon fixation, only to use up macronutrients and invoke the stress response. Over-enrichment of ammonia-N and phosphate-P allowed *Chlamydomonas* to continue cell division and photosynthetic carbon fixation. Comparing control cells by scale, PBR cultures likely had entered N and P deprivation, and possibly starvation, due to depleted intracellular stores after day 2. Flask control cultures experienced the onset of N-limitation only after approximately 10 days of culture time (Chapter 4; Figure 4.1a,d), causing enrichment of KEGG

pathways related to amino acid recycling, and the synthesis and oxidation of starch, both used to power cellular respiration and continued growth, with little lipid biosynthesis (Chapter 4; Table 4.1) (Chapter 4; Figure 4.3), as shown by proteomic analysis.⁷⁵

6.4.3. A metabolic conundrum between growth and the stress response

Nitrogen source, availability and assimilation are critical factors that affect microalgal cellular physiology, growth, and metabolic function.^{96–98} Chlorophytes, just like higher plants, utilize starch as their primary carbohydrate store.¹⁰⁹ Transcript abundance^{35,42} in *C. reinhardtii* experiencing N-starvation has been shown to trigger early synthesis of starch, followed by activation of gametogenesis, down-regulation of protein synthesis, and a redirection of metabolism that funnels carbon towards TAG biosynthesis and storage in lipid bodies, the default stress response for microalgae.^{36,40} This cellular response to N-deprivation by carbon and nitrogen responsive pathways also includes reduced carbon assimilation and chlorophyll biosynthesis, and increased levels of oxidative stress response enzymes.^{43,75,245,270} As mentioned, this starvation response and recovery was demonstrated using P-limitation and starvation.^{37,38} Purple acid phosphatase (PAP) was found to have higher differentially abundant levels during proteomic analysis of control cultures in the flask experiment (Chapter 5, Supplemental findings, Section 5.3.2.2).⁷⁵ PAPs are metalloenzymes that hydrolyse phosphate esters and anhydrides under acidic conditions, and are associated with an acclimation to nutritional phosphate deprivation,²⁵⁸ as demonstrated in phosphate-starved *Arabidopsis* plants, where PAPs scavenged phosphate from extracellular phosphate esters by root cells, and functioned in intracellular vacuolar phosphate recycling.²⁵⁹

Results from the 10 L PBR cultures showed a significant and pronounced decrease in biomass yields in the control condition, which was not over-enriched with ammonia-N or phosphate-P. This finding highlights the detriment to biomass yields of the survival response. Proteomic analysis of stationary phase samples from the 330 mL flask cultures highlighted a second challenge for biofuel applications. In the absence of full N-deprivation, cells in exponential and stationary growth stages counter an initial reduction in carbon assimilation by higher abundances of enzymes involved in amino acid metabolism (Chapter 4; Figure 4.3), including those with carbon backbones, with the net result of no significant difference in biomass growth (Figure 6.3b).^{43,88} It is only after chronic N-deprivation, evident in PBR control cells, that the eventual shunting of photoassimilates in neutral lipid form occurs.^{35,36,43,45,88}

An active area of research in algal biofuels seeks to culture lipid rich microalgae by shunting carbon away from carbohydrate synthesis towards triacylglycerol (TAG) biosynthesis,^{44,45} while still maintaining growth. Cellular metabolism in prokaryotes is governed by sophisticated biochemical networks. In eukaryotic microalgae this complexity is compounded further by the important role of post-transcriptional and post-translational regulation of protein expression and cellular metabolism.^{59,110–112} Tightly controlled and dynamic cellular responses to N availability, then, will dictate cell culture health and productivity in concert with light absorption and carbon assimilation, and it remains to be seen if modification of the default stress response can maintain optimal growth and lipid biosynthesis in a strain cultured outdoors in high light.^{7,12} The present PBR experiment further delineates the evolutionary tradeoffs between biosynthesis of starch and oil.⁴⁷ This ancient metabolic chassis continues to use highly conserved molecular survival mechanisms to shunt and compartmentalize C and N to the detriment of culture yields over longer durations,^{36,40} and at production scales.³⁷ With regards to wastewater

processing, this pilot scale study provided further evidence that over-enrichment of N did not adversely affect growth or cellular physiology. This finding provides optimism that continued improvements in breeding programs, bioprocess optimization, and potentially new species found through bioprospecting, can be made.

6.4.4. Development of dual-purpose candidates and consortia

Projection of yields at the large-scale from performance at the small is uncertain at best when dealing with complex metabolic dynamics in high-density cell cultures. Using the average maximum biomass achieved by *C. reinhardtii* cultured in wastewater medium in the PBR system of $0.48 \pm 0.04 \text{ g L}^{-1}$ over 5 days, that also removed $3.79 \pm 0.06 \text{ mg L}^{-1}$ (99.4 %) of TP, $4.41 \text{ mg L}^{-1} \pm 0.04$ (97.2 %) of nitrate-N, and $17.15 \text{ mg L}^{-1} \pm 0.06$ (99.4 %) of ammonia-N, it is feasible to envision a scaled up PBR or pond system able to treat 100 L of wastewater in the same 5 day time period, remove $2.8 \times 10^{-5} \text{ kg}$ of TP, $3.3 \times 10^{-5} \text{ kg}$ of N-nitrate, and $1.3 \times 10^{-4} \text{ kg}$ of N-ammonia, and produce $3.6 \times 10^{-3} \text{ kg}$ of algal biomass, assuming 75% efficiency. Scaling to 1000 L, or two orders of magnitude larger, either by multiplying the number of PBR columns or moving directly to outdoor ponds, would theoretically remove $3 \times 10^{-4} \text{ kg}$ of TP, $3 \times 10^{-4} \text{ kg}$ of N-nitrate, and $1 \times 10^{-1} \text{ kg}$ of N-ammonia, and produce $4 \times 10^{-2} \text{ kg}$ of biomass, assuming 75% efficiency, in the same 5 day time period. *Chlamydomonas* removed TP and inorganic nitrogen in solution efficiently in both 10L PBR and 330mL flask cultures and achieved results comparable to the literature. Nonetheless, biomass yields were lower than other microalgae cultured in real and synthetic wastewater. In comparison to the two promising candidates identified in Chapter 3,²³ *Monoraphidium minutum* sp. and *Tetraselmis suecica* sp.,

Chlamydomonas did not demonstrate the desired dual-purpose traits of high nutrient removal efficiency and biomass productivity.

Principle findings of this study were that the use of AWW medium containing nitrate-N and ammonia-N resulted in significantly higher biomass yields at the PBR scale than nutrient-replete control containing only nitrate-N. Control cultures showed evidence of the onset of nutrient starvation. Treatment had no significant effect on final biomass yields at the flask scale. Although not directly comparable by statistical analysis, cells cultured in wastewater media showed higher final biomass concentration and biomass productivity in the PBR cultures than flask cultures. Cells cultured in control medium had similar final biomass yields, but higher biomass productivity in the PBR cultures. *Chlamydomonas* did remove nutrients efficiently at the pilot scale, as it did at the bench scale, but again did not accumulate biomass quickly, and failed to demonstrate the desired dual-purpose traits identified in candidates from the literature. *C. reinhardtii* demonstrated a remarkable ability to adapt to environmental conditions associated with mass culturing, including light attenuation, fluid dynamics, and the fundamental metabolic conundrum concerning growth and the N-limitation induced stress response. Comparing results from different studies using different organisms and conditions highlights the limitations of gravimetric, spectrophotometric, and colorimetric analyses alone, in selecting suitable candidates, and inferring physiological states. A systems biology approach is needed to elucidate microalgal responses to environmental conditions associated with mass scale culturing. Of particular interest for biomass production schemes is understanding the budgeting and allocation of photosynthate (ATP and NADPH) among cellular processes,^{1,47,61} and the resultant shunting of C and N to different metabolic compartments of the cell in an effort to maintain growth and a balanced C/N ratio.⁴³ Our findings highlight the importance of nitrogen source, availability,

switching and assimilation in wastewater treatment with or without biofuel feedstock production, and not comparative studies of N-limitation or starvation using nitrate-N or ammonia-N alone.

Future work characterizing the adaptive response of enzymes to P-limitation and/or starvation is needed to understand tightly controlled and dynamic cellular responses to P availability that dictate cell culture health and productivity in concert with light absorption and carbon assimilation. Furthermore, accounting for bacterial contamination in actual and projected yields, and examining the potentially beneficial effects of microbial consortia^{198,269} for enhanced nutrient removal and/or biomass and secondary compound production, represents a promising avenue of research beyond studies using only mono-cultured microalgae at the small or large-scales. Our primary objective remains the characterization of metabolic responses to wastewater processing applicable to the development of candidate strains or microbial consortia, suitable for outdoor culturing in secondary municipal effluent and/or agricultural wastewater as part of a larger feedstock production scheme. To this end, samples from this PBR experiment will be subjected to shotgun proteomic and functional enrichment analysis, in an effort to better elucidate the tightly regulated biochemical processes of nitrogen metabolism and assimilation, photosynthetic carbon fixation, and carbohydrate and lipid biosynthesis.

Acknowledgements

We wish to thank Dr. Darwin Lyew for assistance in modifying the photobioreactor system for suspended microalgae, input on mass culturing, and critical review of this manuscript; Drs. Vijaya Raghavan, Valérie Orsat and Robert Williams (Department of Bioresource Engineering, McGill University) for support on engineering and culturing; Dr. Graham Bell (Department of Biology, McGill University) for providing the *C. reinhardtii* (CC-2936 wild type mt+) strain;

and Drs. Etienne Low-Décarie (School of Biological Sciences, University of Essex) and Eric J. Pederson (Department of Biology, McGill University) for assistance with the statistical program R. This research was funded by a Natural Sciences and Engineering Research Council of Canada (NSERC) Discovery grant (RGPIN 355743-13), a Canada Foundation for Innovation (CFI) equipment grant (CFI/Exp/Lefsrud/#23635), and McGill University, QC, Canada.

Chapter 7: Final summary, significance and conclusions

Connecting statement

This chapter provides a summary of the, main conclusions, and the significance of findings reported in this doctoral dissertation. A dissertation summary, methodologies developed, and the experimental findings concerning the potential of wastewater treatment using microalgae and shotgun proteomics are presented. The significance, originality, and contributions to knowledge of this research are stated. At the end of Chapter 7 areas of potential future research in the fields of microalgal biology, biotechnology, and proteomics are discussed in relation to the dissertation research reported here.

7. Final summary, significance and conclusions

7.1. Dissertation summary

The global objectives of this research dissertation were to investigate biomass growth and nutrient removal in microalgae, and to apply shotgun proteomics as a technique for evaluating the metabolic response to simulated wastewater processing. This research involved multi-disciplinary approaches - including aquatic biology, microbiology, systems biology, bioprocess and bioreactor engineering, biochemistry and cellular physiology, and bioinformatics. Developing and refining the shotgun proteomics workflow required a firm grasp of analytical and protein chemistry, chromatography, statistics, and the theoretical and practical principles of mass spectrometry. Each chapter of this dissertation is built upon increasing layers of research complexity. Different disciplines were integrated in order to develop questions, design experiments, and reach conclusions of biological significance concerning the potential and challenges of wastewater treatment using microalgae.

Chapter 1 served as an introduction and presented the background concerning the biological feasibility and the economic reality of wastewater treatment coupled biofuel feedstock production using microalgae. Also included were the objectives for each of three chapter manuscripts reporting experimental results and conclusions.

Chapter 2 provided a comprehensive literature review of all relevant aspects of microalgal biology and biotechnology related to this dissertation. This included a primer on biological mass spectrometry (MS), liquid chromatography (LC), execution of a label-free MS/MS shotgun proteomics experiment, and the steps necessary for interpretation of high throughput (HT) MS data sets, including mass informatics, differential analysis, functional enrichment, and bioinformatics tools and databases.

Chapter 3 (Manuscript 1) reported results from the first experiment of this doctoral dissertation.²³ The objective of this six species screen was to identify dual-purpose candidates capable of high rates of total phosphorus (TP) removal and growth. Three freshwater – *Chlorella* sp., *Monoraphidium minutum* sp. and *Scenedesmus* sp. – and three marine – *Nannochloropsis* sp., *N. limnetica* sp., and *Tetraselmis suecica* sp. – species were propagated in batch mode using 165 mL bench scale flask cultures over 16 days to quantify TP removal and growth as a function of increasing phosphate-P loadings. Experimental design used high light, a light/dark cycle of 14/10 hours, and no CO₂ supplementation. Two dual-purpose candidates were identified, the freshwater *Monoraphidium minutum* sp. and the marine *Tetraselmis suecica* sp.

Chapter 4 (Manuscript II) reported results from the principal experiment of this doctoral dissertation.⁷⁵ The sequenced *Chlamydomonas reinhardtii* was cultured in batch mode using 330 mL bench scale flask cultures over 12 days under continuous illumination and no CO₂ supplementation to investigate nitrogen and phosphorus uptake, growth, and metabolic responses to wastewater processing by comparing culture group proteomes. Our approach compared two conditions: (1) artificial wastewater containing nitrate and ammonia and (2) nutrient-sufficient control containing nitrate as sole form of nitrogen. Remarkably, treatment had no significant effect on final biomass concentration. A comparison of culture group proteomes, however, revealed significant differences. Label-free shotgun proteomic analysis identified 2358 proteins, of which 92 were significantly differentially abundant. Proteomic analysis showed over-enrichment of ammonia-N did not adversely affect cellular physiology or yields in wastewater-cultured cells. In comparison to the other microalgae in the literature, and top performers identified in Chapter 3 (Manuscript 1), *Chlamydomonas* did remove N and P efficiently at the bench scale, but did not demonstrate the desired dual-purpose traits of high rates of nutrient

removal and biomass accumulation. Nonetheless, enriched pathways identified in artificial wastewater, notably, photosynthetic carbon fixation and biosynthesis of plant hormones, and those in nitrate only control, most notably, nitrogen, amino acid, and starch metabolism, represent potential targets for genetic improvement and strain optimization that require further elucidation.

Chapter 5 (Manuscript II, Supplemental findings) reported additional differentially abundant proteins of interest not discussed in Chapter 4, including biosynthesis related, stress related, poorly annotated, and unknown proteins.⁷⁵ Wastewater-cultured cells showed higher relative levels of biosynthesis proteins related to B complex vitamins and cobalamin, and stress proteins related to iron deficiency. Control cells showed higher levels of histone superfamily proteins, sugar metabolism and nitrogen regulation proteins, and nutrient limitation and oxidative stress response proteins. Control had a higher abundance of poorly annotated and unknown proteins, but not proteins associated with neutral lipid biosynthesis. Proteomic analysis found that N-limitation had not adversely affected cellular physiology or biomass yields in control cells at day 12, due in part to the role of stress response proteins. Enriched pathways related to the stress response in control, most notably, glycolysis/gluconeogenesis, glutathione metabolism, oxidative phosphorylation, peroxisome and proximal tubule bicarbonate reclamation also represent potential targets for genetic improvement requiring further elucidation.

Chapters 4 and 5, taken together, demonstrated the implementation and refinement of a shotgun proteomics method, and the development and execution of a bioinformatics workflow to compare the proteomes of flask samples taken in lag phase. This approach uncovered remarkable adaptations to the different treatments as revealed by a comparison of group proteomes, despite

no significant difference in final biomass detected using gravimetric and spectrophotometric analyses.

In Chapter 6 (Manuscript III) *Chlamydomonas* was propagated in batch mode in 10L cultures over 5 days using a pilot scale photobioreactor (PBR) system. The objective was to examine growth and nutrient removal responses to wastewater processing, and to compare performance obtained at the pilot scale to that obtained at the bench scale (Chapters 4 and 5, Manuscript II). The same strain of *C. reinhardtii* cultured in identical control and wastewater treatment media as reported in Chapters 4 and 5 was used. As in Chapters 3, 4 and 5, the dual-purpose traits of high rates of nutrient removal and biomass growth were sought, and evaluated using similar gravimetric, spectrophotometric and colorimetric analysis. Treatment was found to have a highly significant effect on final biomass, where wastewater cultures showed higher biomass concentration. *Chlamydomonas* removed nutrients efficiently, as it did at the bench scale, but again did not accumulate biomass quickly at the pilot scale, and failed to demonstrate the desired dual-purpose traits identified in candidates from Chapter 3. Cells cultured in wastewater media showed higher final biomass concentration and biomass productivity in the PBR cultures. Cells cultured in control medium had comparable final biomass yields, but higher biomass productivity in the PBR cultures, which showed evidence of nutrient starvation. Results were reported and discussed within the context of metabolic constraints to microalgal mass culturing, and with insights obtained from proteomic results obtained at the bench scale in Chapter 4 and 5.

In sum total this dissertation demonstrated how shotgun proteomics and functional enrichment analysis can be integrated into fundamental biological research concerning microalgae, and generate insight into physiology and genetics. Furthermore, it showed relevance

for the selection and development of candidate strains, and in the optimization of environmental applications such as wastewater treatment or feedstock production for biofuels. Future areas of inquiry include generation of peptide and protein lists for targeted proteomics and absolute quantitation of protein abundance, identification of potential mutagenic targets for genetic manipulation, candidate selection and breeding programs, and integration of proteomic techniques and HT data sets with metabolomics and RNA sequencing (RNA-seq) platforms. Furthermore, with continued technical advances in instrumentation and bioinformatics platforms, a more routine use of proteomics as a monitoring tool for both monocultures and microbial consortia in wild and industrial settings alike is feasible. Lastly, because of the highly conserved photosynthetic and nitrogen assimilatory machinery in the chloroplast, insights surrounding growth and nutrient removal in microalgae can inform higher plant physiology, and vice versa.

7.2. Methodology

An in-house microalgae platform for culturing and maintaining stable seed monocultures for present and future experiments was successfully implemented at the outset of this dissertation research. At present up to 8 different species and/or strains of photoautotrophic microalgae, including cyanobacteria, have been maintained simultaneously, with the capacity for heterotrophic microalgae culturing as well.

In order to study microalgae cultured at the pilot scale, a PBR system was successfully modified for use with liquid media, compressed air, and continuous light. The PBR system consisted of four modular glass vertical tubular columns, each with inner diameter of 10.16 cm, height of 1.37 m, and culture volume of 10.02 L. Filter compressed air was introduced at the base of the columns using air spargers to promote mixing and gas exchange. Air was

supplemented with CO₂ in a ratio of (97/3, v/v) by using air flow meters and an electronic mixer. Continuous illumination (24 h) using banks of cool white fluorescent bulbs was achieved, and cultures propagated under non-sterile conditions.

A label-free shotgun proteomics platform was successfully developed and applied to compare the proteomes of photoautotrophic microalgae cultured in simulated wastewater containing nitrate and ammonia, and a nutrient-sufficient control that contained nitrate only. This required adapting and optimizing an in-house shotgun proteomics platform capable of yielding high-quality and reproducible HT MS data from microalgae samples, using protocols originally developed by Drs. Robert L. Hettich, Nathan VerBerkmoes and colleagues at Oak Ridge National Laboratory (Oak Ridge, TN, USA) using prokaryotes,^{104,198,221} then eukaryotic yeast,⁷⁶ then modified here for microalgae and green plants (Chapter 9, Section 9.1, Appendix A). This included harvesting of pellet, protein extraction, in-solution digestion, sample clean up, column packing, and instrument methods for performance of two-dimensional liquid chromatography nano-electrospray ionization tandem mass spectrometry (2D LC–nanoESI–MS/MS) using a linear ion trap mass spectrometer (LTQ XL). Challenges related to microalgae, particularly removal of lipids, salts, and algal cell impurities, required the modification of a previous elution gradient⁷⁶ into a 24 h 12-step MudPIT method⁷⁵ to maximize the elution of peptides from the column into the ionization source (Chapter 9, Section 9.1.3, Appendix A). This optimization resulted in the identification of 2358 proteins across four biological replicates of *C. reinhardtii* cultured at the flask scale in two treatment conditions (Chapters 4 and 5, Manuscript II).

Because our proteome analysis was performed using a low mass accuracy ion trap for MS and MS/MS, we employed Scaffold software to apply empirical and statistical approaches to the entire replicate data set. We selected individual peptide and protein probability thresholds to

limit false positive identifications, as determined by reverse database hits. For this reason, despite using a low mass accuracy detector, this target-decoy approach allowed specificity to be maintained and our data set achieved similar false positive protein identification rates as could be obtained with high mass accuracy data, albeit at reduced sensitivity. A mass informatics methodology was used whereby MS/MS spectra were extracted from Thermo RAW files that corresponded to a single biological replicate and then compared to theoretical tryptic peptide sequences using Proteome Discoverer (v1.4)/SEQUEST HT algorithm (v1.3) (Thermo Fisher Scientific, San Jose, CA). SEQUEST HT-assigned peptide spectrum matches (PSMs) from the 8 biological flask samples (2 conditions, 4 replicates) were loaded into Scaffold (v4.0.7, Proteome Software, Inc., Portland, OR) and PSM probabilities assigned by Scaffold's local false discovery rate (FDR) Bayesian algorithm, and an X! Tandem re-search to increase sequence coverage. Protein identifications were initially filtered to require ≥ 3 unique peptides in at least one biological sample, followed by defining protein and PSM probability filters to achieve $\leq 1\%$ global protein and peptide FDR, estimated using reverse database search results.

The development of a bioinformatics platform for differential analysis and functional enrichment relied on web-based tools, followed by extensive manual curation to confirm results and determine the statistical and biological significance of differences detected in the *C. reinhardtii* proteomes. In addition to controlling for false positive protein identifications, it was necessary to control the FDR when screening for differential abundance on a proteome scale. We first applied a minimum spectral count filter of four spectral counts.²²⁶ Then, significant differential relative abundance was assessed using the QSpec algorithm (v1.2.2), which computes Z-statistics and allows global FDR to be controlled.¹⁷⁰ The QSpec program normalized total spectral counts by adjusting MS data using a Poisson distribution by the total sum sample-

by-sample, and the normalized length of proteins across all samples to allow for relative abundance quantitation. All proteins were evaluated with a Z-statistic $\geq |3.69|$ threshold, corresponding to a directional FDR_{up} or FDR_{down} of 5% (0.05).

Functional enrichment was performed using the web-based annotation integration tool Algal Functional Annotation Tool (AFAT) which contained integrated annotation data for biological pathways, ontology terms, and protein families for *C. reinhardtii* and *Arabidopsis thaliana*. Hypergeometric testing by AFAT determined the significance of functional enrichment terms with rank and assignment of a *p*-value, where each enrichment test was considered independent.¹⁵⁵ Significantly differentially expressed protein transcript IDs were queried against the entire *C. reinhardtii* genome. Manual curation of bioinformatics results and verification using multiple ontology, pathway, and protein family resources was required due to *in silico* generation of many annotation results for *C. reinhardtii* and *A. thaliana* that were not experimentally verified.

Extensive literature searches and data mining of all 92 statistically significant differentially expressed proteins were required to confirm protein function, cellular location, and biological process. Functional attributes of the differential data sets were manually analyzed using the JGI Phytozome annotation (*Chlamydomonas* v9.1 and *Arabidopsis* v9.1), the incomplete annotation from the *Chlre* v5.3.1 JGI build including the Kyoto Encyclopedia of Genes and Genomes (KEGG), Eukaryotic Orthologous Group (KOG), Panther, Pfam and best *Arabidopsis* TAIR10 hits. Pattern searches of GO annotation data from *A. thaliana* were used to produce GOSLIM files targeting specific processes and functions. Lastly, metabolic mapping was performed using the KEGG pathway mapping software iPath2.0 to visualize functional enrichment, and differences between treatment conditions.¹⁸⁰

7.3. Microalgae and wastewater treatment

The doctorate dissertation findings summarized here come from examining growth and nutrient uptake responses in unsequenced and sequenced microalgae, at the bench and pilot bioreactor scales, to simulated wastewater processing. Each dissertation chapter served to build on the complexity of analysis and experimental questions, and culminated in a comparative shotgun proteomic analysis of wastewater-cultured microalgae to elucidate functional enrichment of metabolic pathways, and gain biological insight.

7.3.1. Chapter 3: Manuscript I

Despite the short sexual cycles present in microalgae, and decades of research, as of yet, no strain with demonstrably improved productivities, under full sunlight in outdoor scale up conditions, has been reported.^{7,12} Chapter 3 (Manuscript I) posited that microalgae differ in uptake of phosphorus (P) and growth, making the identification of top performers fundamental. The objective of this species screen was to identify dual-purpose candidates capable of high rates of TP removal and growth. Three freshwater – *Chlorella* sp., *Monoraphidium minutum* sp. and *Scenedesmus* sp. – and three marine – *Nannochloropsis* sp., *N. limnetica* sp., and *Tetraselmis suecica* sp. – species were batch cultured in flasks over 16 days to quantify TP removal from solution and growth as a function of P loads (control, and 5, 10, and 15 mg L⁻¹ enrichment of control). Experimental design used 100 $\mu\text{mol m}^{-2} \text{s}^{-1}$ of light, a light/dark cycle of 14/10 hours, and no CO₂ enrichment.

Total phosphorus uptake was found to be dependent on species, duration of exposure, and treatment, with significant interaction effects. Growth was found to be dependent on species and

treatment. Of interest was the finding that not all species showed increased TP removal with increasing P addition, and no species demonstrated higher growth. Also unexpected was that the two marine picoplankton species, *Nannochloropsis* sp and *N. limnetica* sp. performed poorly across all treatments, despite recent interest in the use of picoplankton for outdoor feedstock production.³⁷

The observed linear growth rate data from this study was not expected. At higher TP loads it was expected these cultures would show higher biomass and optical density measurements, and a distinct J curve. Exponential growth of microalgae was reported in a screen of 30 strains of microalgae that included *Chlorella* sp., *Scenedesmus* sp., *Nannochloropsis* sp., and *Tetraselmis suecica* sp.,³⁷ and *Neochloris oleoabundans* sp. cultured in anaerobically digested dairy manure.⁴⁸ Linear trend lines fitted to growth data and lower biomass productivities were most likely caused by excess P addition with an insufficient supply of light and/or carbon. Also, the lower N/P ratio in the treatments may have affected P uptake and growth, where responses of autotrophs to single enrichment of N or P was not as effective in provoking the growth response as N + P enrichment.¹⁰³

Two promising dual-purpose candidates were identified. At the 10 mg L⁻¹ treatment *Monoraphidium minutum* sp. removed 6.66 mg L⁻¹ ± 0.60 SE (67.1 %) of TP at day 8, 7.86 mg L⁻¹ ± 0.28 SE (79.3 %) at day 16, and biomass accumulation of 0.63 g L⁻¹ ± 0.06 SE at day 16. At the 10 mg L⁻¹ treatment *Tetraselmis suecica* sp. removed 6.98 mg L⁻¹ ± 0.24 SE (79.4 %) of TP at day 8, 7.30 mg L⁻¹ ± 0.60 SE (83.0 %) at day 16, and biomass accumulation of 0.55 g L⁻¹ ± 0.02 SE at day 16. Biomass yields are lower than many published reports for biomass and biofuel applications. However the biomass yields and P removal efficiencies are within the range of studies for many recent peer reviewed studies using microalgae cultured in wastewater. Using

the maximum biomass achieved by *Monoraphidium* sp. for the 10 mg L⁻¹ treatment of 0.63 g L⁻¹ ± 0.06 SE at day 16 (0.039 g L⁻¹ day⁻¹), and removing 7.86 mg L⁻¹ ± 0.28 SE of TP also at day 16, it is feasible to envision a outdoor scale up PBR or pond system able to treat 100 L of wastewater, remove 5.90×10^{-4} kg of P and produce 4.70×10^{-2} kg of algal biomass, assuming 75% efficiency. These species merit further study using high-density wastewater cultures, lipid profiling, and potentially gel-based liquid chromatography-mass spectrometry (GeLC/MS)⁵⁸ in order to assess further suitability for a nutrient removal and biomass/biofuel production scheme.

7.3.2. Chapter 4: Manuscript II

Chapter 4 (Manuscript II) posited that a systems biology understanding of the role of nitrogen source and availability is needed to elucidate cellular processes leading to the shunting of carbon into different metabolic compartments – oil or starch.⁴⁷ Evolution of the basic cell cycle in microalgae included the development of signaling networks reliant on post-transcriptional and post-translational modifications to regulate protein expression and metabolic adaptations to changing environments and stressors. Just as in the candidate species screen (Chapter 3, Manuscript I), the expected response by *Chlamydomonas* to higher nutrient loadings in the wastewater group was enhanced biomass accumulation (Chapter 4, Manuscript II). Furthermore, the expected physiological response of higher nutrient loadings in the wastewater flask cultures was enhanced P and N removal efficiency.

At the bench scale using flask cultures (Chapter 4), final biomass concentration in *Chlamydomonas*, as measured gravimetrically, was found to be 0.19 g L⁻¹ ± 0.02 SD and 0.23 g L⁻¹ ± 0.06 SD for wastewater and control groups, respectively, where treatment had no significant effect (ANOVA F_{1,8} = 3.807; *p* = 0.063). Uptake of TP, nitrate-N, and ammonia-N in

solution was followed over 12 days. Additional statistical analysis showed *C. reinhardtii* consumed phosphorus at an exponential rate in both treatments (ANOVA $F_{1,8} = 0.33$ $p = 0.58$), with a half life in the media of 0.71 ± 0.21 SD days. *C. reinhardtii* consumed ammonia at an exponential rate in the wastewater treatment, halving the concentration every 3.13 ± 0.18 SD days. When ammonia was nearly depleted after 10 days of growth, *C. reinhardtii* started consuming nitrate at a rate of 1.7 ± 0.34 SD days. In the control treatment, which lacked ammonia, nitrate was consumed at an exponential rate with a halving of the concentration every 2.25 ± 0.26 SD days. Once uptake was initiated, the rate of nitrate consumption was comparable in both treatments. Despite the increased availability of nitrogen in the form of ammonia, a preferred source of nitrogen for green algae and higher plants, wastewater cells did not grow faster, accumulate higher biomass, or uptake nutrients faster at the bench scale.

For this reason it was hypothesized that if microalgae cells subjected to different treatments adapt dynamically to their respective conditions, then a comparison of their proteomes should demonstrate physiological differences and metabolic adaptations at the level of cellular pathway. The development and application of an in-house shotgun proteomics and bioinformatics platform (Chapter 9, Section 9.1, Appendix A) to compare samples from control and wastewater flasks showed just that. Namely, that despite no significant difference in final biomass accumulation between treatment groups, proteomic analysis captured the dynamic adaptation by *Chlamydomonas* to the different culture conditions. Label-free shotgun proteomic analysis identified 2358 of which 92 were significantly differentially abundant. Remarkably, even after 12 days wastewater cells showed higher relative abundances of photosynthetic antenna proteins, enzymes related to carbon fixation, and biosynthesis of amino acids and secondary metabolites. Control cells showed higher abundances of enzymes and proteins related

to nitrogen metabolism and assimilation, synthesis and utilization of starch, amino acid recycling, evidence of oxidative stress, and little lipid biosynthesis.

The insignificant difference in final biomass concentration and OD₆₈₀ further demonstrated that even in increasingly N-limited media, *C. reinhardtii* continued to grow and attempt to balance its C/N ratio without invoking the stress response of TAG biosynthesis associated with N-deprivation.⁴³ This remarkable ability of *Chlamydomonas* to rapidly adjust to favourable and unfavourable abiotic conditions¹ due to the flexibility of its metabolism⁸⁸ was demonstrated in this doctoral dissertation. While the shift in proteomes was not as dramatic as would be expected using harsh perturbation, such as comparing nutrient-sufficient cells to nutrient-deprived, for example, findings in Manuscript II highlighted the resilience of eukaryotic microalgae. Of interest for scale up production was that proteomic analysis found that N-limitation did not adversely affect growth or biomass yields in control cells at the flask bench scale after 12 days, and over-enrichment of ammonia-N did not adversely affect cellular physiology or yields in wastewater cells. Overall, results were in agreement with previous findings on nitrogen sensing, recycling of nitrogen to sustain growth, and decreased overall protein turnover in favor of those critical for survival in cells entering N-limitation.^{35,39,41,43,62,245}

Results showed 32 proteins enriched in 17 KEGG pathways, and 28 proteins also enriched in 17 KEGG pathways, for wastewater and control, respectively. In wastewater, Photosynthesis—antenna proteins, Carbon fixation in photosynthetic organisms, Pentose phosphate pathway, Biosynthesis of plant hormones, and Biosynthesis of alkaloids derived from shikimate pathway make up the top-5 enriched pathways by AFAT significance score and manual curation. In the control group Nitrogen metabolism, Alanine, aspartate and glutamate metabolism, Pyrimidine metabolism, Glycolysis/Gluconeogenesis and Arginine and proline

metabolism made up the top-5 enriched pathways. A number of enriched enzymes and proteins were found to be of interest for further analysis, including 7 related to carbon fixation, amino acid metabolism and starch metabolism, and an additional 9 related to nitrogen metabolism.

Chapter 4 (Manuscript II) provided insight into the importance of nitrogen source, ammonia and/or nitrate, availability, and switching, and to date is the first study to perform shotgun proteomics on wastewater-cultured microalgae, and the first to use both N sources in a comparative proteomics study, that we know of. The response of a eukaryotic microalgal proteome to experimental conditions highlighted tightly controlled pathways essential to the maintenance of culture health and productivity in concert with light absorption and carbon assimilation. This sophisticated regulation, in concert with light absorption, plays a critical role in determining cell culture health, productivity, growth, and the metabolic partitioning of carbon. Enriched pathways in artificial wastewater, notably, photosynthetic carbon fixation and biosynthesis of plant hormones, and those in nitrate only control, most notably, nitrogen, amino acid, and starch metabolism, represent potential targets for genetic improvement requiring targeted elucidation. Future mutagenic selection and/or metabolic dissection of these targets could further enhance understanding of growth and nutrient removal dynamics in microalgae and higher plants. Findings also demonstrated the power of LC–MS/MS proteomic analysis to detect metabolic responses to subtle changes in environmental conditions, and not just harsh perturbation.

7.3.3. Chapter 5: Manuscript II, Supplemental findings

In the previous Chapter 4 (Manuscript II) we performed a label-free comparative shotgun proteomic analysis of wastewater-cultured *C. reinhardtii* at the bench scale. *Chlamydomonas*

demonstrated a remarkable ability to adapt to the availability and source of nitrogen in each respective culture condition, as evidenced by the insignificant difference in final biomass and comparable nutrient removal rates. In Chapter 5 (Manuscript II, Supplemental findings), we reported additional significant differentially abundant proteins of interest not discussed in Chapter 4, including biosynthesis related, stress related, poorly annotated, and unknown proteins.

Comparison of proteomes revealed wastewater cells had higher relative levels of biosynthesis proteins related to B complex vitamins and cobalamin, and stress proteins related to iron deficiency. Control cells showed higher levels of histone superfamily proteins, sugar metabolism and nitrogen regulation proteins, and nutrient limitation and oxidative stress response proteins. Control had a higher abundance of poorly annotated and unknown proteins, but not proteins associated with neutral lipid biosynthesis. Enriched pathways in wastewater included RNA degradation, thiamine metabolism and one carbon pool by folate, and those in nitrate only control, notably, calcium signaling, systemic lupus erythematosus, protein processing in endoplasmic reticulum and Arf/Sar family. Proteome analysis found that N-limitation did not adversely affect cellular physiology or biomass yields in control cells at day 12, due in part to the role of stress response proteins. Enriched pathways related to the stress response in control, included most notably, glycolysis/gluconeogenesis, glutathione metabolism, oxidative phosphorylation, peroxisome and proximal tubule bicarbonate reclamation. Differential abundance analysis and functional enrichment identified a number of enzymes and potential gene targets in both culture conditions that represent potential targets for genetic improvement, and require further elucidation using discovery and targeted proteomic techniques.

7.3.4. Chapter 6: Manuscript III

Chapters 4 and 5 (Manuscript II) posited that an evolutionary tradeoff between growth and lipid biosynthesis in microalgae represents a metabolic conundrum central to a decades long discrepancy between actual yields and scale up projections by academia and industry alike. Furthermore, the use of sequenced strains could inform development of dual-purpose candidates capable of high rates of growth and nutrient removal for wastewater treatment, in turn subsidizing biomass production, including feedstock for biofuels.

In Chapter 6 (Manuscript III), the same strain of *C. reinhardtii* studied at the bench scale was cultured in batch mode under continuous illumination for 5 days using a pilot scale photobioreactor (PBR) system in order to investigate and compare nutrient uptake and growth responses of scale up wastewater processing. Our approach compared two identical growth medium conditions as in Chapters 4 and 5 (Manuscript II), and cultures were supplemented with CO₂ and propagated under non-sterile conditions. *Chlamydomonas* removed phosphorus and nitrogen from solution efficiently in both culture conditions, and at comparable rates to other studies in the literature.^{33,121–124} By day 5, *C. reinhardtii* removed 3.79 mg L⁻¹ ± 0.06 SE (99.4 %) of TP, 4.41 mg L⁻¹ ± 0.04 SE (97.2 %) of nitrate-N, and 17.15 mg L⁻¹ ± 0.06 SE (99.4 %) of ammonia-N in the AWW condition, and 1.10 mg L⁻¹ ± 0.02 SE (98.7 %) of TP and 11.30 mg L⁻¹ ± 0.18 SE (97.5 %) of nitrate-N in the CTRL condition. Final biomass concentration was 0.48 mg L⁻¹ ± 0.04 SE for wastewater, and 0.24 mg L⁻¹ ± 0.02 SE in control.

Culture condition was found to have a highly significant effect on final biomass accumulation (ANOVA F_{1,8} = 37.99; *p* = 3.33 E-06). At the 10 L pilot scale culture volume, final biomass densities of 0.48 ± 0.04 g L⁻¹ and 0.24 ± 0.02 g L⁻¹ for wastewater and control, respectively, corresponded to biomass productivities of 0.24 g L⁻¹ day⁻¹ and 0.12 g L⁻¹ day⁻¹,

respectively, when adjusted for time (2 days exponential growth). These results were compared to biomass yields from the same strain propagated at the bench scale using 330 mL flask culture volumes, continuous high light, and sterile conditions with no CO₂ supplementation. Final biomass was $0.19 \pm 0.01 \text{ g L}^{-1}$ for AWW and $0.23 \pm 0.02 \text{ g L}^{-1}$ in CTRL, where culture condition had no significant effect (ANOVA $F_{1,8} = 3.807$; $p = 0.063$). Both conditions achieved the same relatively low biomass productivity rate of $0.02 \text{ g L}^{-1} \text{ day}^{-1}$, when adjusted for time in days. Cells cultured in control medium showed similar final biomass yields, but higher biomass productivity in the PBR cultures, and evidence of nutrient starvation. Cells cultured in wastewater media showed higher final biomass and biomass productivity in the PBR cultures.

Lower biomass yields were expected and observed at the bench scale^{23,25,26,37} and pilot scale³⁷ for *C. reinhardtii* as compared to other reported freshwater and marine eukaryotic microalgae cultured in real and synthetic wastewater. Of particular interest was the finding that treatment had no significant effect on final biomass in the flask cultures, and that final biomass was significantly higher in the wastewater treatment at the PBR scale. A review of the literature (Chapter 2) showed that the highly conserved and tightly regulated chloroplast mechanisms of photosynthesis and nitrogen assimilation greatly affect the shunting of carbon towards lipid biosynthesis or carbohydrates. Studies using microalgae suggested continued protein and nucleotide biosynthesis in non-limited nitrogen conditions (wastewater group), and decreased chlorophyll production, light absorption, and cell division in nitrogen limited conditions (control group).^{35,41,43,245}

The complete removal of macronutrients from solution by day 2 in both the PBR culture groups suggested that differences in biomass accumulation are mainly attributed to N and P loadings. It was hypothesized⁴⁰ and demonstrated⁴¹ that consumption of chlorophyll continues to

support growth after exhaustion of extracellular N pools. In the PBR control cultures cells appeared yellow-green,^{40,62} and larger and globular in shape, compared to a dark green color in wastewater cells. This observation is supported by proteomic studies of cells adapting to harsh N perturbation, when sampled at early time points demonstrated dramatic and immediate changes in primary metabolism,^{39,43,62} with changes in C/N balance and TAG accumulation occurring only under sustained chronic conditions.^{43,62} It has to be mentioned that lower biomass productivities were also found using nutrient-deprived growth medium,³⁷ including the same response of neutral lipid accumulation due to P-limitation, as that associated with N-limitation, as demonstrated in marine species,^{37,38} and very likely control group cells at the pilot scale.

By using the average maximum biomass achieved by *C. reinhardtii* cultured in wastewater medium in the PBR system of 0.48 ± 0.04 SE g L⁻¹ over 5 days, that also removed $3.79 \text{ mg L}^{-1} \pm 0.06$ SE (99.4 %) of TP, $4.41 \text{ mg L}^{-1} \pm 0.04$ SE (97.2 %) of nitrate-N, and $17.15 \text{ mg L}^{-1} \pm 0.06$ SE (99.4 %) of ammonia-N, a scaled up PBR or pond system could feasibly treat 100 L of wastewater in the same 5 day time period, remove 2.8×10^{-5} kg of TP, 3.3×10^{-5} kg of N-nitrate, and 1.3×10^{-4} kg of N-ammonia, and produce 3.6×10^{-3} kg of algal biomass, assuming 75% efficiency. By scaling to 1000 L, or two orders of magnitude larger, either by increasing the number of PBR columns or moving directly to outdoor ponds, would theoretically remove 3×10^{-4} kg of TP, 3×10^{-4} kg of N-nitrate, and 1×10^{-1} kg of N-ammonia, and produce 4×10^{-2} kg of biomass, assuming 75% efficiency, in the same 5 day time period. Thus, *C. reinhardtii* did not demonstrate the desired dual-purpose traits of high nutrient removal efficiency and biomass productivity at either the flask or PBR scales. This finding was in itself not surprising given the status of *Chlamydomonas* as a model organism, and the difficulty experienced culturing the microalga at the 10L pilot scale without CO₂ enrichment.

Chlamydomonas did demonstrate a remarkable ability to adapt to environmental conditions associated with mass culturing, including light attenuation, fluid dynamics, and nutrient limitation. This study highlights the importance of characterizing microalgae cultured in wastewater containing both ammonia and nitrate, and further highlighted the metabolic conundrum that limits biomass feedstock production schemes, where biomass growth and lipid yields are metabolically constrained and opposed. As demonstrated at the bench scale, over-enrichment of ammonia-N had no detrimental effect on cells cultured in wastewater, however N-limitation and P-limitation most certainly affected culture health and biomass yields.

7.4. Statement of originality, significance and contribution to knowledge

The chapter manuscripts of this doctoral dissertation have made contributions to knowledge in microalgal biology, algae and plant proteomics, and environmental and industrial applications such as wastewater treatment and biofuel production. The following are findings of originality, significance, and contributions to knowledge listed by chapter manuscript.

- 1) The screen of six different unsequenced species of microalgae in Chapter 3 (Manuscript 1) to identify dual-purpose candidates capable of high rates of P removal and growth made the following contributions.
 - Established in-house platform and protocols for maintaining stable monocultures and axenic seed cultures of different species of microalgae for current and future research.
 - Identified 1 freshwater, *Monoraphidium minutum* sp., and 1 marine, *Tetraselmis suecica* sp., dual-purpose candidates with potential for use and further research into scalable wastewater treatments.

2) Shotgun proteomic analysis of flask samples from Chapters 4 and 5 (Manuscript II and Supplemental findings) yielded a number of original and significant findings.

- Adapted and optimized in-house shotgun proteomics platform capable of yielding high-quality and reproducible high throughput MS data from eukaryotic green microalgae, including pellet harvesting, protein extraction, in-solution digestion, sample clean up, column packing, and instrument methods for performance of two-dimensional liquid chromatography nano-electrospray ionization tandem mass spectrometry (2D LC–nanoESI–MS/MS) using a linear ion trap (LTQ XL) mass spectrometer.
- Modified a 6-step MudPIT elution gradient into a 24 h 12-step gradient with strong reproducibility for analysis of green algae and plant samples.
- Established in-house mass informatics and bioinformatics workflows to analyze *C. reinhardtii* data sets. The bioinformatics workflow leveraged publicly available online resources and databases for *C. reinhardtii* and *A. thaliana*, including tools for data normalization, differential expression analysis, functional enrichment, pathway analysis and visualization. Workflow enabled elucidation of protein function, location, and regulation in both eukaryotic microalgae and plants.
- Label-free shotgun proteomic analysis identified 2358 proteins, of which 92 were significantly differentially abundant (42 in wastewater and 50 in control). Of these, 32 in wastewater, and 28 in control, were mapped to 17 KEGG pathways, respectively.

- Provided insight into the importance of nitrogen source – ammonia and/or nitrate – and to date is the first study to perform shotgun proteomics on wastewater-cultured microalgae, where both nitrate-N and ammonia-N are present in a treatment.
- Uncovered remarkable differences in proteome responses of *C. reinhardtii* that traditional gravimetric, spectrophotometric and colorimetric techniques failed to detect.
- Demonstrated that subtle manipulations in environmental conditions can be captured in proteomic analysis of *C. reinhardtii*, and not just harsh perturbation comparing nutrient enrichment with nutrient deprivation.
- Identified a number of enriched enzymes and proteins of interest for further targeted proteomic analysis, including 7 related to carbon fixation, amino acid metabolism and starch metabolism, and an additional 9 related to nitrogen metabolism.
- Identified a number of stress response proteins of interest for further elucidation.

3) Culturing the sequenced eukaryotic green microalga *C. reinhardtii* at the pilot scale in Chapter 6 (Manuscript III) contributed the following:

- Modified an existing vertical column PBR system for suitability in culturing suspended microalgae in liquid medium with a bubble column, CO₂ supplementation, gas mixing and a uniform lighting system, including modifiable configurations of light emitting diodes, for current and future research.
- Examined scale up wastewater processing and compared results to the bench scale.
- Confirmed that *C. reinhardtii* is not a robust dual-purpose candidate for scalable wastewater treatment.

- Speculated that dynamic adaptations to available ammonia and/or nitrate may have been taking place using proteomics results at the bench scale. Demonstrated the limitations of gravimetric, spectrophotometric and colorimetric analyses alone as tools for inferring changes in cellular physiology.
- Generated samples for proteomic analysis.

7.5. Future research

The work presented in this dissertation attempted to improve the present understanding of the response of microalgae to wastewater processing at the levels of cell culture and cellular pathway. Findings from the candidate screening (Chapters 3), and particularly conclusions reached concerning the proteomic response of wastewater-cultured microalgae (Chapters 4 and 5) and scale up of culture volume using a PBR system (Chapter 6), have implications for future algal and plant research, and high-density biomass production in general. In sum total this dissertation demonstrated how shotgun proteomics and functional enrichment can be integrated into fundamental research concerning algal physiology and genetics to generate biological insight. Furthermore, it showed relevance in the selection of potential candidate strains, identification of genetic targets, and the optimization of environmental applications such as wastewater treatment. Future areas of inquiry include generation of lists for targeted proteomics and absolute quantitation of gene expression, integration with RNA sequencing (RNA-seq) and metabolomics data, identification of potential mutagenic targets for genetic manipulation, candidate selection and breeding programs. With technical advances, a more routine use of proteomics as a monitoring tool for both monocultures and microbial consortia in wild and industrial settings alike. Lastly, because of the highly conserved photosynthetic and nitrogen

assimilatory machinery in the chloroplast, insights surrounding growth and nutrient removal in microalgae can inform plant physiology, and vice versa.

7.5.1. Discovery and targeted proteomics

The platforms and workflows reported here can serve in the short run as a starting point for future multi-state and/or time course discovery proteomic work to compare nitrogen source, availability, sensing, and dynamic metabolic responses to subtle manipulations of macronutrients, including phosphorus, and/or sub-optimal culture conditions. For example, this workflow can be expanded to investigate time course studies.^{43,59} Multi-state experiments make use of hierarchical clustering of differentially expressed proteins to identify protein groups and/or families associated with different conditions or adaptations.⁷⁴ Tradeoffs exist as to identifying greater numbers of proteins versus a comparison of broader arrays of samples/conditions. Overall, given the continued improvement in high mass accuracy instruments, and decreasing costs, a long term strategy of attempting to perform experiments with a broad array of biological replicates and conditions and time points may be best.

Furthermore, proteomic data can also be integrated with metabolomic analysis to combine insights into enzyme abundance and pathway enrichment, with metabolic flux.^{39,43,62} Discovery proteomics can also be pursued using unsequenced strains by way of gel-based liquid chromatography-mass spectrometry (GeLC/MS).^{58,59} The effects of decreasing sequencing costs,¹⁵⁴ and increased curation and annotation of algae and plant databases coincide with the adoption of large-scale MS-based proteomic and molecular genetic studies. To that end using MS-based proteomics for the identification of critical regulators of genes, proteins, and metabolites as promising targets for genetic and metabolic engineering should continue to

intensify in algae. At present N-limitation and induction of fatty acid (FA) biosynthesis are of high interest for industry, academia and government laboratories. Equally interesting for algae and plant researchers would be the continued characterization of shifts in proteome responses when cells are introduced back into favorable nitrogen environments.³⁹ Proteomic analysis of P-starvation and recovery in eukaryotic microalgae has not been studied to the extent of N-starvation. Lipid profiling^{37,38} suggests P-limitation proteomic studies could contribute to understanding algal physiology and environmental applications. Lipid profiling showed a return in lipid composition for polar lipids and sterols associated with growth within a week.³⁷ At the time of this dissertation, changes in the proteome associated with the breakdown of FA and triacylglycerols (TAGs) accumulated bodies in support of cell recovery is also not well known.

In the medium term targeted proteomics has much to offer algae and plant proteomic research. As mentioned, technical advances in chromatography (nano-HPLC separation), MS instrumentation (high-resolution, sensitivity and mass-accuracy) and data processing have enabled low cost label-free quantitation.¹⁶⁶ Further developments in these areas have also spurred advances in single and multiple reaction monitoring (SRM/MRM) and creation of full scan (MS1 and MS/MS) targeted proteomic methods.^{271,272} High-quality and reproducible HT MS data from shotgun proteomic experiments can be used to generate target lists of assays, chromatogram libraries,²⁷³ peptides and proteins of interest for use in relative and absolute quantitation of gene products, including protein and small molecules. The integration⁷⁸ of RNA-seq^{63,64} and MS-based shotgun proteomics⁷⁹ suggests that in the near term, more cost effective and comprehensive understandings of biological systems, including bioremediation applications using microalgae, can be achieved.

7.5.2. Community proteomics and bioprocess monitoring

In community ecology, the idea that diversity within ecosystems increases stability²⁷⁴ and that more diverse plant communities are more productive was proposed very early on.²⁷⁵ Directly controlled species composition in 147 replicate grassland plots found that productivity increased significantly with diversity, as did complete utilization of the limiting nutrient nitrogen.²⁷⁶ Similarly, the human gut flora affords enriched metabolism and synthesis of compounds.²⁷⁷ Developments in biological MS and informatic platforms from the study of complex microbial consortia²²¹ can also improve the current poor understanding of growth, nutrient uptake and photosynthetic dynamics found in high-density wastewater mono and mixotrophic microalgae cultures. Metaproteomic studies include acid mine drainage,^{77,222} enhanced biological phosphorus removal (EBPR)¹⁹⁸ using activated sludge, and methanogenic degradation of terephthalate.²⁷⁸ Lastly, continued technical advances in mass spectrometry and informatics may afford more routine proteomic study and monitoring of candidate strains.²⁷⁹

This dissertation research sought to integrate shotgun proteomics and functional analysis into fundamental biological research concerning algal physiology and the environmental application of wastewater treatment. The effort and results may inform candidate selection and breeding programs, identification of genetic targets, and provide insights for higher plants. In light of accelerating technical developments in HT MS, it may contribute incremental progress towards the use of algal proteomics as a monitoring and diagnostic tools for bioprocess optimization,⁷⁶ and the study of both monocultures and microbial consortia in industrial and wild settings.⁷⁷ Building on this dissertation is the continued elucidation of candidate pathways and targets in bench and pilot scale cultures for development of robust microalga or consortia of

microalga and/or microbes, suitable for scalable outdoor treatment of secondary municipal effluent and/or agricultural wastewater as part of a larger feedstock production scheme.

Chapter 8: References

8.1. References

- (1) Behrenfeld, M. J.; Halsey, K. H.; Milligan, A. J. Evolved physiological responses of phytoplankton to their integrated growth environment. *Philos. Trans. R. Soc., B* **2008**, 363 (1504), 2687–2703.
- (2) Falkowski, P. G.; Katz, M. E.; Knoll, A. H.; Quigg, A.; Raven, J. A.; Schofield, O.; Taylor, F. J. R. The evolution of modern eukaryotic phytoplankton. *Science* **2004**, 305 (5682), 354–360.
- (3) Pulz, O.; Gross, W. Valuable products from biotechnology of microalgae. *Appl. Microbiol. Biotechnol.* **2004**, 65, 635–648.
- (4) Richmond, A. Economic applications of micro algae. In: *Handbook of Microalgal Culture*; Richmond, A., Ed.; Blackwell Science Ltd: Oxford, UK, **2004**; pp 255–353.
- (5) Weyer, K. M.; Bush, D. R.; Darzins, A.; Willson, B. D. Theoretical maximum algal oil production. *BioEnergy Res.* **2010**, 3 (2), 204–213.
- (6) Zhu, X.-G.; Long, S. P.; Ort, D. R. What is the maximum efficiency with which photosynthesis can convert solar energy into biomass? *Curr. Opin. Biotechnol.* **2008**, 19 (2), 153–159.
- (7) Walker, D. A. Biofuels, facts, fantasy, and feasibility. *J. Appl. Phycol.* **2009**, 21 (5), 509–517.
- (8) van Beilen, J. B. Why microalgal biofuels won't save the internal combustion machine. *Biofuels, Bioprod. Biorefin.* **2010**, 4 (1), 41–52.
- (9) Chisti, Y. Biodiesel from microalgae. *Biotechnol. Adv.* **2007**, 25 (3), 294–306.
- (10) Savage, D. F.; Way, J.; Silver, P. A. Defossilizing fuel: how synthetic biology can transform biofuel production. *ACS Chem. Biol.* **2008**, 3 (1), 13–16.
- (11) Georgianna, D. R.; Mayfield, S. P. Exploiting diversity and synthetic biology for the production of algal biofuels. *Nature* **2012**, 488 (7211), 329–335.
- (12) Klein-Marcuschamer, D.; Chisti, Y.; Benemann, J. R.; Lewis, D. A matter of detail: assessing the true potential of microalgal biofuels. *Biotechnol. Bioeng.* **2013**, 110 (9), 2317–2322.
- (13) McGinn, P. J.; Dickinson, K. E.; Park, K. C.; Whitney, C. G.; MacQuarrie, S. P.; Black, F. J.; Frigon, J.-C.; Guio, S. R.; O'Leary, S. J. B. Assessment of the bioenergy and

- bioremediation potentials of the microalga *Scenedesmus* sp. AMDD cultivated in municipal wastewater effluent in batch and continuous mode. *Algal Res.* **2012**, *1* (2), 155–165.
- (14) De Bhowmick, G.; Subramanian, G.; Mishra, S.; Sen, R. Raceway pond cultivation of a marine microalga of indian origin for biomass and lipid production: a case study. *Algal Res.* **2014**, *6*, 201–209.
 - (15) Uduman, N.; Qi, Y.; Danquah, M. K.; Forde, G. M.; Hoadley, A. Dewatering of microalgal cultures: a major bottleneck to algae-based fuels. *J. Renew. Sustain. Energy* **2010**, *2* (1), 012701.
 - (16) Clarens, A. F.; Resurreccion, E. P.; White, M. A.; Colosi, L. M. Environmental life cycle comparison of algae to other bioenergy feedstocks. *Environ. Sci. Technol.* **2010**, *44* (5), 1813–1819.
 - (17) Pate, R.; Klise, G.; Wu, B. Resource demand implications for us algae biofuels production scale-up. *Appl. Energy* **2011**, *88* (10), 3377–3388.
 - (18) Courchesne, N. M. D.; Parisien, A.; Wang, B.; Lan, C. Q. Enhancement of lipid production using biochemical, genetic and transcription factor engineering approaches. *J. Biotechnol.* **2009**, *141* (1), 31–41.
 - (19) Araya, B.; Gouveia, L.; Nobre, B.; Reis, A.; Chamy, R.; Poirrier, P. Evaluation of the simultaneous production of lutein and lipids using a vertical alveolar panel bioreactor for three *Chlorella* species. *Algal Res.* **2014**, *6*, 218–222.
 - (20) Del Campo, J. A.; García-González, M.; Guerrero, M. G. Outdoor cultivation of microalgae for carotenoid production: current state and perspectives. *Appl. Microbiol. Biotechnol.* **2007**, *74* (6), 1163–1174.
 - (21) Rasala, B. A.; Muto, M.; Lee, P. A.; Jager, M.; Cardoso, R. M. F.; Behnke, C. A.; Kirk, P.; Hokanson, C. A.; Crea, R.; Mendez, M.; Mayfield, S. P. Production of therapeutic proteins in algae, analysis of expression of seven human proteins in the chloroplast of *Chlamydomonas reinhardtii*. *Plant Biotechnol. J.* **2010**, *8* (6), 719–733.
 - (22) Gregory, J. A.; Li, F.; Tomosada, L. M.; Cox, C. J.; Topol, A. B.; Vinetz, J. M.; Mayfield, S. Algae-produced Pfs25 elicits antibodies that inhibit malaria transmission. *PLoS One* **2012**, *7* (5), e37179.
 - (23) Patel, A.; Barrington, S.; Lefsrud, M. Microalgae for phosphorus removal and biomass production: a six species screen for dual-purpose organisms. *GCB Bioenergy* **2012**, *4* (5), 485–495.
 - (24) Sheehan, J.; Dunahay, T.; Benemann, J.; Roessler, P. *A Look Back at the U.S. Department of Energy's Aquatic Species Program Biodiesel from Algae*. U.S. Report NREL/TP-580-

- 24190; National Renewable Energy Laboratory: Golden, CO, 1998; p 323.
- (25) Christenson, L.; Sims, R. Production and harvesting of microalgae for wastewater treatment, biofuels, and bioproducts. *Biotechnol. Adv.* **2011**, *29* (6), 686–702.
 - (26) Pittman, J. K.; Dean, A. P.; Osundeko, O. The potential of sustainable algal biofuel production using wastewater resources. *Bioresour. Technol.* **2011**, *102* (1), 17–25.
 - (27) Lundquist, T.J.; Woertz, I.C.; Quinn, N.W.T.; Benemann, J.R. *A Realistic Technology and Engineering Assessment of Algae Biofuel Production*; Berkeley, California, 2010; p 153.
 - (28) Falkowski, P.; Scholes, R. J.; Boyle, E.; Canadell, J.; Canfield, D.; Elser, J.; Gruber, N.; Hibbard, K.; Högberg, P.; Linder, S.; Mackenzie, F. T.; Moore, B., III.; Pedersen, T.; Rosenthal, Y.; Seitzinger, S.; Smetacek, V.; Steffen, W. The global carbon cycle: a test of our knowledge of earth as a system. *Science* **2000**, *290* (5490), 291–296.
 - (29) Smith, V. H.; Tilman, G. D.; Nekola, J. C. Eutrophication: impacts of excess nutrient inputs on freshwater, marine, and terrestrial ecosystems. *Environ. Pollut.* **1999**, *100* (1), 179–196.
 - (30) Oswald, A. W. J.; Gotaas, H. B.; Golueke, C. G.; Kellen, W. R.; Gloyna, E. F.; Hermann, E. R. Algae in waste treatment [with discussion]. *Sewage Ind. Waste.* **1957**, *29* (4), 437–457.
 - (31) Celekli, A.; Yavuzatmaca, M.; Bozkurt, H. Modeling of biomass production by *Spirulinaplatensis platensis* as function of phosphate concentrations and pH regimes. *Bioresour. Technol.* **2009**, *100* (14), 3625–3629.
 - (32) Celekli, A.; Balci, M.; Bozkurt, H. Modelling of *Scenedesmus obliquus*; function of nutrients with modified gomperztz model. *Bioresour. Technol.* **2008**, *99* (18), 8742–8747.
 - (33) Aslan, S.; Kapdan, I. K. Batch kinetics of nitrogen and phosphorus removal from synthetic wastewater by algae. *Ecol. Eng.* **2006**, *28* (1), 64–70.
 - (34) Mulbry, W.; Kondrad, S.; Buyer, J. Treatment of dairy and swine manure effluents using freshwater algae: fatty acid content and composition of algal biomass at different manure loading rates. *J. Appl. Phycol.* **2008**, *20* (6), 1079–1085.
 - (35) Msanne, J.; Xu, D.; Konda, A. R.; Casas-Mollano, J. A.; Awada, T.; Cahoon, E. B.; Cerutti, H. Metabolic and gene expression changes triggered by nitrogen deprivation in the photoautotrophically grown microalgae *Chlamydomonas reinhardtii* and *Coccomyxa* sp. C-169. *Phytochemistry* **2012**, *75*, 50–59.
 - (36) Hu, Q.; Sommerfeld, M.; Jarvis, E.; Ghirardi, M.; Posewitz, M.; Seibert, M.; Darzins, A. Microalgal triacylglycerols as feedstocks for biofuel production: perspectives and advances. *Plant J.* **2008**, *54* (4), 621–639.

- (37) Rodolfi, L.; Chini Zittelli, G.; Bassi, N.; Padovani, G.; Biondi, N.; Bonini, G.; Tredici, M. R. Microalgae for oil: Strain selection, induction of lipid synthesis and outdoor mass cultivation in a low-cost photobioreactor. *Biotechnol. Bioeng.* **2009**, *102* (1), 100–112.
- (38) Reitan, K. I.; Rainuzzo, J. R.; Olsen, Y. Effect of nutrient limitation on fatty acid and lipid content of marine microalgae. *J. Phycol.* **1994**, *30* (6), 972–979.
- (39) Valledor, L.; Furuhashi, T.; Recuenco-Muñoz, L.; Wienkoop, S.; Weckwerth, W. System-level network analysis of nitrogen starvation and recovery in *Chlamydomonas reinhardtii* reveals potential new targets for increased lipid accumulation. *Biotechnol. Biofuels* **2014**, *7* (1), 171.
- (40) Spoehr, H. A.; Milner, H. W. The chemical composition of *Chlorella*; effect of environmental conditions. *Plant Physiol.* **1949**, *24* (1), 120–149.
- (41) Li, Y.; Horsman, M.; Wang, B.; Wu, N.; Lan, C. Q. Effects of nitrogen sources on cell growth and lipid accumulation of green alga *Neochloris oleoabundans*. *Appl. Microbiol. Biotechnol.* **2008**, *81* (4), 629–636.
- (42) Miller, R.; Wu, G.; Deshpande, R. R.; Vieler, A.; Gärtner, K.; Li, X.; Moellering, E. R.; Zäuner, S.; Cornish, A. J.; Liu, B.; Bullard, B.; Sears, B. B.; Kuo, M.-H.; Hegg, E. L.; Shachar-Hill, Y.; Shiu, S.-H.; Benning, C. Changes in transcript abundance in *Chlamydomonas reinhardtii* following nitrogen deprivation predict diversion of metabolism. *Plant Physiol.* **2010**, *154* (4), 1737–1752.
- (43) Lee, D. Y.; Park, J.-J.; Barupal, D. K.; Fiehn, O. System response of metabolic networks in *Chlamydomonas reinhardtii* to total available ammonium. *Mol. Cell. Proteomics* **2012**, *11* (10), 973–988.
- (44) Radakovits, R.; Jinkerson, R. E.; Darzins, A.; Posewitz, M. C. Genetic engineering of algae for enhanced biofuel production. *Eukaryot. Cell* **2010**, *9* (4), 486–501.
- (45) Yu, W.-L.; Ansari, W.; Schoepp, N. G.; Hannon, M. J.; Mayfield, S. P.; Burkart, M. D. Modifications of the metabolic pathways of lipid and triacylglycerol production in microalgae. *Microb. Cell Fact.* **2011**, *10* (91), 1–11.
- (46) Merchant, S. S.; Kropat, J.; Liu, B.; Shaw, J.; Warakanont, J. TAG, you're it! *Chlamydomonas* as a reference organism for understanding algal triacylglycerol accumulation. *Curr. Opin. Biotechnol.* **2012**, *23* (3), 352–363.
- (47) Johnson, X.; Alric, J. Central carbon metabolism and electron transport in *Chlamydomonas reinhardtii*: metabolic constraints for carbon partitioning between oil and starch. *Eukaryotic Cell* **2013**, *12* (6), 776–793.
- (48) Levine, R. B.; Costanza-Robinson, M. S.; Spatafora, G. A. *Neochloris oleoabundans* grown on anaerobically digested dairy manure for concomitant nutrient removal and

- biodiesel feedstock production. *Biomass and Bioenergy* **2011**, 35 (1), 40–49.
- (49) Dudley, J. W. From means to QTL: the illinois long-term selection experiment as a case study in quantitative genetics. *Crop Sci.* **2007**, 47 (53), 520–531.
- (50) Zuidhof, M. J.; Schneider, B. L.; Carney, V. L.; Korver, D. R.; Robinson, F. E. Growth, efficiency, and yield of commercial broilers from 1957, 1978, and 2005. *Poult. Sci.* **2014**, 93 (1), 1–13.
- (51) Moose, S. P.; Mumm, R. H. Molecular plant breeding as the foundation for 21st century crop improvement. *Plant Physiol.* **2008**, 147 (3), 969–977.
- (52) Fernie, A. R.; Schauer, N. Metabolomics-assisted breeding: a viable option for crop improvement? *Trends Genet.* **2009**, 25 (1), 39–48.
- (53) Elena, S. F.; Lenski, R. E. Evolution experiments with microorganisms: the dynamics and genetic bases of adaptation. *Nat. Rev. Genet.* **2003**, 4 (6), 457–469.
- (54) Bell, G. Experimental evolution of heterotrophy in a green alga. *Evolution* **2013**, 67 (2), 468–476.
- (55) Perrineau, M.-M.; Gross, J.; Zelzion, E.; Price, D. C.; Levitan, O.; Boyd, J.; Bhattacharya, D. Using natural selection to explore the adaptive potential of *Chlamydomonas reinhardtii*. *PLoS One* **2014**, 9 (3), e92533.
- (56) Goodson, C.; Roth, R.; Wang, Z. T.; Goodenough, U. Structural correlates of cytoplasmic and chloroplast lipid body synthesis in *Chlamydomonas reinhardtii* and stimulation of lipid body production with acetate boost. *Eukaryotic Cell* **2011**, 10 (12), 1592–1606.
- (57) Boyle, N. R.; Page, M. D.; Liu, B.; Blaby, I. K.; Casero, D.; Kropat, J.; Cokus, S. J.; Hong-Hermesdorf, A.; Shaw, J.; Karpowicz, S. J.; Gallaher, S. D.; Johnson, S.; Benning, C.; Pellegrini, M.; Grossman, A.; Merchant, S. S. Three acyltransferases and nitrogen-responsive regulator are implicated in nitrogen starvation-induced triacylglycerol accumulation in *Chlamydomonas*. *J. Biol. Chem.* **2012**, 287 (19), 15811–15825.
- (58) Guarnieri, M. T.; Nag, A.; Smolinski, S. L.; Darzins, A.; Seibert, M.; Pienkos, P. T. Examination of triacylglycerol biosynthetic pathways via de novo transcriptomic and proteomic analyses in an unsequenced microalga. *PLoS One* **2011**, 6 (10), e25851.
- (59) Guarnieri, M. T.; Nag, A.; Yang, S.; Pienkos, P. T. Proteomic analysis of *Chlorella vulgaris*: potential targets for enhanced lipid accumulation. *J. Proteomics* **2013**, 93, 245–253.
- (60) Hirasawa, M.; Tripathy, J. N.; Sommer, F.; Somasundaram, R.; Chung, J.-S.; Nestander, M.; Kruthiventi, M.; Zabet-Moghaddam, M.; Johnson, M. K.; Merchant, S. S.; Allen, J. P.; Knaff, D. B. Enzymatic properties of the ferredoxin-dependent nitrite reductase from

- Chlamydomonas reinhardtii*. Evidence for hydroxylamine as a late intermediate in ammonia production. *Photosynth. Res.* **2010**, *103* (2), 67–77.
- (61) Cardol, P.; Forti, G.; Finazzi, G. Regulation of electron transport in microalgae. *Biochim. Biophys. Acta* **2011**, *1807* (8), 912–918.
 - (62) Wase, N.; Black, P. N.; Stanley, B. A.; DiRusso, C. C. Integrated quantitative analysis of nitrogen stress response in *Chlamydomonas reinhardtii* using metabolite and protein profiling. *J. Proteome Res.* **2014**, *13* (3), 1373–1396.
 - (63) González-Ballester, D.; Casero, D.; Cokus, S.; Pellegrini, M.; Merchant, S. S.; Grossman, A. R. RNA-seq analysis of sulfur-deprived *Chlamydomonas* cells reveals aspects of acclimation critical for cell survival. *Plant Cell* **2010**, *22* (6), 2058–2084.
 - (64) Castruita, M.; Casero, D.; Karpowicz, S. J.; Kropat, J.; Vieler, A.; Hsieh, S. I.; Yan, W.; Cokus, S.; Loo, J. A.; Benning, C.; Pellegrini, M.; Merchant, S. S. Systems biology approach in *Chlamydomonas* reveals connections between copper nutrition and multiple metabolic steps. *Plant Cell* **2011**, *23* (4), 1273–1292.
 - (65) De la Fuente van Bentem, S.; Hirt, H. Using phosphoproteomics to reveal signalling dynamics in plants. *Trends Plant Sci.* **2007**, *12* (9), 404–411.
 - (66) Timmins, M.; Zhou, W.; Rupprecht, J.; Lim, L.; Thomas-Hall, S. R.; Doebbe, A.; Kruse, O.; Hankamer, B.; Marx, U. C.; Smith, S. M.; Schenk, P. M. The metabolome of *Chlamydomonas reinhardtii* following induction of anaerobic H₂ production by sulfur depletion. *J. Biol. Chem.* **2009**, *284* (35), 23415–23425.
 - (67) May, P.; Wienkoop, S.; Kempa, S.; Usadel, B.; Christian, N.; Rupprecht, J.; Weiss, J.; Recuenco-Munoz, L.; Ebenhöf, O.; Weckwerth, W.; Walther, D. Metabolomics- and proteomics-assisted genome annotation and analysis of the draft metabolic network of *Chlamydomonas reinhardtii*. *Genetics* **2008**, *179* (1), 157–166.
 - (68) Stauber, E. J.; Hippler, M. *Chlamydomonas reinhardtii* proteomics. *Plant Physiol. Biochem.* **2004**, *42* (12), 989–1001.
 - (69) Nguyen, H. M.; Baudet, M.; Cuiné, S.; Adriano, J.-M.; Barthe, D.; Billon, E.; Bruley, C.; Beisson, F.; Peltier, G.; Ferro, M.; Li-Beisson, Y. Proteomic profiling of oil bodies isolated from the unicellular green microalga *Chlamydomonas reinhardtii*: with focus on proteins involved in lipid metabolism. *Proteomics* **2011**, *11* (21), 4266–4273.
 - (70) Baba, M.; Suzuki, I.; Shiraiwa, Y. Proteomic analysis of high-CO₂-inducible extracellular proteins in the unicellular green alga, *Chlamydomonas reinhardtii*. *Plant Cell Physiol.* **2011**, *52* (8), 1302–1314.
 - (71) Terashima, M.; Specht, M.; Naumann, B.; Hippler, M. Characterizing the anaerobic response of *Chlamydomonas reinhardtii* by quantitative proteomics. *Mol. Cell.*

Proteomics **2010**, 9 (7), 1514–1532.

- (72) Yates, J. R.; Cociorva, D.; Liao, L.; Zabrouskov, V. Performance of a linear ion trap-orbitrap hybrid for peptide analysis. *Anal. Chem.* **2006**, 78 (2), 493–500.
- (73) Washburn, M. P.; Wolters, D.; Yates, J. R. III. Large-scale analysis of the yeast proteome by multidimensional protein identification technology. *Nat. Biotechnol.* **2001**, 19 (3), 242–247.
- (74) Abraham, P.; Giannone, R. J.; Adams, R. M.; Kalluri, U.; Tuskan, G. A.; Hettich, R. L. Putting the pieces together: high-performance LC-MS/MS provides network-, pathway-, and protein-level perspectives in *Populus*. *Mol. Cell. Proteomics* **2013**, 12 (1), 106–119.
- (75) Patel, A. K.; Huang, E. L.; Low-Décarie, E.; Lefsrud, M. G. Comparative shotgun Proteomic analysis of wastewater cultured microalgae: nitrogen sensing and carbon fixation for growth and nutrient removal in *Chlamydomonas reinhardtii*. *J. Proteome Res.* **2015**, 14 (8), 3051–3067.
- (76) Huang, E. L.; Orsat, V.; Shah, M. B.; Hettich, R. L.; VerBerkmoes, N. C.; Lefsrud, M. G. The temporal analysis of yeast exponential phase using shotgun proteomics as a fermentation monitoring technique. *J. Proteomics* **2012**, 75 (17), 5206–5214.
- (77) Goltsman, D. S. A.; Denef, V. J.; Singer, S. W.; VerBerkmoes, N. C.; Lefsrud, M.; Mueller, R. S.; Dick, G. J.; Sun, C. L.; Wheeler, K. E.; Zemla, A.; Baker, B. J.; Hauser, L.; Land, M.; Shah, M. B.; Thelen, M. P.; Hettich, R. L.; Banfield, J. F. Community genomic and proteomic analyses of chemoautotrophic iron-oxidizing “*Leptospirillum rubrum*” (Group II) and “*Leptospirillum ferrodiazotrophum*” (Group III) bacteria in acid mine drainage biofilms. *Appl. Environ. Microbiol.* **2009**, 75 (13), 4599–4615.
- (78) Wang, X.; Liu, Q.; Zhang, B. Leveraging the complementary nature of RNA-seq and shotgun proteomics data. *Proteomics* **2014**, 14 (23), 2676–2687.
- (79) Wang, X.; Slebos, R. J. C.; Wang, D.; Halvey, P. J.; Tabb, D. L.; Liebler, D. C.; Zhang, B. Protein identification using customized protein sequence databases derived from RNA-seq data. *J. Proteome Res.* **2012**, 11 (2), 1009–1017.
- (80) Snow, A. A.; Smith, V. H. Genetically engineered algae for biofuels: a key role for ecologists. *Bioscience* **2012**, 62 (8), 765–768.
- (81) Lesk, A. M. *Introduction to Bioinformatics*, 3rd ed.; Oxford University Press: Oxford, UK, 2008. pp. 432.
- (82) Gould, S. B.; Waller, R. F.; McFadden, G. I. Plastid evolution. *Annu. Rev. Plant Biol.* **2008**, 59, 491–517.
- (83) Harris, E.H. *Chlamydomonas* in the laboratory. In *The Chlamydomonas Sourcebook*, 2nd

- ed.; Stern, DB.; Harris, EH., Eds.; Academic Press: New York, 2009; Vol. 1, pp. 241–302.
- (84) Moseley, J.; Grossman, A. R. Phosphate metabolism and responses to phosphorus deficiency. In *The Chlamydomonas sourcebook*, 2nd ed.; Stern, DB.; Harris, EH., Eds.; Academic Press: New York, 2009; Vol. 2, pp. 189–216.
 - (85) Maul, J. E.; Lilly, J.W.; Cui, L.; DePamphilis, C. W.; Miller, W.; Harris, E. H.; Stern, D. B. The *Chlamydomonas reinhardtii* plastid chromosome: islands of genes in a sea of repeats. *Plant Cell* **2002**, *14* (11), 2659–2679.
 - (86) Fernández, E.; Galván, A. Nitrate assimilation in *Chlamydomonas*. *Eukaryot. Cell* **2008**, *7* (4), 555–559.
 - (87) Arabidopsis Genome Initiative. Analysis of the genome sequence of the flowering plant *Arabidopsis thaliana*. *Nature* **2000**, *408* (6814), 796–815.
 - (88) Merchant, S. S.; Prochnik, S. E.; Vallon, O.; Harris, E. H.; Karpowicz, S. J.; Witman, G. B.; Terry, A.; Salamov, A.; Fritz-Laylin, L. K.; Maréchal-Drouard, L.; Marshall, W. F.; Qu, L.-H.; Nelson, D. R.; Sanderfoot, A. A.; Spalding, M. H.; Kapitonov, V. V.; Ren, Q.; Ferris, P.; Lindquist, E.; Shapiro, H.; Lucas, S. M.; Grimwood, J.; Schmutz, J.; Cardol, P.; Cerutti, H.; Chanfreau, G.; Chen, C.-L.; Cognat, V.; Croft, M. T.; Dent, R.; Dutcher, S.; Fernández, E.; Ferris P.; Fukuzawa, H.; González-Ballester, D.; González-Halphen, D.; Hallmann, A.; Hanikenne, M.; Hippler, M.; Inwood, W.; Jabbari, K.; Kalanon, M.; Kuras, R.; Lefebvre, P. A.; Lemaire, S. D.; Lobanov, A. V.; Lohr, M.; Manuell, A.; Meier, I.; Mets, L.; Mittag, M.; Mittelmeier, T.; Moroney, J. V.; Moseley, J.; Napoli, C.; Nedelcu, A. M.; Niyogi, K.; Novoselov, S. V.; Paulsen, I. T.; Pazour, G.; Purton, S.; Ral, J.-P.; Riaño-Pachón, D. M.; Riekhof, W.; Rymarquis, L.; Schroda, M.; Stern, D.; Umen, J.; Willows, R.; Wilson, N.; Zimmer, S. L.; Allmer, J.; Balk, J.; Bisova, K.; Chen, C.-J.; Elias, M.; Gendler, K.; Hauser, C.; Lamb, M. R.; Ledford, H.; Long, J. C.; Minagawa, J.; Page, M. D.; Pan, J.; Pootakham, W.; Roje, S.; Rose, A.; Stahlberg, E.; Terauchi, A. M.; Yang, P.; Ball, S.; Bowler, C.; Dieckmann, C. L.; Gladyshev, V. N.; Green, P.; Jorgensen, R.; Mayfield, S.; Mueller-Roeber, B.; Rajamani, S.; Sayre, R. T.; Brokstein, P.; Dubchak, I.; Goodstein, D.; Hornick, L.; Huang, Y. W.; Jhaveri, J.; Luo, Y.; Martínez, D.; Ngau, W. C. A.; Otiilar, B.; Poliakov, A.; Porter, A.; Szajkowski, L.; Werner, G.; Zhou, K.; Grigoriev, I. V.; Rokhsar, D. S.; Grossman, A. R. The *Chlamydomonas* genome reveals the evolution of key animal and plant functions. *Science* **2007**, *318* (5848), 245–250.
 - (89) Gray, M. W.; Boer, P. H. Organization and expression of algal (*Chlamydomonas reinhardtii*) mitochondrial DNA. *Philos. Trans. R. Soc., B* **1988**, *319* (1193), 135–147.
 - (90) Specht, E.; Miyake-Stoner, S.; Mayfield, S. Micro-algae come of age as a platform for recombinant protein production. *Biotechnol. Lett.* **2010**, *32* (10), 1373–1383.
 - (91) Huntley, M. E.; Redalje, D. G. CO₂ Mitigation and renewable oil from photosynthetic microbes: a new appraisal. *Mitig. Adapt. Strateg. Glob. Chang.* **2007**, *12* (4), 573–608.

- (92) Allen, J. F. Photosynthesis of ATP – electrons, proton pumps, rotors, and poise. *Cell* **2002**, *110* (3), 273–276.
- (93) Finazzi, G.; Moreau, H.; Bowler, C. Genomic insights into photosynthesis in eukaryotic phytoplankton. *Trends Plant Sci.* **2010**, *15* (10), 565–572.
- (94) Finazzi, G. The central role of the green alga *Chlamydomonas reinhardtii* in revealing the mechanism of state transitions. *J. Exp. Bot.* **2005**, *56* (411), 383–388.
- (95) Pulz, O. Photobioreactors: production systems for phototrophic microorganisms. *Appl. Microbiol. Biotechnol.* **2001**, *57* (3), 287–293.
- (96) Forde, B. G. Local and long-range signaling pathways regulating plant responses to nitrate. *Annu. Rev. Plant Biol.* **2002**, *53* (1), 203–224.
- (97) Lam, H.-M.; Coschigano, K. T.; Oliveira, I. C.; Melo-Oliveira, R.; Coruzzi, G. M. The molecular-genetics of nitrogen assimilation into amino acids in higher plants. *Annu. Rev. Plant Physiol. Plant Mol. Biol.* **1996**, *47* (1), 569–593.
- (98) Rexach, J.; Fernández, E.; Galván, A. The *Chlamydomonas reinhardtii* *Nar1* gene encodes a chloroplast membrane protein involved in nitrite transport. *Plant Cell* **2000**, *12* (8), 1441–1453.
- (99) Hase, T.; Schürmann, P.; Knaff, D. B. The interaction of ferredoxin with ferredoxin-dependent enzymes. In *Photosystem I*; Golbeck, J., Ed.; Springer: Dordrecht, The Netherlands, 2006; pp. 477–498.
- (100) Hoff, T.; Truong, H.-N.; Caboche, M. The use of mutants and transgenic plants to study nitrate assimilation. *Plant, Cell Environ.* **1994**, *17* (5), 489–506.
- (101) Elser, J. J.; Fagan, W. F.; Denno, R. F.; Dobberfuhl, D. R.; Folarin, A.; Huberty, A.; Interlandi, S.; Kilham, S. S.; McCauley, E.; Schulz, K. L.; Siemann, E. H.; Sterner, R. W. Nutritional constraints in terrestrial and freshwater food webs. *Nature* **2000**, *408* (6812), 578–580.
- (102) Elser, J. J.; Marzolf, E. R.; Goldman, C. R. Phosphorus and nitrogen limitation of phytoplankton growth in the freshwaters of north america: a review and critique of experimental enrichments. *Can. J. Fish. Aquat. Sci.* **1990**, *47*, (7), 1468–1477.
- (103) Elser, J. J.; Bracken, M. E. S.; Cleland, E. E.; Gruner, D. S.; Harpole, W. S.; Hillebrand, H.; Ngai, J. T.; Seabloom, E. W.; Shurin, J. B.; Smith, J. E. Global analysis of nitrogen and phosphorus limitation of primary producers in freshwater, marine and terrestrial ecosystems. *Ecol. Lett.* **2007**, *10* (12), 1135–1142.
- (104) Thompson, M. R.; Chourey, K.; Froelich, J. M.; Erickson, B. K.; VerBerkmoes, N. C.; Hettich, R. L. Experimental approach for deep proteome measurements from small-scale

- microbial biomass samples. *Anal. Chem.* **2008**, *80* (24), 9517–9525.
- (105) Guschina, I. A.; Harwood, J. L. Lipids and lipid metabolism in eukaryotic algae. *Prog. Lipid Res.* **2006**, *45* (2), 160–186.
 - (106) Han, X.; Gross, R. W. global analyses of cellular lipidomes directly from crude extracts of biological samples by esi mass spectrometry: a bridge to lipidomics. *J. Lipid Res.* **2003**, *44* (6), 1071–1079.
 - (107) Roessler, P. G. Environmental control of glycerolipid metabolism in microalgae: commercial implications and future research directions. *J. Phycol.* **1990**, *26* (3), 393–399.
 - (108) Schenk, P. M.; Thomas-Hall, S. R.; Stephens, E.; Marx, U. C.; Mussnug, J. H.; Posten, C.; Kruse, O.; Hankamer, B. Second generation biofuels: high-efficiency microalgae for biodiesel production. *BioEnergy Res.* **2008**, *1* (1), 20–43.
 - (109) Thompson, G. A. Lipids and membrane function in green algae. *Biochim. Biophys. Acta* **1996**, *1302* (1), 17–45.
 - (110) Kirk, M. M.; Kirk, D. L. Translational regulation of protein synthesis, in response to light, at a critical stage of volvox development. *Cell* **1985**, *41* (2), 419–428.
 - (111) Gillham, N. W.; Boynton, J. E.; Hauser, C. R. Translational regulation of gene expression in chloroplasts and mitochondria. *Annu. Rev. Genet.* **1994**, *28* (36), 71–93.
 - (112) Mayfield, S. P.; Yohn, C. B.; Cohen, A.; Danon, A. Regulation of chloroplast gene expression. *Annu. Rev. Plant Physiol. Plant Mol. Biol.* **1995**, *46* (1), 147–166.
 - (113) Reboloso-Fuentes, M. M.; Navarro-Pérez, A.; García-Camacho, F.; Ramos-Miras, J. J.; Guil-Guerrero, J. L. Biomass nutrient profiles of the microalga *Nannochloropsis*. *J. Agric. Food Chem.* **2001**, *49* (6), 2966–2972.
 - (114) Brennan, L.; Owende, P. Biofuels from microalgae – a review of technologies for production, processing, and extractions of biofuels and co-products. *Renew. Sustain. Energy Rev.* **2010**, *14* (2), 557–577.
 - (115) Dreesen, I. A. J.; Charpin-El Hamri, G.; Fussenegger, M. Heat-stable oral alga-based vaccine protects mice from *Staphylococcus aureus* infection. *J. Biotechnol.* **2010**, *145* (3), 273–280.
 - (116) Rasala, B. A.; Lee, P. A.; Shen, Z.; Briggs, S. P.; Mendez, M.; Mayfield, S. P. Robust expression and secretion of xylanase1 in *Chlamydomonas reinhardtii* by fusion to a selection gene and processing with the FMDV 2A peptide. *PLoS One* **2012**, *7* (8), e43349.
 - (117) Benemann, J. R.; Weissman, J. C.; Koopman, B. L.; Oswald, W. J. Energy production by

- microbial photosynthesis. *Nature* **1977**, 268 (5615), 19–23.
- (118) Mulbry, W.; Kebede-Westhead, E.; Pizarro, C.; Sikora, L. Recycling of manure nutrients: use of algal biomass from dairy manure treatment as a slow release fertilizer. *Bioresour. Technol.* **2005**, 96 (4), 451–458.
 - (119) Pizarro, C.; Kebede-Westhead, E.; Mulbry, W. Nitrogen and phosphorus removal rates using small algal turfs grown with dairy manure. *J. Appl. Phycol.* **2005**, 14 (6), 469–473.
 - (120) Kebede-Westhead, E.; Pizarro, C.; Mulbry, W. W. Treatment of swine manure effluent using freshwater algae: production, nutrient recovery, and elemental composition of algal biomass at four effluent loading rates. *J. Appl. Phycol.* **2006**, 18 (1), 41–46.
 - (121) Shi, J.; Podola, B.; Melkonian, M. Removal of nitrogen and phosphorus from wastewater using microalgae immobilized on twin layers: an experimental study. *J. Appl. Phycol.* **2007**, 19 (5), 417–423.
 - (122) Hoffmann, J. P. Wastewater treatment with suspended and nonsuspended algae. *J. Phycol.* **1998**, 34 (5), 757–763.
 - (123) Martínez, M.; Sánchez, S.; Jiménez, J. .; El Yousfi, F.; Muñoz, L. Nitrogen and phosphorus removal from urban wastewater by the microalga *Scenedesmus obliquus*. *Bioresour. Technol.* **2000**, 73 (3), 263–272.
 - (124) Olguín, E. J.; Galicia, S.; Mercado, G.; Pérez, T. Annual productivity of *Spirulina* (*Arthrospira*) and nutrient removal in a pig wastewater recycling process under tropical conditions. *J. Appl. Phycol.* **2003**, 15 (2), 249–257.
 - (125) González, L. E.; Cañizares, R. O.; Baena, S. Efficiency of ammonia and phosphorus removal from a colombian agroindustrial wastewater by the microalgae *Chlorella vulgaris* and *Scenedesmus dimorphus*. *Bioresour. Technol.* **1997**, 60 (3), 259–262.
 - (126) de-Bashan, L. E.; Bashan, Y. Recent advances in removing phosphorus from wastewater and its future use as fertilizer (1997-2003). *Water Res.* **2004**, 38 (19), 4222–4246.
 - (127) Deviller, G.; Aliaume, C.; Nava, M. A. F.; Casellas, C.; Blancheton, J. P. High-rate algal pond treatment for water reuse in an integrated marine fish recirculating system: effect on water quality and sea bass growth. *Aquaculture* **2004**, 235 (1), 331–344.
 - (128) Powell, N.; Shilton, A. N.; Pratt, S.; Chisti, Y. Factors influencing luxury uptake of phosphorus by microalgae in waste stabilization ponds. *Environ. Sci. Technol.* **2008**, 42 (16), 5958–5962.
 - (129) Kong, Q-x.; Li, L.; Martinez, B.; Chen, P.; Ruan, R. Culture of microalgae *Chlamydomonas reinhardtii* in wastewater for biomass feedstock production. *Appl. Biochem. Biotechnol.* **2010**, 160 (1), 9–18.

- (130) Wang, L.; Min, M.; Li, Y.; Chen, P.; Chen, Y.; Liu, Y.; Wang, Y.; Ruan, R. Cultivation of green algae *Chlorella* sp. in different wastewaters from municipal wastewater treatment plant. *Appl. Biochem. Biotechnol.* **2010**, *162* (4), 1174–1186.
- (131) Fenton, O.; Ó hUallacháin, D. Agricultural nutrient surpluses as potential input sources to grow third generation biomass (microalgae): a review. *Algal Res.* **2012**, *1* (1), 49–56.
- (132) de-Bashan, L. E.; Moreno, M.; Hernandez, J.-P.; Bashan, Y. Removal of ammonium and phosphorus ions from synthetic wastewater by the microalgae *Chlorella vulgaris* coimmobilized in alginate beads with the microalgae growth-promoting bacterium *Azospirillum brasilense*. *Water Res.* **2002**, *36* (12), 2941–2948.
- (133) Chini Zittelli, G.; Rodolfi, L.; Biondi, N.; Tredici, M. R. Productivity and photosynthetic efficiency of outdoor cultures of *Tetraselmis suecica* in annular columns. *Aquaculture* **2006**, *261* (3), 932–943.
- (134) Borowitzka, M. A. Commercial production of microalgae: ponds, tanks, tubes and fermenters. *J. Biotechnol.* **1999**, *70* (1), 313–321.
- (135) Miyamoto, K.; Wable, O.; Benemann, J. R. Vertical tubular reactor for microalgae cultivation. *Biotechnol. Lett.* **1988**, *10* (10), 703–708.
- (136) Carvalho, A. P.; Meireles, L. A.; Malcata, F. X. Microalgal reactors: a review of enclosed system designs and performances. *Biotechnol. Prog.* **2006**, *22* (6), 1490–1506.
- (137) Sánchez Mirón, A.; Contreras Gómez, A.; García Camacho, F.; Molina Grima, E.; Chisti, Y. Comparative evaluation of compact photobioreactors for large-scale monoculture of microalgae. *J. Biotechnol.* **1999**, *70* (1), 249–270.
- (138) Amer, L.; Adhikari, B.; Pellegrino, J. Technoeconomic analysis of five microalgae-to-biofuels processes of varying complexity. *Bioresour. Technol.* **2011**, *102* (20), 9350–9359.
- (139) Rosello Sastre, R.; Csögör, Z.; Perner-Nochta, I.; Fleck-Schneider, P.; Posten, C. Scale-down of microalgae cultivations in tubular photo-bioreactors—a conceptual approach. *J. Biotechnol.* **2007**, *132* (2), 127–133.
- (140) Perner-Nochta, I.; Posten, C. Simulations of light intensity variation in photobioreactors. *J. Biotechnol.* **2007**, *131* (3), 276–285.
- (141) Molina Grima, E.; Acién Fernández, F. G.; García Camacho, F.; Chisti, Y. Photobioreactors: light regime, mass transfer, and scaleup. *J. Biotechnol.* **1999**, *70* (1), 231–247.
- (142) Yates, J. R. Mass spectrometry from genomics to proteomics. *Trends Genet.* **2000**, *16*, (1), 5–8.

- (143) McCormack, A. L.; Schieltz, D. M.; Goode, B.; Yang, S.; Barnes, G.; Drubin, D.; Yates, J. R., III. Direct analysis and identification of proteins in mixtures by LC/MS/MS and database searching at the low-femtomole level. *Anal. Chem.* **1997**, *69* (4), 767–776.
- (144) Tabb, D. L.; McDonald, W. H.; Yates, J. R., III. DTASelect and contrast: tools for assembling and comparing protein identifications from shotgun proteomics. *J. Proteome Res.* **2002**, *1* (1), 21–26.
- (145) Yamaguchi, K.; Beligni, M. V.; Prieto, S.; Haynes, P. A.; McDonald, W. H.; Yates, J. R., III; Mayfield, S. P. Proteomic characterization of the *Chlamydomonas reinhardtii* chloroplast ribosome: identification of proteins unique to the 70 S ribosome. *J. Biol. Chem.* **2003**, *278* (36), 33774–33785.
- (146) Schmidt, M.; Geßner, G.; Luff, M.; Heiland, I.; Wagner, V.; Kaminski, M.; Geimer, S.; Eitzinger, N.; Reissenweber, T.; Voytsekh, O.; Fiedler, M.; Mittag, M.; Kreimer, G. Proteomic analysis of the eyespot of *Chlamydomonas reinhardtii* provides novel insights into its components and tactic movements. *Plant Cell* **2006**, *18* (8), 1908–1930.
- (147) Keller, L. C.; Romijn, E. P.; Zamora, I.; Yates, J. R., III; Marshall, W. F. Proteomic analysis of isolated *Chlamydomonas* centrioles reveals orthologs of ciliary-disease genes. *Curr. Biol.* **2005**, *15* (12), 1090–1098.
- (148) Jamers, A.; Blust, R.; De Coen, W. Omics in algae: paving the way for a systems biological understanding of algal stress phenomena? *Aquat. Toxicol.* **2009**, *92* (3), 114–121.
- (149) Förster, B.; Mathesius, U.; Pogson, B. J. Comparative Proteomics of high light stress in the model alga *Chlamydomonas reinhardtii*. *Proteomics* **2006**, *6* (15), 4309–4320.
- (150) Naumann, B.; Busch, A.; Allmer, J.; Ostendorf, E.; Zeller, M.; Kirchhoff, H.; Hippler, M. Comparative quantitative proteomics to investigate the remodeling of bioenergetic pathways under iron deficiency in *Chlamydomonas reinhardtii*. *Proteomics* **2007**, *7* (21), 3964–7379.
- (151) Kim, Y. K.; Yoo, W. I.; Lee, S. H.; Lee, M. Y. Proteomic analysis of cadmium-induced protein profile alterations from marine alga *Nannochloropsis oculata*. *Ecotoxicology* **2005**, *14* (6), 589–596.
- (152) Gillet, S.; Decottignies, P.; Chardonnet, S.; Le Maréchal, P. Cadmium response and redoxin targets in *Chlamydomonas reinhardtii*: a proteomic approach. *Photosynth. Res.* **2006**, *89* (2), 201–211.
- (153) Wang, S.-B.; Chen, F.; Sommerfeld, M.; Hu, Q. Proteomic analysis of molecular response to oxidative stress by the green alga *Haematococcus pluvialis* (Chlorophyceae). *Planta* **2004**, *220* (1), 17–29.

- (154) DePristo, M. A.; Banks, E.; Poplin, R.; Garimella, K. V.; Maguire, J. R.; Hartl, C.; Philippakis, A. A.; del Angel, G.; Rivas, M. A.; Hanna, M.; McKenna, A.; Fennell, T. J.; Kernysky, A. M.; Sivachenko, A. Y.; Cibulskis, K.; Gabriel, S. B.; Altshuler, D.; Daly, M. J. A framework for variation discovery and genotyping using next-generation DNA sequencing data. *Nat. Genet.* **2011**, *43* (5), 491–498.
- (155) Lopez, D.; Casero, D.; Cokus, S. J.; Merchant, S. S.; Pellegrini, M. Algal Functional Annotation Tool: a web-based analysis suite to functionally interpret large gene lists using integrated annotation and expression data. *BMC Bioinf.* **2011**, *12* (1), 282.
- (156) Motoyama, A.; Yates, J. R., III. Multidimensional LC separations in shotgun proteomics. *Anal. Chem.* 2008, *80* (19), 7187–7193.
- (157) Carvalho, P. C.; Fischer, J. S. G.; Chen, E. I.; Yates, J. R., III; Barbosa, V. C. PatternLab for proteomics: a tool for differential shotgun proteomics. *BMC Bioinformatics* **2008**, *9* (1), 1–14.
- (158) Peng, J.; Elias, J. E.; Thoreen, C. C.; Licklider, L. J.; Gygi, S. P. Evaluation of multidimensional chromatography coupled with tandem mass spectrometry (LC/LC–MS/MS) for large-scale protein analysis: the yeast proteome. *J. Proteome Res.* **2003**, *2* (1), 43–50.
- (159) Link, A. J.; Eng, J.; Schieltz, D. M.; Carmack, E.; Mize, G. J.; Morris, D. R.; Garvik, B. M.; Yates, J. R., III. Direct analysis of protein complexes using mass spectrometry. *Nat. Biotechnol.* **1999**, *17* (7), 676–682.
- (160) Olsen, J. V; Ong, S.-E.; Mann, M. Trypsin cleaves exclusively C-terminal to arginine and lysine residues. *Mol. Cell. Proteomics* **2004**, *3*, (6), 608–614.
- (161) Eng, J. K.; McCormack, A. L.; Yates, J. R., III. An approach to correlate tandem mass spectral data of peptides with amino acid sequences in a protein database. *J. Am. Soc. Mass Spectrom.* **1994**, *5* (11), 976–989.
- (162) Mann, M.; Hendrickson, R. C.; Pandey, A. Analysis of proteins and proteomes by mass spectrometry. *Annu. Rev. Biochem.* **2001**, *70* (1), 437–473.
- (163) Kuster, B.; Schirle, M.; Mallick, P.; Aebersold, R. Scoring proteomes with proteotypic peptide probes. *Nat. Rev. Mol. Cell Biol.* **2005**, *6* (7), 577–583.
- (164) Nesvizhskii, A. I.; Aebersold, R. Interpretation of shotgun proteomic data: the protein inference problem. *Mol. Cell. Proteomics* **2005**, *4* (10), 1419–1440.
- (165) Yates, J. R.; Ruse, C. I.; Nakorchevsky, A. Proteomics by mass spectrometry: approaches, advances, and applications. *Annu. Rev. Biomed. Eng.* **2009**, *11*, 49–79.
- (166) Wang, H.; Alvarez, S.; Hicks, L. M. Comprehensive comparison of iTRAQ and label-free

LC-based quantitative proteomics approaches using two *Chlamydomonas reinhardtii* strains of interest for biofuels engineering. *J. Proteome Res.* **2012**, *11* (1), 487–501.

- (167) Liu, H.; Sadygov, R. G.; Yates, J. R., III. A model for random sampling and estimation of relative protein abundance in shotgun proteomics. *Anal. Chem.* **2004**, *76* (14), 4193–4201.
- (168) Gygi, S. P.; Corthals, G. L.; Zhang, Y.; Rochon, Y.; Aebersold, R. Evaluation of two-dimensional gel electrophoresis-based proteome analysis technology. *Proc. Natl. Acad. Sci. U. S. A.* **2000**, *97* (17), 9390–9395.
- (169) Florens, L.; Carozza, M. J.; Swanson, S. K.; Fournier, M.; Coleman, M. K.; Workman, J. L.; Washburn, M. P. Analyzing chromatin remodeling complexes using shotgun proteomics and normalized spectral abundance factors. *Methods* **2006**, *40* (4), 303–311.
- (170) Choi, H.; Fermin, D.; Nesvizhskii, A. I. Significance analysis of spectral count data in label-free shotgun proteomics. *Mol. Cell. Proteomics* **2008**, *7* (12), 2373–2385.
- (171) Zeger, S. L.; Karim, M. R. Generalized linear models with random effects; a gibbs sampling approach. *J. Am. Stat. Assoc.* **1991**, *86* (413), 79–86.
- (172) Tusher, V. G.; Tibshirani, R.; Chu, G. Significance analysis of microarrays applied to the ionizing radiation response. *Proc. Natl. Acad. Sci. U. S. A.* **2001**, *98* (9), 5116–5121.
- (173) Mariani, T. J.; Budhraja, V.; Mecham, B. H.; Gu, C. C.; Watson, M. A.; Sadovsky, Y. A Variable fold change threshold determines significance for expression microarrays. *J. Fed. Am. Soc. Exp. Biol.* **2003**, *17* (2), 321–323.
- (174) Oberg, A. L.; Vitek, O. Statistical design of quantitative mass spectrometry-based proteomic experiments. *J. Proteome Res.* **2009**, *8* (5), 2144–2156.
- (175) Finn, R. D.; Bateman, A.; Clements, J.; Coggill, P.; Eberhardt, R. Y.; Eddy, S. R.; Heger, A.; Hetherington, K.; Holm, L.; Mistry, J.; Sonnhammer, E. L. L.; Tate, J.; Punta, M. Pfam: the protein families database. *Nucleic Acids Res.* **2014**, *42*, 222–230.
- (176) Hendrickson, E. L.; Lamont, R. J.; Hackett, M. Tools for interpreting large-scale protein profiling in microbiology. *J. Dent. Res.* **2008**, *87* (11), 1004–1015.
- (177) Tatusov, R. L.; Koonin, E. V.; Lipman, D. J. A genomic perspective on protein families. *Science* **1997**, *278* (5338), 631–637.
- (178) Tatusov, R. L.; Fedorova, N. D.; Jackson, J. D.; Jacobs, A. R.; Kiryutin, B.; Koonin, E. V.; Krylov, D. M.; Mazumder, R.; Mekhedov, S. L.; Nikolskaya, A. N.; Rao, B. S.; Smirnov, S.; Sverdlov, A. V.; Vasudevan, S.; Wolf, Y. I.; Yin, J. J.; Natale, D. A. The COG database: an updated version includes eukaryotes. *BMC Bioinformatics* **2003**, *4* (41), 1–14.
- (179) Ashburner, M.; Ball, C. A.; Blake, J. A.; Botstein, D.; Butler, H.; Cherry, J.; Davis, A. P.;

- Dolinski, K.; Dwight, S. S.; Eppig, J. T.; Harris, M. A.; Hill, D. P.; Issel-Tarver, L.; Kasarskis, A.; Lewis, S.; Matese, J. C.; Richardson, J. E.; Ringwald, M.; Rubin, G. M.; Sherlock, G. Gene Ontology: tool for the unification of biology. The Gene Ontology Consortium. *Nat. Genet.* **2000**, *25* (1), 25–29.
- (180) Yamada, T.; Letunic, I.; Okuda, S.; Kanehisa, M.; Bork, P. iPath2.0: interactive pathway explorer. *Nucleic Acids Res.* **2011**, *39*, W412–W415.
- (181) Hill, J.; Nelson, E.; Tilman, D.; Polasky, S.; Tiffany, D. Environmental, economic, and energetic costs and benefits of biodiesel and ethanol biofuels. *Proc. Natl. Acad. Sci. U.S.A.* **2006**, *103*, 11206–11210.
- (182) Lardon, L.; Hélias, A.; Sialve, B.; Steyer, J.-P.; Bernard, O. Life-cycle assessment of biodiesel production from microalgae. *Environ. Sci. Technol.* **2009**, *43* (17), 6475–6481.
- (183) Subhadra, B. G. Comment on “environmental life cycle comparison of algae to other bioenergy feedstocks.” *Environ. Sci. Technol.* **2010**, *44* (9), 3641–3642.
- (184) Reijnders, L. Do biofuels from microalgae beat biofuels from terrestrial plants? *Trends Biotechnol.* **2008**, *26* (7), 349–350.
- (185) Stephens, E.; Ross, I. L.; King, Z.; Mussnug, J. H.; Kruse, O.; Posten, C.; Borowitzka, M. A.; Hankamer, B. An economic and technical evaluation of microalgal biofuels. *Nat. Biotechnol.* **2010**, *28* (2), 126–128.
- (186) Collet, P.; Hélias, A.; Lardon, L.; Ras, M.; Goy, R.-A.; Steyer, J.-P. Life-cycle assessment of microalgae culture coupled to biogas production. *Bioresour. Technol.* **2011**, *102* (1), 207–214.
- (187) Gibson, D. G.; Glass, J. I.; Lartigue, C.; Noskov, V. N.; Chuang, R.-Y.; Algire, M. A.; Benders, G. A.; Montague, M. G.; Ma, L.; Moodie, M. M.; Merryman, C.; Vashee, S.; Krishnakumar, R.; Assad-Garcia, N.; Andrews-Pfannkoch, C.; Denisova, E. A.; Young, L.; Qi, Z.-Q.; Segall-Shapiro, T. H.; Calvey, C. H.; Parmar, P. P.; Hutchison, C. A, III.; Smith, H. O.; Venter, J. C. Creation of a bacterial cell controlled by a chemically synthesized genome. *Science* **2010**, *329* (5987), 52–56.
- (188) Masson, S.; Pinel-Alloul, B.; Smith, V. H. Total phosphorus-chlorophyll *a* size fraction relationships in southern Québec lakes. *Limnol. Oceanogr.* **2000**, *45* (3), 732–740.
- (189) MacDonald, G. K.; Bennett, E. M. Phosphorus accumulation in Saint Lawrence river watershed soils: a century-long perspective. *Ecosystems* **2009**, *12* (2), 621–635.
- (190) de-Bashan, L. E.; Bashan, Y. Immobilized microalgae for removing pollutants: review of practical aspects. *Bioresour. Technol.* **2010**, *101* (6), 1611–1627.
- (191) Ahluwalia, S. S.; Goyal, D. Microbial and plant derived biomass for removal of heavy

- metals from wastewater. *Bioresour. Technol.* **2007**, 98 (12), 2243–2257.
- (192) Lee, K.; Lee, C.-G. Effect of Light/dark cycles on wastewater treatments by microalgae. *Biotechnol. Bioprocess Eng.* **2001**, 6 (3), 194–199.
- (193) Martínez Sancho, M.E.; Jiménez Castillo, J.M.; El Yousfi, F. Photoautotrophic consumption of phosphorus by *Scenedesmus obliquus* in a continuous culture. Influence of light intensity. *Process Biochem.* **1999**, 34 (8), 811–818.
- (194) Jiménez-Pérez, M.V.; Sánchez-Castillo, P.; Romera, O.; Fernández-Moreno, D.; Pérez-Martínez, C. Growth and nutrient removal in free and immobilized planktonic green algae isolated from pig manure. *Enzyme Microb. Technol.* **2004**, 34 (5), 392–398.
- (195) Kilham, S. S.; Kreeger, D. A.; Lynn, S. G.; Goulden, C. E.; Herrera, L. COMBO: a defined freshwater culture medium for algae and zooplankton. *Hydrobiologia* **1998**, 377 (1), 147–159.
- (196) Guillard, R. R. L.; Ryther, J. H. Studies of marine planktonic diatoms: *I. Cyclotella nana* Hustedt, and *Detonula confervacea* (Cleve) gran. *Can. J. Microbiol.* **1962**, 8, (2), 229–239.
- (197) Wetzel, R. G.; Likens, G. E. *Limnological Analyses*, 3rd ed.; Springer: New York, 2000. pp 85–112.
- (198) Wilmes, P.; Andersson, A. F.; Lefsrud, M. G.; Wexler, M.; Shah, M.; Zhang, B.; Hettich, R. L.; Bond, P. L.; VerBerkmoes, N. C.; Banfield, J. F. Community proteogenomics highlights microbial strain-variant protein expression within activated sludge performing enhanced biological phosphorus removal. *ISME J.* **2008**, 2 (8), 853–864.
- (199) Eilers, P. H. C.; Peeters, J. C. H. A model for the relationship between light intensity and the rate of photosynthesis in phytoplankton. *Ecol. Modell.* **1988**, 42 (2), 199–215.
- (200) Merchuk, J. C.; Garcia-Camacho, F.; Molina-Grima, E. Photobioreactor design and fluid dynamics. *Chem. Biochem. Eng. Q.* **2007**, 21 (4), 345–355.
- (201) Aitchison, P. A.; Butt, V. S. The relation between the synthesis of inorganic polyphosphate and phosphate uptake by *Chlorella vulgaris*. *J. Exp. Bot.* **1973**, 24, (3), 497–510.
- (202) Hernandez, J.-P.; de-Bashan, L. E.; Bashan, Y. Starvation enhances phosphorus removal from wastewater by the microalga *Chlorella* sp. co-immobilized with *Azospirillum brasilense*. *Enzyme Microb. Technol.* **2006**, 38 (1), 190–198.
- (203) Voltolina, D.; Cordero, B.; Nieves, M.; Soto, L. Growth of *Scenedesmus* sp. in artificial wastewater. *Bioresour. Technol.* **1999**, 68 (3), 265–268.

- (204) Droop, M. R. The nutrient status of algal cells in batch culture. *J. Mar. Biol. Assoc. United Kingdom* **1975**, *55*, (3), 541–555.
- (205) Lau, P.S.; Tam, N.F.Y.; Wong, Y.S. Effect of algal density on nutrient removal from primary settled wastewater. *Environ. Pollut.* **1995**, *89* (1), 59–66.
- (206) Ruiz-Marin, A.; Mendoza-Espinosa, L. G.; Stephenson, T. Growth and nutrient removal in free and immobilized green algae in batch and semi-continuous cultures treating real wastewater. *Bioresour. Technol.* **2010**, *101* (1), 58–64.
- (207) Azov, Y.; Shelef, G. The effect of pH on the performance of high-rate oxidation ponds. *Water Sci. Technol.* **1987**, *19* (12), 381–383.
- (208) Ogbonna, J. C.; Yada, H.; Tanaka, H. Kinetic study on light-limited batch cultivation of photosynthetic cells. *J. Ferment. Bioeng.* **1995**, *80* (3), 259–264.
- (209) Hessen, D. O.; Færøvig, P. J.; Andersen, T. Light, nutrients, and P:C ratios in algae: grazer performance related to food quality and quantity. *Ecology* **2002**, *83* (7), 1886–1898.
- (210) Valledor, L.; Furuhashi, T.; Hanak, A.-M.; Weckwerth, W. Systemic cold stress adaptation of *Chlamydomonas reinhardtii*. *Mol. Cell. Proteomics* **2013**, *12* (8), 2032–2047.
- (211) Ball, S. G.; Dirick, L.; Decq, A.; Martiat, J.-C.; Matagne, R. F. Physiology of starch storage in the monocellular alga *Chlamydomonas reinhardtii*. *Plant Sci.* **1990**, *66* (1), 1–9.
- (212) Chen, M.; Tang, H.; Ma, H.; Holland, T. C.; Ng, K. Y. S.; Salley, S. O. Effect of nutrients on growth and lipid accumulation in the green algae *Dunaliella tertiolecta*. *Bioresour. Technol.* **2011**, *102* (2), 1649–1655.
- (213) Grossman, A. Acclimation of *Chlamydomonas reinhardtii* to its nutrient environment. *Protist* **2000**, *151* (3), 201–224.
- (214) Blaby, I. K.; Blaby-Haas, C. E.; Tourasse, N.; Hom, E. F. Y.; Lopez, D.; Aksoy, M.; Grossman, A.; Umen, J.; Dutcher, S.; Porter, M.; King, S.; Witman, G. B.; Stanke, M.; Harris, E. H.; Goodstein, D.; Grimwood, J.; Schmutz, J.; Vallon, O.; Merchant, S. S.; Prochnik, S. The *Chlamydomonas* genome project: a decade on. *Trends Plant Sci.* **2014**, *19* (10), 672–680.
- (215) Grossman, A.R.; Croft, M.; Gladyshev, V. N.; Merchant, S. S.; Posewitz, M. C.; Prochnik, S.; Spalding, M. H. Novel metabolism in *Chlamydomonas* through the lens of genomics. *Curr. Opin. Plant Biol.* **2007**, *10* (2), 190–198.
- (216) Sack, L.; Zeyl, C.; Bell, G.; Sharbel, T.; Reboud, X.; Bernhardt, T.; Koelewyn, H. Isolation of four new strains of *Chlamydomonas reinhardtii* (Chlorophyta) from soil samples. *J. Phycol.* **1994**, *30* (4), 770–773.

- (217) Wehr, J. D.; Brown, L. M.; Vanderelst, I. E. Hydrogen ion buffering of culture media for algae from moderately acidic, oligotrophic waters. *J. Phycol.* **1986**, 22 (1), 88–94.
- (218) Grobbelaar, J. U. Algal nutrition—mineral nutrition. In *Handbook of Microalgal Culture: Biotechnology and Applied Phycology*; Richmond, A., Ed.; Blackwell Publishing Ltd: Oxford, UK, 2003; pp. 95–115.
- (219) Nuñez, V. J.; Voltolina, D.; Nieves, M.; Piña, P.; Medina, A.; Guerrero, M. Nitrogen budget in *Scenedesmus obliquus* cultures with artificial wastewater. *Bioresour. Technol.* **2001**, 78 (2), 161–164.
- (220) Voltolina, D.; Gómez-Villa, H.; Correa, G. Nitrogen removal and recycling by *Scenedesmus obliquus* in semicontinuous cultures using artificial wastewater and a simulated light and temperature cycle. *Bioresour. Technol.* **2005**, 96 (3), 359–362.
- (221) VerBerkmoes, N. C.; Russell, A. L.; Shah, M.; Godzik, A.; Rosenquist, M.; Halfvarson, J.; Lefsrud, M. G.; Apajalahti, J.; Tysk, C.; Hettich, R. L.; Jansson, J. K. Shotgun metaproteomics of the human distal gut microbiota. *ISME J.* **2009**, 3 (2), 179–189.
- (222) Ram, R.J.; VerBerkmoes, N.C.; Thelen, M.P.; Tyson, G.W.; Baker, B. J.; Blake, R.C., II.; Shah, M.; Hettich, R. L.; Banfield, J. F. Community proteomics of a natural microbial biofilm. *Science* **2005**, 308 (5730), 1915–1920.
- (223) McDonald, W. H.; Ohi, R.; Miyamoto, D. T.; Mitchison, T. J.; Yates, J. R. III. Comparison of three directly coupled HPLC MS/MS strategies for identification of proteins from complex mixtures: single-dimension LC-MS/MS, 2-phase MudPIT, and 3-phase MudPIT. *Int. J. Mass Spectrom.* **2002**, 219 (1), 245–251.
- (224) Craig, R.; Beavis, R. C. TANDEM: Matching proteins with tandem mass spectra. *Bioinformatics* **2004**, 20 (9), 1466–1467.
- (225) Searle, B. C. Scaffold: a bioinformatic tool for validating MS/MS-based proteomic studies. *Proteomics* **2010**, 10 (6), 1265–1269.
- (226) Old, W. M.; Meyer-Arendt, K.; Aveline-Wolf, L.; Pierce, K. G.; Mendoza, A.; Sevinsky, J. R.; Resing, K. A.; Ahn, N. G. Comparison of label-free methods for quantifying human proteins by shotgun proteomics. *Mol. Cell. Proteomics* **2005**, 4 (10), 1487–1502.
- (227) Schaub, J.; Clemens, C.; Kaufmann, H.; Schultz, T. W. Advancing biopharmaceutical process development by system-level data analysis and integration of omics data. In *Genomics and Systems Biology of Mammalian Cell Culture*; Hu, W.-S.; Zeng, A.-P., Eds.; Springer: Berlin, 2012; pp. 133–163.
- (228) Yuan, J.; Doucette, C. D.; Fowler, W. U.; Feng, X.-J.; Piazza, M.; Rabitz, H. A.; Wingreen, N. S.; Rabinowitz, J. D. Metabolomics-driven quantitative analysis of ammonia assimilation in *E. Coli*. *Mol. Syst. Biol.* **2009**, 5, 302.

- (229) Martin, T.; Oswald, O.; Graham, I. A. *Arabidopsis* seedling growth, storage lipid mobilization, and photosynthetic gene expression are regulated by carbon:nitrogen availability. *Plant Physiol.* **2002**, *128* (2), 472–481.
- (230) Zhang, S.; Zheng, C.; Lanza, I. R.; Nair, K. S.; Raftery, D.; Vitek, O. Interdependence of Signal processing and analysis of urine ^1H NMR spectra for metabolic profiling. *Anal. Chem.* **2009**, *81* (15), 6080–6088.
- (231) Mussnug, J. H.; Thomas-Hall, S.; Rupprecht, J.; Foo, A.; Klassen, V.; McDowall, A.; Schenk, P. M.; Kruse, O.; Hankamer, B. Engineering photosynthetic light capture: impacts on improved solar energy to biomass conversion. *Plant Biotechnol. J.* **2007**, *5* (6), 802–814.
- (232) Chida, H.; Nakazawa, A.; Akazaki, H.; Hirano, T.; Suruga, K.; Ogawa, M.; Satoh, T.; Kadokura, K.; Yamada, S.; Hakamata, W.; Isobe, K.; Ito, T.; Ishii, R.; Nishio, T.; Sonoike, K.; Oku, T. Expression of the algal cytochrome *c6* gene in *Arabidopsis* enhances photosynthesis and growth. *Plant Cell Physiol.* **2007**, *48* (7), 948–957.
- (233) Rudra, D.; Warner, J. R. What better measure than ribosome synthesis? *Genes Dev.* **2004**, *18* (20), 2431–2436.
- (234) Abe, J.; Kubo, T.; Takagi, Y.; Saito, T.; Miura, K.; Fukuzawa, H.; Matsuda, Y. The transcriptional program of synchronous gametogenesis in *Chlamydomonas reinhardtii*. *Curr. Genet.* **2004**, *46* (5), 304–315.
- (235) Siersma, P. W.; Chiang, K.-S. Conservation and degradation of cytoplasmic and chloroplast ribosomes in *Chlamydomonas reinhardtii*. *J. Mol. Biol.* **1971**, *58* (1), 167–185.
- (236) Pérez-Pérez, M. E.; Florencio, F. J.; Crespo, J. L. Inhibition of target of rapamycin signaling and stress activate autophagy in *Chlamydomonas reinhardtii*. *Plant Physiol.* **2010**, *152* (4), 1874–1888.
- (237) Chen, C.; Gibbs, M. Some enzymes and properties of the reductive carboxylic acid cycle are present in the green alga *Chlamydomonas reinhardtii* F-60. *Plant Physiol.* **1992**, *98* (2), 535–539.
- (238) Igarashi, D.; Tsuchida, H.; Miyao, M.; Ohsumi, C. Glutamate:glyoxylate aminotransferase modulates amino acid content during photorespiration. *Plant Physiol.* **2006**, *142* (3), 901–910.
- (239) Timm, S.; Nunes-Nesi, A.; Pärnik, T.; Morgenthal, K.; Wienkoop, S.; Keerberg, O.; Weckwerth, W.; Kleczkowski, L. A.; Fernie, A. R.; Bauwe, H. A Cytosolic pathway for the conversion of hydroxypyruvate to glycerate during photorespiration in *Arabidopsis*. *Plant Cell* **2008**, *20* (10), 2848–2859.
- (240) Ravanel, S.; Gakière, B.; Job, D.; Douce, R. The specific features of methionine

- biosynthesis and metabolism in plants. *Proc. Natl. Acad. Sci. U.S.A.* **1998**, 95 (13), 7805–7812.
- (241) Herrmann, K. M. The shikimate pathway: Early steps in the biosynthesis of aromatic compounds. *Plant Cell* **1995**, 7 (7), 907–919.
- (242) Kalamaki, M. S.; Alexandrou, D.; Lazari, D.; Merkouropoulos, G.; Fotopoulos, V.; Pateraki, I.; Aggelis, A.; Carrillo-López, A.; Rubio-Cabetas, M. J.; Kanellis, A. K. Over-expression of a tomato N-acetyl-L-glutamate synthase gene (*SNAGSI*) in *Arabidopsis thaliana* results in high ornithine levels and increased tolerance in salt and drought stresses. *J. Exp. Bot.* **2009**, 60 (6), 1859–1871.
- (243) Dastoor, Z.; Dreyer, J.-L. Potential role of nuclear translocation of glyceraldehyde-3-phosphate dehydrogenase in apoptosis and oxidative stress. *J. Cell Sci.* **2001**, 114 (9), 1643–1653.
- (244) Zala, D.; Hinckelmann, M.-V.; Yu, H.; Lyra da Cunha, M. M.; Liot, G.; Cordelières, F. P.; Marco, S.; Saudou, F. Vesicular glycolysis provides on-board energy for fast axonal transport. *Cell* **2013**, 152 (3), 479–491.
- (245) Gutiérrez, R. A.; Lejay, L. V.; Dean, A.; Chiaromonte, F.; Shasha, D. E.; Coruzzi, G. M. Qualitative network models and genome-wide expression data define carbon/nitrogen-responsive molecular machines in *Arabidopsis*. *Genome Biol.* **2007**, 8, R7.
- (246) Li, X.; Benning, C.; Kuo, M.-H. Rapid triacylglycerol turnover in *Chlamydomonas reinhardtii* requires a lipase with broad substrate specificity. *Eukaryotic. Cell* **2012**, 11 (12), 1451–1462.
- (247) Lea, P. J.; Mifflin, B. J. Glutamate synthase and the synthesis of glutamate in plants. *Plant Physiol. Biochem.* **2003**, 41 (6), 555–564.
- (248) Quesada, A.; Gómez, I.; Fernández, E. Clustering of the nitrite reductase gene and a light-regulated gene with nitrate assimilation loci in *Chlamydomonas reinhardtii*. *Planta* **1998**, 206 (2), 259–265.
- (249) Paul, J. H.; Cooksey, K. E. Regulation of asparaginase, glutamine synthetase, and glutamate dehydrogenase in response to medium nitrogen concentrations in a euryhaline *Chlamydomonas* species. *Plant Physiol.* **1981**, 68 (6), 1364–1368.
- (250) Muñoz-Blanco, J.; Cardenas, J. Changes in glutamate dehydrogenase activity of *Chlamydomonas reinhardtii* under different trophic and stress conditions. *Plant Cell Environ.* **1989**, 12 (2), 173–182.
- (251) Vizcaíno, J. A.; Deutsch, E. W.; Wang, R.; Csordas, A.; Reisinger, F.; Ríos, D.; Dienes, J. A.; Sun, Z.; Farrah, T.; Bandeira, N.; Binz, P.-A.; Xenarios, I.; Eisenacher, M.; Mayer, G.; Gatto, L.; Campos, A.; Chalkley, R. J.; Kraus, H.-J.; Albar, J. P.; Martinez-Bartolomé, S.;

- Apweiler, R.; Omenn, G. S.; Martens, L.; Jones, A. R.; Hermjakob, H. ProteomeXchange provides globally co-ordinated proteomics data submission and dissemination. *Nat. Biotechnol.* **2014**, *32* (3), 223–226.
- (252) Croft, M. T.; Warren, M. J.; Smith, A. G. Algae need their vitamins. *Eukaryotic Cell* **2006**, *5* (8), 1175–1183.
- (253) Benhamed, M.; Bertrand, C.; Servet, C.; Zhou, D.-X. *Arabidopsis* *GCN5*, *HDI1*, and *TAF1/HAF2* interact to regulate histone acetylation required for light-responsive gene expression. *Plant Cell* **2006**, *18* (11), 2893–2903.
- (254) Wittenberg, G.; Danon, A. Disulfide bond formation in chloroplasts: formation of disulfide bonds in signaling chloroplast proteins. *Plant Sci.* **2008**, *175* (4), 459–466.
- (255) Niewiadomski, P.; Knappe, S.; Geimer, S.; Fischer, K.; Schulz, B.; Unte, U. S.; Rosso, M. G.; Ache, P.; Flügge, U.-I.; Schneider, A. The *Arabidopsis* plastidic glucose 6-phosphate/phosphate translocator *GPT1* is essential for pollen maturation and embryo sac development. *Plant Cell* **2005**, *17* (3), 760–775.
- (256) Pfalz, J.; Liere, K.; Kandlbinder, A.; Dietz, K.-J.; Oelmüller, R. pTAC2, -6, and -12 are components of the transcriptionally active plastid chromosome that are required for plastid gene expression. *Plant Cell* **2006**, *18* (1), 176–197.
- (257) Page, M. D.; Allen, M. D.; Kropat, J.; Urzica, E. I.; Karpowicz, S. J.; Hsieh, S. I.; Loo, J. A.; Merchant, S. S. Fe sparing and Fe recycling contribute to increased superoxide dismutase capacity in iron-starved *Chlamydomonas reinhardtii*. *Plant Cell* **2012**, *24* (6), 2649–2665.
- (258) Hurley, B. A.; Tran, H. T.; Marty, N. J.; Park, J.; Snedden, W. A.; Mullen, R. T.; Plaxton, W. C. The dual-targeted purple acid Phosphatase isozyme AtPAP26 is essential for efficient acclimation of *Arabidopsis* to nutritional phosphate deprivation. *Plant Physiol.* **2010**, *153* (3), 1112–1122.
- (259) Tran, H. T.; Hurley, B. A.; Plaxton, W. C. Feeding hungry plants: the role of purple acid phosphatases in phosphate nutrition. *Plant Sci.* **2010**, *179* (1), 14–27.
- (260) Brocker, C.; Vasiliou, M.; Carpenter, S.; Carpenter, C.; Zhang, Y.; Wang, X.; Kotchoni, S. O.; Wood, A. J.; Kirch, H.-H.; Kopečný, D.; Nebert, D. W.; Vasiliou, V. Aldehyde dehydrogenase (ALDH) superfamily in plants: gene nomenclature and comparative genomics. *Planta* **2013**, *237* (1), 189–210.
- (261) Dietz, K. J.; Horling, F.; König, J.; Baier, M. The function of the chloroplast 2-cysteine peroxiredoxin in peroxide detoxification and its regulation. *J. Exp. Bot.* **2002**, *53* (372), 1321–1329.
- (262) Eriksson, M.; Karlsson, J.; Ramazanov, Z.; Gardeström, P.; Samuelsson, G. Discovery of

- an algal mitochondrial carbonic anhydrase: molecular cloning and characterization of a low-CO₂-induced polypeptide in *Chlamydomonas reinhardtii*. *Proc. Natl. Acad. Sci. U.S.A.* **1996**, 93 (21), 12031–12034.
- (263) Ohnishi, N.; Mukherjee, B.; Tsujikawa, T.; Yanase, M.; Nakano, H.; Moroney, J. V.; Fukuzawa, H. Expression of a low-CO₂-inducible protein, LCII, increases inorganic carbon uptake in the green alga *Chlamydomonas reinhardtii*. *Plant Cell* **2010**, 22 (9), 3105–3117.
- (264) Nedelcu, A. M. Sex as a response to oxidative stress: stress genes co-opted for sex. *Proc. R. Soc., B* **2005**, 272 (1575), 1935–1940.
- (265) Barbosa, M. J.; Albrecht, M.; Wijffels, R. H. Hydrodynamic stress and lethal events in sparged microalgae cultures. *Biotechnol. Bioeng.* **2003**, 83 (1), 112–120.
- (266) Masson, S.; Pinel-Alloul, B.; Dutilleul, P. Spatial heterogeneity of zooplankton biomass and size structure in southern Quebec lakes: variation among lakes and within lake among epi-, meta- and hypolimnion strata. *J. Plankton Res.* **2004**, 26 (12), 1441–1458.
- (267) Wang, L.; Li, Y.; Chen, P.; Min, M.; Chen, Y.; Zhu, J.; Ruan, R. R. anaerobic digested dairy manure as a nutrient supplement for cultivation of oil-rich green microalgae *Chlorella* sp. *Bioresour. Technol.* **2010**, 101 (8), 2623–2628.
- (268) Lau, P. S.; Tam, N. F. Y.; Wong, Y. S. Influence of organic-n sources on an algal wastewater treatment system. *Resour. Conserv. Recycl.* **1994**, 11 (1), 197–208.
- (269) García Martín, H.; Ivanova, N.; Kunin, V.; Warnecke, F.; Barry, K. W.; McHardy, A. C.; Yeates, C.; He, S.; Salamov, A. A.; Szeto, E.; Dalin, E.; Putnam, N. H.; Shapiro, H. J.; Pangilinan, J. L.; Rigoutsos, I.; Kyrpides, N. C.; Blackall, L. L.; McMahon, K. D.; Hugenholtz, P. Metagenomic analysis of two enhanced biological phosphorus removal (EBPR) sludge communities. *Nat. Biotechnol.* **2006**, 24 (10), 1263–1269.
- (270) Vidal, E. A.; Gutiérrez, R. A. A systems view of nitrogen nutrient and metabolite responses in *Arabidopsis*. *Curr. Opin. Plant Biol.* **2008** 11, (5), 521–529.
- (271) MacLean, B.; Tomazela, D. M.; Shulman, N.; Chambers, M.; Finney, G. L.; Frewen, B.; Kern, R.; Tabb, D. L.; Liebner, D. C.; MacCoss, M. J. Skyline: an open source document editor for creating and analyzing targeted proteomics experiments. *Bioinformatics* **2010**, 26, (7), 966–968.
- (272) Sherrod, S. D.; Myers, M. V.; Li, M.; Myers, J. S.; Carpenter, K. L.; MacLean, B.; MacCoss, M. J.; Liebner, D. C.; Ham, A.-J. L. Label-free quantitation of protein modifications by pseudo selected reaction monitoring with internal reference peptides. *J. Proteome Res.* **2012**, 11 (6), 3467–3479.
- (273) Sharma, V.; Eckels, J.; Taylor, G. K.; Shulman, N. J.; Stergachis, A. B.; Joyner, S. A.;

- Yan, P.; Whiteaker, J. R.; Halusa, G. N.; Schilling, B.; Gibson, B. W.; Colangelo, C. M.; Paulovich, A. G.; Carr, S. A.; Jaffe, J. D.; MacCoss, M. J.; MacLean, B. Panorama: a targeted proteomics knowledge base. *J. Proteome Res.* **2014**, *13* (9), 4205–4210.
- (274) Elton, C. S. *The Ecology of Invasions by Plants and Animals*, 18th ed.; Methuen: London, 1958. pp. 181.
- (275) Darwin, C. *The Origin of Species by Means of Natural Selection, Or the Preservation of the Favored Races in the Struggle for Life*; Murray: London, 1859. pp. 458.
- (276) Tilman, D.; Reich, P. B.; Knops, J. M. H. Biodiversity and ecosystem stability in a decade-long grassland experiment. *Nature* **2006**, *441* (7093), 629–632.
- (277) Gill, S. R.; Pop, M.; Deboy, R. T.; Eckburg, P. B.; Turnbaugh, P. J.; Samuel, B. S.; Gordon, J. I.; Relman, D. A.; Fraser-Liggett, C. M.; Nelson, K. E. Metagenomic analysis of the human distal gut microbiome. *Science* **2006**, *312* (5778), 1355–1359.
- (278) Wu, J.-H.; Wu, F.-Y.; Chuang, H.-P.; Chen, W.-Y.; Huang, H.-J.; Chen, S.-H.; Liu, W.-T. Community and proteomic analysis of methanogenic consortia degrading terephthalate. *Appl. Environ. Microbiol.* **2013**, *79*, (1), 105–112.
- (279) Huang, E. L.; Lefsrud, M. G. Temporal analysis of xylose fermentation by *Scheffersomyces stipitis* using shotgun proteomics. *J. Ind. Microbiol. Biotechnol.* **2012**, *39* (10), 1507–1514.

Chapter 9: Appendices

9.1. Appendix A: Proteomic sample preparation and instrument setup

9.1.1. Sample preparation for small samples of microalgae

Cell pellets were processed through a single tube cell lysis and protein digestion method reported previously for prokaryotes and yeast^{76,104,221} and adapted and optimized for eukaryotic microalgae.⁷⁵

- a) Immediately harvest and process biological samples in random order at the same time as a single batch. Each biological replicate represents a sample for processing and injection into the mass analyzer.
- b) Centrifuge ~ 150 mL of suspended microalgae cells at $\sim 10^7$ cells mL⁻¹ at ~ 25 °C for 15 min at $3000 \times g$.
- c) Immediately quench ~ 25 mg of wet cell pellet in liquid nitrogen and store at - 80 °C.
- d) Thaw and solubilize on ice in 100 μ L of lysis buffer to extrude proteins (Tris/10 mM CaCl₂ at pH 7.6 and 6 M guanidine/10 mM dithiothreitol (DTT)). Use LC–MS water.
- e) Seal tube with parafilm.
- f) Sonicate in an ice slurry bath for 5 cycles of 30 s each, with a 30 s cool-down period between cycles.
- g) Vortex every 2 min for the first hour, place on tube rotator and incubate at 37 °C for 12 h (or overnight).
- h) Dilute guanidine solution samples further with further with 50 mM Tris/10 mM CaCl₂.
- i) Dilute sequencing grade trypsin with 50 mM Tris/10 mM CaCl₂ (ie. 20 μ g in 100 μ L) and add 20 μ g of trypsin to each sample (ie. ~ 100 μ L).
- j) Incubate a further 12 h at 37 °C.
- k) Add a second aliquot of same amount of sequencing grade trypsin. Incubate further 6 h.
- l) Add 1 M DTT to a final concentration of 20 mM. Very important that final concentration is ~ 20 mM. (ie. 154.25 mg in 1 mL of Tris/10 mM CaCl₂ and add 2 μ g).
- m) Incubate for an additional 1h at 37 °C.
- n) Centrifuge for 10 min at $5\text{--}6000 \times g$ and discard pellet.
- o) Clean and desalt supernatant sample via solid-phase extraction with Sep-Pak Plus C-18 cartridges (WAT020515, Waters Limited, Mississauga, ON).
- p) Samples from clean up are concentrated, solvent exchanged to 95% H₂O/5% CAN/0.1% formic acid.
- q) Filter (Ultrafree-MC UFC30HV00, pore size 0.45 μ m, EMD Millipore, Billerica, MA), and store at -80 °C.

9.1.2. LTQ XL parameters for data-dependent acquisition of tandem MS/MS spectra

The LTQ XL was calibrated using ESI source with MRFA, caffeine, and Ultramark. The instrument tune was performed using automatic optimization with 52426 m/z as target (MRFA), as performed for yeast proteomics.⁷⁶

- a) For ESI source: sheath gas= 0, aux gas= 0, sweep gas= 0, spray voltage= 195-225kV, capillary temp= 275C, capillary voltage= 47, tube lens= 110
- b) Ion optics: Multipole 00 offset= -45, Lens 0 voltage= -4, multipole 0 offset = -525, lens 1 voltage= -28, gate lens voltage= -22, multipole 1 offset= -155, multipole RF amplitude V p-p = 400, front lens= -575
- c) ACG target: full ms= 3e4, SIM= 1e4, MSn= 2e4, zoom= 3000
- d) Instrument setup for MS/MS and data-dependent:
 - 1) 6 total scan events, 1 full and 5 dependent. 5 MS/MS per 1 full MS
 - 2) Global mass range: 0 to 100,000
 - 3) Global mass width: Should be 05
 - 4) Dynamic exclusion: repeat count =1, repeat duration=30s, exclusion list size=100, exclusion duration= 60s, exclusion mass width: by mass, 15 low and high
 - 5) Activation Page for each scan event:
 - i. Activation type: CID
 - ii. Default charge state: always 3
 - iii. Isolation width= 3
 - iv. Normalized collision energy= 35
 - v. Activation Q= 025
 - vi. Activation time= 30 ms
 - vii. For the current scan event, minimum signal threshold=1000, select mass determined from the full scan, select Nth most intense ion Scan event 2 should be 1st most intense ion from scan event 1, scan 3 should be for the 2nd most intense from scan event 1

9.1.3. 2D LC elution gradient

Peptide analysis was accomplished using online two-dimensional liquid chromatography interfaced with a linear ion trap mass spectrometer (LTQ, Thermo Fisher Scientific, San Jose, CA).^{221,222} For performance of label-free shotgun proteomics using Multi-dimensional Protein Identification Technology (MudPIT).⁷³ For each sample injection, peptides were bomb-loaded onto a biphasic MudPIT back column packed with ~ 5 cm strong cation exchange (SCX) resin followed by ~ 5 cm C₁₈ reversed phase (RP) (Luna 5 μ m 100A and Aqua 5 μ m 100A, Phenomenex, Torrance, CA).²²³ Peptide-loaded columns were first washed for 30 min off-line with LC-MS grade H₂O (0.1% F.A) to remove salts and algal cell impurities, then placed in-line with a front column with an integrated nanospray emitter tip (100 μ m i.d., 360 μ m o.d., 15 μ m i.d. tip, New Objective, Woburn, MA) packed with ~15 cm of C₁₈ RP material, and analyzed via 24 h, 12 step MudPIT 2D LC-nanoESI-MS/MS adapted and optimized for eukaryotic microalgae from previously described methods.^{198,223}

Solvent A: 95 water, 5 ACN, 01 formic acid

Solvent B: 30 water, 70 ACN, 01 formic acid

Solvent D: 500mM Ammonium Acetate in Solvent A

All flow rates were approximated and measured at the tip.

Run 1					
Time (min)	Flow (nl/min)	A	B	C	D
0	450	100	0	0	0
45	450	50	50	0	0
55	450	0	100	0	0
60	450	100	0	0	0
Run 2					
Time (min)	Flow (nl/min)	A	B	C	D
0	450	100	0	0	0
5.0	450	100	0	0	0
5.10	450	90	0	0	10
7.00	800	90	0	0	10
7.10	800	100	0	0	0
10.00	450	100	0	0	0
120.00	450	50	50	0	0
Run 3					
Time (min)	Flow (nl/min)	A	B	C	D
0.00	450	100	0	0	0
5.00	450	100	0	0	0
5.10	450	85	0	0	15
7.00	800	85	0	0	15
7.10	800	100	0	0	0
10.00	450	100	0	0	0
120.00	450	50	50	0	0
Run 4					
Time (min)	Flow (nl/min)	A	B	C	D
0.00	450	100	0	0	0
5.00	450	100	0	0	0
5.10	450	80	0	0	20
7.00	450	80	0	0	20
7.10	450	100	0	0	0
10.00	450	100	0	0	0
120.00	450	50	50	0	0
Run 5					
Time (min)	Flow (nl/min)	A	B	C	D
0.00	450	100	0	0	0
5.00	450	100	0	0	0
5.10	450	75	0	0	25
7.00	800	75	0	0	25

7.10	800	100	0	0	0
10.00	450	100	0	0	0
120.00	450	50	50	0	0

Run 6

Time (min)	Flow (nl/min)	A	B	C	D
0.00	450	100	0	0	0
5.00	450	100	0	0	0
5.10	450	70	0	0	30
7.00	800	70	0	0	30
7.10	800	100	0	0	0
10.00	450	100	0	0	0
120.00	450	50	50	0	0

Run 7

Time (min)	Flow (nl/min)	A	B	C	D
0.00	450	100	0	0	0
5.00	450	100	0	0	0
5.10	450	65	0	0	35
7.00	800	65	0	0	35
7.10	800	100	0	0	0
10.00	450	100	0	0	0
120.00	450	50	50	0	0

Run 8

Time (min)	Flow (nl/min)	A	B	C	D
0.00	450	100	0	0	0
5.00	450	100	0	0	0
5.10	450	60	0	0	40
7.00	800	60	0	0	40
7.10	800	100	0	0	0
10.00	450	100	0	0	0
120.00	450	50	50	0	0

Run 9

Time (min)	Flow (nl/min)	A	B	C	D
0.00	450	100	0	0	0
5.00	450	100	0	0	0
5.10	450	55	0	0	45
7.00	800	55	0	0	45
7.10	800	100	0	0	0
10.00	450	100	0	0	0
120.00	450	50	50	0	0

Run 10

Time (min)	Flow (nl/min)	A	B	C	D
0.00	450	100	0	0	0
5.00	450	100	0	0	0
5.10	450	50	0	0	50

7.00	800	50	0	0	50
7.10	800	100	0	0	0
10.00	450	100	0	0	0
120.00	450	50	50	0	0

Run 11

Time (min)	Flow (nl/min)	A	B	C	D
0.00	450	100	0	0	0
5.00	450	100	0	0	0
5.10	450	40	0	0	60
7.00	800	40	0	0	60
7.10	800	100	0	0	0
10.00	450	100	0	0	0
120.00	450	50	50	0	0

Run 12

Time (min)	Flow (nl/min)	A	B	C	D
0.00	450	100	0	0	0
5.00	450	100	0	0	0
5.10	450	40	0	0	60
15.00	800	40	0	0	60
16.10	800	100	0	0	0
25.00	450	100	0	0	0
40.00	450	80	20	0	0
100.00	450	0	100	0	0



NEW FRONT
COLUMN
CLEAN


Time (min)	Flow (nl/min)	A	B	C	D
0	300	0	100	0	0
5	300	0	100	0	0
30	300	100	0	0	0
35	300	100	0	0	0


9.2. Appendix B: Publishing agreements

Rightslink® by Copyright Clearance Center

<https://s100.copyright.com/AppDispatchServlet>



[Home](#) [Create Account](#) [Help](#)  Live Chat

 **Title:** Multidimensional LC Separations in Shotgun Proteomics
Author: Akira Motoyama, John R. Yates
Publication: Analytical Chemistry
Publisher: American Chemical Society
Date: Oct 1, 2008
Copyright © 2008, American Chemical Society

LOGIN

If you're a [copyright.com](#) user, you can login to RightsLink using your copyright.com credentials. Already a [RightsLink](#) user or want to [learn more?](#)

PERMISSION/LICENSE IS GRANTED FOR YOUR ORDER AT NO CHARGE

This type of permission/license, instead of the standard Terms & Conditions, is sent to you because no fee is being charged for your order. Please note the following:

- Permission is granted for your request in both print and electronic formats, and translations.
- If figures and/or tables were requested, they may be adapted or used in part.
- Please print this page for your records and send a copy of it to your publisher/graduate school.
- Appropriate credit for the requested material should be given as follows: "Reprinted (adapted) with permission from (COMPLETE REFERENCE CITATION). Copyright (YEAR) American Chemical Society." Insert appropriate information in place of the capitalized words.
- One-time permission is granted only for the use specified in your request. No additional uses are granted (such as derivative works or other editions). For any other uses, please submit a new request.

If credit is given to another source for the material you requested, permission must be obtained from that source.

[BACK](#)[CLOSE WINDOW](#)

Copyright © 2015 Copyright Clearance Center, Inc. All Rights Reserved. [Privacy statement](#). [Terms and Conditions](#).
Comments? We would like to hear from you. E-mail us at customer@copyright.com

Permission for Figure 2.2. Reprinted with permission from Motoyama, A.; Yates, J. R.

Multidimensional LC separations in shotgun proteomics. *Anal. Chem.* **2008**, 80 (19), 7187–7193.

Copyright 2008, American Chemical Society.).


RightsLink®
[Home](#)
[Account Info](#)
[Help](#)
[Live Chat](#)


Title: Microalgae for phosphorus removal and biomass production: a six species screen for dual-purpose organisms

Author: Anil Patel, Suzelle Barrington, Mark Lefsrud

Publication: GCB Bioenergy

Publisher: John Wiley and Sons

Date: Feb 11, 2012

© 2012 Blackwell Publishing Ltd

Logged in as:

Anil Patel

[LOGOUT](#)

Order Completed

Thank you for your order.

This Agreement between Anil K Patel ("You") and John Wiley and Sons ("John Wiley and Sons") consists of your license details and the terms and conditions provided by John Wiley and Sons and Copyright Clearance Center.

Your confirmation email will contain your order number for future reference.

[Get the printable license.](#)

License Number	3637750036491
License date	May 28, 2015
Licensed Content Publisher	John Wiley and Sons
Licensed Content Publication	GCB Bioenergy
Licensed Content Title	Microalgae for phosphorus removal and biomass production: a six species screen for dual-purpose organisms
Licensed Content Author	Anil Patel, Suzelle Barrington, Mark Lefsrud
Licensed Content Date	Feb 11, 2012
Licensed Content Pages	11
Type of use	Dissertation/Thesis
Requestor type	Author of this Wiley article
Format	Print and electronic
Portion	Full article
Will you be translating?	No
Order reference number	DOI: 10.1111/j.1757-1707.2012.01159.x
Title of your thesis / dissertation	Microalgae for wastewater treatment and biomass production: a comparative analysis of growth and nutrient removal using shotgun proteomics
Expected completion date	Aug 2015
Expected size (number of pages)	275
Requestor Location	Anil K Patel Bioresource Eng. McGill University Macdonald Stewart Building 21111 Lakeshore Road Ste-Anne-de-Bellevue, QC H9X 3V9 Canada

Permission for Chapter 3, Manuscript I. Reprinted with permission from Patel, A.; Barrington, B.; Lefsrud, M. Microalgae for phosphorus removal and biomass production: a six species screen for dual-purpose organisms. *GCB Bioenergy* **2011**, 4 (5), 485-495. Copyright 2012, John Wiley and Sons.).


RightsLink®
[Home](#)
[Create Account](#)
[Help](#)
[Live Chat](#)

Title:

Comparative shotgun proteomic analysis of wastewater cultured microalgae: Nitrogen sensing and carbon fixation for growth and nutrient removal in *Chlamydomonas reinhardtii*

Author:

Anil K Patel, Eric Lu Huang, Etienne Low-Décarie, et al

Publication: Journal of Proteome Research

Publisher: American Chemical Society

Date: May 1, 2015

Copyright © 2015, American Chemical Society

LOGIN

If you're a **copyright.com** user, you can login to RightsLink using your copyright.com credentials. Already a **RightsLink** user or want to [learn more?](#)

PERMISSION/LICENSE IS GRANTED FOR YOUR ORDER AT NO CHARGE

This type of permission/license, instead of the standard Terms & Conditions, is sent to you because no fee is being charged for your order. Please note the following:

- Permission is granted for your request in both print and electronic formats, and translations.
- If figures and/or tables were requested, they may be adapted or used in part.
- Please print this page for your records and send a copy of it to your publisher/graduate school.
- Appropriate credit for the requested material should be given as follows: "Reprinted (adapted) with permission from (COMPLETE REFERENCE CITATION). Copyright (YEAR) American Chemical Society." Insert appropriate information in place of the capitalized words.
- One-time permission is granted only for the use specified in your request. No additional uses are granted (such as derivative works or other editions). For any other uses, please submit a new request.

[BACK](#)
[CLOSE WINDOW](#)

Copyright © 2015 Copyright Clearance Center, Inc. All Rights Reserved. [Privacy statement](#). [Terms and Conditions](#). Comments? We would like to hear from you. E-mail us at customer@copyright.com

Permission for Chapter 4 and 5, Manuscript II. Reprinted with permission from Patel, A.K.; Huang, E.L.; Low-Décarie, E.; Lefsrud, M. G. Comparative shotgun proteomic analysis of wastewater-cultured microalgae: nitrogen sensing and carbon fixation for growth and nutrient removal in *Chlamydomonas reinhardtii*. *J. Proteome Res.* **2015**, *14* (8), 3051-3067. Copyright 2015, American Chemical Society.).